Evaluation of an Adeno-associated virus-vector based broadly reactive influenza vaccine

D I S S E R T A T I O N

zur Erlangung des akademischen Grades

D o c t o r r e r u m n a t u r a l i u m

(Dr. rer. nat.)

im Fach Biologie

Eingereicht an der

Lebenswissenschaftlichen Fakultät

Der Humboldt-Universität zu Berlin

Von

Daniel Demminger

Präsidentin der Humboldt-Universität zu Berlin
Prof. Dr.-Ing. Dr. Sabine Kunst

Dekan der Lebenswissenschaftlichen Fakultät
Prof. Dr. Bernhard Grimm

Gutachter/innen: 1.....PD Dr. Thorsten Wolff.....
2.....Prof. Dr. Andreas Herrmann .....
3.....Prof. Dr. Benedikt Kaufer .....

Tag der mündlichen Prüfung: 7. Mai 2019

ZUSAMMENFASSUNG

Influenza Viren stellen eine große Bedrohung der öffentlichen Gesundheit dar, die mit hoher Morbidität und Mortalität besonders in Kindern und älteren Menschen assoziiert ist. Zudem verursacht die Erkrankung beträchtliche sozio-ökonomische Kosten. Die saisonale Grippeschutzimpfung induziert eine neutralisierende Antikörperantwort, welche sich gegen antigene Bereiche im Kopfbereich des viralen Oberflächenproteins Hämagglutinin (HA) richtet. In diesen Bereichen tritt jedoch verstärkt Antigendrift auf, wodurch die Effektivität der saisonalen Grippeimpfung auf den Impfstamm beschränkt wird, während keine ausreichende Schutzwirkung gegenüber viralen Driftvarianten oder neu entstehenden pandemischen und zoonotischen Viren besteht. Eine effektivere und breit reaktive oder sogar universelle Grippeimpfung wird daher dringend benötigt.

Die Entdeckung breit reaktiver Antikörper gegen konservierte Bereiche, wie dem HA-Stammbereich, hat die Erforschung von Impfstrategien vorangetrieben, mit deren Hilfe gezielt breit reaktive Antikörper induziert werden können. Chimären HA oder Headless HA erzielten in diesem Zusammenhang bereits vielversprechende Ergebnisse. Beide Antigenkonzepte beruhen dabei auf dem Prinzip des Ausschlusses der immundominanten, jedoch hoch variablen Regionen im HA-Kopfbereich, um eine Fokussierung der Immunantwort auf immunsubdominante, aber konservierte Bereiche im HA-Stammbereich zu erzielen. Zudem bergen innovative Impfstoffplattformen, wie zum Beispiel Adeno-assoziierte Virus (AAV)-Vektoren, ein immenses Potenzial. AAV-Vektoren können in Zellkultur hergestellt werden, sie können ohne die Verwendung von Nadeln intranasal verabreicht werden und sind für die Verwendung im Menschen zugelassen. Zudem wird die Immunogenität des Antigens durch die AAV-Vektor vermittelte Expression, welche der Antigenexpression im Verlauf einer natürlichen Influenza Virus Infektion gleicht, positiv beeinflusst.

In der vorliegenden Arbeit führte die Immunisierung mit AAV-Vektoren, die wildtypisches HA, Chimäre HA oder Nukleoprotein exprimieren, zur Induktion breit reaktiver Antikörper in Mäusen, nicht aber die Immunisierung mit Headless HA exprimierenden AAV-Vektoren oder inaktiviertem Grippeimpfstoff. Die Schutzwirkung ging einher mit der Fähigkeit der AAV-Vektor Impfstoffe FcγR-aktivierende Antikörper zu induzieren, wodurch in der Maus vermutlich FcγR-vermittelte Effektormechanismen wie zum Beispiel Antikörper vermittelte zelluläre Zytotoxizität ausgelöst wurden, die zum Schutz der Tiere gegenüber einer Influenza führten. Interessanterweise löste nicht nur die AAV-vektor vermittelte Impfung mit Chimären HA, sondern auch mit wildtypischem HA eine Antikörperantwort gegen den HA-Stammbereich aus. Dies deutet darauf hin, dass die Immundominanz des HA-Kopfbereiches allein durch die AAV-Vektor vermittelt Expression des Antigens abgemildert werden konnte. Abschließend konnte zum ersten Mal die Schutzwirkung einer AAV-Vektor Immunisierung gegen HA im Frettchen demonstriert werden. Die in dieser Arbeit beschriebenen Ergebnisse zeigen somit das große Potenzial von AAV-Vektoren als Impfvehikel für eine breit reaktive Grippeschutzimpfung auf.

SUMMARY

Influenza viruses represent a severe threat to public health, associated with high morbidity and mortality especially in children and the elderly. Moreover, the disease is associated with substantial socio-economic costs. A seasonal vaccine is available, which readily leads to the induction of neutralizing antibodies against antigenic sites in the head domain of the viral surface protein hemagglutinin (HA). These antigenic sites are, however, prone to antigenic drift. Therefore, seasonal vaccination induces only strain specific protection, while it is not effective against drifted seasonal virus strains and emerging pandemic or zoonotic viruses. Hence, there is an urgent need for a more effective and broader reactive or even universal influenza vaccine.

The discovery of broadly reactive antibodies against highly conserver regions such as the HA-stalk domain has prompted a great interest into research on vaccination strategies to induce broadly protective HA antibodies. Concepts such as chimeric HA and headless HA have been developed, which show promising results with respect to the induction of protective HA-stalk antibodies. Both antigen concepts rely on the principle of avoiding immunodominant but strain specific epitopes to re-focus immunity towards conserved but immunosubdominant epitopes in the HA-stalk. Aside from rational antigen development, also innovative vaccine delivery platforms such as Adeno-associated virus (AAV)-vectors offer an attractive developmental perspective. AAV-vectors can be readily manufactured in cell culture, they can be applied without needles into the nose, and the vector system is licensed for use in humans. Furthermore, AAV-vectored antigen expression, which resembles antigen processing as it occurs during natural infection with influenza virus, will likely positively influence the immunogenicity of the antigen.

In this thesis, it could be shown that only immunization with AAV-vectors expressing wildtype HA, chimeric HA or nucleoprotein induced broad protection in mice, but not vaccination with AAV-vectors expressing headless HA or an inactivated influenza vaccine. Intriguingly, protection was associated with the ability of the AAV-vectored vaccines to potently induce FcγR-activating antibodies, indicating that protection is mediated by FcγR-mediated effector mechanisms such as antibody-dependent cellular cytotoxicity. Surprisingly, not only chimeric HA but also wildtype HA induced antibodies against the HA-stalk when expressed from an AAV-vector, suggesting that AAV-vectored antigen expression can mitigate the immunodominance of virus strain-specific epitopes in the HA-head. Importantly, for the first time a protective effect AAV-vectored immunization towards HA could be shown in ferrets. Thus, results described in this thesis suggest a large potential for the development of AAV-vectors as carriers for a broadly protective influenza vaccine.

TABLE OF CONTENT

1. INTRODUCTION

1.1. INFLUENZA VIRUSES

1.1.1. GENERAL INTRODUCTION

Influenza viruses are negative sensed, single stranded RNA viruses with a segmented genome, which belong to the family of *Orthomyxoviridae* (*1*). Within the influenza viruses, only the genera A, B and C are able to infect humans. A fourth genus, influenza D viruses, is connected to infections in cattle and pigs (*2*). Influenza A viruses show a very broad host range, covering several avian and mammalian species, while influenza B virus infections are mainly restricted to humans with occasional outbreaks in marine mammals (*3, 4*). Influenza A viruses are further subtyped according to the combination of their surface proteins hemagglutinin (HA) and neuraminidase (NA) (e.g. H1N1). To date, 18 HA (H1 – H18) and 11 NA (N1 – N11) subtypes have been antigenically differentiated, with intra- and intersubtype sequence variations of HA of up to 20 % or 30 – 70 %, respectively (*5-7*) (Figure 1). However, only the subtypes H1N1, H2N2, H3N2, H5N1, H5N6, H6N1, H7N7, H7N9, H9N2, and H10N7 have been reported to infect humans (*8, 9*) (Figure 2). Additionally, influenza A viruses are divided into group 1 and group 2 viruses based on the HA amino acid sequence (Figure 1). Influenza B viruses are sub-classified into lineages, whereas viruses circulating in humans belong to the Yamagata or Victoria lineage that diverged from each other in the 1920s.

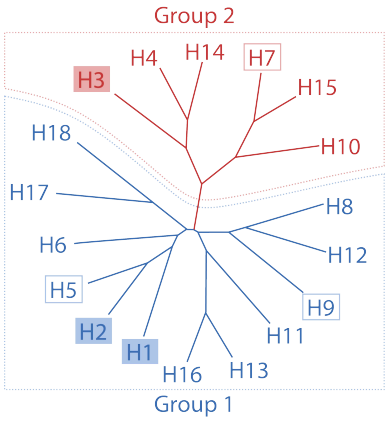

Figure 1: Phylogenetic tree of Influenza A virus HA
Influenza A virus HA are divided into two groups based on their amino acid sequences (Group 1 and Group 2). Influenza A virus subtypes that have been circulating in humans (filled rectangles) and such with pandemic potential (empty rectangles) are marked. (modified from Wu *et al.*, Trends Microbiol (2014))

Influenza A and B viruses cause recurrent epidemics of respiratory illness in humans, i.e. the "flu season", whereas influenza C virus infections generally occur during childhood and cause only mild disease (*10*). For temperate climate areas the epidemic season starts in November and ends in March. Seasonal influenza viruses are directly transmitted from person to person via aerosols produced during coughing and sneezing or by contact with contaminated surfaces and fomites (*9*). Replication of seasonal influenza viruses takes place mainly in ciliated cells of trachea and bronchi, but attachment to alveolar type II pneumocytes, alveolar macrophages and dendritic cells in the lower respiratory tract may occur (*11, 12*). After an incubation period of one to two days, typical influenza disease, i.e. "the flu", is characterized by a sudden onset of high fever in combination with cough, head- and general aches, chills, fatigue, sore throat or sneezing (*13*). Usually, symptoms last no longer than one to two weeks before people recover without need for medical attendance (*9*). However, complications such as pneumonia, bronchitis, sinusitis and otitis may occur, which can be life-threatening.

The annual global attack rate is estimated to be 5 – 10 % in adults and 20 – 30 % in children. The viral infection causes annually three to five million cases of severe illness, 290 000 to 650 000 of which become fatal. Persons at highest risk for complications are pregnant women, children at the age of 6 – 59 months, the elderly (≥69 years) and health care workers. Additionally, influenza can exacerbate chronic health conditions such as asthma, immune deficiencies or chronic cardiopulmonary diseases (*9*). The resulting economic costs for health systems and due to loss of productivity in the population are substantial (*14*).

Morbidity and mortality can even increase dramatically in case of pandemics, which occur in non-predictable, irregular intervals when a virus undergoes major antigenic changes and is introduced into a population which is immunologically naïve to it (*15, 16*). One of the most prominent examples is the 1918 H1N1 pandemic, the so called "Spanish flu", which is estimated to have caused up to 50 million deaths worldwide (*17*) (Figure 2). A related virus caused the most recent pandemic in 2009 ("Swine Flu") (*15*).

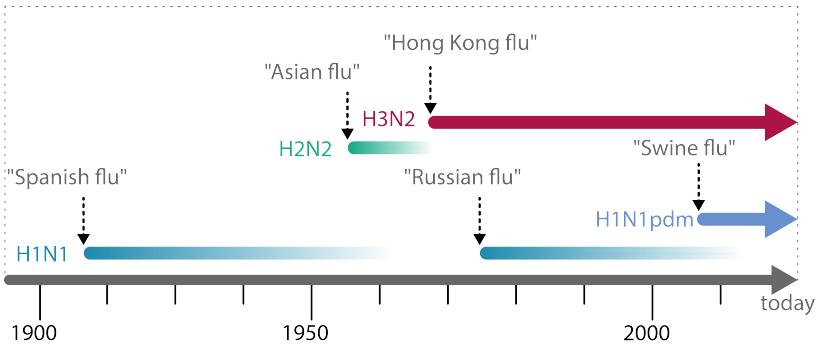

Figure 2: Influenza A viruses circulating in the human population
Viruses of three HA (H1, H2 and H3) and two NA (N1 and N2) subtypes circulated in humans during the last century. Four pandemic viruses emerged, replacing the by that time circulating subtypes: The H1N1 pandemic virus in 1918-1919 ("Spanish Flu", 50 million deaths), the H2N2 pandemic virus in 1957 ("Asian Flu", 1.1 million deaths), the H3N2 pandemic virus in 1968 ("Hong Kong flu", 1.0 million deaths) and most recently, the H1N1 pandemic virus in 2009 ("Swine flu", 0.5 million deaths). In 1977 a virus related to the H1N1 virus from 1950 re-emerged ("Russian flu"). At the moment, viruses of the subtypes H3N2 and H1N1 are circulating in humans. (modified from Palese, Nat Med (2004))

Since the end of the last century an increasing number of direct zoonotic transmissions of avian influenza viruses to humans have been reported (*18*). The severity of the disease ranges from mild to very aggressive depending on the infecting virus subtype (*8*). With H5N1 viruses for instance a mortality rate of about 50 % is reported, which is much higher than for seasonal influenza viruses (*18*). Although being hardly transmissible from human to human, there is potential for avian influenza viruses to acquire mutations enabling them for direct human to human transmission which increases their pandemic potential (*19-21*). The constant threat of seasonal and pandemic influenza viruses as well as emerging zoonotic strains emphasizes the urgent need for more effective prophylactic and therapeutic countermeasures, which is antagonized by the ever changing nature of the virus.

1.1.2. MORPHOLOGY

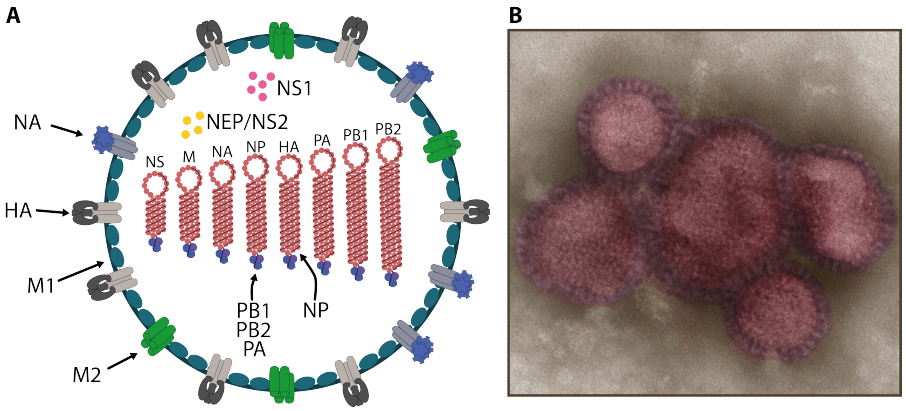

Figure 3: Morphology of influenza A virus particles
(A) Schematic drawing of an influenza A virus particle. Hemagglutinin (HA), Neuraminidase (NA) and M2 protein are embedded into the host cell derived lipid membrane. The Matrix protein (M1) lines the inner side of the envelope. Within the particle, accessory proteins NS1 and NEP/NS2 as well as the viral RNP complexes are located. The RNP complexes consist of one of the eight viral RNA segments, the Nucleoprotein (NP) and the RdRp-complex (PB1, PB2 and PA). **(B)** Negative stain transmission electron micrograph of A/California/7/2009 (H1N1)pdm influenza virus. (Courtesy of Gudrun Holland and Norbert Bannert (RKI), 85.000 x magnifications, false color)

Influenza A virions are spherical or pleomorphic particles with diameters of 80 – 120 nm (spherical) to more than 300 nm (filamentous). The virion envelope is derived from the host cell lipid membrane and harbors three viral membrane proteins (*22*): Hemagglutinin (HA) and neuraminidase (NA), which form characteristic spikes that project about 10 – 14 nm from the membrane, and matrix protein 2 (M2) (Figure 3). HA is the most abundant of the membrane proteins, being 4–times more abundant than NA and 10–100 – times more than M2 (*23*).

The interior of the envelope is lined by matrix protein 1 (M1) and contains the ribonucleoprotein (RNP) complexes (*24*). These comprise the viral (v)RNA segments, the nucleoprotein (NP), and the viral RNA-dependent-RNA-polymerase (RdRp) complex, which consists of the subunits polymerase acid (PA), polymerase basic 1 (PB1) and polymerase basic 2 (PB2) (*25*).

Table 1: Proteome of influenza A viruses
Proteins are categorized as membrane, internal or non-structural virion protein. Not all of the accessory proteins are expressed by all influenza isolates and the function or existence of some has yet to be determined. (modified from Vasin *et al.*, Virus Res (2014))

membrane	internal	non-structural
	PB1 / PB2 / PA Replication/Transcription (RdRp subunits)	**PB1-F2** Virulence factor
HA (3-mer) Attachment, Fusion	**NP** RNA encapsidation nucleo-cytoplasmic RNP transport	**PB1-N40** Replication factor
NA (4-mer) Release (Sialidase, receptor destroying enzyme)	**M1** Virion structure, virion assembly	**PB2-S1** Antagonist of antiviral host response
M2 (4-mer) Uncoating (Proton specific ion channel)	**NS1** Antagonist of antiviral host response	**PA-X** Virulence factor
M42 Replacement of M2	**NEP/NS2** Nuclear export of RNPs	**PA-N155, PA-N182** Unknown function
		NS3 Host adaption (mouse)
		NEG8/NSP (hypothetical) Unknown function

Also, the accessory nonstructural protein 1 (NS1) and nuclear export protein/nonstructural protein 2 (NEP/NS2) were shown to be part of the virion (*26*) (Figure 3). The individual RNP display double-helical rod-like structures of about 50 – 150 nm in length (*24, 27*). The eight vRNA are approximately 890-2350 nucleotides in length, whereas the coding region is flanked by non-coding regions that contain the regulatory sequences needed for transcription and replication (*28-31*). Influenza A viruses increase their coding capacity by ribosomal leaky scanning and open reading frame shifting (e.g. PB1 or PA segment) or alternative splicing (e.g. M1, M2 and NS segment), which eventually results in the expression of a minimum of ten proteins (*32-37*) (Table 1).

1.1.3. REPLICATION

Attachment of influenza viruses to the host cell is mediated by binding of HA on the viral surface to its receptor on the cell membrane: glycoproteins or glycolipids that carry a terminal N-acetylneuraminic (sialic) acid (*38-41*). Hence, the receptor is ubiquitously expressed in many animal species. Avian and human influenza viruses preferentially target sialic acid that is linked to a penultimate galactose residue either via α(2,3)-linkage or α(2,6)-linkage, respectively (*42-46*). Corresponding to the fact that influenza is a respiratory or enteric infection in humans or avian species, respectively, in humans α(2,6)-linked sialic acid predominate the respiratory tract, while α(2,3)-linkage is most common in the avian intestine (*11*). The receptor-specificity depends on amino acids at several positions within the receptor binding site (RBS) of HA (*47-50*) (Figure 4). The preference for different conformations of the receptor contributes to the species specificity of human and avian influenza viruses. An increased relative abundance of α(2,3)-linked sialic acid in the human lower respiratory tract can partially explain the ability of avian viruses to infect humans with very low efficiency, but cause high lung pathology at the same time (*51*). However, amino acid changes in the RBS that alter the receptor-specificity may be a prerequisite for efficient infection and spread of avian viruses after transmission to humans (*52, 53*).

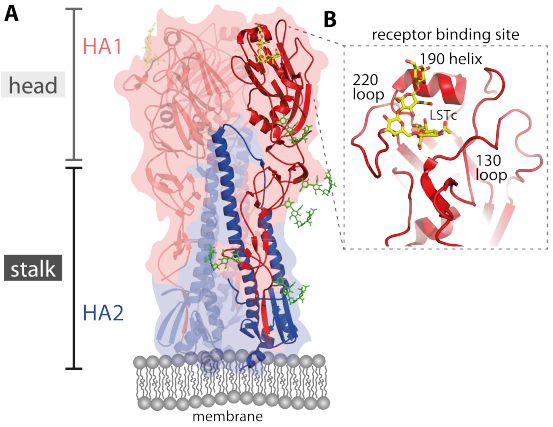

Figure 4: Structure of trimeric HA and the receptor binding site
(A) Three dimensional structure of HA. Glycan residues (green) on HA1 (red) and HA2 (blue) are depicted. Position of the head and stalk domain is indicated **(B)** Magnification of the RBS with main structural features 130 loop, 190 helix and 220 loop. The receptor analogue LSTc is depicted (yellow). (PDB: 3UBE)

After attachment of HA to the receptor, clathrin-mediated endocytosis is triggered and the virus is taken up into the cell (*54*). Also, HA is responsible for fusion of the viral and host cell membrane resulting in escape of the RNP complexes from the endosome into the cytoplasm. To become fusogenic each monomer of the trimeric HA has to be cleaved from the precursor protein HA0 into the subunits HA1 and HA2 (Figure 5, A and B). Although leaving the overall HA conformation quite unchanged, cleavage generates a metastable state of HA, with the newly formed positively charged N-terminus of HA2, the so called fusion peptide, being buried in a

cavity within the HA monomer (*55*) (Figure 5B). Acidification to a pH of about 5 - 6 triggers an irreversible conformational change (*56*): Re-folding of HA results in exposition of the fusion peptide and its approximation towards the endosomal membrane, in which it is ultimately inserted (Figure 5C). HA, now being anchored via HA2 into both the viral and the cellular membrane, undergoes further rearrangement steps that bend the molecule in half and allow the two membranes to come into close proximity and eventually fuse, resulting in formation of a pore through which the RNP complexes escape into the cytoplasm (*57-60*) (Figure 5, C and D).

Before release of the RNP into the cytoplasm, protons have to enter the viral particle through the pH-gated M2 ion channel, which results in the disruption of interactions of M1 with the RNP (*61, 62*). For transcription and replication, the RNP complexes are transported into the nucleus through interactions of cellular importins with the nuclear localization signals within NP and the RdRp (*63*). Within the nucleus, the RdRp transcribes mRNA carrying a 5'–cap and a Poly(A) tail from the vRNA segments. Transcription is initiated on a 5'–capped primer which is cleaved from cellular pre-mRNA (so called "cap snatching") (*64, 65*). Unlike cellular mRNA, influenza viral mRNA are polyadenylated by reiterative copying of a polyuracil stretch within the vRNA (*66, 67*). Hereafter, mRNA are exported from the nucleus and translated by the cellular translation machinery (*68*). Proteins harboring nuclear localization signals (e.g. NP or polymerase subunits) are subsequently transported into the nucleus (*69*). Membrane proteins are translated at the rough endoplasmic reticulum, trafficked to the Golgi apparatus and sorted to cholesterol-rich lipid rafts at the apical plasma membrane (*70*).

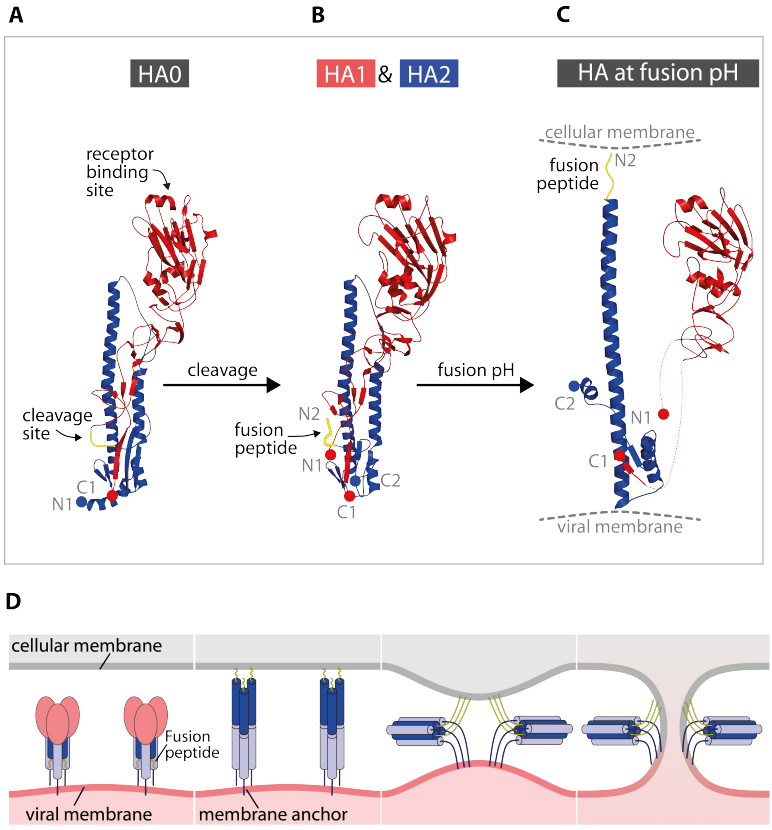

Figure 5: Conformations of HA during the fusion process
(A) Structure of the uncleaved HA precursor, HA0 (only one monomer is shown). The position of the C- and N-terminus is indicated (blue/red circles). In the uncleaved molecule, the cleavage site (yellow) is projecting from surface of the structure forming a loop between HA1 (red) and HA2 (blue). **(B)** Matured HA with cleaved HA1 and HA2 subunit. The newly generated C- and N-termini are indicated (circels: N1 and C1 of HA1 red; N2 and C2 of HA2 blue). The fusion peptide is located at the N-terminus of HA2 (N2). **(C)** At fusion pH, conformational changes in HA2 lead to repositioning of the fusion peptide towards the cellular membrane while the RBS domain in HA1 is preserved. **(D)** Schematic representation of the conformational changes during fusion. HA2 alone is shown in the right three panels (PDB structures: 1RD8, 1RU7, 1HTM, 2VIR). (modified from Hughson, Curr Biol (1997); Bullogh, Nat (1994))

During this process, the proteins are correctly folded and monomers are assembled to their oligomeric forms, e.g. three HA monomers form a trimer (Table 1) (*71*). Additionally, post-translational modifications occur, such as addition of several glycosylations and palmitoylations to HA (Figure 4) (*72-74*).

Eventually, a switch from transcription to synthesis of full length complementary (c)RNA occurs, which in turn serve as templates for the replication of the genomic vRNA segments (*75-77*). The newly formed RNP complexes are exported from the nucleus through an interaction with M1 and NEP/NS2 and transported to the apical site of the cell (*69, 78, 79*). The viral components assemble at the lipid raft domains and the virus particles bud from the plasma membrane (*80*). During this process, a selective packaging mechanism ensures that particles contain all eight RNP complexes (*81*). Because HA binds to sialic acids on the host cell surface also during budding, NA's sialidase activity is needed to finally release the progeny virions from the cell surface (*82-84*). For the virus to become infective, HA0 has to be cleaved into HA1 and HA2, as mentioned above. For most HA subtypes that contain a single arginine in their cleavage site (Q/E-X-R), this process is mediated by proteases expressed by influenza viruses target cells in the human respiratory tract such as Clara, HAT or TMPRSS2 (*85-87*). However, some HA of the subtypes H5 and H7 contain a polybasic cleavage site (R-X-R/K-R) (*88*). The proteases responsible for cleavage of these HA, i.e. subtilisin-like proteases such as furin, show very wide tissue distribution, which might be related to the systemic and highly virulent courses of infection seen with these viruses (*89, 90*) (see 1.1.1).

1.2. IMMUNITY TO INFLUENZA VIRUSES

1.2.1. GENERALITIES ON CELLS AND MECHANISMS INVOLVED IN AN IMMUNE RESPONSE

Breathing not only enables gas exchange which is vital for life, but also constantly exposes the respiratory tract to a large number of pathogens. To fight intruders, the human body is equipped with sophisticated defense mechanisms: the immune system.

The first physical barrier to pathogens is the mucociliary epithelium of the respiratory tract. If viruses circumvent this barrier, epithelial and endothelial cells as well as lung resident innate immune cells including dendritic cells (DC) and alveolar macrophages represent the first line of defense (*91*). Influenza virus triggers an intrinsic response by activation of pattern recognition receptors, i.e. Toll-like-, RIG-I-like-, and NOD-like-receptors, which recognize "non-self" pathogen-associated molecular patterns, such as viral single stranded RNA (*92*). This response induces the production of antiviral and inflammatory cytokines, including type I interferon (IFN) and TNFα, leading to recruitment and activation of further innate immune effector cells (*91*). The production of IFN-stimulated gene products counteracts the infection by establishment of an antiviral state in infected as well as neighboring non-infected cells. Also, damage-associated molecular patterns, e.g. extracellular mitochondrial DNA, can activate innate cells (*93*). The complement system can inhibit influenza virus through direct lysis or activation of innate cells as well (*94*). Alveolar macrophages as well as monocytes and neutrophils which enter the site of infection from the blood stream become activated and phagocytose pathogens as well as debris of infected cells, or produce antimicrobial molecules (e.g. reactive oxygen species) (*95, 96*). Natural

killer cells (NK cells) are able to recognize infected cells and are equipped with several mechanisms to eliminate them (perforin/granzyme pathway or FasL/Fas interaction) (*97*).

By bridging innate and adaptive immunity, DC represent the most important professional antigen presenting cells (APC) besides macrophages and B-cells (*98*). APC, like all other nucleated cells, present endogenously produced peptide antigen on MHC class I molecules (MHCI) on their surface. In addition, they express MHC class II molecules (MHCII) allowing them to present exogenously acquired peptide antigens, too (*99*). Moreover, some APC are able to present exogenous antigen on MHCI, so called 'cross presentation', and vice versa, also presentation of endogenous antigen on MHCII plays a role during influenza virus infection (*100, 101*). DC take up antigen via endocytosis of viral products or debris of infected cells, by direct infection or by trogocytosis (*102*). The abundance, accessibility and mode of presentation of the antigen will likely define the outcome of the immune response (*103*). After antigen uptake, DC home to draining lymph nodes where they present the antigen to naïve, antigen-specific T-cells. Following engagement of the antigen-MHC complex with the T-cell receptor in the presence of co-stimulatory signals, T-cells clonally expand, acquire a specific set of effector functions and migrate to the site of infection (*99*). Different subsets of lung resident DC ($CD103^+$, $CD11b^+$, pDC) were shown to preferentially activate different T-cell subsets during influenza infection (*97, 102*).

$CD8^+$ T-cells differentiate into cytotoxic T lymphocytes (CTL) after recognition of antigen-MHCI complexes. CTL are the primary cell type eliminating influenza virus infected cells via induction of apoptosis (perforin/granzyme pathway; FasL/Fas interaction, TRAIL mediated) and secretion of pro-inflammatory cytokines (*104*). Interestingly, $CD8^+$ T-cells also play a role in regulating the immune response at the end of the infection (*105*). Influenza virus-specific CTL can be found in all individuals older than 15 years of age, with the dominant proportion being specific for epitopes in internal virion proteins such as NP and M1 (*106, 107*).

Recognition of antigen-MHCII complexes by $CD4^+$ T-cells induces their differentiation into several functionally different effector cell types. These stimulate, modulate or regulate the immune response ("helper cells"). Among these, T_H1 cells bias the immune response towards inflammation and stimulate the maturation of CTL (*99*). Influenza virus infection is generally associated with a strong T_H1-type response. Though being non-essential for their primary activation, the establishment of an efficient CTL memory is also strongly dependent on $CD4^+$ T-cell help (*108*). Interestingly, cytotoxic $CD4^+$ T-cell can also directly eliminate influenza virus infected lung epithelial cells (*109*). In contrast to that, T_H2 cells and particularly T follicular helper (T_{FH}) cells in the lymphoid organs promote the production of antibodies by inducing maturation of B-cells and antibody class switch (*110*). Another helper cell subset, T_H17 cells, can promote clearing of the infection by enhancing CTL and B-cell responses, while T_{Reg} cells where shown to limit $CD8^+$ T-cell effector functions, thus, preventing immunopathology (*109, 111*).

After clearance of the infection, the effector T-cell pools contract and long lived memory T-cells remain. Memory cells re-activate their effector functions more rapidly and potently compared to naïve cells (*112*). Moreover, their localization not only to lymphoid organs (central memory T-cell, T_{CM}) but to the site of infection (effector memory T-cells, T_{EM}; resident memory

T-cell, T_{RM}) accelerates their response. Particularly lung T_{RM} cells were found to confer long lasting protection against influenza virus infection (*113*).

B-cells can recognize not only peptide-MHC complexes but also linear or conformational epitopes in proteins (*99*). Interestingly, while influenza virus surface antigens, e.g. HA, are considered to be primary inducers of a humoral response, also antibodies against internal antigens such as NP can be induced during infection (*114, 115*). Upon recognition, B-cells endocytose their antigen and present peptide-MHCII complexes to antigen specific, activated $CD4^+$ T-cells (i.e. T_{FH} cells) in the draining lymph nodes. The interaction of B and T-cell leads to proliferation of the B-cell and differentiation into antibody secreting plasma cells that leave the lymphoid organ. Some B-cells reside in the lymphoid tissue and, promoted by T_{FH} cells, increase their effectivity and functionality by affinity maturation and antibody class switch (see 1.2.2) (*116*). As with T-cells, a B-cell memory is established after clearance of the infection which can be recalled within hours after second exposure (*116*). For influenza virus infections also $CD4^+$ T-cell independent activation of B-cells was described, although efficient B-cell memory relies on $CD4^+$ T-cell help (*117*).

Adequately balanced cellular and humoral immune responses can efficiently clear the infection. However, a misregulated response may lead to immunopathology (*118*). Furthermore, though establishment of a memory T and B-cell response makes vaccination possible in the first place, it can also lead to immunopathology if not considered cautiously during a vaccine's design process (*118, 119*).

1.2.2. STRUCTURE AND FUNCTIONS OF ANTIBODY MOLECULES

To react and adapt to the immense number of different pathogens which infect the organism during life time, the immune system is able to generate a nearly unlimited, highly variable repertoire of antigen specific antibody molecules. The antibody molecule (ca. 150 kDa) consists of two identical heavy (50 kDa) and two identical light (25 kDa) chains, which are linked to each other via disulfide bonds (*99*) (Figure 6). The heavy and light chains consist of four or two immunoglobulin (Ig) domains, respectively. Each Ig domain is composed of several β-sheets arranged in a characteristic β-barrel. Antigen binding occurs at a highly variable region in the first Ig domain of the molecule (variable region: V_H or V_L). Due to the β-barrel arrangement, the antigen binding site is formed by highly variable loops at the tip of the antibody molecule, the so called complementarity determining regions (CDR). Each antibody molecule contains three CDR loops of the light (CDR_L1-3) and three of the heavy chain (CDR_H1-3). The adjacent Ig domains are more conserved (constant region: C_H1-3 or C_L). A second function of antibodies besides antigen binding is the activation of other cells and mediators of the immune system. Activation of these effector functions is mediated by the C-terminal Fc region of the antibody. Whereas the V_L / V_H, C_L / C_H1 and C_H3 / C_H3 are associated with each other, there is no such connection due to the presence of carbohydrates moieties at the interface of the two C_H2 domains (*120*).

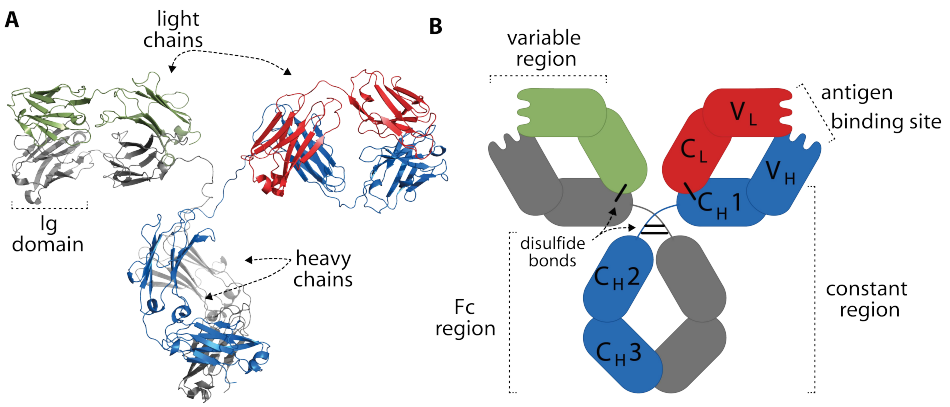

Figure 6: Structure of a classical antibody molecule
(A) Three dimensional structure of an IgG2a molecule showing Ig domains of light (green and red) and heavy (grey and blue) chains (PDB: 1IGT). **(B)** Schematic drawing of an Ig molecule. The position of the antigen binding site within the variable region of the antibody (V_L and V_H) is indicated. The constant region (C_L and C_H1-3) makes up the 'stalk' of the Y-shaped antibody, which is also called the Fc region (C_H2 and 3) (color coding as in (a)).

The human immune system produces about 10^{11} antibody specificities at a given time, which might be an underestimate being limited by the absolute number of B-cells. This immense diversity is achieved through several mechanisms such as i) random joining of V(D)J segments during B-cell maturation via somatic recombination within the genome loci coding for the variable region, ii) unspecific insertion of nucleotides during this process (i.e. junctional diversity), iii) random combination of heavy and light chains with different variable regions in one antibody molecule and iv) somatic hypermutation of the variable region after B-cell activation and selection for high affinity antibodies (affinity maturation) (*121-124*). In addition to mechanisms affecting the binding specificity, also the constant region of the heavy chain is variable: A recombination event within the activated B-cell switches the expressed heavy chain constant region gene segment (μ, δ, γ, ε or α) and thereby the antibody's isotype (IgM, IgD, IgG, IgE or IgA) (*99*). Antibody isotypes show differential spatial and temporal appearance: after primary infection IgM molecules dominate the immune response. Later, IgG molecules are produced and become the most abundant isotype in the serum. Furthermore, IgA play a pivotal role during infections with respiratory pathogens like influenza virus due to presence in the mucosa of the respiratory tract (*125*). The antibody isotypes are specialized in different effector functions such as neutralization, opsonization, complement activation as well as activation of other immune effector cells. In part, these differences are accounted for by varying affinities of the antibody isotype's Fc region for Fc-gamma receptors (FcγR) on immune cells.

1.2.3. FC-GAMMA RECEPTORS

FcγR are expressed on a variety of leukocyte populations, including NK cells, macrophages, monocytes, neutrophils, basophils and mast cells (*126*). Interestingly, DC and B-cells do express FcγR, indicating their role in shaping adaptive cellular and humoral immunity as well (*120*). Based on the stoichiometry and mode of binding, FcγR are classified into type I and type II receptors (Figure 7) (*127*). Type I FcγR vary with respect to their potential to activate different downstream signaling cascades and their affinity for IgG isotypes (Figure 7A). They are, therefore, categorized into activating (human: FcγRI, IIA, IIC, IIIA, IIIB; mouse: FcγRI, III, IV) and inhibitory

(human/mouse: FcγRIIB) type I FcγR (*128*). While most cells co-express activating and inhibitory type I FcγR, NK cells and B-cells express only one activating or inhibitory receptor at a time, respectively. Although type I FcγR subclass members were shown to bind several IgG isotypes *in vitro*, there is evidence that *in vivo* binding is more restricted to individual IgG isotypes (*120*).

The type I receptor molecule consists of two or three IgG-like domains (D1-D3) (Figure 7A). Type I FcγR signaling is, with the exception of the GPI-linked FcγRIIIB, initiated at ITAM (activating) or ITIM (inhibitory) domains within the ligand-binding domain (FcγRIIA, FcγRIIC and FcγRIIB) or within the associated adaptor molecule (e.g. FcR γ chain, FcγRI, FcγRIIIA) (*126*) (Figure 7A). Phosphorylation of ITAM or ITIM domains triggers Ca^{2+}-dependent or MAP-kinase-signal transduction cascades, eventually resulting in activation of a multitude of cellular effector functions, resulting in activation, regulation, and modulation of immune responses (see below) (*120*).

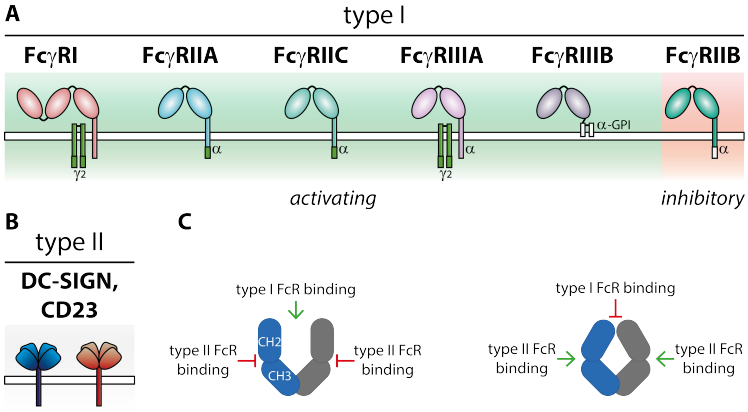

Figure 7: Human type I and type II Fcγ-receptors
(**A**) Type I FcγR are related to the Ig-receptor superfamily and categorized into activating and inhibitory receptors according to the signaling cascades they initiate. (**B**) Type II FcγR belong to the C-type lectin receptor family. (**C**) Binding of type I and type II receptors to the Fc region is mutually exclusive and regulated by differential glycosylation of C_H2, altering the conformation of the Fc region. Thereby, further diversification of the functional effector response is enabled. (adapted from Pincetic *et al.*, Nat Rev Immunol (2014); Bruhns, Blood (2012))

Signaling triggered by type II FcγR is less well defined compared to type I receptor signaling, but results in activation of several effector functions, too, interestingly including upregulation of type I FcγR surface expression (*129*). Intriguingly, structural analysis revealed that type I FcγR bind to the interface between the two heavy chains of the Fc part, thereby precluding binding of a second FcγR to the same antibody molecule (Figure 7C) (*130, 131*). Thus, only immune complexes in which multiple antibody molecules are present can efficiently crosslink and activate type I FcγR (*132*). In contrast, type II FcyR bind a region between C_H2 and C_H3 on each heavy chain, thus allowing binding of two receptor molecules to one antibody molecule at a time (Figure 7C) (*127*). The Fc region can adapt two conformations depending on the glycosylation status of C_H2, rendering the binding of type I and type II receptors to on antibody molecule mutually exclusive (Figure 7C) (*133*). In fact, it was shown that Fc glycosylation patterns change dynamically after immunization with an inactivated influenza vaccine (*129*). Selection of high affinity B-cell receptors (BCR) was augmented after engagement of type II FcγR on B-cells,

followed by upregulation and engagement of the inhibitory type I FcγRIIB, which eventually raised the threshold for BCR activation (*129*). Thus, further diversification and regulation of the effector immune response is enabled (*129, 134*). Also, Fc glycoengineering, i.e. the targeted manipulation of the antibody molecule's glycosylation pattern, has been employed to enhance or augment cytotoxic activity of therapeutic antibodies, including anti-tumor antibodies (*135*). Another example for the important role of FcγR during establishment of adaptive immune responses is their regulation of T-cell activation. Here, relative abundance of activating and inhibitory type I FcγR on DC regulates antigen uptake and inflammatory cytokine secretion, and thus T-cell activation (*135*). Two major innate effector mechanisms triggered via Fc-FcγR interactions are antibody-dependent phagocytosis (ADP) and antibody-dependent cellular cytotoxicity (ADCC) (*95, 96, 136*). ADCC and ADP are mediated mainly by NK cells, monocytes, macrophages and neutrophils (*126*). In NK cells, FcγR engagement leads to activation of perforin/granzyme or FasL/Fas pathways (*137*). Neutrophils where shown to produce reactive oxygen species upon stimulation of FcγR (*96*). However, the exact mechanism underlying neutrophil-mediated cytotoxicity remains elusive and might involve extracellular trap formation (*136, 138, 139*). Recently, it was shown that ADP is induced in alveolar macrophages during murine influenza (*95*). In fact, Fc-FcγR interactions confer specificity to these otherwise non-adaptive innate effector mechanisms.

1.2.4. Natural infection and seasonal influenza vaccination induce strain specific antibodies

As influenza viruses replicate at high rates, complete prevention of infection, i.e. sterile immunity, represents the most efficient defense mechanism for the organism (*140*). Accordingly, natural infection or seasonal vaccination induces mainly antibodies which are directed against the attachment and fusion mediating HA. Antibodies against the other viral surface proteins NA or M2e play minor roles as they interfere with later steps of the influenza virus life cycle (*141, 142*). As mentioned above, also antibodies against internal proteins such as NP may be involved in protection (*143*).

Sterile immunity is conferred via sterical hindrance of neutralizing antibodies that bind near the RBS within the membrane proximal HA globular head, and thereby block the interaction of HA with its receptor (Figure 4). Additionally, antibodies can mimic the receptor and prevent attachment by inserting a single CDR loop into the narrow cavity at the RBS (*144*). Although neutralizing antibodies against the HA-head can confer lifelong protection against the same virus, they are considered to have only narrow or strain-specific reactivity (*145*). Major antigenic sites surrounding the RBS in the HA-head have been mapped in early studies, which show very high sequence variability enabling rapid emergence of viral immune escape mutants (*146-149*). The main mechanisms driving these variations are i) the insertion of point mutations into the influenza virus genome by the error-prone RdRp ('antigenic drift'), which generates amino acid changes along with variations in the glycosylation pattern of the protein, and ii) the re-assortment of genome segments during co-infection of different influenza viruses ('antigenic shift'). Antigenic drift thus leads to a more gradual change of the antigenicity. This, however, can generate escape

mutants also within one flu season. Antigenic shift can lead to the emergence of new viruses that are introduced into an immunologically naïve population (1.1.1) (*150*).

The seasonal inactivated vaccine induces neutralizing antibodies against the HA-head, which show only narrow binding breadth. Rapid and unpredictable antigenic changes of the viruses pose *the* major obstacle to the production of an efficient influenza vaccine: A mismatch between the viruses circulating throughout the season and the viruses that are contained in the vaccine will result in a dramatic reduction of the effectiveness of the seasonal influenza vaccine.

1.3. VACCINATION AGAINST INFLUENZA VIRUSES

1.3.1. CURRENT INFLUENZA VACCINES

First historical reports on outbreaks of influenza date back more than 400 years before Christ (*151*). Since then, numerous severe influenza pandemics were documented, with the most devastating being the H1N1 pandemic in 1918, and the most recent the H1N1 pandemic in 2009 (Figure 2). The etiology of the disease was resolved only in 1933, with the isolation of influenza A virus from nasal secretions of an infected patient (*152*). The discovery of the virus quickly prompted research on influenza vaccines and antivirals, which was propelled by the appearance of new virus subtypes during the last century (Figure 2) (*153, 154*). Three classes of antivirals are currently available for prophylactic and therapeutic treatment of influenza: blockers of the M2 ion channel (e.g. Amantadine), inhibitors of NA activity (e.g. Oseltamivir), and inhibitors of PA endonuclease activity (e.g. Boloxavir). M2 inhibitors are, however, not recommended anymore due to the rapid induction of viral resistance mutations during treatment (*155*). Oseltamivir, although being no longer listed on the 'core list' of the 'WHO Model Lists of Essential Medicines' *(156),* is still considered to be an effective influenza therapeutic, though alternatives would be desirable (*157*). The recently licensed PA inhibitor Boloxavir showed promising results in a clinical trial compared to Oseltamivir (*158*). However, the emergence of a resistance mutation which decreased susceptibility was noted during treatment (*158*). Therefore, and because the aforementioned antivirals are almost exclusively limited to therapeutic use, vaccination is the most effective countermeasure against influenza. Consequently, influenza vaccination is recommended for all people at high risk for severe influenza, i.e. persons at the extremities of age, pregnant women or persons suffering from underlying chronic health conditions as well as those at elevated risk for infection, e.g. health care workers (*159*) (see 1.1.1).

The current seasonal influenza vaccine is tri- or quadrivalent (TIV or QIV), thus containing antigen from two circulating influenza A strains (i.e. H1N1 and H3N2) and from either one or both influenza B lineages. In Germany, the use of QIV is recommended by the Standing Committee on Vaccination (*Ständige Impfkomission*, STIKO) since 2018, thus minimizing the risk for a vaccine mismatch with the influenza B components (*160*). While originally composed of whole inactivated virus (WIV), the inactivated vaccine currently includes either split virus or viral subunits (surface proteins HA and NA), showing lower reactogenicity and adverse effects than WIV (*154, 161*). Though used less commonly recombinant HA and virosomal vaccines are available as well (*162, 163*). Most commonly, vaccine preparations are applied intramuscularly but also formulations for intradermal application are available (*164*). In addition to inactivated

vaccines, live-attenuated influenza vaccines (LAIV) are used as an intranasal administration (*165*). Mimicking natural infection LAIV triggers a protective mucosal humoral and cellular immune response being superior to inactivated vaccines in children (*166*). Nevertheless, reduced efficiency of LAIV in non-naïve adults and concerns as to possible genetic reversion of the attenuated viruses restricts their more general use (*167, 168*). Aside from seasonal vaccines, monovalent preparations containing pandemic viruses (H1N1)pdm and such with pandemic potential (H5N1) are available as measures for preparedness for an unforeseen pandemic (*169*).

Since influenza viruses evolve constantly, also the vaccine components have to be adapted permanently to match the circulating viruses. To this end, the WHO collects influenza virus surveillance data globally throughout the year resulting in recommendations regarding the viral strains which should be included in the vaccine (February/March, Northern hemisphere) (*170*). Usually, national public health and legal authorities follow these recommendations and commission private manufacturers to produce the vaccine (*171*). Bulk manufacturing is most frequently done in embryonated chicken eggs (until September, Northern hemisphere) (*172*). Beforehand, most human influenza viruses have to be adapted to high-yield egg-based production either by repeated passaging or classical re-assortment (until April, Northern hemisphere) (*170*). This can, however, lead to undesirable changes of their antigenicity (*173*). Additionally, the limited availability of vaccine-quality eggs restricts vaccine supply for the world's population. On the contrary, cell culture-based production platforms are readily up scalable and yield high amounts of virus progeny (*174*). Several cell cultures have been evaluated and licensed for vaccine production, among them MDCK cells (canine) and Vero cells (simian) (*175, 176*). Although adaption of vaccine viruses to (non-human) cell culture might be necessary, too, their versatility make them particularly useful for the preparation of (pre-) pandemic vaccines, i.e. when time is limited (*177, 178*).

Following growth, the virus is concentrated, purified, chemically inactivated and fragmented (until October/November, Northern hemisphere) (*170*). In parallel, reference reagents for testing the vaccine products are produced which are used for quality control of the vaccine before its release and distribution (*170*). The vaccine is standardized to contain 15 µg of each HA antigen component. It is administered shortly before the start of the seasonal epidemic, e.g. for the Northern hemisphere from October/November on (*159*). Persons such as the elderly, for whom seasonal vaccination is particularly recommended, generally respond poorly to immunologic stimuli (*159, 179*). To increase the immunogenicity of the seasonal vaccine, thus, licensed in some EU countries is the use of higher antigen doses (up to 60 µg per HA component), intradermal administration, or the addition of immuno-stimulatory compounds, i.e. adjuvants like the oil-in-water emulsions MF59 or AS03 (*165, 169, 180*). Additionally, innovative delivery systems and adjuvants are under investigation to complement the inactivated seasonal vaccine (*181, 182*).

Table 2: Vaccine effectiveness against influenza virus subtypes
Left: Pooled vaccine effectiveness in the seasons 2010 – 2015 (with 95 % confidence interval thereof in brackets) is reduced in case of a H3N2 mismatch especially in the vulnerable group of people of 65-years of age and older (adapted from Rondy *et al.*, J Infect (2017)). Right: Pooled vaccine effectiveness in the seasons 2004 - 2015 varies for the individual vaccine components (adapted from Belongia *et al.*, Lancet Infect Dis (2016)).

	A/H3N2	vaccine effectiveness (95% CI)
matched	all	52 % (39 - 66)
	16-64 years	59 % (38 - 80)
	65 years and older	43 % (33 - 53)
mismatched	all	29 % (13 - 44)
	16-64 years	46 % (30 - 61)
	65 years and older	14 % (-3 - 30)

virus subtype	vaccine effectiveness (95% CI)
A/pdmH1N1	67 % (29 - 85)
A/H3N2	33 % (26 - 39)
B	61 % (57 - 65)

Due to the complexity of the recommendation process and the long manufacturing period there is a risk for the vaccine components to not match the actually seasonally circulating strains. Vaccine mismatches occur quite often and are associated with a reduced effectiveness of the vaccine against the mismatched component especially in the vulnerable group of person >65-years of age (Table 2) (*183, 184*). Aside from mismatched components, the vaccine's efficacy is mainly influenced by the status of the immune system of the vaccine recipient, which is in turn mainly dependent on age and health status. Thus, the approximate overall influenza seasonal vaccine effectiveness rate is only 40 – 60 % even in case of a good vaccine match, while apparently vaccine effectiveness varies for each subtype (Table 2) (*185*). The relatively low vaccine effectiveness can lead to individual mistrust and hesitancy towards influenza vaccination (*186*). In fact, this is reflected by low overall vaccination coverage rates in most European countries (*187*). To improve protective efficacy and thus trust in influenza vaccination and vaccine coverage, research on innovative vaccine platforms and broadly reactive antigens, so called 'universal influenza vaccines', is essential (*188-191*).

1.3.2. BROADLY REACTIVE ANTIBODIES AGAINST INFLUENZA VIRUSES

In the early 1980's, Graves *et al.* discovered that cross reactive antibodies could be induced when influenza virus particles where treated with acid and the detergent DTT before immunization of rabbits (*192*). This treatment removed the HA1 subunit from the virion, resulting in the induction of a cross-reactive HA2-specific antibody response. As mentioned above, the membrane distal globular head domain of HA which consists of the internal part of HA1 is highly variable (Figure 8; see 1.2.4). On the contrary, the membrane proximal part of HA, the so called 'stalk domain', which is comprised of HA2 and the terminal parts of HA1, is highly conserved among influenza viruses (*150*). The cross-reactive antibodies identified by Graves *et al.* where likely directed against conserved epitopes in the HA-stalk domain (*192*).

In fact, one decade later the first broadly reactive HA-stalk binding antibody, C179, was obtained from mice immunized with an H2N2 virus, which reacted with various group 1 influenza A viruses (*193, 194*). The importance of this finding remained unappreciated until other broadly reactive HA-stalk binding antibodies were extracted from human PBMC several years later (*195, 196*).

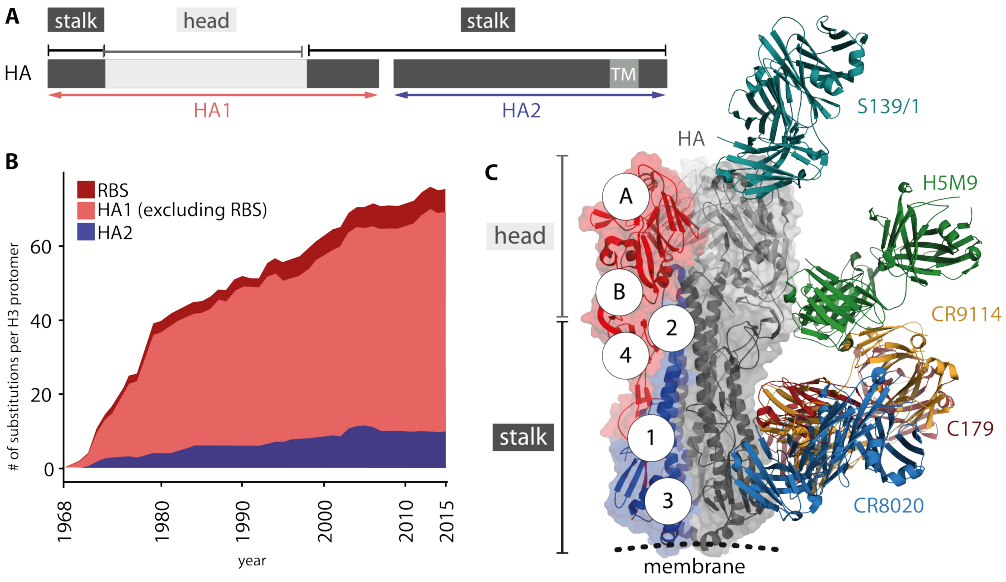

Figure 8: Conserved epitopes within HA
(**A**) Schematic representation of HA1 and HA2 domain of HA (TM: transmembrane domain). In the three dimensional molecule the head domain is comprised of the internal part of HA1 (light grey) while the HA-stalk domain consists of parts of HA1 and HA2 (dark grey). (**B**) Cumulative number of amino acid substitutions in H3 HA from 1968 – 2015 for HA1 including or excluding the RBS (dark red or light red, respectively) or for HA2 (blue) (adapted from Wu *et al.*, J Mol Biol (2017)). (**C**) Three dimensional structure of HA together with Fab fragments of broadly binding antibodies. Although antibodies C179 (red, PDB: 4HLZ), CR8020 (blue, PDB: 3SDY) and CR9114 (orange, PDB: 4FQI) bind similar sites within the HA-stalk they show different binding breadth. Broadly reactive antibodies against the HA-head can bind the RBS, i.e. S139/1 (cyan, PDB: 4GMS), or other regions, i.e. H5M9 (green, PDB: 4MHH). All antibody structures were mapped onto the H2N2 HA of PDB 4HLZ (adapted from Lee *et al.*, Curr Top Microbiol Immunol (2017)). Accordingly, two conserved epitopes in the head have been identified (A (RBS): in influenza A and influenza B viruses; B (vestigial esterase): in influenza B virus). Four conserved epitopes were defined in the HA-stalk domain (#1 (α-helix): influenza A virus group 1; #2 (upper long α-helix) and #3 (fusion peptide): influenza A virus group 2; #4 (HA1 c-terminus): influenza B virus). (adapted from Neu *et al.*, Curr Opin Immunol (2016))

Although targeting similar regions within the HA-stalk, the antibodies differ in their binding breadth (*197*) (Figure 8). Like C179, antibodies CR6261 or F10 bind only to the HA of group 1 influenza A viruses (*198, 199*), while antibody CR8020 binds to group 2 viruses only (*200*). In contrast, antibody FI6v3 shows promiscuous binding to almost all influenza A virus HA (*201*). Remarkably, binding to influenza A and B viruses was demonstrated for antibody CR9114 (*202*). Interestingly, most HA-stalk binding antibodies recognize conformational epitopes and do not bind to the post-fusion HA conformation (*196, 200, 203*).

The discovery of broadly reactive HA antibodies has not been restricted to antibodies targeting epitopes within the HA-stalk domain (Figure 8C): as certain residues in the RBS are functionally highly conserved, several RBS-targeting broadly reactive antibodies such as S139/1 were isolated (*204, 205*). Most, if not all of them reach into the receptor binding pocket with one of their CDR_H loops and mimic the receptor (*196*). However, the high variability of the residues surrounding the RBS limits their affinity and reactivity breadth (*204*). Other antibodies like H5M9 target highly conserved epitopes in other parts of the HA-head domain, including the vestigial esterase domain of influenza B viruses (*206*) (Figure 8C). Eventually, in addition to the classical highly variable antigenic sites, six different conserved antigenic sites were defined so far in the HA-head or -stalk domain of group 1 and 2 influenza A and of influenza B viruses (Figure 8C) (*207*).

1.3.3. EFFECTOR MECHANISMS OF BROADLY REACTIVE ANTIBODIES AGAINST INFLUENZA VIRUSES

Since non-RBS targeting antibodies cannot block the attachment of the virus to the host cell, they may interfere with later steps of the viral replication cycle (Figure 9). As described in section 1.1.3, the HA-stalk domain plays an important role during fusion of the viral and endosomal membranes (Figure 5). In fact, antibodies were identified that interfere with this step by blocking the conformational changes of HA during acidification of the endosome (*200, 203, 208*) (Figure 9 B). HA-stalk antibodies, furthermore, interfere with budding and egress of the virus or maturation of HA (*209, 210*) (Figure 9, C and D). Intriguingly, even sterical inhibition of NA activity by an HA-stalk binding antibody was described (*211*).

Aside from direct inhibition of steps in the replication cycle, the viral particle can be lysed by the complement system, which is potently activated by HA-stalk antibodies (*94, 212*) (Figure 9F). Interestingly, also FcγR-mediated effector mechanisms such as ADCC seem to be of major importance for non-RBS binding antibody-mediated protection (*95, 96, 136*) (Figure 9E, see 1.2.3). Broadly-reactive ADCC-activating antibodies against H7N9 and H5N1 subtype viruses were found in individuals who were not exposed to these viruses before (*213*). The absence of neutralizing antibodies against these novel viruses indicates that the ADCC-activating antibodies are not directed against the RBS (*213*). Likewise, broadly protective, but non-neutralizing antibodies against (H1N1)pdm were found before the first pandemic wave in 2009 in children, who were not exposed to the same or structurally related H1N1 viruses before (*214*). ADCC-activating antibody titers were shown to rise with age, likely due to repeated influenza infection or vaccination (*213, 215*). However, in non-human primates vaccination with human TIV did not prime ADCC-activating antibodies, while infection with H1N1 or H3N2 virus did (*216*). Nevertheless, pre-existing ADCC-activating antibody titers could be boosted in humans by inactivated vaccine, indicating that efficient priming (e.g. by natural infection or LAIV immunization) of an ADCC-activating antibody response is imperative (*217-221*).

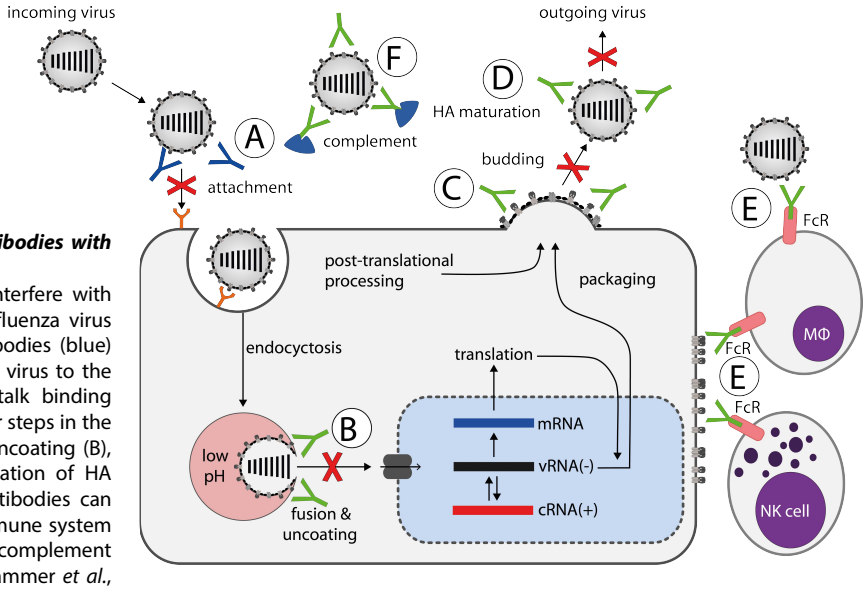

Figure 9: Interference of antibodies with the influenza virus life cycle
Antibodies against HA can interfere with different steps during the influenza virus life cycle. Head binding antibodies (blue) can inhibit attachment of the virus to the host cell receptor (A). HA-stalk binding antibodies (green) inhibit later steps in the replication cycle like fusion/uncoating (B), budding/egress (C) or maturation of HA (D). Additionally, HA-stalk antibodies can activate other cells of the immune system by FcR interactions (E) or the complement system (F). (adapted from Krammer *et al.*, Curr Opin Virol (2013))

The protective potency of ADCC-activating monoclonal HA-stalk antibodies was proven *in vivo* employing FcγR-KO mice or antibody variants no longer able to activate FcγR (*222-225*). Effector functions of neutrophils and alveolar macrophages seem to be critical in this regard (*95, 96*). While initially it was apparent that only HA-stalk antibodies mediate FcγR activation, it is now evident that any broadly reactive non-RBS binding antibody can elicit FcγR activity (*222, 223*). Intriguingly, this holds also true for broadly reactive antibodies against NA (*223*). Furthermore, intrinsically poorly FcγR-activating NA-inhibiting (NAI^{pos}) antibodies can co-operate with HA-specific antibodies and enhance their FcγR-activation potency (*226*). On the contrary, HAI^{pos}-antibodies which bind to the sialic acid binding pocket in the RBS are no potent inducers of FcγR activity (*227*). In fact, it was demonstrated that HAI^{pos} antibodies can inhibit FcγR-activation by HA-stalk antibodies although they do not prevent their binding to the HA-stalk (*226*). Therefore, in addition to Fc-FcγR interaction, also the accessibility and functionality of the sialic acid binding pocket in the RBS is necessary for activation of FcγR-mediated effector functions (*224, 227-229*). A model is proposed, according to which two concomitant interactions are required to potently activate effector functions: i) interaction of HAI^{neg} antibodies with FcγR and ii) interaction of the RBS with sialic acid on the immune cell (*227*). However, it is unclear whether the RBS-sialic acid interaction only stabilizes the HA or acts as a co-receptor (*136*). Recent finding of an exceptional influenza B HA antibody which can block receptor attachment (HAI^{pos}) and mediated ADCC indicate that more research is needed to define the ultimate requirements for HA-specific FcγR-activating antibodies (*230, 231*).

Moreover, FcγR-activating antibodies against the internal proteins NP and M1 were readily found in humans and also could mediate protection after passive transfer in mice (*143, 232, 233*). Although the presence of NP and M1 on the surface of infected cells was described, further investigation on their *in vivo* significance and contribution to protection of ADCC-activating antibodies against internal influenza virus proteins seems to be necessary (*114, 234*).

In a pig vaccination model antibody-dependent enhancement of disease (ADE) associated with HA-stalk antibodies was described (*235*). Here, HA-stalk antibodies potentially cross-linked the viral fusion peptide with the cellular membrane and rather promoted infection then prevented it. Other studies in pigs linked ADE to intradermal delivery only while vaccination of mice would not induce ADE antibodies (*236, 237*). Furthermore, non-neutralizing but FcγR-activating antibodies occasional can enhance disease by increasing uptake and replication of virus in FcγR-expressing cells (e.g. macrophages) (*127*). This has also been shown for influenza viruses (*238, 239*). Also, pathologic deposition of immune complexes in the tissue can result in increased FcγR-mediated cytotoxicity and inflammation (*127*). Though the exact reason for ADE might not be well understood, the phenomenon must be carefully considered when designing a vaccine which particularly aims at the induction of non-neutralizing antibodies.

Although functionally constrained, epitopes in the HA-stalk are under selective pressure as well, and immune escape virus mutants can arise (*240, 241*). Interestingly, viruses seem to escape either via complete abolishment of antibody binding or by increase of the fusion activity of the

HA, allowing fusion even in the presence of the antibody (*240*). However, immune escape is associated with a loss of viral fitness (*240*).

1.3.4. HA-STALK ANTIBODIES ARE RARELY INDUCED IN NATURE

Most HA-stalk antibodies show a similar mode of binding as they use hydrophobic residues of their CDR_H to contact a highly conserved pocket within the HA-stalk (*124, 196*) (Figure 6, Figure 8). Some antibodies quiet untypically use solely their heavy chain to interact with HA (*201, 242*). A great number of HA-stalk antibodies employs the VH1-69 antibody germline gene locus (*243, 244*). However, non-VH1-69 HA-stalk antibodies have been described which sometimes emulate the binding modalities of VH1-69 (*196, 201, 245*). VH1-69 codes for important hydrophobic anchor residues at the apices of the CDR_H loops that directly contact the HA-stalk (*124, 246*). A genetic polymorphism in humans at these positions can diminish the HA-stalk antibody response (*247*). The development of high-affinity VH1-69 HA-stalk antibodies does apparently not rely on the extensive acquisition of somatic mutations, indicating their general potential to rapidly be induced (*121, 246*). However, HA-stalk antibodies are rare in the human population (*248*). The impaired induction of HA-stalk antibodies by natural infection or seasonal vaccination could be explained by the immunodominance of epitopes in the HA-head. According to Angeletti and Yewdell, factors mainly influencing antibody immunodominance include antigen quantity and accessibility, the frequency and affinity of B-cell precursors, T-cell help, and the immunization conditions, besides minor factors including genetic background, age, and environment (*249*). In fact, poor accessibility of stalk epitopes by BCR was shown to occasionally occur and result in a HA-head-biased response (*250, 251*). Also, the above mentioned restricted VH-germline gene usage and increased poly-/auto-reactivity (e.g. DNA cross-reactivity) of stalk-reactive B-cells can further result in a reduced number of available HA-stalk specific naïve B-cells (*244, 252*). Interestingly, the form of antigen and route of administration also was shown to critically influence the immunodominance hierarchy, whereas intranasal infection with an active virus mounted antibodies covering more antigenic sites on HA as compared to intramuscular or intraperitoneal administration of inactivated virus (*253*).

Nevertheless, antibodies against conserved epitopes within HA are able to broadly protect humans against influenza (*254*). In fact, the extinction of the seasonal H1N1 strain circulating before 2009 was attributed to an increase of HA-stalk antibodies following infection or vaccination with the 2009 pandemic influenza virus, which was also supported in a mouse model (*243, 255, 256*). Li *et al.* describe a model, in which broadly reactive but otherwise immunosubdominant memory B-cells against conserved epitopes in HA become predominantly reactivated during infection with a divergent influenza strain due to the lack of memory B-cells against the divergent HA-head (*257*). This phenomenon, a specific case of original antigenic sin, might generally be responsible for the extinction of seasonal viruses by an emerging pandemic strain (*258, 259*). Indeed, during a period of only minor antigenic drift, i.e. when HA-head domains of circulating viruses were closely related to each other, substantial increase over time could only by detected for antibodies against the immunodominant HA-head, while HA-stalk antibody levels increased only modestly (*260*). Stronger induction of HA-stalk antibodies was

seen, however, in individuals being seropositive for more divergent influenza virus subtypes harboring more variable HA-head domains (*260*). Similarly, the induction of HA-stalk antibodies by a (H1N1)pdm vaccine was impaired in presence of pre-existing HA-head specific antibodies against the pandemic virus (*252*). Not only antigenic shift but also periods of marked antigenic drift can lead to an increase of HA-stalk antibodies and older people who have longer histories of exposure to divergent influenza viruses also tend to have higher levels of HA-stalk antibodies (*261-263*). Interestingly, also the extent polyclonality and isotype distribution of the HA-stalk antibody response seems to influence the potency of protection (*264*).

Although induction of HA-stalk antibodies seems to be more frequent after natural infection, also their induction after vaccination was described (*250, 265-269*). However, due to immunodominance of epitopes in the HA-head, efficient induction of HA-stalk antibodies by vaccination requires development of innovative antigens and delivery concepts.

1.3.5. VACCINE CONCEPTS TO INDUCE BROADLY REACTIVE ANTIBODIES AGAINST HA

Several antigen concepts were described in the literature that aim at the induction of antibodies against conserved regions in the HA, such as the stalk domain. These include i) sequential vaccination with diverse antigens, ii) vaccination with minimal antigens, iii) vaccination with consensus antigens and iv) vaccination with glycan-modified antigens (*259*).

i) Diverse antigens: Chimeric HA (cHA) contain the stalk domain of one influenza virus subtype but the head domain of other exotic subtypes (e.g. H1 stalk and H13 head), which are currently not circulating in humans, and are thus expected to lack pre-existing immunity in the population (*270, 271*) (Figure 10). Hence, vaccination with cHA resembles the immunologic phenomenon described above (see 1.3.4): after repetitive exposure to different cHA which all contain an identical HA-stalk, the immune response towards broadly reactive epitopes is boosted. The immune response against variable epitopes in the divergent exotic HA-heads is inferior because it would have to be induced *de novo* against each cHA *(272)*. cHA were used to induce broadly protective HA-stalk reactive antibodies in mice and ferrets (*273-281*) (Figure 10). Furthermore, a formulation of inactivated split influenza virus carrying a cHA on its surface is evaluated in a phase I/II clinical trial underlining the potential of the approach (*282*).

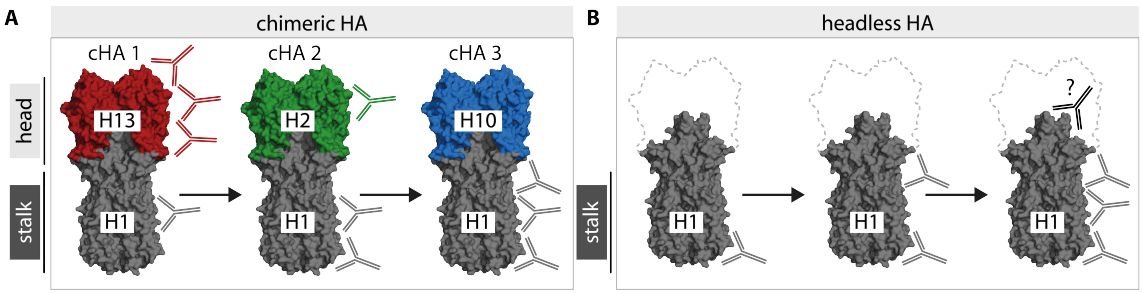

Figure 10: Chimeric and headless HA can be used to boost HA-stalk reactive antibodies
(A) Sequential immunization with chimeric HA (cHA) that contain the identical stalk domain (e.g. H1) but exotic head domains (e.g. H13, H2 or H10) induces re-focussing of the immune response from dominant head epitopes (red) to conserved stalk epitopes (grey). **(B)** Headless-HA lack dominant epitopes in the head completely and therefore induce antibodies to conserved stalk epitopes (grey). Antibodies against regions not exposed in the wildtype HA (black) might also be induced. (adapted from Krammer, Curr Opin Virol (2016))

ii) Minimal antigens: Minimal antigens represent either epitopes, structural features (e.g. long α-helix) or specific domains of HA (e.g. stalk) which lack unwanted epitopes (e.g. in the head) (*259*). Although strategies using epitopes coupled to immunogenic carrier particles and the display of HA-stalk epitopes embedded in the HA-head were evaluated, the majority of research focusses on so called headless HA (*283, 284*). Headless HA completely lack the HA-head domain due to deletion of the respective region in the open reading frame of HA (*285*) (Figure 10). As mentioned above, most HA-stalk antibodies recognize conformational epitopes (*196*). Since the HA-stalk is metastable, removal of the complete head can readily lead to misfolding into undesired antigenic conformation, i.e. the post fusion conformation (Figure 5) (*286*). This is, however, not the case for most cHA, where the exotic head seems to stabilize the HA-stalk conformation (*271*). In fact, early headless HA versions, in which the HA-head was substituted with a short linker did not display the correct conformation of the stalk as evidenced by the lack of binding of well characterized conformational HA-stalk antibodies (*287-289*). Nevertheless, broadened protection in mice and rabbits was achieved. To improve antigenicity, more recent headless HA versions contained additional mutations to stabilize the neutral pH conformation of the HA-stalk, including removal of newly generated hydrophobic surfaces as well as removal of the HA cleavage site or alterations of disulfide bonds (*290-293*). Moreover, the addition of trimerization motifs to the membrane proximal part of the headless HA resulted in a significantly improved conformation and antigenicity (*236, 289, 294-296*). Recently, two very advanced headless HA have been reported by Yassine *et al.* and Impagliazzo *et al.*, in which the membrane distal end was stabilized as well and/or the headless HA was fused to a carrier particle (*297, 298*). Exceptional broad protection was demonstrated in mice, ferrets and non-human primates and was associated with a rise in ADCC-activating antibody titers (*297, 298*). Although recent headless HA seem to have overcome issues regarding the HA-stalk conformation, the addition of heterologous stabilizing elements (trimerization motifs, carrier particles) may result in a skewed immune response towards these highly immunogenic elements (*285*).

iii) Optimized/centralized antigens: Broad protection in several animal models including mice and ferrets could be induced with consensus or computationally optimized broadly reactive (e.g. COBRA) HA antigens containing at each position the most prevalent, i.e. conserved, amino acid (*299, 300*). Also, ancestral HA sequences can be used to induce broadly protective antibodies (*301*). Furthermore, conserved epitopes of different HA variants can be combined in one construct (mosaic antigen) (*302, 303*).

iv) Glycan-modified antigens: Influenza viruses use the addition or removal of surface glycans to escape the immune response (*304*). However, this can be harnessed to modulate and broaden the immune response by unmasking otherwise hidden epitopes (*259*). Two strategies were successfully used to induce broadly protective antibodies against the HA-stalk: i) removal of glycans on the HA-stalk that interfere with recognition of these moderately immunogenic epitopes or ii) addition of glycans to the HA-head to shield the immunodominant epitopes (*304-306*).

1.3.6. OTHER ANTIGENS TO INDUCE BROAD PROTECTION AGAINST INFLUENZA

Aside from HA, research on universal influenza vaccines mainly focusses on the target antigens NP, the highly conserved extracellular domain of M2 (M2e), and to a lower extent also M1, while recently NA was described as highly promising broadly reactive antigen candidate (*307, 308*). While M2e and NA vaccine candidates aim at the induction of an antibody response, NP and M1 mainly focus on eliciting a strong cellular immune response (*309*). Vaccination with complete proteins, as well as T-cell and B-cell epitope vaccines are under evaluation in a multitude of studies. Furthermore, some concepts include linking of the antigen to an immune stimulatory carrier such as bacterial or viral subunits (cholera toxin subunit A, Hepatitis B virus core protein), or receptors and agonist of the host immune system (TLR5, CD11c), or virus like particles (*237, 310, 311*). The feasibility of new production methods, e.g. in plants, and new adjuvants is tested (*182, 312*). Additionally, innovative delivery platforms such DNA and RNA vaccines and viral vectors are under intensive investigation (*307, 313, 314*).

1.3.7. VIRAL VECTORS AS CARRIERS FOR INFLUENZA VACCINES

The use of viral vectors as carriers for influenza vaccines is appealing, since they offer possible solutions to some of the problems associated with the vaccine manufacturing cycle as discussed in section 1.3.1. For example, it is possible with viral vectors to express genes *in vivo* without the need for production and purification of antigen in chicken eggs. Moreover, antigens are expressed *in situ* in their desired conformation. Comparable to the antigen expression during natural infection, vectored antigens are subjected to cognate antigen processing pathways, which is likely positively modulating the immune response (*313*). Hence, different vectors (Poxvirus, Alphavirus, Herpesvirus, Vesicular stomatitis virus (VSV), Newcastle disease virus, Baculovirus, Parainfluenza virus, Adenovirus (AdV), Adeno-associated virus) were tested for the induction of strain-specific or broadly protective immunity with different native (HA, NA, NP, M1, M2, PB2) and modified antigens (HA-stalk, M2e) in several animal species including mice, ferrets, pigs and non-human primates, as well as avian species (*313*). Intriguingly, cHA immunization also induced protective HA-stalk antibodies in a virus vectored vaccine approach in mice and ferrets, albeit the immunization regimen required change of the vectors (VSV pseudotypes to AdV to influenza B virus) (*276, 278, 279*). Modified vaccine virus Ankara (MVA) virus vectors which express a headless HA alone or in combination with other antigens (NP, M2e) were used as well (*315*). Interestingly, MVA-vectored headless HA only afforded protection when it was co-expressed together with NP, indicating some limitations to a virus vectored headless HA approach (*315*). Nevertheless, production of high amount of virus vectors according to good manufacturing production criteria is still costly (*316*). Also, inherent pathogenicity of some virus vectors raises concerns regarding their safety in humans (*317, 318*). Pre-existing immunity in humans against viral vectors poses a challenge to development of a virus vector vaccine (*319-321*). Thus, the choice of the right viral vector system might be critical for the success of an influenza vaccine approach. Adeno-associated virus vectors seem to be well suited for this purpose.

1.4. AAV-VECTORS

Adeno-associated viruses (AAV) where identified as contamination in an Adenovirus preparation in 1965 (*322*). Belonging to the family of *Parvoviridae*, AAV is a non-enveloped virus with icosahedral capsid symmetry (ca. 20 nm in diameter) (*323*). The encapsidated single stranded DNA genome is about 4.7 kb in length and either of negative or positive polarity. The genome is flanked by non-coding *cis*-active sequences, the inverted terminal repeats (ITR), which have important functions during replication and potential integration of the genome (*324*) (Figure 11). Two open reading frames (*rep* and *cap*) code for seven major proteins: Rep78, Rep68, Rep52 and Rep40 are important factors for replication and integration of the genome, while capsid proteins VP1, VP2 and VP3 are structural parts of the virion. The expression of these proteins is initiated from three different promotors (p5, p19 and p40) (*324*). Additionally, mRNA splicing and also antisense transcription and translation can increase the coding capacity, and further accessory proteins were described to play a role during AAV life cycle (*324, 325*). As members of the genus *Dependovirus*, AAV relies on co-infection with helper viruses such as Adenovirus or Herpes Simplex virus for efficient replication (*326*). Also, Hepatitis B virus and Bocavirus 1 can act as helper viruses underlining that a multitude of viral and host factors are being exploited by AAV, including proteins and RNA, but that the minimum which is absolutely required may still yet be ill-defined (*327, 328*).

Vectors based on AAV are 'gutless', meaning they completely lack viral genes and only contain the ITR between which the transgene and regulatory elements for its expression are placed (*326*) (Figure 11B). *Rep* and *Cap* genes as well as helper genes required for production of AAV-vector particles have to be provided in *trans (329)*. AAV-vectors, thus, can be produced from a three-plasmid system (transgene / AAV genes / helper genes) without contaminations of wildtype AAV and helper viruses. Interestingly, AAV-vector genomes (containing AAV2 ITR) can be transencapsidated in heterologous capsids of various subtypes with e.g. other tissue specificities (*330*).

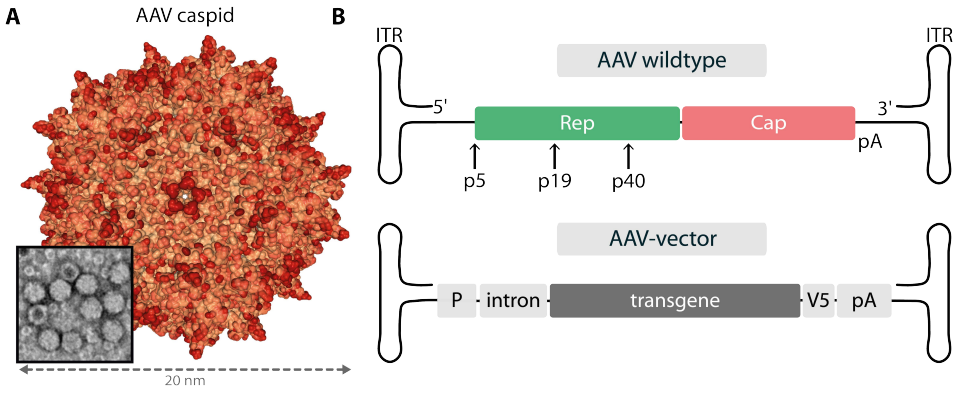

Figure 11: Capsid and genome structure of AAV
(A) 3D structure model of an AAV capsid (PDB: 1LP3, color-gradient: b-factor) with inset showing negative stain electron microscopic picture of purified AAV capsids. **(B)** schematic drawing of a wildtype AAV genome (top) with inverted terminal repeats (ITR), Rep and Cap genes and position of promotors (p5, p19, p40). The AAV-vector (bottom) completely lacks rep and cap genes but contains an expression cassette comprised of a promotor (P), an irrelevant intron, the transgene, a V5-tag and a polyadenylation/termination signal (pA).

AAV genomes persist predominantly as episomal circular concatemers (*331*). Impressively, expression is extremely durable (1 year and longer) and persisting genomes are apparently neither cleared from the cells nor epigenetically silenced (*332, 333*). Most likely signals or higher order structures in the ITR regulate persistence of AAV-vectors (*325*). Furthermore, integration was described for AAV with an integration hotspot being the chromosomal region 19q13.4. This is due to the presence of an AAV Rep protein binding element in this region, which eventually leads to recruitment of the host non-homologous recombination machinery in a Rep-dependent manner (*334, 335*). Along the same lines, Nault *et al.* reported that AAV integration caused hepatic cell carcinoma in humans (*336*). However, the conclusions drawn by Nault *et al.* were argued by other groups, thus, the true impact of AAV-associated oncogenicity remains elusive (*318, 337*). In fact, also protection from cervical cancer in AAV infected women was demonstrated (*338*). Since AAV-vectors completely lack *rep* gene integration is extremely unlikely (*339*) (Figure 11). Also, toxicity was seen only after administration of high vector doses or with specific cell lines (embryonic stem cells) (*340, 341*). The licensure of AAV-vectors for gene therapy for the treatment of familial lipoprotein lipase deficiency (alipogene tiparvovec (Glybera®)) and retinitis pigmentosa (voretigene neparvovec (Luxturna®)) in the EU and the USA and its use in over a hundred clinical trials definitely underlines their safety (*324, 342, 343*).

AAV genomes were extracted from the epithelia of the respiratory tract, tonsils and adenoids after co-infection with an AdV but also from other human tissue like muscle, spleen, blood and the urogenital tract of women (*325*). Interestingly, human leucocytes were found recently to be positive for AAV at high frequencies indicating that these cells may be a natural reservoir (*344*). Many different AAV serotypes have been isolated from human tissues and from tissues of other animal species, including primates but also snakes (*321*). Serotypes vary regarding their capsid identity between 99 % and 50 % while the most widely used serotypes in clinical studies are human origin AAV2, AAV1, AAV6, AAV8 and rhesus origin AAVrh.10 (*324*). AAV serotypes show specific tissue tropisms, thus, allowing specific targeting of transgene expression to the desired site of the body by selection of a distinct capsid (*345*). These differences are likely due to differential receptors usage of each serotype (*345*). Hence, attachment of AAV serotypes to a variety of specific glycan and/or protein receptors was shown (*346*). Recently, a putatively universal AAV receptor (AAVR) was identified, which seems to be essential for most, including AAV2 and AAV9, but not all AAV serotypes (*347-349*). After attachment, capsids are endocytosed in a clathrin-dependent or independent manner and trafficked retrograde to the Golgi apparatus (*350-352*). AAV capsids eventually escape into cytoplasm and accumulate perinuclear before they are imported into the nucleus by host importins, and the genome is uncoated (*353-355*). Replication takes place in dedicated foci within the nucleus where the second strand of the genome is complemented mediated by Rep proteins and host DNA repair machinery (*356, 357*). As mentioned above, genomes either persist in a concatemerized form (without helper functions) or progeny virus is produced (in presence of helper functions) (*324*). Capsid assembly takes place within the nucleus, where also progeny genomes are packed (*358*).

Initial infection with AAV occurs very early in life. Neutralizing antibodies against multiple serotypes can be found in humans, indicating the great extent of cross-reactivity of these antibodies (*359*). However, the prevalence varies for each AAV serotype: AAV2 has the highest prevalence (30-60 %) of neutralizing antibodies while other serotypes, including AAV9, show only moderate prevalence (15-30 %). Neutralizing and total antibodies correlate, thus, 70 % and 45 % humans are sero-positive for AAV2 and AAV9, respectively (*319, 359*). AAV-specific T-cells can be found from an early age on but their prevalence is lower compared to AAV antibodies. Cellular and humoral responses do not correlate. However, T-cells also show extended cross-reactivity. Most prevalent T-cells display a memory phenotype and exert cytotoxic effector functions upon activation (*359*). To circumvent immune responses against AAV and to prevent neutralization of the vector, different strategies are being evaluated: isolation of new (non-human) serotypes, modification of existing capsids and creation of new capsids by directed evolution. Furthermore, improvement of the production methods to yield highly pure virus vector stocks which can be administered in lower doses (*326, 359*). In addition, transgene production can be optimized with self-complementary AAV-vectors which package genomes containing both DNA strands and, thus, do not require the rate limiting step of second DNA strand synthesis (*360*).

Intriguingly, AAV-vectors were also used to actively or passively immunize against several viral pathogens including human immunodeficiency virus, human papillomavirus virus, respiratory syncytial virus, severe acute respiratory syndrome coronavirus, and influenza virus (*361*).

1.4.1. AAV-VECTORS FOR INFLUENZA VACCINATION

AAV-vectors were used as vehicles for influenza vaccines in very few studies either as active immunization (serotypes AAV2, AAV8, AAV rh32.33 or AAV9, expressing HA, NP and M1) (*362-364*) or passive immunization (serotypes AAV8 and AAV9, expressing HA-specific antibodies) (*365-367*). Interestingly, in the passive immunization studies broad protection was achieved with AAV-vectors expressing three HA-stalk binding antibodies, namely F10, CR6261, FI6, in young, aged and immunodeficient mice, as well as ferrets (*365-368*). AAV-vectors seem to be particularly suited for such passive immunization approaches due to the durable expression of the respective antibody (*361*).

The first study describing an active AAV-vectored influenza vaccine was published in 2001 (*364*). Xin *et al.* focused on the development of AAV-vectors as carrier for an HIV vaccine. The authors, however, also intranasally immunized mice with an AAV2-vector expressing the HA of A/Puerto Rico/8/1934(H1N1) (PR8) with or without simultaneous immunization with AAV-IL2. This was done to proof that an AAV-vector vaccine was not only immunogenic against HIV, but also induced protective immunity, which was shown in a lethal influenza mouse model. Mice were partially but significantly protected from homologous influenza virus challenge and AAV-IL2 further adjuvanted the protective effect which was attributed to an enhancement of cell mediated immunity (*364*). Furthermore, in another study Lin *et al.* transferred pooled human serum into mice before intramuscular immunization with AAVrh32.22 or AAV8 expressing PR8 NP. This experiment was intended to analyze pre-existing immunity in humans against AAVrh32.22, a new

rhesus monkey AAV-vector serotype (*363*). AAVrh32.22-NP immunized mice were completely and AAV8-NP immunized mice partially protected against homologous influenza challenge, which on the one hand proved that human serum does not interfere with AAVrh32.22 but with AAV8, and on the other hand represented the first report on an successful AAV-vectored influenza vaccine against the internal NP protein (*363*).

More recently, Sipo *et al.* used AAV2/9-vectors (AAV2 ITR and AAV9 capsid) which expressed codon-optimized A/Mexico/4603/2009 (H1N1)pdm HA, NP and M1 proteins (*362*). AAV9, which was used in the aforementioned study, has some remarkable features making it particularly suited to serve as a vaccine vector against respiratory diseases. The AAV9 capsid coding sequence was isolated and reconstructed from human tissue (*321*). As for most AAV serotypes, AAV9 sero-prevalence is quite high in humans (about 45 %) (*319*). However, neutralizing factors not only show lower prevalence (about 30 %) but 70 % of the tested individuals present low (1:20) AAV9 neutralizing antibody titers (*319*). Therefore, AAV9 might have an advantage for use in humans in the context of pre-existing immunity over other AAV serotypes (*319*). AAV9 was shown to target alveolar epithelial cells *in vivo* where it stably expressed transgene over month (*369-371*). Most importantly, AAV9 was re-administrable into the respiratory tract of mice due to the lack of neutralizing antibodies in bronchoalveolar lavage fluid even in the presence of neutralizing serum antibodies (*369*). Sipo *et al.* reported the induction of T-cell as well as antibody responses against all antigens after intramuscular immunization with a combination of AAV-HA/AAV-NP/AAV-M1, with the strongest T-cell and antibody response against NP or HA, respectively (*362*). As expected, no neutralizing antibodies were detected against the heterologous PR8. For homologous (H1N1)pdm challenge, mice were vaccinated with each AAV-vector alone or with the trivalent combination. Interestingly, AAV-HA as well as AAV-H1/AAV-NP/AAV-M1 induced sterile immunity resulting in complete protection without weight loss of the animals (*362*). AAV-NP also completely protected animals, which was most likely mediated by strong cell-mediated immunity. However, these animals did show signs of disease due to the lack of neutralizing antibodies. AAV-M1 alone was not able to protect the mice (*362*). Intriguingly, AAV-HA/AAV-NP/AAV-M1 also partially protected animals from challenge with the heterologous PR8 which was associated with slightly reduced lung virus loads. The authors concluded that heterologous protection is mediated by broadly reactive cell-mediated NP-specific immunity in absence of cross-neutralizing HA-specific antibodies against PR8 (*362*). However, in a follow up study cross-protection against PR8 after intramuscular immunization with an AAV9-vector expressing A/California/7/09(H1N1pdm) (Cal/7/9) NP was only seen after introduction of the major CTL epitope ($NP_{366-374}$) of PR8 into the NP of Cal/7/9 (*371*). Also, immunization with an AAV-vector expressing an epitope chain comprised of the major CTL epitope of most influenza A virus NP proteins induced a non-functional T-cell response which failed to protect animals (*371*). These somehow contradictory findings indicate that further evaluation of the contribution of cell-mediated and humoral immunity to heterologous protection with an AAV-vectored vaccine against influenza is necessary. However, they also underline the

enormous potential of AAV9-vectors for the use as vehicles for broadly protective influenza vaccines.

1.5. AIM OF STUDY

The current seasonal influenza vaccine has unsatisfactory low overall effectiveness especially in the population being at high risk for influenza-associated complications (*183*). Moreover, protection is virus strain specific and, thus, the vaccine has little to no effectiveness against non-vaccine strains, i.e. drifted seasonal and emerging pandemic or zoonotic strains. Hence, a more effective and broadly reactive vaccine is highly desirable in view of improvement of public health (*190, 191*).

Recently, antigens have been described, which in contrast to the current vaccine aim at the induction of immunity (humoral and/or cellular) against conserved regions in influenza virus antigens, including for instance the HA-stalk domain (*272*). Furthermore, research and development of innovative vaccine delivery platforms such as AAV-vectors is considered important (*190, 191*). These cannot only help to overcome challenges associated with the vaccine manufacturing cycle, but also directly influence the immune response and enhance immunogenicity of the antigen (*314*).

The aim of this thesis was to evaluate the feasibility of AAV-vectors as broadly reactive influenza vaccine carriers and identify immunization regimens, i.e. antigens or combinations thereof, which would induce broad protection against challenge infection. Therefore, breadth and quality of the humoral immune response after vaccination of mice with AAV-vectors expressing either wildtype influenza antigens (HA, NP) or antigens particularly aiming at the induction of antibodies against the HA-stalk (chimeric HA, headless HA) was assessed. Thereupon it was evaluated, whether one of the measured immunological parameters, such as neutralizing antibodies or FcγR-activating antibodies, could be correlated with protection of mice against homologous or heterologous influenza virus challenge. Finally, the protective effect against homologous viral challenge was investigated for the first time in ferrets, which represent the gold-standard animal model for influenza in humans. A detailed knowledge of the effects of the AAV-vector on the immunogenicity of influenza virus antigens and their protective efficacy will likely facilitate the progression to clinical evaluation of AAV-vectors as carriers for a broadly-reactive influenza vaccine as characterized herein.

2. MATERIALS

Animals:	
Mice: C57BL/6NCrl	Charles River (Sulzfeld, Germany)
Ferrets *Mustela putorius furo*	EuroFerret (Denmark)

Immortalized cell lines:	
HEK 293T	*Homo sapiens* embryonic kidney cells, epithelial, adherent, DMEM
MDCKII	*Canis familiaris* kidney cells, epithelial-like, adherent, MEM
BW5147 (& derivates)	*Mus musculus* thymus cells, T-cell, suspension, R10

Chemo-competent bacteria:	
Escherichia coli (DH5α™) subcloning efficiency (genotype: F- φf80lacZΔM15 Δ(lacZYA-argF) U169 recA1 endA1 hsdR17(rk-, mk+) phoA supE44 thi-1 gyrA96 relA1 λ-)	2xYT medium, Thermo Fisher Scientific Inc. (Waltham, USA)

Influenza A viruses:	
A/California/7/2009 (H1N1)pdm	**Mouse infections:** NIBSC ref. 39570, $10^{7.6}$TCID$_{50}$/ml, NYMC X-181 (hyH1N1sw); 5:3 reassortant: HA, NA, PB1 of Cal/7/9 (H1N1)pdm in the background of A/PR/8/34 (H1N1) **All others:** virus grown on embryonated chicken eggs and purified by ultracentrifugation, source: National reference center (NRC) at RKI
A/California/7/2009 (H1N1)pdm whole inactivated virus (WIV)	inactivated and purified X-181 (H1N1)pdm virus (charge BII/1/15), source: NIBSC
A/Mexico/InDRE4487/2009(H1N1)pdm	**Ferret Infections:** 10^5 TCID$_{50}$/ml, source: PEI
A/Puerto Rico/8/1934 (H1N1)	**Mouse infections:** NIBSC ref. 39560; $10^{9.1}$TCID$_{50}$/ml **All others:** virus grown on embryonated chicken eggs and purified by ultracentrifugation, source: FG17 (RKI)
A/Puerto Rico/8/1934 (H1N1) WIV	inactivated and purified A/PR/8/34 (H1N1) virus (charge BII/19/14), source: NIBSC

Influenza A viruses:	
HA/NA-1918 x WSN/1933 (H1N1)	6:2 reassortant: HA and NA of A/Brevik Mission/1/1918 (H1N1) in the background of A/WSN/1933 (H1N1), source: FG17 (BSL3) (RKI)
A/Widgeon/Denmark/66174/G18/2004 (H2N3)	Source: NRC at RKI
X31 (H3N2)	6:2 reassortant: HA and NA of A/Aichi/2/1968 (H3N2) in the background of A/PR/8/34 (H1N1) **Mouse infections:** NIBSC ref. 39600; $10^{9.3}TCID_{50}$/ml **All others:** virus grown on embryonated chicken eggs and purified by ultracentrifugation, source: FG17 (RKI)
X31 (H3N2) WIV	inactivated and purified X-31 (H3N2) virus (charge BII/21/14), source: NIBSC
A/Panama/2007/1999 (H3N2)	virus grown on embryonated chicken eggs and purified by ultracentrifugation, source: FG17 (RKI)
A/Viet Nam/1203/2004 (H5N1)	virus grown on embryonated chicken eggs and purified by ultracentrifugation, source: FG17 (BSL3) (RKI)
A/Anhui/1/2013 (H7N9)	virus grown on embryonated chicken eggs and purified by ultracentrifugation, source: FG17 (BSL3) (RKI)
A/Mallard/Nordvorpommern/Wv9417/2004 (H10N7)	virus grown on embryonated chicken eggs and purified by ultracentrifugation, source: NRC at RKI
A/Gull/Maryland/707/1977 (H13N6)	virus grown on embryonated chicken eggs and purified by ultracentrifugation, source: FG17 (RKI)

Plasmids (not constructed during this work):		
pAAV-MCS	empty AAV-vector	Agilent Technologies (Santa Clara, USA)
pHelper	Helper plasmid expressing Adenovirus E2A, E4, VA genes	

Plasmids (not constructed during this work):		
p5E18-VD2/9	Helper plasmid expressing AAV2 rep and AAV9 cap gene	Isaac Sipo (FG18, RKI Berlin, (*362*))
pAAV-HA	HA of Cal/7/9 (H1N1)pdm, codon opt. for *mus musculus*	
pAAV-NP	NP of Cal/7/9 (H1N1)pdm, codon opt. for *mus musculus*	
pAAV-GFP	Green fluorescent protein of Renilla reniformis, humanized	

Primers and probes:	
AAV insert sequencing fw	5'-CCACCAGACATAATAGCG-3'
AAV insert sequencing ref (=Sp6 promoter 3' primer)	5'-ATTTAGGTGACACTATAG-3'
AAV qPCR (CMV promoter) fw	5'-TGGAGTTCCGCGTTACATAACTTAC-3'
AAV qPCR (CMV promoter) rev	5'-CTATTGGCGTTACTATGGGAACATAC-3'
AAV Probe (CMV promoter)	5'-FAM-CCTGGCTGACCGCCCAACGAC-BBQ-3'

Enzymes:	
Fast AP Thermosensitive Alkaline Phosphatase 1 U/µl	Thermo Fisher Scientific Inc. (Waltham, USA)
FastDigest® *BamHI*	
FastDigest® *Bsu36I*	
FastDigest® *HindIII*	
FastDigest® *HpaI*	
FastDigest® *SmaI*	
Pierce® Universal Nuclease for cell lysis (Benzonase) 250 U/µl	
T4 DNA Ligase 5 U/µl	

Commercial antibodies:	
ADK9	Anti-AAV9 (intact particle) Origin: mouse (monoclonal: ADK9, IgA) Progen (Heidelberg, Germany)
Anti-FluA virion	Anti-influenza A virion Antigen: 'strain USSR (H1N1)' Origin: goat 5315-0064 Bio-Rad (Hercules, USA)
anti-GAPDH	Anti-human GAPDH Origin: rabbit Cell Signaling Technologies (Danvers, USA)

Commercial antibodies:	
anti-HA2	Anti-pdmH1N1 HA2 Origin: rabbit Biorbyt (Cambridge, UK)
Biotin-IL-2	Anti-mouse-IL2, biotinylated Origin: rat (monoclonal: JES6-5H4, IgG2b) BD Biosciences (Franklin Lakes, USA)
C179	Anti-HA-stalk domain (conformational) Antigen: A/Okuda/57 (H2N2) Origin: mouse (monoclonal: M145, IgG2a) TaKaRa Bio Inc. (Shiga, Japan)
donkey-anti-mouse IgG (H&L)-AF488 goat-anti-mouse-IgA-HRP	Thermo Fisher Scientific Inc. (Waltham, USA)
IL-2	Anti-mouse-IL2 Origin: rat (monoclonal: JES6-1A12, IgG2a) BD Biosciences (Franklin Lakes, USA)
rabbit-anti-goat (H&L)-HRP rabbit-anti-mouse (H&L)-HRP	Agilent Technologies Inc. (Santa Clara, USA)
Streptavidin-HRP	Streptavidin conjugated to HRP 016-030-084 Jackson ImmunoResearch Laboratories Inc. (West Grove, USA)
V5-Tag	Anti-V5-Tag Origin: mouse (monoclonal: SV5-Pk1, IgG2a) Bio-Rad (Hercules, USA)

Kits:	
QIAamp MinElute Virus Spin Kit QIAfilter Plasmid Maxi Kit QIAquick PCR Purification Kit	Qiagen (Hilden, Germany)
Invisorb® Spin DNA Extraction Kit Invisorb® Spin Plasmid Mini Two	Stratec Molecular GmbH (Berlin, Germany)
1-Step™ Ultra TMB-ELISA Substrate Solution Pierce® BCA protein assay kit Platinum® *Taq* DNA Polymerase SuperSignal™ West Dura Extended Duration Substrate	Thermo Fisher Scientific Inc. (Waltham, USA)

Software:	
GraphPad Prism 7.03	GraphPad Software, Inc.
Adobe Photoshop CS6 v.13 extended	Adobe Systems Inc.
Chemostar Professional	Intas Science Imaging Instruments GmbH
Zen 2012 (blue/black)	Carl Zeiss Microscopy GmbH
Intas GDS	Intas Science Imaging Instruments GmbH

Software:	
Geneious 10.0.5	Biomatters Ltd.
Microsoft Office 2010	Microsoft Corporation
Adobe Illustrator CS6	Adobe Systems Inc.
Endnote X7.4	Thomson Reuters
Reader Control Software	BMG Labtech
MARS Data Analysis Software	BMG Labtech
BD Cell Quest Pro	BD Biosciences
PyMol 1.7.2.1	Schrödinger, LLC

Consumables and Equipment:	
Amicon® Ultra-15 centrifugal filter units	Merck KGaA (Darmstadt, Germany)
Flow cytometer FACSCalibur	BD Biosciences (Franklin Lakes, USA)
Optima™-L 100K ultracentrifuge with 70-Ti rotor	Beckman coulter (Brea, USA)
Quick-Seal® (1x3.5 inch) ultracentrifugation tubes	
Cell culture incubator	Binder GmbH (Tuttlingen, Germany)
Agarose gel system Mini-Sub®	BioRad (Hercules, USA)
Mini-Protean® system	
PowerPac™ 300W HC / Basic	
Trans-Blot® SD semi-dry Transfer cell	
Gel dryer Phero-Temp 40	Biotec-Fischer GmbH (Reiskirchen, Germany)
Micropipettes Research® plus	Eppendorf (Hamburg, Germany)
Thermomixer compact	
5417R cooling centrifuge	
Water bath DC10	Thermo Haake GmbH (Karlsruhe, Germany)
Intas UV transilluminator system	Intas (Göttingen, Germany)
Advanced Fluorscence and ECL Imager	
CKX41 inverse bright field microscope	Olympus (Tokio, Japan)
LightCylcer® 480 II instrument	Roche (Basel, Switzerland)
Orbital shaker Certomat® H	Sartorius Stedim Biotech (Göttingen, Germany)
Shaker Roto-Shake Genie®	Scientific Industries Inc (Bohemia, USA)
Shaker Vortex Genie® 2	

Consumables and Equipment:	
Cell culture plastic consumables	Sarstedt (Nürnbrecht, Germany) Carl Roth (Karlsruhe, Germany) GE Healthcare (Little Chalfont, UK) TTP AG (Trasadingen, Switzerland) Greiner Bio One (Solingen, Germany) Brand GmbH+KoKG(Wertheim, Germany) Thermo Fisher Scientific Inc. (Waltham, USA)
centrifuge Sorvall LYNX 4000 superspeed	Thermo Fisher Scientific Inc. (Waltham, USA)
ELISA Plates Nunc Maxisorb™	
Heraeus™ Pico™ 17 microcentrifuge	
NanoDrop™ 8000 UV/Vis Spectrophotometer	
Sterile work bench Herasafe™ KS12	

Chemicals & substances:	
Iodixanol, 60 %	Axis Shield (Oslo, Norway)
Bacto-agar Tryptone Yeast extract	BD Biosciences (Franklin Lakes, USA)
Bovine serum albumin (BSA), 30%	MP Biomedicals (Eschwege, Germany)
Midori green advanced DNA stain	Nippon Genetics Europe (Düren, Germany)
Polyethylenimine (PEI), molecular weight ca. 25 kDA	Polyscience Inc. (Hirschberg, Germany)
Chicken red blood cells	Preclinics (Potsdam, Germany)
TEMED Triton X-100	SERVA Electrophoresis GmbH (Heidelberg, Germany)
Isofluran, 1 ml/ml	CP-Pharma HandelsGmbH (Burgdorf, Germany)
Amersham™ Protran® Premium Western blotting nitrocellulose membranes Filter paper	Whatman (Maidstone, USA)
Avicel microcrystalline cellulose	FMC Corporation (Philadelphia, USA)

Chemicals & substances:	
Agarose NEEO Ultra Quality Ammoniumpersulfat (APS) Boric acid $C_6H_5O_7Na_3 \cdot 2H_2O$ DTT Ethanol, ≥99.9 % Formaldehyde, 37 % Glycerole Glycine H_2O_2, 30% H_2SO_4, 2.5 M Kanamycin KIO_4 L-Gluatmine Methanol, ≥99.9 % $MgCl_2$ Na_2CO_3 NaCl Pefabloc® SC-protease-inhibitor PFA Roti®-Blue 5x concentrate Rotiphorese® Gel 30 (37.5:1) SDS, 20 % Skimmed milk powder TRIS Tween-20 β-Mercaptoethanol	Carl Roth (Karlsruhe, Germany)
1 Kb Plus DNA Ladder 6x DNA Loading Dye DMEM KH_2PO_4 Lipofectamine™2000 MEM Na_2HPO_4 Opti®-MEM PageRuler™ Prestained Protein Ladder, 10 to 180 kDa PBS Penicillin/Streptomycin, 10 000 U/ml RPMI	Thermo Fisher Scientific Inc. (Waltham, USA)

Chemicals & substances:	
Acetone Ampicillin $C_6H_8O_7 \cdot H_2O$ $CaCl_2$ Crystal Violet DAPI DEAE-dextran EDTA Fetal bovine serum (FBS) KCl Na_3VO_4 Na-deoxycholat $NaHCO_3$ $NaHCO_3$ Phenol red Ponceau S Sodiumpyruvate, 100 mM Succrose TPCK-treated trypsin	Merck KGaA (Darmstadt, Germany)

Buffers, media and solutions:	
2xYT agar plates	1.5 % (w/v) bacto-agar 100 mg/l ampicillin in 2xYT medium
2xYT medium, pH=7.2	1.6 % (w/v) tryptone 1.0 % (w/v) yeast extract 171 mM NaCl 100 mg/l ampicillin in ddH_2O
Acetone, 80 %	(v/v) in PBS
Cell lysis buffer (RIPA)	10 mM Tris/HCl (pH=8) 150 mM NaCl 0.5 mM EDTA (pH=8) 0.1 % SDS 1 % Triton X-100 2 mM Na_3VO_4 1 mM Pefablock®
Chicken red blood cells, 1%	(v/v) in PBS
Coomassie de-staining solution	10 % (v/v) ethanol 5 % (v/v) acetic acid in ddH_2O
Coomassie fixation solution	30 % (v/v) ethanol 10 % (v/v) acetic acid in ddH_2O

Buffers, media and solutions:	
Coomassie staining solution	20 % Roti®-Blue 5x concentrate 20 % (v/v) ethanol in ddH_2O
Crystal violet solution, 1x	10 % (v/v) formaldehyde 10% (v/v) crystal violet stock solution, 10x in ddH_2O
Crystal violet stock solution, 10x	20 % (v/v) ethanol 1 % (w/v) crystal violet in ddH_2O
DEAE-dextran, 1 %	in ddH_2O
DMEM	10 % (v/v) FBS 2 mM L-glutamine 100 mg/l penicillin/streptomycin in DMEM
ELISA coating buffer, 50 mM pH=9.6	71.4 mM $NaHCO_3$ 28.6 mM Na_2CO_3 in ddH2O
L-glutamine, 200 mM	in ddH_2O
Glycerol, 1 %	(v/v) in PBS
H_2O_2, 3 %	(v/v) in PBS
KIO_4, 0.011 M	(w/v) in PBS
MEM	10 % (v/v) FBS 2 mM L-glutamine 100 mg/l penicillin/streptomycin in MEM
MEM infection	0.2 % (v/v) BSA 2 mM L-glutamine 100 mg/l penicillin/streptomycin in MEM
Na-deoxycholat, 0.5 %	(v/v) in PBS
$NaHCO_3$, 5 %	in ddH_2O
PBS	137 mM NaCl 2.7 mM KCl 80.9 mM Na_2HPO_4 1.5 mM KH_2PO_4 in ddH_2O
PBS^{++}	1 mM $MgCl_2$ 1 mM $CaCl_2$ in PBS
PBS-MK	25 mM KCl 5 mM $MgCl_2$ in PBS
$PBST^{0.05\%-0.1\%}$	0.05 – 0.1 % (v/v) Tween-20 in PBS

Buffers, media and solutions:	
Polyethylenimine (PEI) solution	2.58 g/l (w/v) in ddH_2O
pH solutions, 0.1 M pH=7.2 – 4.4/+DTT	$C_6H_8O_7 \cdot H_2O$ / $C_6H_5O_7Na_3 \cdot H_2O$ 7.0: 0 mM / 100 mM 5.8: 16.0 mM / 84.0 mM 5.4: 25.5 mM / 74.5 mM 5.0: 35.0 mM / 65.0 mM 4.4: 49.5 mM / 50.5 mM 4.4+DTT: pH=4.4 + 0.1 M DTT in ddH_2O
PFA, 4 %	in ddH_2O
Phenol red, 0.5 %	(w/v) in PBS
R10	10 % (v/v) FBS 2 mM L-glutamine 100 mg/l penicillin/streptomycin 1 mM Na-pyruvat 50 µM β-mercaptoethanol in RPMI
SDS-PAGE running buffer, 10x	250 mM Tris 1.92 M glycine 34 mM SDS
SDS-PAGE sample buffer, 6x	500 mM Tris/HCl (pH=6.8) 12 mM EDTA (pH=8) 12 % (w/v) SDS 60 % (v/v) glycerol 0.6 % (w/v) bromophenol blue 5 % (v/v) β -mercaptoethanol
Semi viscous overlay medium (Plaque assay)	0.2 % (w/v) BSA 0.05 % (w/v) $NaHCO_3$ 0.01 % (w/v) DEAE-dextran 2 mM L-glutamine 100 mg/l penicillin/streptomycin 1.25 % (w/v) Avicell 1-2 µg/ml TPCK-treated trypsin in MEM
Semidry blotting buffer	40 mM Tris 30 mM glycine 1.3 mM SDS 20 % (v/v) ethanol in ddH_2O

Buffers, media and solutions:	
SOC-medium	2.0 % (w/v) tryptone 5 % (w/v) yeast extract 10 mM NaCl 2.5 mM KCl 20 mM $MgCl_2$ in ddH_2O
Sucrose-NTE, 25 %	25 % sucrose 1 M NaCl 0.1 M Tris M EDTA (pH=8.0) in ddH_2O
Sulfuric acid, 1M	in ddH_2O
TBE buffer, 10x	0.89 M Tris 0.89 M boric acid 10 mM EDTA (pH=8.0) in ddH_2O
$TBST^{0.05\%}$	100 mM Tris/HCl (pH=8.0) 1.5 M NaCl 0.05 % (v/v) Tween-20 in ddH_2O
TPCK-treated trypsin, 1 mg/ml	in ddH_2O

3. METHODS

3.1. CELL CULTURE

Cells were maintained at 5 % CO_2 and 37°C in a humidified environment in cell line specific culture medium. In order to maintain optimal growth, adherent cell cultures were sub-cultured when they reached about 90 % confluency. Therefore, cell culture medium was aspirated and the cells were washed once with PBS. Trypsin-versene was added to the cell culture vessel which was then incubated at 37°C until all cells were detached from the vessel's surface. Cell culture medium was added and a fraction of the cells was transferred into a fresh cell culture vessel.

Non adherent cell cultures were sub-cultured before pH changes in the cell culture medium were indicative. Therefore, the cell culture medium was transferred to 50 ml tubes and centrifuged at 500 RCF for 5 min. After this, supernatant was aspirated and the cells were resuspended in fresh cell culture medium. A fraction of the cell was transferred into a fresh cell culture vessel.

3.2. TRANSFECTION

3.2.1. LIPOFECTAMINE®-TRANSFECTION

Transfection of MDCKII cells with Lipofectamine®2000 (Thermo Fisher Scientific) was done as indicated by the manufacturer, whereas a 1 µg DNA per 2 µl Lipofectamin®2000 reagent was used.

3.2.2. PEI-TRANSFECTION

Transfection of 293T cells with polyethylenimine (PEI) was done as in Reed *et al.*, 2006 (*372*). Briefly, a 2.58 µg/ml PEI (linear, MW 25 kDa) solution in water was prepared according to the publication mentioned above and stored at -20°C until use. For optimal transfection efficiency, cells were seeded into cell culture vessels the day before transfection. DNA and PEI were mixed in adequate cell culture medium without FBS in a ratio of 1 µg DNA per 2 µl of PEI solution. The mixture was incubated at RT for 15 min before it was dropped directly into the cell culture supernatant. A change of the cell culture medium before or after the transfection was not performed. After 24-48 h of incubation at 5 % CO_2 and 37°C, cells were further processed for SDS-PAGE, immunofluorescence etc. (see below).

3.3. PRODUCTION AND QUANTIFICATION OF INFLUENZA VIRUSES

3.3.1. PRODUCTION AND PURIFICATION OF INFLUENZA VIRUS PREPARATIONS

To produce sufficient amounts of influenza virus, eleven day old embryonated chicken eggs were inoculated with 1000 PFU of virus per 100 µl PBS^{++} per egg and incubated at 37°C for 48 h in a humidified environment. Eggs were then refrigerated overnight at 4°C, before the eggshell was opened and the allantoic fluid was harvested. Debris was removed by centrifugation at 3000 RPM at 4°C. The cleared allantoic fluid was poured on top of a 5 ml 25 %-sucrose cushion and centrifuged at 24 000 RMP at 4°C for 1.5 h. The supernatant was aspirated and 1-2 ml PBS was added to the pellet before it was left at 4°C overnight. The resuspended pellet was aliquoted and stored at -80°C. Protein concentration of the purified influenza virus preparation was determined with Pierce™ bicinchoninic acid (BCA) protein assay kit (Thermo Fisher Scientific) according to the manufacturer's instructions.

A Hemagglutination assay was performed by serially diluting the virus preparation twofold in 50 µl PBS in V-bottom shaped 96-well plate. 50 µl of 1 % chicken red blood cells in PBS were added to each well and the plate was incubated at 4°C for 20 min. The Hemagglutination titer was determined as reciprocate of the last dilution of the virus preparation at which agglutination still can be observed.

3.3.2. INFLUENZA VIRUS TITRATION BY PLAQUE FORMING ASSAY

MDCKII cells were seeded in 12-well plates the day before infection. Virus containing samples were serially diluted tenfold in 200 µl PBS^{++} with 0.2 % BSA. The cells were washed once with PBS^{++} before 0.15 ml of the virus dilution was added per well and the plates were incubated at room temperature for 45°C with occasional gentle agitation. After inoculation, cells were washed once again and semi-viscous overlay-medium containing 1-2 µg/ml TPCK-treated trypsin was added to the wells and the plates were incubated at 5 % CO_2 and 37°C for 48 h. The overlay-medium was then removed and cells were washed once with PBS and simultaneously fixed and stained with crystal violet solution at room temperature for 15 min. After aspiration of the staining solution, the cells were washed once with water and air-dried. Due to the cytolytic effect of influenza viruses, infected cells of cell culture monolayers become visible as a so called 'plaque' and can be counted. Viral titers are expressed as plaque forming units per ml (PFU/ml) and are determined by multiplying the number of plaques with the reciprocal dilution factor divided by 0.15 (with respect to the volume used for inoculation).

3.4. PRODUCTION, PURIFICATION AND QUANTIFICATION OF RECOMBINANT AAV-VECTORS

In principle, the Iodixanol-based purification protocol as suggested by Strobel *et al.* (*373*) with minor modifications was used for the production of recombinant AAV-vectors (Figure 12). Typically, 15-20 15-cm dishes of 293T cells per AAV-vector preparation were seeded the day before transfection. Cells were then transfected with the plasmids mentioned below by using PEI transfection protocol (see 3.2.2, Table 3). The amount of each plasmid used per 15-cm dish corresponds to an equimolar ratio of the plasmids.

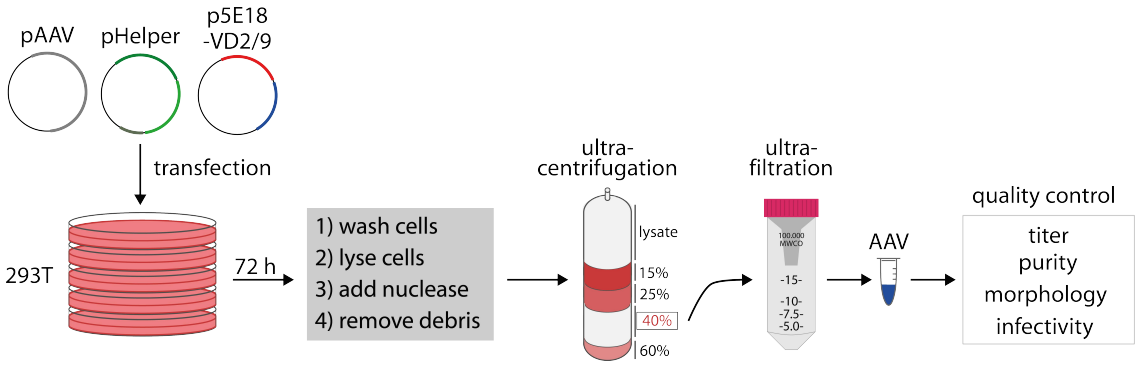

Figure 12: Schematic representation of the AAV-vector production process

Table 3: Amount of transfected plasmid DNA for production of recombinant AAV-vectors

	amount per 15-cm dish
pAAV	9 µg
p5E18-VD2/9	10 µg
pHelper	15 µg
PEI	68 µl

72 hours after transfection, cell culture medium was aspirated and ca. 10 ml PBS-MK were added. Cells were resuspended and centrifuged at 2000 RCF for 10 min. After removal of the supernatant 5 ml PBS-MK containing 0.5 % Na-deoxycholat and 0.5 µl/ml benzonase were added for lysis of the cells and the cell pellet was resuspended by vortexing. The lysate was incubated at 37°C for 1 h and vortexed every 15 min. To remove cellular debris from the crude AAV-vector preparation, samples were centrifuged at 10 000 RCF for 15 min and supernatant containing the AAV-vectors was harvested. To purify the AAV-vectors from cellular components, a discontinuous Iodixanol gradient isopycnic centrifugation was performed. To this end, the crude lysate was transferred into ultracentrifugation tubes and underlaid with a discontinuous Iodixanol gradient (Table 4). Centrifugation was carried out at 300 000 RCF at 18°C for 2.5 h. In order to not disturb to gradient acceleration and break were set to low.

Table 4: Composition of Iodixanol gradient steps

Final Iodixanol concentration	60% Iodixanol (ml)	PBS-MK (ml)	5 M NaCl (ml)	phenol red (µl)	Vol. in tube (ml)
15 %	2,4	5,3	1,9	14,4	8,0
25 %	3,0	4,2	-	10,8	6,0
40 %	6,4	3,2	-	-	8,0
60 %	6,0	-	-	3,0	5,0

Subsequently, the ultracentrifugation tube was punctured with a needle and ca. 5 ml of the AAV-vector containing 40 %-phase were extracted with the help of a syringe. 25 ml of PBS-MK were added and the sample was passed through a 0.45 µm pore size syringe filter. Afterwards, ultra-centrifugal filter units (molecular weight cutoff 100 000 kDA) were used to concentrate the sample to approximately 1-2 ml of pure AAV-vector by centrifugation at ca. 3000 RCF for 30 min. The purified product was stored at -80°C.

3.4.1. TITRATION OF THE GENOMIC CONTENT OF THE AAV-VECTOR PREPARATIONS

For titration of the AAV-vector preparation a quantitative real-time PCR (qPCR) was performed to measure the amount per microliter of product of viral genomes that are resistant to DNase digestion, i.e. the number of intact viral particles that encapsidate an AAV-vector genome.

First, 10 µl of the purified AAV-vector were digested with 0.5 µl/ml Benzonase at 37°C for 1 h. Afterwards, viral genomic DNA was extracted according to the manual of the QIAamp MinElute Virus Spin Kit (Qiagen) and eluted in 100 µl water (i.e. 10^{-1} dilution of original material). The

eluate was further serially diluted tenfold with water and the dilutions 10^{-3} to 10^{-6} were used in the qPCR (Table 5).

Table 5: Reaction components and conditions of the qPCR for AAV-vector titration

Component	Volume (20 µl reaction)
Aqua dest.	10,84 µl
10X PCR buffer (minus Mg)	2,00 µl
50 mM $MgCl_2$	2,00 µl
10 mM dNTPs (each)	1,60 µl
10 µM forward primer	0,60 µl
10 µM reverse primer	0,60 µl
10 µM Taqman-probe	0,20 µl
5 U/µl Platinum®-Taq DNA polymerase	0,16 µl
Sample (10^{-3} to 10^{-6} AAV DNA extraction)	2,00 µl

PCR conditions		
Initially denature	95°C 10 min	
denature	95°C 15 sec	40 cycles
anneal	60°C 20 sec	
elongate	72°C 10 sec	

The PCR was performed in white 96-well plates in a LightCycler®480 (Roche) instrument. Fluorescence was red at the beginning of each annealing cycle and quantification was calculated with the "Abs Quant/2nd Derivative Max" setting within the LightCycler®480 Software. For this purpose, a standard was included on the 96-well plate. The standard was prepared by restriction digesting pAAV plasmid DNA with *SmaI*. After separation of the digested pAAV plasmid DNA in an agarose gel, the respective band, i.e. a dsDNA cassette containing the complete AAV genome, was cut out and the DNA fragment was purified according to the manual of the Invisorb® Spin DNA Extraction Kit (Stratec). The concentration of the dsDNA was measured with a NanoDrop™ 8000 spectrophotometer (Thermo Fisher Scientific) and set to 1 µg/ml. The absolute number of ssDNA molecules in this 1 µg/ml stock solution was calculated with the formula $N_{DNA} = N_A \times (10^{-9} / MW)$, where N_{DNA} is the number of DNA molecules in the stock solution, N_A is the Avogadro constant and MW the molecular weight of the DNA fragment, which is calculated with the formula $MW = (A_n \times 313.2) + (T_n \times 304.2) + (C_n \times 289.2) + (G_n \times 329.2) + 79.0$, where A_n, T_n, C_n and G_n is the number of each of the respective nucleotides within the DNA fragment (Table 6). The standard stock solution was then serially diluted tenfold and the 10^{-3} to 10^{-6} dilutions were used for qPCR.

Table 6: Concentration of qPCR standards for AAV-vector titrations

AAV-vector	DNA molecules per µl stock solution	DNA molecules per µl standard dilution (10^{-3} to 10^{-6})
HA (used also for cHA)	4.33×10^8	4.33×10^5 to 4.33×10^2
HL HA (used also for mHL)	5.27×10^8	5.27×10^5 to 5.27×10^2
NP	4.63×10^8	4.63×10^5 to 4.63×10^2
GFP	9.00×10^8	9.00×10^5 to 9.00×10^2

3.4.2. ASSESSMENT OF PURITY OF THE AAV-VECTOR PREPARATIONS

The degree of purity of the AAV-vector preparation was assessed by separation of 10 µl of the preparation in a SDS-PAGE (see 3.6.2) followed by Coomassie staining of the gel (see 3.6.4). Before SDS-PAGE, samples were mixed 1:1 with 2x sample buffer with β-mercaptoethanol and boiled at 95°C for 5 min.

3.4.3. MORPHOLOGICAL ANALYSIS OF THE AAV-VECTOR PREPARATIONS

To confirm integrity and morphology of the AAV-vectors, an ELISA with an AAV9-capsid-specific antibody (ADK9) was performed, which recognizes its epitope only on the intact capsid (*374*). Additionally, electron micrographs were taken from the AAV preparations.

3.4.3.1. ADK9 CONFORMATIONAL CAPSID ELISA

96-well ELISA plates were coated with 50 µl/well of a twofold dilution of the AAV-vector preparations in coating buffer at 4°C overnight. The next day, plates were blocked with 3 % skimmed milk in PBST at 37°C for 1 h. 50 µl of ADK9 diluted 1:250 in blocking buffer were added to each well and the plates were incubated at 37°C for 1-2 h. After washing the plates three times with PBST, 50 µl of secondary anti-mouse-IgA HRP conjugated antibody were added in a 1:1000 dilution to each well and the plates were incubated at 37°C for 1 h. 50 µ/well ELISA-substrate were added to the plates after washing them three times. The color reaction was stopped by the addition of 50 µl 1M sulfuric acid per well and optical density (OD) was red at 450 nm.

3.4.3.2. ELECTRON MICROGRAPHS

Transmission electron microscopy was performed at the RKI by Lars Möller in cooperation with the *Centre for Biological Threats and Special Pathogens 4 (ZBS4): Advanced Light and Electron Microscopy*. Briefly, after negative stain of AAV-vector preparations with uranylacetat, samples were examined on a JEM-2100 200 kilovolt transmission electron microscope (Jeol).

3.4.3.3. ASSESSMENT OF AAV-VECTORED TRANSGENE EXPRESSION AFTER *IN VITRO* TRANSDUCTION

Infectivity of the AAV-vectors was assessed on 293T cells, since this cell line represents one of the very few being susceptible to AAV9 infection. 293T cells were seeded in 12-well plates the day before transduction. 20-40 µl of the AAV-vector preparation were then directly added to the cell culture medium. The next day, cell culture medium was exchanged with fresh medium and the cells were incubated for another 48 h before they were processed for SDS-PAGE and Western blot, immunofluorescence or flow cytometry (see 3.6.1, 3.6.2, 3.6.3, 3.7.1, 3.7.2).

3.5. CONSTRUCTION OF PAAV-PLASMIDS

3.5.1. PLASMID CONSTRUCTION

A headless HA version of the A/California/7/09 (H1N1)pdm HA was constructed by exchanging the amino acids between cysteine 52 and cysteine 277 in HA1 with a short linker (4x glycine) (*288*). A *Bsu36I* restriction sites was generated downstream of the linker by introducing a silent mutation into the corresponding DNA sequence (C213T → P284P). A *HindIII* restriction site followed by a Kozak sequence (ACC**ATG**A) and a *BamHI* restriction site were added to the 5' and 3' end of the DNA fragment, respectively.

Modified headless (mHL) HA were constructed by adapting the amino acid changes mentioned in Yassine *et al.*, 2016 (mHL1) or Impagliazzo *et al.*, 2016 (mHL2) to the A/California/7/09 (H1N1)pdm HA (*297, 298*). Of each of the mHL a version with (+TM) and without transmembrane domain was designed. Therefore, the terminal 36 amino acids were deleted to yield the mHL without transmembrane domain. A *HindIII* restriction site followed by a Kozak sequence and a *BamHI* restriction site were added to the 5' and 3' end of the DNA fragment, respectively.

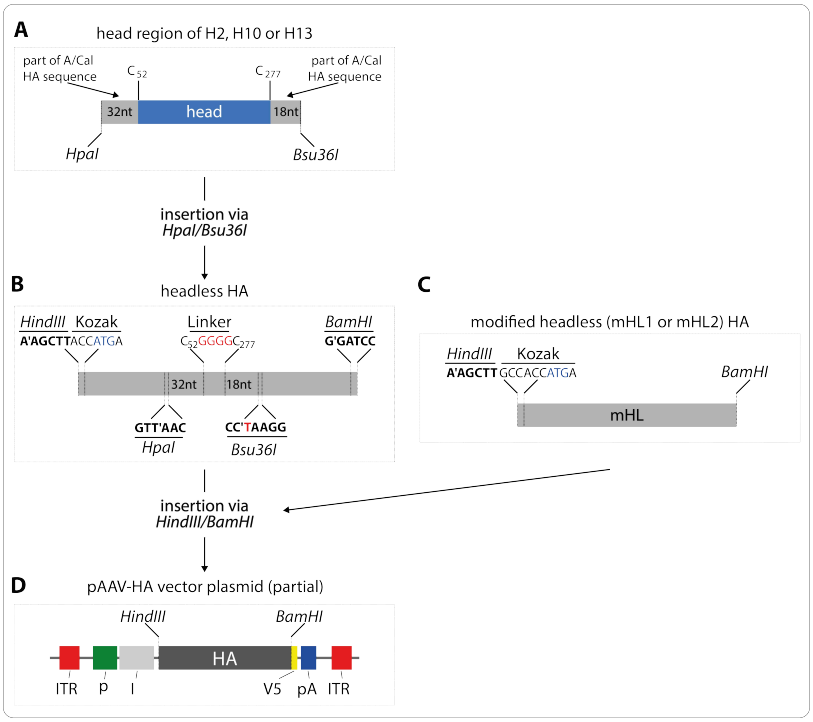

Figure 13: Schematic representation of the synthesized HA constructs and fragments
as described in section 3.5.1.
(A) Head regions (C_{52}-C_{277}) of H2, H10 and H13 HA with flanking (H1N1)pdm sequences and *HpaI* and *Bsu36I* restriction sites (**B)** headless HA containing an insertion of 4xG linker (in red) between C_{52}-C_{277}. The positions of a *HpaI* and *Bsu36I* restriction sites upstream and downstream of the two C within HA are marked, the latter was generated by silent mutation (C→T, marked as red in the sites' nucleotide sequence). The headless HA sequence is flanked by a *HindIII* restriction site plus Kozak sequence (start codon in blue) and a *BamHI* restriction site. (**C**) The sequences of the modified headless (mHL1 and mHL2) are also flanked by a *HindIII* restriction site plus Kozak sequence (start codon in blue) and a *BamHI* restriction site. (**D**) The pAAV-vector contains two long terminal repeat regions (LTR) at both ends, a CMV promoter (p), an irrelevant intron (I), a V5 Tag (V5) which is fused to the transgene, a poly adenylation and termination signal (pA) and the transgene, which is in this case HA, that is flanked by a *HindIII* and a *BamHI* restriction site.

To generate chimeric HA (cHA) proteins, the head regions of the avian H2N3, H10N7 and H13N6 influenza viruses, defined as the region between cysteine 52 and cysteine 277, were used (*270*). 32 and 18 nucleotides of A/California/7/09 (H1N1)pdm HA upstream or downstream of cysteine 52 and cysteine 277, respectively, were added to the avian head regions. These additional nucleotides included a naturally occurring *HpaI* restriction site and a *Bsu36I* restriction site that was generated by the silent mutation mentioned above at the 5' and 3' end, respectively. All DNA fragments were codon-optimized to murine gene expression and synthesized commercially (GeneArt, Invitrogen, Thermo Fisher Scientific).

Table 7: pAAV plasmid designation and insert

plasmid	HA version	comment
pAAV-HA	wildtype HA	A/California/7/09 HA (H1N1)pdm
pAAV-HA1	chimeric HA	H2N3 head + (H1N1)pdm stalk
pAAV-cHA2	chimeric HA	H10N7 head + (H1N1)pdm stalk
pAAV-cHA3	chimeric HA	H13N6 head + (H1N1)pdm stalk
pAAV-HL	headless HA protein	as in Steel *et al.*, 2010 (*288*) adapted to (H1N1)pdm
pAAV-mHL1	mod. headless protein	as in Yassine *et al.*, 2016 (*297*) adapted to (H1N1)pdm
pAAV-mHL2	mod. headless protein	as in Impagliazzo *et al.*, 2016 (*298*) adapted to (H1N1)pdm

For the construction of the cHA, headless HA fragment was restriction digested with *HpaI* and *Bsu36I*, 5' ends of the DNA fragment were dephosphorylated with alkaline phosphatase and ligated through T4 ligase with *HpaI* / *Bsu36I* restriction digested H2N3, H10N7 and H13N6 head fragments to yield cHA1, cHA2 and cHA3, respectively. Subsequently, to yield the final AAV-vectors, the headless HA, the mHL and the three cHA were restriction digested with *BamHI* and *HindIII* and ligated with pAAV-HA (*362*), which was also restriction digested with these enzymes and dephosphorylated (Table 7). All procedures were done according to the manufacturer's instructions. Correctness of the plasmid constructs was analyzed by restriction digestion with *BamHI* and *HindIII* and sequencing.

3.5.2. SEQUENCING

Sanger DNA sequencing was done according to the manufacturer's instructions with the BigDye® Terminator 3.1 sequencing kit (Applied Biosystems) using the following protocol and insert sequencing primers (see section 2) (Table 8).

Table 8: Protocol for Sanger sequencing PCR

Component	Volume (10 µl reaction)
Aqua dest.	ad 10 µl
5x ABI reaction buffer	1.5 µl
Primer 10 µM	0.5 µl
BigDye® 3.1 mix	1.0 µl
DNA	200 ng

PCR conditions		
Initially denature	90°C / 1 min	
denature	96°C / 10 sec	25 cycles
anneal	40°C / 5 sec	
elongate	60°C / 4 min	

3.6. BIOCHEMICAL METHODS

3.6.1. PREPARATION OF CELL LYSATES

Cell culture medium was aspirated and the cells were washed once with ice cold PBS. Fresh, ice-cold PBS was added and the cells were detached from the cell culture vessel with a cell scraper. After centrifugation at 2 500 RCF at 4°C for 2 min, PBS was aspirated and lysis buffer was added in which the cell pellet was resuspended. Subsequently, the lysates were incubated on ice for

20 min before they were centrifuged at 10 000 RCF at 4°C for 10 min. Supernatant was harvested and stored at -20°C.

3.6.2. SDS-PAGE

Polyacrylamide gels were produced in-house by first casting the separation gel between a short and a spacer glass plate with a spacer width of 0.75 mm (gels for Coomassie staining) or 1.5 mm (all others) (Table 9). After complete polymerization of the separation gel the stacking gel was layered over it and a 10-well comb was inserted. Finally, the gel was transferred into a vertical gel chamber and running buffer was added. Generally, protein samples (see 3.6.1) or purified virus samples (4 – 8 µg/lane) were prepared for SDS-PAGE by mixing them with 6x sample buffer with β-mercaptoethanol and boiling at 95°C for 5 min before they were loaded on the gel and separated by applying a constant electric current of 25 mA/gel to it.

Table 9: Composition of acrylamide gels for SDS-PAGE

Amounts are sufficient for one 1.5 mm gel.

component	separation gel 10 %	stacking gel 5%
30 % Acrylamide/ Bisacrylamide (29:1)	3.3 ml	0.83 ml
ddH_2O	4.0 ml	2.8 ml
1.5 M Tris-HCl pH 8.8	2.5 ml	-
0.5 M Tris-HCl pH 6.8	-	1.25 ml
10 % SDS	100 µl	50 µl
10 % APS	100 µl	50 µl
TEMED	6 µl	6 µl

3.6.3. PROTEIN TRANSFER AND WESTERN BLOT

Proteins were transferred from acrylamide gels to nitrocellulose membrane by stacking three layers of Whatman paper, one nitrocellulose membrane, the acrylamide gel and another three layers of Whatman paper between the anode and the cathode of a semi-dry blotting apparatus and applying a constant electric current of 80 mA/gel to it for 80 min.

After protein transfer, nitrocellulose membranes were blocked with 5 % skimmed milk in TBST at room temperature for 1 h. Primary antibody or mouse serum (1:500) was diluted in 5 % skimmed milk in TBST and added to the membrane which was incubated at 4°C overnight. The next day HRP-conjugated secondary antibody was added after excessive washing with TBST. After another round of excessive washing, SuperSignal™ West Dura Extended Duration Substrate (Thermo Fisher Scientific) was added to the nitrocellulose membrane according to the manufacturer's instructions. Chemiluminescence was detected with a ChemiDoc™ imager and the corresponding software (BioRad).

3.6.4. COOMASSIE STAINING

After SDS-PAGE acrylamide gels were incubated in Coomassie fixation solution at room temperature for 30 min. The fixation solution was replaced with 1x Roti®-Blue (Roth) Coomassie staining solution and the gel was incubated at room temperature overnight. The next day

Coomassie destaining solution was added and the gel was incubated until areas without sample were destained completely. The gel was then rinsed with water and dried in a vacuum gel drying apparatus.

3.7. IMMUNOFLUORESCENCE STAINING

3.7.1. IMMUNOFLUORESCENCE STAINING ON COVERSLIDES

4 % PFA was added directly to the cell culture medium in a 1:1 ratio (final [PFA]: 2 %) and plates were left at 4°C for 15 min. The supernatant was aspirated and 100 % ice-cold methanol was added (Note: there was no negative effect of methanol permeabilization on conformation of the antigens (as assessed by C179 staining) compared to other methods (e.g. Tween20, Triton x-100, saponin) (data not shown)). After 10 min the methanol was removed and the cells were washed once with PBST before they were blocked with 5 % skimmed milk and 10 % FBS in PBST at 37°C for 1 h. Serum or commercial primary antibodies were added to the cells appropriately diluted in 50 µl blocking buffer for 1-2 h at 37°C. After washing the cells three times with PBST 50 µl dye-conjugated secondary antibody (1:1000) and DAPI were added to the cells for 1 h at 37°C before the cells were washed again three times with PBST, one time with desalted water, mounted with Mowiol, and inspected under a Zeiss Axio Observer D1 inverted epifluorescence microscope or Zeiss LSM 780 confocal laser scanning microscope.

3.7.2. STAINING FOR ANALYSIS VIA FLOW CYTOMETRY

Cells expressing transfected proteins were detached from cell culture vessel with trypsin versene and transferred to 15 ml centrifugation tubes. After centrifugation (500 RCF, 5 min) 2 % PFA was added, cell were resuspended and fixed at 4°C for 20 min. The cells were centrifuged, supernatant was aspirated and 100 % ice-cold methanol was added at -20°C for 10 min. After washing the cells two times with PBST, the cells were resuspended in 5 % skimmed milk and 10 % FBS in PBST and transferred into a 96-well plate (50 µl per well). The plates were centrifuged after 1 h incubation at 37°C before 50 µl/well serum or primary antibody at an appropriate dilution was added for 1-2 h at 37°C. After washing the cells three times with PBST 50 µl dye-conjugated secondary antibody (1:1000) were added to the cells for 1 h at 37°C before the cells were washed again three times with PBST. Fluorescence was measured with a BD FACSCalibur™ flow cytometer (BD). Analysis was done with BD CellQuest™ Pro.

3.8. SEROLOGICAL METHODS

3.8.1. ELISA

96-well high-binding ELISA plates were coated with antigen (4-8 µg/ml purified influenza virus or 1:500 dilution of AAV) in 50 µl coating buffer at 4°C overnight. The next day coating buffer was aspirated and plates were blocked with 100 µl 5 % skimmed milk in PBST at 37°C for 1 h. Blocking buffer was removed and 50 µl/well serum serially diluted in blocking buffer were added to each well and the plates were incubated at 37°C for 1-2 h. After washing the plates three times with PBST, 50 µl of secondary HRP conjugated antibody were added in a 1:1000 dilution to each well and the plates were incubated at 37°C for 1 h. 50 µ/well ELISA-substrate were added to the plates after washing them three times. The color reaction was stopped by the addition of 50 µl 1M sulfuric acid per well and OD was red at 450 nm.

3.8.2. CONFORMATIONAL CHANGE ELISA

96-well ELISA plates were coated with antigen (4-8 µg/ml purified influenza virus) in 50 µl coating buffer at 4°C overnight. The next day coating buffer was aspirated and plates were incubated with 50 µl/well of different 0.1 M citric acid – sodium citrate buffer solutions (pH = 7.2, 5.8, 5.4, 5.0, 4.4 or 4.4 + 0.1 DTT) at room temperature for 30 min. Afterwards, the plates were washed two times with PBST and then blocked and incubated with antibody as indicated above (see 3.8.1).

3.8.3. IN-CELL ELISA

MDCKII cells were seeded in 96-well plates and transfected as described under 3.2.1. 48 h post transfection, 4 % PFA was added directly to the cell culture medium in a 1:1 ratio (final [PFA]: 2 %) and plates were left at 4°C for 15 min. The supernatant was aspirated and 100 µl 100 % ice-cold methanol were added. After 10 min the methanol was removed and the cells were washed once with PBST before they were blocked with 100 µl of 5 % skimmed milk and 10 % FBS in PBST at 37°C for 1 h. After quenching of the endogenous peroxidase with 100 µl of 3 % H_2O_2 at room temperature for 30 min, 50 µl of mouse serum or C179 antibody in blocking buffer were added to each well at a dilution of 1:250 for 1 h at 37°C. After washing the cells three times with PBST, 50 µl HRP-conjugated secondary antibody (1:1000) and was added to the cells for 1 h at 37°C before the cells were washed again three times with PBST and 50 µ/well ELISA-substrate were added to the plates after washing them three times. The color reaction was stopped by the addition of 50 µl 1M sulfuric acid per well and OD was red at 450 nm.

3.8.4. INFLUENZA VIRUS MICRONEUTRALIZATION ASSAY (MN)

MN was performed as outlined in He *et al.*, 2015 (*375*), which is an extended version of a WHO recommended protocol (*376*) to capture effects of anti-HA (stalk) antibodies on events in the late viral replication cycle. MDCKII cells were seeded in 96-well plates one day before the assay. Sera were inactivated by heating to 56°C for 30 min and subsequently diluted 1:20 in MEM with 0.2 % BSA with 1 µg/ml TPCK-treated trypsin. 1:20 diluted sera were serially diluted twofold in MEM with 0.2 % BSA with 1 µg/ml TPCK-treated trypsin. Additionally, two control dilutions (cell ctrl. and virus ctrl.) where prepared which did not contain serum. 3.5 $x10^4$ PFU influenza virus (mouse) or 2 $x10^2$ PFU (ferret) in 25 µl MEM with 0.2 % BSA with 1 µg/ml TPCK-treated trypsin were added to 25 µl of each serum dilution and the virus ctrl. wells. No virus was added to the cell ctrl. wells, instead only MEM 0.2 % BSA with 1 µg/ml TPCK-Treated trypsin was added and all plates were incubated at 37°C for 1 h. The final starting serum dilution was now 1:40. MDCKII cells were washed once with PBS^{++} and the serum/virus mixture (50 µl) was transferred to the cells. The cells were inoculated at 37°C for 1 h before they were washed once with PBS^{++} and 50 µl serum in the identical dilution as before was added to each well in MEM with 0.2 % BSA with 1 µg/ml TPCK-treated trypsin.

After 24 h incubation at 5 % CO_2 and 37°C, cell culture medium was aspirated, cells were fixed with 80 % ice-cold acetone for 10 min at room temperature, air dried and blocked with 5 % skimmed milk in PBST for 45 min at 37°C before endogenous peroxidase was quenched with 100 µl/well 3 % H_2O_2 at room temperature for 30 min. Cells were washed once with PBST and

50 µl/well primary polyclonal goat anti-influenza antibody (5315-0064, BioRad; 1:1000 in blocking buffer) were added for 1-2 h at 37°C. After washing the plates 3-times with PBST, 50 µl secondary HRP-conjugated anti-goat antibody were added to the cells diluted 1:1000 in blocking buffer and they were incubated at 37°C for 1 h. Cells were washed 3-times and 50 µl ELISA-substrate were added. After color development the reaction was stopped with 50 µl 1 M sulfuric acid and OD was red at 450 nm. Neutralization was calculated with the following formula, whereas resulting values that were above 1 were set to be 1 and values that were below 0 were set to be 0:

$$\text{MN (fold)} = 1 - \frac{\text{OD}_{\text{well}} - \text{mean}_{\text{OD all cell ctrl. wells}}}{\text{mean}_{\text{OD all wells of resp. dilution}}}$$

3.8.5. HEMAGGLUTINATION INHIBITION ASSAY (HAI)

For inactivation, 1 volume of serum was mixed with 0.5 volumes of 8 µg/ml TPCK-treated trypsin and incubated at 56°C for 30 min. Samples were cooled down to room temperature and 3 volumes of 0.011 M KIO_4 were added before samples were incubated at room temperature for 15 min. Afterwards, 3 volumes of 1 % glycerol were added and samples were incubated at room temperature for 15 min. Finally, 12.5 volumes of PBS were added to reach a starting dilution of 1:20. The sera were further diluted twofold in 25 µl PBS in a V-bottom shaped 96-well plate. Additionally, two control dilutions (no virus ctrl. and no serum ctrl.) where prepared which did not contain serum. 4 HA units of virus in 25 µl PBS were added to each well except for the no virus ctrl to which only 25 µl PBS were added (starting dilution of serum 1:40). The plates were incubated at 37°C for 1 h. 50 µl of 1 % chicken red blood cells in PBS were added to each well and the plate was incubated at 4°C for 20 min. The HAI titer is determined as reciprocate of the last dilution of serum at which agglutination is still inhibited.

3.8.6. AAV MICRONEUTRALIZATION ASSAY (AAV MN)

AAV MN was principally performed as described by Meliani *et al.*, 2015 (*377*). 293T cells were seeded in 96-well plates. The next day, serum was pre-diluted 1:50 in FBS and inactivated at 56°C for 30 min. Semi-log10 dilutions of the serum were prepared in FBS, starting with the 1:50 pre-dilution. Additionally, two control dilutions (cell ctrl. and virus ctrl.) where prepared which did not contain serum. AAV-GFP was diluted in DMEM with 0 % FBS to 2.22 $x10^{10}$ GC/ml. 27 µl of each serum dilution and virus ctrl. were mixed with 27 µl of AAV GFP dilution (i.e. 6 $x10^{8}$ GC/well) and incubated at 37°C for 1 h. 27 µl of DMEM with 0 % FBS were added to the cell ctrl. . 20 µl of the serum/virus mixture were added directly to the cell culture medium of the 293T 96-well plate and cells were incubated at 5 % CO_2 and 37°C for 48 h.

Cell culture medium was aspirated and cells were washed once with PBS before trypsin-versene was added and the cells were left at 37°C until a single cell suspension was established. Cell culture medium was added to the cells and the plates were centrifuged at 500 RCF for 5 min. Supernatant was aspirated and 0.5 % PFA was added at room temperature for 15 min. Finally, PBS was added and the plates were centrifuged again before fresh PBS was added, cells were resuspended and green fluorescence was measured with a BD FACSCalibur™ flow cytometer (BD). Analysis was done with BD CellQuest™ Pro.

3.8.7. FC-GAMMA RECEPTOR ASSAY (INFECTION & TRANSFECTION BASED)

The FcγR assay (courtesy of Prof. Dr. med. Hartmut Hengel, Universitätsklinikum Freiburg) is based on the protocols described in Corrales-Aguilar *et al.*, 2013 and Van den Hoecke *et al.*, 2017 (*225, 378*). BW 5147 reporter cell lines that stably express chimeric surface receptors comprising the extracellular domain of the murine FcγRI, -IIB, -III or -IV and the intracellular signaling module of the murine CD3-ζ chain were produced by lentiviral transduction as described in (*225, 378, 379*). Upon activation of the FcγR by immune complexes IL-2 is produced which is quantified by ELISA. MDCKII cells were seeded into 96-well plates one day before they were washed once with PBS^{++} and infected with 1 $x10^4$ PFU/100 µl per well influenza virus in MEM with 0.2 % BSA without TPCK-treated trypsin, or mock infected. No washing was performed after infection. Alternatively, MDCKII cells were seeded into 96-well plates one day before they were transfected with 0.4 µg plasmid DNA using the Lipofectamine™ protocol mentioned above (see 3.2.2) or mock transfected. On the following day, cell culture medium was exchanged with fresh medium. The next day, serum was inactivated at 56°C for 30 min and twofold dilutions were prepared in 50 µl R10 medium starting with a dilution of 1:50. Cell culture medium was aspirated and 50 µl/well of the serum dilution were added for 1 h at 37°C. 50 µl of only the 1:50 dilution were added to mock infected or transfected wells. During the incubation period, FcγR cells were counted and concentration was set to 1-2 $x10^5$ cells per 200 µl R10 medium. The MDCKII cells were washed once with PBS^{++} and 200 µl FcγR cells per well were added before the cells were incubated over night at 5 % CO2 and 37°C. Finally, ELISA plates were coated with 1 µg/ml anti-IL2 antibody in 50 µl coating buffer overnight at 4°C.

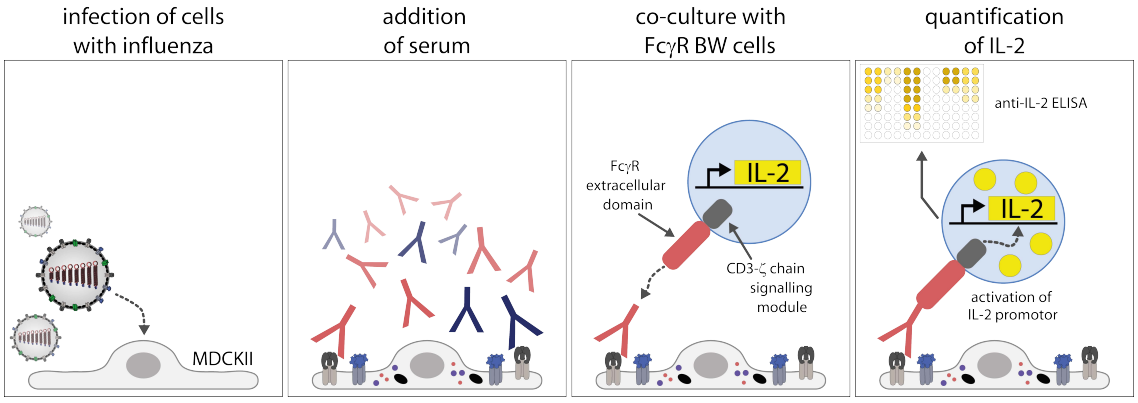

Figure 14: Schematic representation of the experimental protocol of the influenza virus infection-based FcγR assay as described in section 3.8.7; modified from (*378*).

The next day, 100 µl PBS with 0.1 % Tween-20 and 5 % FBS were added to the MDCKII / FcγR co-culture and cells were resuspended 5 times in order to lyse the cells and release the IL-2. ELISA coating buffer was aspirated and plates were blocked with PBST with 10 % FBS at room temperature for 1 h. 150 µl of the MDCKII / FcγR co-culture supernatant were transferred to the ELISA plates before they were incubated at room temperature for 1-2 h. After washing the plates three times with PBST, 50 µl of 1 µg/ml biotinylated anti-IL2 antibody were added to each well and the plates were incubated at room temperature for 1 h. 50 µl per well HRP-conjugated

streptavidin was added in a 1:1000 dilution after washing the plates three times with PBST. After 30 min incubation at room temperature the plates were washes again three times with PBST and 50 µl of ELISA substrate were added. After color development the reaction was stopped with 50 µl 1 M sulfuric acid and OD was red at 450 nm. FcγR activation was calculated by subtracting the mean of the mock infected or transfected wells (i.e. background) from the infected or transfected wells.

3.9. MICE

6 - 8 week old female C57BL/6NCrl mice were purchased from Charles River. The animals were allowed to acclimate to the housing conditions for one week prior to any experiment. Mice were kept in a 12/12 h light-dark cycle at 22°C, with an air exchange rate of 10 – 12 times per day in groups of 5 animals per cage containing enrichment.

All experiments were performed in accordance with protocols approved by the *Landesamt für Gesundheit und Soziales* (LAGeSo) Berlin (reference numbers G 0256/14, G 254/15, G 0255/16).

3.9.1. IMMUNIZATION

Animals were anesthetized with Isofluran and immunized either intramuscularly or intranasally with the respective vaccines (Table 10) in a volume of 50 µl PBS which was evenly distributed to both posterior limbs and nostrils, respectively.

Table 10: Doses of vaccines used for mouse immunization studies

Vaccine	Immunization route	Dose per mouse
AAV	intramuscular	1 x10^{10} vg
	intranasal	1 x10^{11} vg
WIV	intramuscular/intranasal	20 µg

3.9.2. INFECTION

Animals were anesthetized with Isofluran and infected intranasally with a lethal dose of influenza virus (Table 11) in a volume of 50 µl PBS which was evenly distributed to both nostrils. Mice were monitored daily for survival and weight loss and general signs of disease until day 14 where they were anesthetized and sacrificed and lungs were harvested (see 3.9.4). Animals that lost more than 20 % of their initial weight or reached another humane endpoint were euthanized immediately.

Table 11: Lethal doses of influenza viruses used for mouse infection studies

Virus	$TCID_{50}$ / mouse
A/California/7/09 (H1N1)pdm	7.94 x10^{3}
A/Puerto Rico/8/34 (H1N1) – low dose	2.51 x10^{4}
A/Puerto Rico/8/34 (H1N1) – high dose	5.01 x10^{4}
X31 (H3N2)	1.00 x10^{5}

3.9.3. BLOOD COLLECTION AND SERUM PREPARATION

Blood sampling was done before each immunization and before the challenge infection of the mice. Animals were anesthetized with Isofluran and blood was drawn from the retrobulbar plexus

and left at room temperature for ca. 30 min. The coagulated blood samples were centrifuges at 2500 RCF for 30 min and the supernatant, i. e. the serum, was harvested and stored at -80°C.

3.9.4. LUNG HOMOGENIZATION

Lungs of mice were harvested and stored at -80°C. Subsequently, all organs were thawed on ice and lung tissue was weighted. The lungs were transferred into FastPrep® Lysing Matrix D tubs (MP Biomedicals) and 1 ml cold PBS was added before the tissue was homogenized in a FastPrep-24™ apparatus at 6 m/sec for 40 sec. Afterwards, FastPrep® tubes were centrifuged at 4000 RPM and 8°C for 5 min and supernatant was transferred into fresh 1.5 ml-tubes which were centrifuged again at 10 000 RPM and 8°C for 5 min. Again, supernatant was transferred into 15 ml-tubes and PBS was added to reach a final volume of 10-times the lung weight (i.e. 0.1 g lung tissue – 1 ml PBS). The diluted lung homogenates were aliquoted and stored at -80°C.

3.10. FERRETS

Experiments with ferrets were done in cooperation with the group of Prof. Dr. Veronika von Messling (Division of Veterinary Medicine, Paul-Ehrlich-Institut (Langen)). Daniel Demminger went to the PEI for the first immunization and for the complete challenge period and assisted during all experimental procedures except for homogenization and titration of ferret organ samples, titration of nasal washes and IPMA for influenza-specific ferret serum antibodies, which were done by Lisa Walz and Yvonne Krebs at the PEI. All other serological assays and all analyses were done by Daniel Demminger. (Immuno-)Histological staining and examination of ferret organ samples was done by Kristina Dietert from the group of Prof. Dr. Achim D. Gruber (Department of Veterinary Medicine, Institute of Veterinary Pathology, Freie Universität (Berlin)).

3.10.1. ANIMALS

16 four month old male ferrets (*Mustela putorius furo*) were obtained from Euroferret (Denmark) and housed at the Paul-Ehrlich-Institut (Langen). Animals were acclimated to the housing conditions and sero negativity to circulating influenza viruses was confirmed by IPMA (data not shown). For experiments, animals were housed in groups of four.

3.10.2. IMMUNIZATION

Animals were anesthetized with ketamine (100 mg/kg) and medetomidine (0.05 mg/kg), and immunized either intranasally with AAV-vector vaccines in a volume of 250 µl PBS which was evenly distributed to both nostrils, or intramuscularly with human QIV into one posterior limb (Table 10).

Table 12: Doses of vaccines used for ferret immunization studies

Vaccine	Immunization route	Dose per ferret
AAV	intranasal	1.875 x10^{12} vg
QIV ***Influsplit Tetra (2017/2018):*** *A/Michigan/45/2015(H1N1)pdm-like* *A/Hong Kong/4801/2014(H3N2)-like* *B/Brisbane/60/2008* *B/Phuket/3073/2013*	intramuscular	human dose (15 µg per HA)

3.10.3. INFECTION

Animals were anesthetized with ketamine (100 mg/kg) and medetomidine (0.05 mg/kg) ,and infected intranasally with a sub-lethal dose of influenza virus (Table 11) in a volume of 200 µl Opti-MEM which was evenly distributed to both nostrils.

Table 13: Doses of influenza viruses used for ferret infection studies

Virus	$TCID_{50}$ / ferret
A/Mexico/InDRE4487/2009 (H1N1)pdm	1 x10^{5}

Ferrets were monitored twice daily for signs of disease using a 0-1-2 scale for activity (normal, calm, depressed), respiratory signs (sneezing, nose exudate and congestion) and general clinical signs. Zero indicates minimal deviation from the physiological state, 1 indicates moderate nasal discharge, congestion and/or occasional sneezing and/or calm temper while 2 indicates severe nasal discharge and/or labored breathing, dyspnea and frequent sneezing and/or depressed manner (*380*). Changes in body weight and body temperature were measured. Nasal washes were collected once a day in which virus titers were determined (see 3.10.6). On day three post infection, animals were exsanguinated and nasal turbinates, trachea and lung were harvested. Nasal turbinates and parts of the traches and the lung where stored at -80°C until further use (see 3.10.4). Trachea and lung samples were also fixed with paraformaldehyde for histopathological examination (see 3.10.7).

3.10.4. SAMPLE COLLECTION (ORGAN, BLOOD, NASAL WASHES)

Blood sampling was done before each immunization and before the challenge infection of the mice. To this end, ferrets were anesthetized with ketamine (100 mg/kg) and medetomidine (0.05 mg/kg), and blood was drawn from the anterior vena cava with Z Serum Sep Activator tubes (Greiner bio-one) which were then centrifuged for 15 min at 1600 RCF before serum was transferred into fresh vessel and stored at -20°C until further use.

Nasal washes where performed on the non-anesthetized animal. Approximately 500 µl of PBS was instilled into one nostril and expectorate was collected into a 50 ml tube. This procedure was repeated until a minimum volume of 400 µl was reached. Debris was removed by centrifugation before virus titers were determined by the $TCID_{50}$ method (see 3.10.6).

Organ samples were thawed, weighed and homogenized in FastPrep® tissue homogenizer according to the manufacturer's instructions, debris were removed by centrifugation and virus titers per gram tissue weight were determined by the $TCID_{50}$ method (see 3.10.6).

3.10.5. DETERMINATION OF SERUM ANTIBODY TITERS

Serum antibody titers against Cal/7/9 virus were determined by immuno-peroxidase monolayer assay (IPMA) as described before (*381*).

3.10.6. VIRUS TITRATION

Virus titration in nasal wash samples and tissue homogenates was done as described before (*381*).

3.10.7. HISTOPATHOLOGY AND IMMUNOHISTOCHEMISTRY

2 µm sections of hematoxylin and eosin stained organ samples were prepared and analyzed microscopically by the board-certified veterinary pathologists Kristina Dietert and Achim D. Gruber to assess character and severity of pathologic lesions using lung specific inflammation score parameters for quantifying influenza virus-induced pneumonia as described (*382*). These parameters included severity of (i) interstitial pneumonia with infiltration by macrophages, lymphocytes, neutrophils (ii) bronchitis, (iii) epithelial necrosis of bronchi, alveoli and, submucosal glands, (iv) perivascular lymphocytic cuffing, and (v) hyperplasia of type II pneumocytes.

Also, influenza A virus antigen was detected via an goat anti-influenza A virion antibody and corresponding phosphatase-conjugated secondary antibody. Binding was detected with the chromogen triamino-tritolyl-methanechloride (Neufuchsin), and slides where counterstained with hematoxylin and eosin. Samples from non-influenza infected ferrets served as negative control for histopathological and immunohistochemical analysis. Neither one of the above mentioned influenza-infection specific parameter nor influenza virus antigen could be detected in these control samples (data not shown).

3.11. STATISTICS

Statistical analyses were performed using GraphPad Prism version 7.03 for Windows (GraphPad Software, La Jolla California USA, www.graphpad.com). Results are presented as mean ±/+ standard deviation or standard error of the mean (linear scales) or as geometric mean (log scales) as indicated in the figure legend. ELISA results are presented as area under the curve (AUC) of the OD (450nm)–serum dilution curve. For comparison of two unmatched groups, a non-paired, non-parametric Mann-Whitney test was used. Analysis of peptide-screen data was done with one-sample t-test (hypothetical value: 1) after normalization to control values obtained for AAV-GFP serum. For comparison of three or more groups a non-paired, non-parametric Kruskal-Wallis test was used in combination with Dunn's posttest. Groups where either compared to a control group or to each other, as indicated in the figure legends. For comparison of matched data, a paired, non-parametric Friedman-test was used in combination with Dunn's posttest. Groups were compared to their individual day sero values. Analysis of survival data was done with log rank Mantel-Cox test comparing treatment groups with each other or to a control group as indicated in the figure legend. Linear regression curves where fitted to the data using the "linear regression"

option. Curves are displayed with the 95% confidence band, i.e. the area that contains the true regression curve with 95% confidence, in the figures. The correlation coefficient (r^2) is reported as measure of goodness-of-fit of the regression together with a p value testing the null hypothesis *is the slope of the best fit curve zero*. Nonlinear regression was performed using the "nonlinear regression - [Inhibitor] vs. response -- Variable slope (four parameters)" option. Default settings where used except for analysis of influenza microneutralization assays, where the fitting was constrained with the setting "Bottom: Shared value for all data set". Correlation coefficient where between $r^2 = 0.93\text{-}0.99$ for all nonlinear regressions. IC_{50} values are reported where indicated.

4. RESULTS

4.1. AAV-VECTORS INDUCE STRONG *IN VITRO* ANTIGEN EXPRESSION

AAV-vectors represent one of the most promising viral vectors not only for use in human gene therapy, but also as carrier for vaccines against viral pathogens including influenza viruses (*361*). Although AAV-vectors have been used for passive immunization with broadly reactive influenza-specific antibodies, there is a lack of knowledge on the influence of AAV-vectored expression of influenza wildtype or broadly reactive antigens on the breadth of the immune response and on protection against influenza virus challenge. In this context, a direct comparison of AAV-vectored and inactivated vaccine is missing, too. Thus, in this thesis the immunogenicity and protective efficacy of AAV-vectors expressing HA, NP, chimeric HA or headless HA was evaluated in mice and compared to immunization with whole inactivated virus (WIV). Finally, AAV-vectored influenza vaccines were also evaluated in the gold-standard human influenza animal model, the ferret.

Based upon the (H1N1)pdm-based AAV9-vectors described by Sipo *et al.*, four additional AAV-vectors were constructed during the first phase of the project (Figure 13) (*362*). (H1N1)pdm viruses, including the prototypic A/California/7/09 (Cal/7/9), caused the most recent influenza pandemic and have been circulating seasonally in humans ever since with only minor antigenic changes. A (H1N1)pdm virus strain has thus been included in the seasonal vaccine from 2010 on (*383*). Therefore, Cal/7/9 was chosen as vaccine virus in this study.

For the generation of an Cal/7/9-based headless HA, the region between $cysteine_{52}$ and $cysteine_{277}$ within the Cal/7/9 HA amino acid sequence, i.e. the HA-head, was replaced with a tetra-glycine linker as described by Steel *et al.* (*288*) (Figure 13B). In the original publication, these particular cysteines were chosen due to their close proximity to each other enabling their connection via a short flexible linker (*288*). Three different cHA were constructed by swapping the respective region in the headless HA with the exotic HA-head regions of the avian viruses H2N2 (cHA1), H10N7 (cHA2) or H13N6 (cHA3) (Figure 13A). Thus, cHA1 and cHA3 contain a HA-head region from group 1 influenza A viruses, while cHA2 contains a group 2 HA-head (Figure 1). Various chimeric combinations of HA-heads and stalks were shown in other studies to behave comparable to their parental counterparts (*271*). Hence, there is apparently no predictor for the resulting overall HA structure. The H2, H10, and H13 HA-head regions were chosen i) based on availability of the parental viruses at the Robert Koch Institute and ii) because they are currently not circulating in humans. Therefore, little to no immunological experience in humans, i.e. immunological naivety, against these virus subtypes can be expected. All constructs/fragments were synthesized *de novo* and optimized to mammalian (i.e. murine) gene expression. cHA and headless HA were eventually inserted into the pAAV-vector plasmid from which they are expressed under the control of a Cytomegalovirus (CMV) promoter enabling ubiquitous tissue expression (*362*). Furthermore, the expressed proteins are tagged with a simian virus 5 epitope tag (V5-tag).

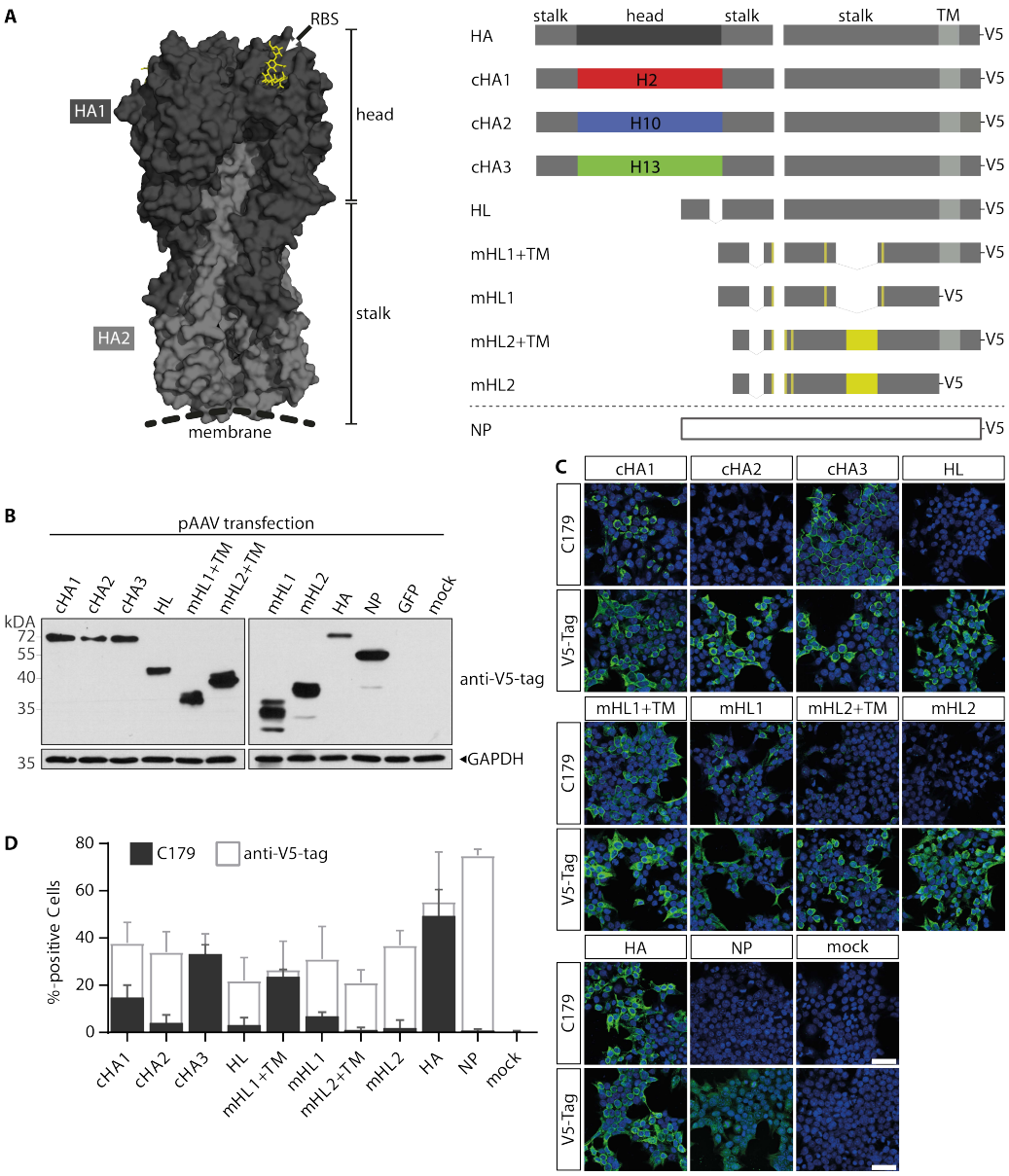

Figure 15: In vitro expression and HA-stalk conformation of the AAV-vectored antigens
(**A**) Three dimensional structure of a trimeric HA protein (PDB: 3UBE). HA1 (black) and HA2 (grey) subunits are indicated as well as the position of the RBS (yellow). The globular HA-head and the membrane proximal stalk domain are indicated. All antigens are based on sequences of A/California/7/2009 (H1N1)pdm virus. cHA1 contains the HA-head region of the HA from an avian H2N2 virus, while cHA2 contains the HA-head from an avian H10N7 and cHA3 from an avian H13N6 virus. While the HA-head region is deleted in headless HA, mHL1 and mHL2 contain further substitutions and/or deletion (yellow) to stabilize the conformation of the HA-stalk. Initially, of each mHL a version with (+TM) and without transmembrane domain was evaluated. All constructs carry a V5-tag at their C-terminus (V5). (**B**) Immunoblot analyses of 293T cell lysates 48 h after transfection with pAAV-vector plasmids. Expression of antigens was detected with anti-V5-tag antibody and equal loading was confirmed with anti-GAPDH antibody. (**C**) Immunofluorescence staining of 293T cells 48 h after transfection with AAV-vector plasmids. Cells were fixed, permeabilized and stained with the conformational HA-stalk antibody C179 or anti-V5-tag antibody and suited dye-conjugated secondary antibody (green). Nuclei are shown in blue (DAPI) (scale bar: 20 µm) (n=3). (**D**) Cells were transfected with pAAV-vector plasmids for 48 h, fixed, permeabilized and stained with C179 (filled bars) or anti-V5-tag (empty bars) antibody and suited dye-conjugated secondary antibody. Amount of antibody-positive cells was quantified by flow cytometry (mean+SD, n=3).

The transgene cassette is flanked by AAV2 ITR which enable transencapdsidation into the AAV9 capsid (Figure 13D). The constructs were named pAAV-HL, pAAV-cHA1, pAAV-cHA2 and pAAV-cHA3.

With the advent of stabilized headless HA, hereafter referred to as modified headless HA (mHL), antigen design concepts as described by Yassine *et al.* (mHL1) and Impagliazzo *et al.* (mHL2) were included at a later time point in the project as well (*297, 298*). These mHL contain substitution which for instance generate additional stabilizing disulfide bridges within the HA-trimer or remove polar and/or hydrophobic surfaces, the undesired exposure of which is associated with the removal of the HA-head. Furthermore, they contain stabilizing trimerization elements at the membrane proximal or distal part of the HA-stalk (*297, 298*).

In this thesis, the sequence alterations described in the aforementioned publications were adapted to the Cal/7/9 HA sequence. In contrast to the unmodified headless HA described by Steel *et al.*, Gen6 (Yassine *et al.*) is stabilized by several amino acid substitutions and deletions within the HA-stalk region, as well as fusion to a nanoparticle carrier, which maintains a native protein fold as shown in the original publication by binding to the conformational HA-stalk antibody CR6261 (*198, 297*). The construct #4900 (Impagliazzo *et al.*) contains a trimerization motif also at the membrane distal end of the HA-stalk in addition to other substitution which increase its stability (*288*). A native protein fold was assessed with the conformational antibodies CR6261 and CR9114 in the original publication (*198, 202, 298*). Due to the high conservation of the amino acids between the parental HA of Gen6 (A/New Caledonia/20/1999 (H1N1)) and #4900 (A/Brisbane/57/2007 (H1N1) and A/California/4/2009 (H1N1)pdm) and the Cal/7/9 HA, it was expected that the adaptation of the respective alterations to the Cal/7/9 HA would result in comparable antigen structures (*297, 298*). While the antigens described in the original publications represent secreted protein (coupled to a nanoparticle carrier in case of Gen6) a version of each mHL with and without the original Cal/7/9 HA transmembrane domain (TM) was generated (mHL+TM or mHL+TM). As with the antigens mentioned above, mHL were optimized to mammalian gene expression, synthesized *de novo* and inserted into the pAAV-vector (Figure 13C; Figure 15A). These constructs were designated pAAV-mHL1, pAAV-mHL1+TM, pAAV-mHL2 and pAAV-mHL2+TM.

High transgene expression could be verified for each antigen after transfection of cells with the pAAV-vector plasmids (Figure 15B). However, wildtype antigens HA and NP as well as mHL1 and mHL2 showed a somewhat higher expression level compared to the cHA, headless HA, mHL1+TM and mHL2+TM (Figure 15B). As mentioned in section 1.3.2, several HA-stalk binding antibodies, such as the prototypic C179, recognize conformational epitopes (*193*). Therefore, C179 was used to approximate whether the HA-stalk domain is folded correctly (Figure 15, C and D). Interestingly, apart from wildtype HA, only cHA3 and mHL1+TM were recognized by C179 comparable to the level of recognition seen with V5-tag antibody (Figure 15, C and D). While cHA1 and mHL1 showed reduced reactivity, the C179 epitope seems not to be intact in cHA2, headless HA, mHL2 and mHL2+TM (Figure 15D). Since mHL1+TM and mHL2+TM did show decreased *in vitro* antigen expression compared to their counterparts without TM, only mHL1 and mHL2 were pursued.

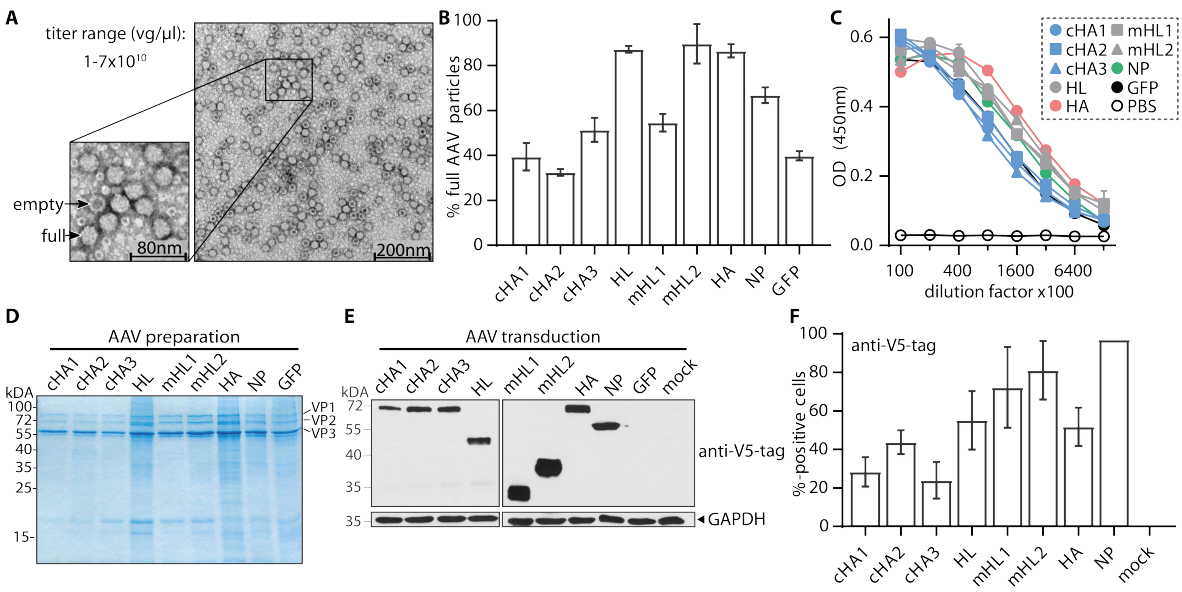

Figure 16: Quality analysis of AAV-vector stocks used for animal trials
(**A**) AAV-vector preparations were analyzed under a transmission electron microscope for impurities, particle dispersion and morphology (shown here: AAV-HA). qPCR titration of AAV-vector stocks yielded titers in the range of 10^{10} vg/µl. (**B**) Full and empty AAV particles were counted on the electron micrographs and a ratio was calculated (min. five pictures; mean±SD). (**C**) 2-fold serial dilutions of AAV-vector stocks were coated on ELISA plates. Intact particles were detected with the conformational AAV9-antibody ADK9 and suited secondary antibody (mean±SD of tech. duplicates, representative result). (**D**) 10 µl of each AAV-vector preparation were separated on SDS-PAGE and proteins were stained with coomassie. The position of the three AAV proteins (VP1, VP2, VP3) is indicated (representative result). (**E**) Immunoblot analyses of 293T cell lysates 72 h after infection with AAV-vectors at an MOI of 10^6. Expression of antigens was detected with anti-V5-tag antibody and equal loading was confirmed with anti-GAPDH antibody (n=3). (**F**) Cells were infected with AAV-vectors at an MOI of 10^6 for 72 h, fixed, permeabilized and stained with anti-V5-tag antibody and suited dye-conjugated secondary antibody. Amount of antibody-positive cells was quantified by flow cytometry (mean+SD, n=2 in tech. duplicates).

Initially, production of AAV-vector stocks was performed in suspension cells grown in spinner bottles (not shown). Although AAV-vector stocks produced that way were successfully used in the experiments outlined in Figure 17 to Figure 19, inter-stock variability prompted further optimization of the production and purification methodology. Finally, a streamlined purification protocol as depicted in Figure 12 was established, with which AAV-vector stocks could be reproducibly produced that contain high amounts of encapsidated viral genomes (vg) (Figure 16, A to D). Particle morphology and integrity of the preparations was assessed by electron microscopy (EM) as well as ELISA with the antibody ADK9, which is specific for intact AAV9 capsids (Figure 16, A and C) (*374*). All preparations contained nearly only intact AAV9 particles in the characteristical icosahedral shape. EM also revealed a high grade of dispersion within the preparation and a medium to high full to empty particle ratio, which will likely positively influence infectivity and immunogenicity (Figure 16, A and B). Coomassie staining of electrophoretically separated AAV-vector preparations together with EM data also indicated high purity of the preparation, while all three AAV capsid proteins (VP1, 2 and 3) could be clearly identified (Figure 16D). As expected, the AAV-vector preparations where highly infective *in vitro* and induced strong antigen expression (Figure 16, E and F). High infectivity and strong transgene expression *in vitro* suggested their suitability for vaccination of animals.

4.2. AAV-HA AND AAV-cHA ARE IMMUNOGENIC IN MICE AFTER INTRAMUSCULAR APPLICATION

To assess immunogenicity of AAV-HA, AAV-cHA and AAV-HL in mice, groups of three to five animals were immunized intramuscularly (i.m.) in three week intervals with $1x10^{10}$ vg according to the scheme depicted in Figure 17A. Different vaccination regimens were tested to evaluate the influence of antigen combinations on broadly reactive HA-stalk antibody responses (Figure 17B): Animals either received AAV-cHA (groups 1 & 2), AAV-HL (groups 7 to 9) or combinations thereof (groups 3 to 6). Additionally, groups of mice were immunized with AAV-HA (group 10) or AAV-GFP (group 11), the latter of which expresses the green fluorescent protein (GFP) and served as non-influenza related negative control antigen.

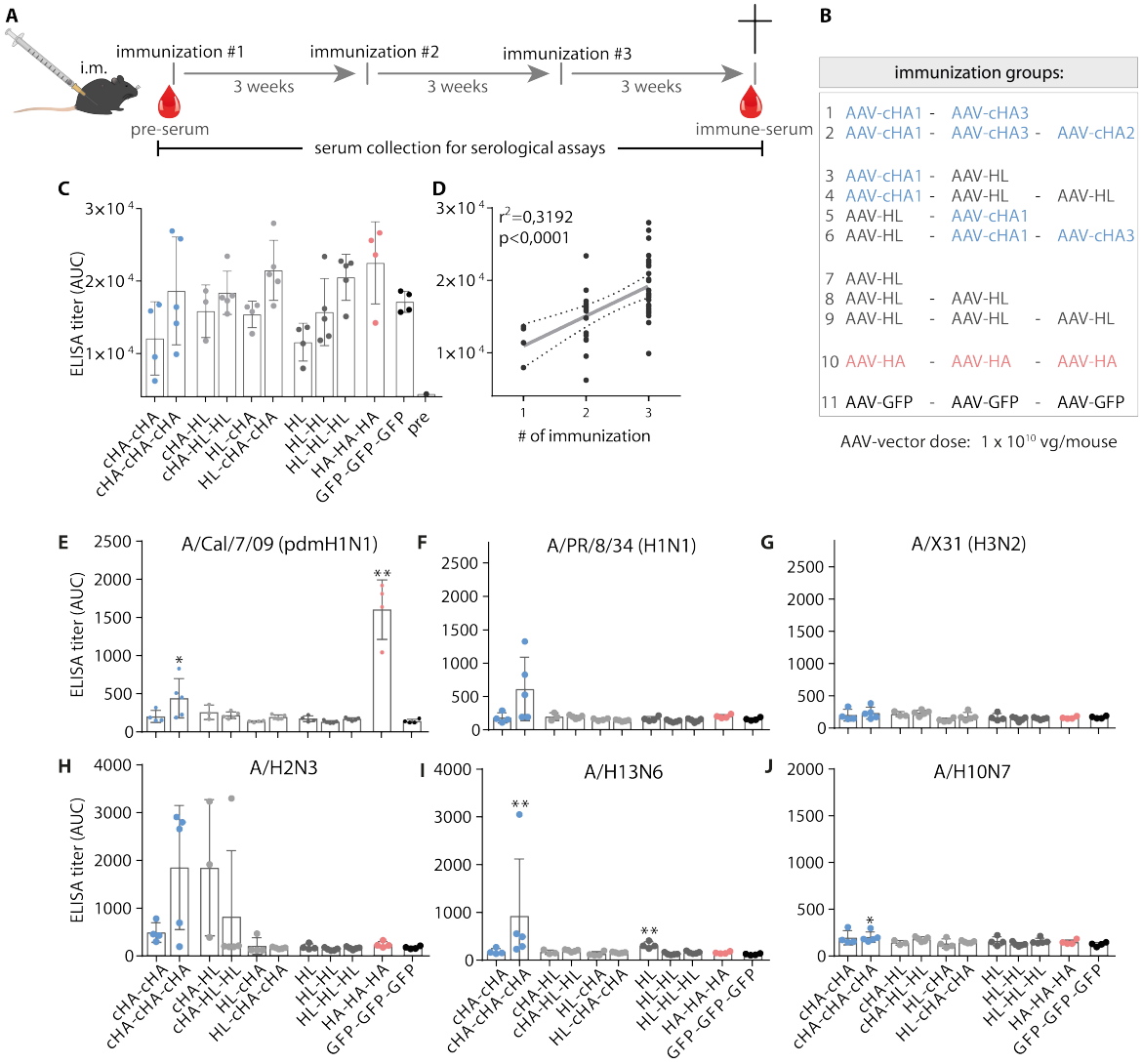

Figure 17: AAV-HA and AAV-cHA, but not AAV-HL is immunogenic in mice after intramuscular application
(**A**) 3 – 6 mice per group were immunized intramuscularly three times in three week intervals. Before the first (pre-serum) and after the last (immune-serum) immunization blood samples were drawn from the animals. (**B**) Immunization groups included in the study (**C**) AAV9-specifc total serum antibody ELISA titers expressed as area under the curve (AUC) (symbols: individual animals; bars: mean ± SD). (**D**) Correlation of AAV9-specific total antibody titers with number of received immunization (symbols: individual animals; line: linear regression curve, dotted lines: 95 % CI band) (**E** to **J**) ELISA titers of serum antibodies against the influenza virus indicated above each panel (symbols: individual animals; bars: mean ± SD). *p<0.05; **p<0.01 (in comparison to AAV-GFP)

Notably, although other studies suggest that the influence of an incorrectly folded HA-stalk domain on the immune response is negligible (*289*), cHA2 was placed at the end of the immunization schedule as this construct showed the least C179-binding (Figure 17B). Before the first (pre-serum) and after the last (immune-serum) immunization serum was obtained from the animals in which AAV9-specific total as well as influenza-specific total and neutralizing antibody titers were determined (Figure 17A).

As expected, all animals developed AAV9-specific serum antibodies which increased with the number of immunization (Figure 17, C and D). Furthermore, a significant increase of homologous Cal/7/9-specific antibodies were detectable in the groups immunized three times with AAV-cHA or AAV-HA (Figure 17E). All other groups remained Cal/7/9-negative, including those receiving only AAV-HL. Interestingly, AAV-cHA but not AAV-HA did also induce antibodies against PR8 and the parental viruses H2N3 and H13N6 (Figure 17F). However, no reactivity was seen against the H3N2 subtype viruses X31 and H10N7, indicating that the AAV-cHA induced broadly reactive antibodies are restricted to group 1 influenza A viruses (Figure 17, G and J). Intriguingly, an increase in antibody titers against H2N3 virus not only in the groups 1 & 2 but also in the groups 3 & 4, which received only a single immunization with AAV-cHA1 indicated that a one-shot vaccination with AAV-vectors might suffice to induce an at least virus-strain specific antibody response (Figure 17H).

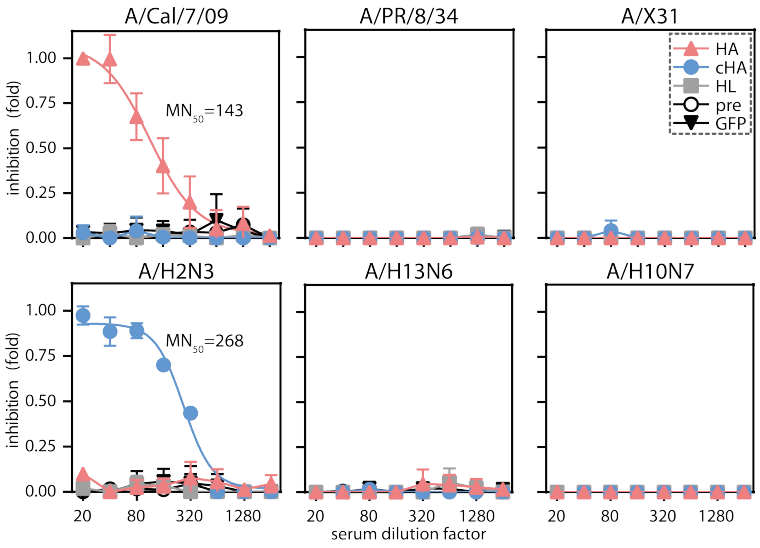

Figure 18: Intramuscular immunization induces strain specific neutralizing antibodies
2-fold serial dilutions of pooled serum were incubated with the virus indicated above each panel for 1 h and added to MDCKII cells for 1 h before cells were washed and fresh serum dilutions were added to capture putative post-attachment effects of serum antibodies as well. After 24 h, influenza virus antigen was detected by immuno-peroxidase staining. Inhibition was calculated, whereas a value of 1 means complete absence of infection. The MN_{50} value, i.e. the reciprocal serum dilution yielding 50 % inhibition, is indicated (mean ± SD, n=3; curve: non-linear regression curve).

No induction of broadly neutralizing serum antibodies against the aforementioned influenza viruses was seen in the groups receiving three AAV-vector immunizations (group 2, 9, 10, 11) (Figure 18). AAV-HA induced Cal/7/9-specific neutralizing antibodies, while AAV-cHA induced H2N3-specific neutralizing antibodies. Thus, neutralization was restricted to the virus whose HA-head was included in the prime immunization of the respective group (Figure 18). These results

indicated that i.m. immunization with AAV-HA and AAV-cHA induces a humoral response in mice while AAV-HL seems not to be immunogenic. Moreover, although AAV-cHA induced a more cross-reactive response, no cross-neutralization of multiple influenza virus subtypes was apparent, which was also the case for AAV-HA.

4.3. INTRANASAL IMMUNIZATION WITH AAV-VECTORS IS EFFECTIVE IN BOOSTING ANTIBODY RESPONSE IN MICE BEING NON-NAÏVE FOR AAV9

In an attempt to investigate the protective efficacy of the AAV-vectored vaccines against influenza virus challenge, another set of mice was immunized i.m. three times in three week intervals with $1x10^{10}$ vg of AAV-HA, AAV-cHA or AAV-HL (Figure 19A). The sequence of the AAV-cHA was changed to completely resemble the pattern of C179-binding to the respective cHA, i.e. AAV-cHA3 – AAV-cHA1 – AAV-cHA2 (Figure 15D). Unexpectedly, and in contrast to AAV-HA, after three i.m. immunizations during this trial no increase of influenza-specific antibody titers against Cal/7/9 was seen for the AAV-cHA and AAV-HL immunized groups (Figure 19B).

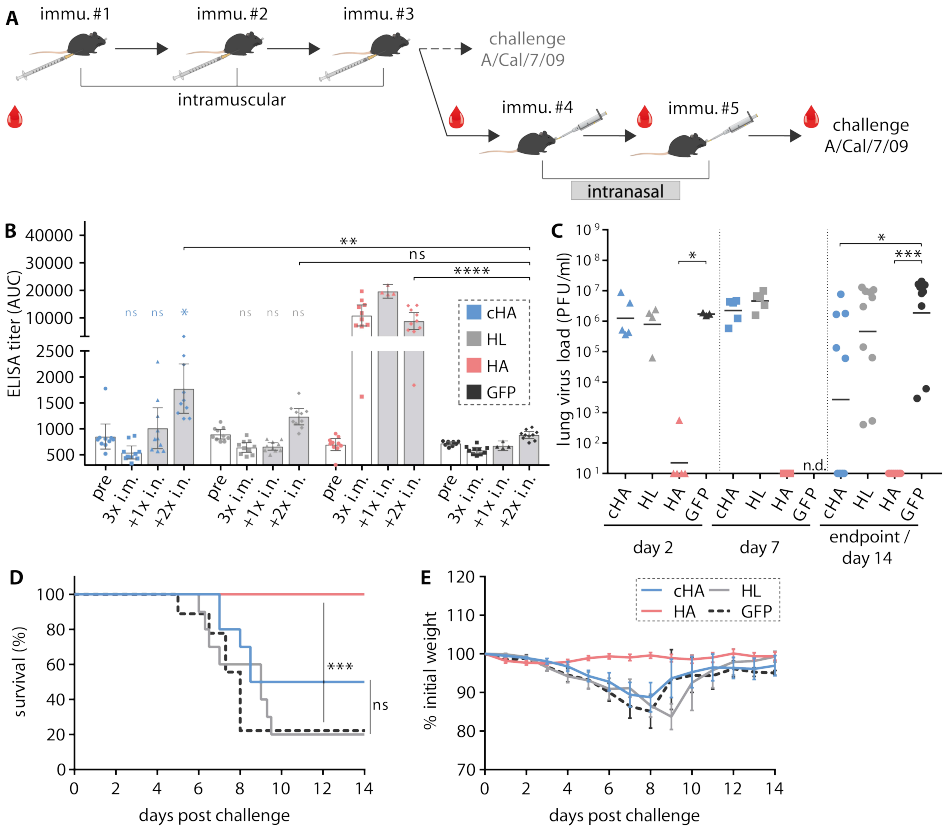

Figure 19: Intranasal application can boost antibodies in AAV-non-naive mice
(**A**) 10 mice per group were immunized intramuscularly three times in three week intervals. Before the first and after the last immunization blood samples were drawn from the animals. Since animals receiving AAV-cHA or AAV-HL were seronegative at this time point, animals were not challenged but further intranasal immunizations were given to these groups. During this period, too, blood samples were collected. After two additional intranasal immunizations, all animals were challenged with a lethal dose of Cal/7/9 and survival and weight loss was monitored. On day 2, day 7 or at the individual humane endpoint, lungs were collected and virus titers were determined. (**B**) Cal/7/9-specific total antibody ELISA titers (symbols: individual animals; bars: mean ± SD) (**C**) Lung virus titers as determined by plaque assay at the indicated time points (line: geometric mean; n.d.: not determined). (**D**) Kaplan-Meier plot of survival data. (**E**) Relative weight loss during challenge period (mean ± SEM). *p<0.05; **p<0.01; ***p<0.001; ****p<0.0001

Apparently, a peculiarity of AAV9 is its ability to be re-administrable to the respiratory tract even in the presence of high titers of AAV9 serum neutralizing antibodies that would otherwise preclude repetitive transduction with the AAV-vector (*369*). Thus, AAV-cHA and AAV-HL immunized mice were given two additional intranasal (i.n.) boosts containing the same amount of AAV-vector as before ($1x10^{10}$ vg) (Figure 19A). In fact, a boosting effect was seen in AAV-cHA immunized mice after the first i.n. immunization which resulted in a significant increase of Cal/7/9-specific antibody titers after the second boost (Figure 19B). No significant boosting effect was seen with AAV-HL. Interestingly, although AAV-HA immunized mice did not receive further immunizations, Cal/7/9-specific antibody titers were nearly unaffected by the longer time interval until challenge (about six month), underlining the beneficial effect of the durable AAV-mediated transgene expression on longevity of the immune response (Figure 19B).

At the end of the immunization period, mice were i.n. challenged with Cal/7/9 ($10^{2.9}$ $TCID_{50}$/mouse in 50 µl). At day two and seven post infection subsets of mice were euthanized and lung virus titers were determined (Figure 19C). Remaining animals were monitored for 14 days for survival and weight loss as this represents the main criteria for severity of influenza disease in mice (*384*). Lungs were harvested after a mouse reached a humane endpoint or at day 14 post infection and virus titers were determined. As indicated in Figure 19D, the challenge virus dose was only sub-lethal and led to 20 % survival in the AAV-GFP immunized animals. However, a significant protective effect was seen with AAV-HA immunization (100 % survival) which was associated with complete lack of weight loss in these animals (Figure 19, D and E). Correspondingly, except for one animal that had an above baseline lung virus titers at day two, all animals were negative for influenza virus already from day two on (Figure 19C). This sterile immunity is most likely induced by neutralizing antibodies against Cal/7/9 in AAV-HA immunized mice (data not shown). Reflecting the magnitude of influenza-specific antibody titers, AAV-cHA immunization induced partial protection which was also associated with a significantly reduced lung virus titer at day 14 (Figure 19, C to E). However, no sterile immunity was induced in these animals (Figure 19C). In contrast to that, no protection was seen with AAV-HL (Figure 19, D and E). These results indicated that i.n. application might be favorable over i.m. administration to induced protective antibody titers with AAV-cHA.

4.4. Intranasal AAV-vector immunization induce broadly reactive antibodies against influenza

Although the headless HA described by Steel *et al.* induced broadly protective immunity when it was applied as DNA/VLP-vaccine or protein antigen as described in the original studies, AAV-HL appeared completely non-immunogenic (see 4.2, 4.3) (*288, 289*). Recent reports by Yassine *et al.* and Impagliazzo *et al.* further underlined the great potential of the headless HA approach for the induction of a broadly protective immunity (*297, 298*). Their advantage over the headless HA described by Steel *et al.* might in part be the more native-like conformation of the HA-stalk (*288*). Hence, it was evaluated whether one of the modified headless HA would be immunogenic in the AAV-vector background.

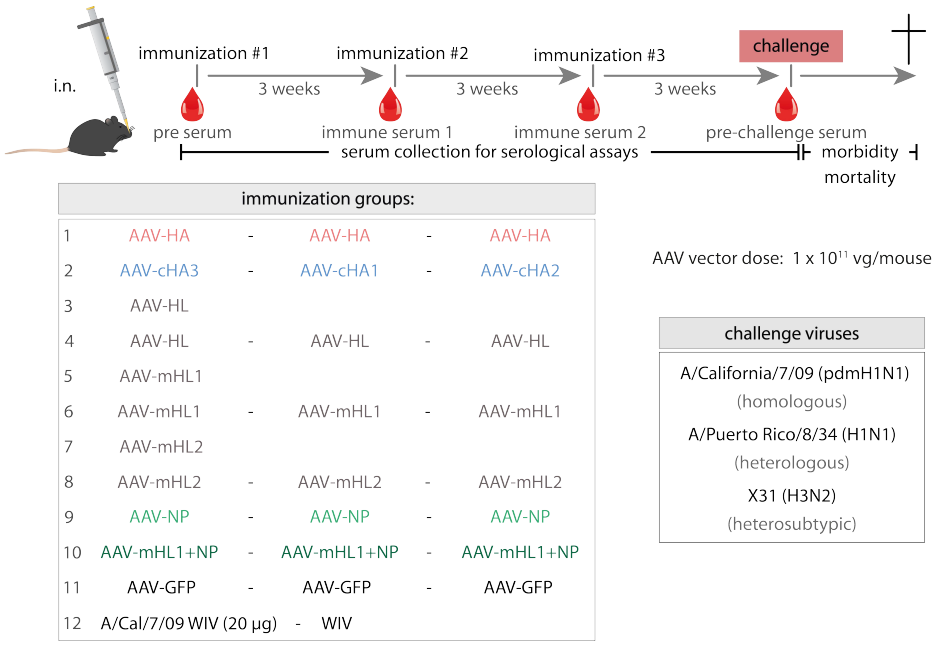

Figure 20: Immunization scheme for intranasal AAV-vector vaccination and challenge trial
Mice were intranasally immunized three times in three week intervals according the scheme depicted in the table. Before each and after the last immunization, blood samples were drawn from the animals which where pooled per group and time point for serological analysis. Three weeks after the last immunization, mice were challenge with Cal/7/9, PR8 or X31. During this time period, survival and weight loss was monitored.

AAV-vectors expressing Cal/7/9-adpated versions of the headless HA by Yassine *et al.* (Gen6; mHL1) and Impagliazzo *et al.* (#4900; mHL2) were constructed and their immunogenicity was evaluated and compared to AAV-HL in mice (*297, 298*). A lack of immunogenicity of a headless HA antigen has also been described in a MVA-vector background (*315*). Interestingly, in the respective study MVA-vectored expression of the headless HA together with NP did induce an immune response superior to the immune response seen with MVA-vectored NP alone, indicating a synergistic effect (*315*). To evaluate whether also the combination of AAV-vectored headless HA and NP would induce a synergistic effect, another experimental group receiving a bivalent AAV-mHL1 + AAV-NP (AAV-mHL1+NP) vaccine was included besides a group receiving monovalent AAV-NP (Figure 20).

Based on the results described in section 4.3, i.n. immunization was used in all following experiments. Mice were i.n. immunized in three week intervals with $1x10^{11}$ vg of AAV-vectors as outlined in Figure 20. Aside from groups receiving three times immunization with AAV-HA, AAV-cHA, AAV-mHL1+NP or AAV-NP, one group was vaccinated two times with Cal/7/9 whole inactivated virus vaccine (WIV), while animals receiving three times AAV-GFP served as negative control group. Though cHA require more than one immunization to refocus the immune response from the HA-head to the stalk domain, headless HA were shown to induce HA-stalk antibodies even after one immunization (Figure 10) (*298*). To evaluate whether this is possible with the AAV-vectored vaccines, AAV-HL, AAV-mHL1 or AAV-mHL2 groups received either one or three immunizations (Figure 20).

Before each and after the last immunization blood was taken from the animals (pre-serum; immune-serum 1, 2, and pre-challenge serum). Different parameters of humoral immunity as

specified in the sections below were determined. Three weeks after immunization #3 mice were challenged with homologous Cal/7/9 (H1N1)pdm, with heterologous PR8 (H1N1) or with heterosubtypic X31 (H3N2) virus (Figure 20).

As in the aforementioned experiment (see 4.2), all animals immunized with AAV-vectors developed high AAV9-specific serum antibody titers, which increased over time (Figure 21A). This was not the case in the WIV immunized group. AAV9-neutralizing serum antibody titers did correlate with total AAV9 antibody titers (Figure 21, B and C). In comparison to the groups receiving only one AAV-vector immunization, a boosting effect of AAV9 antibodies was apparent in groups receiving three immunizations (Figure 21A). This indicates that serum neutralizing antibodies did not preclude intranasal re-administration of the AAV-vector.

Influenza virus-specific total serum antibody binding was analyzed against a panel of ten viruses from both antigenic groups including viruses from subtypes circulating in humans (H1N1, H3N2), pandemic viruses ((H1N1)pdm from 2009 and 1918) and viruses bearing zoonotic potential (H7N9, H5N1) (Figure 22A). As expected, AAV-HA and AAV-NP showed the strongest increase and induced the highest endpoint total antibody titers against the homologous Cal/7/9-virus (Figure 22, B and C). Also, AAV-cHA and WIV induced significantly higher antibody titers against this virus compared to the AAV-GFP immunized control group (Figure 22B).

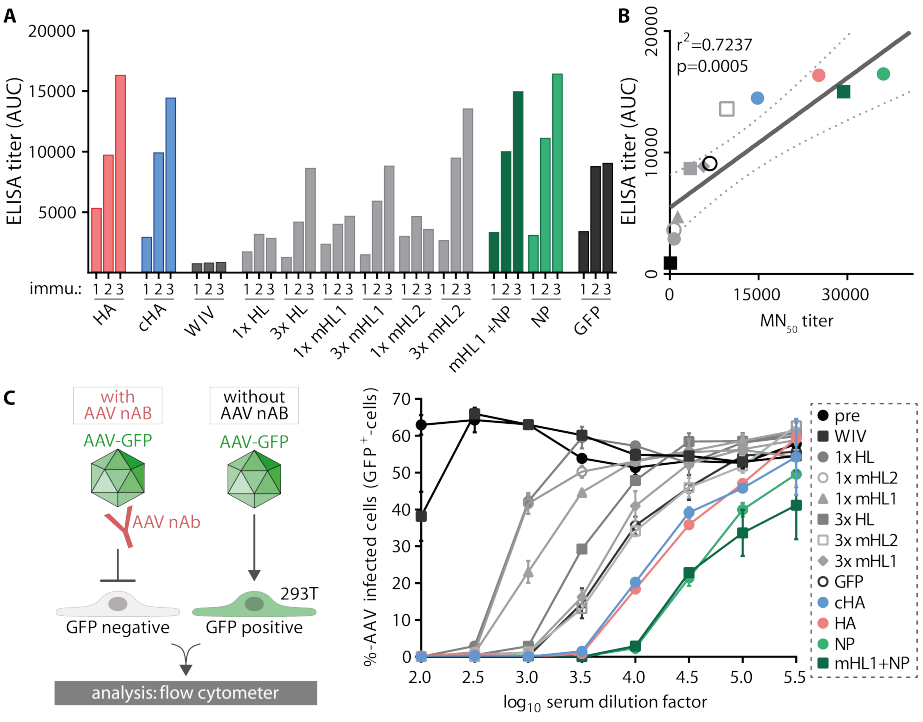

Figure 21: AAV total and neutralizing antibodies correlate with each other
(**A**) AAV9-specific total serum antibody ELISA titers in pooled sera at indicated time points. (**B**) Correlation of AAV9-specific total serum antibody ELISA titers and AAV9-specific neutralizing antibody titers (line: linear regression curve, dotted lines: 95 % CI band). (**C**) As indicated in the cartoon, AAV-GFP particles were incubated with serial dilutions of pooled pre-challenge serum for 1 h before they were added to 293T. After 48 h the number of GFP-positive cells was quantified by flow cytometry (mean ± SD of tech. duplicate, representative result). MN_{50} titers were determined as reciprocal serum dilution yielding 50 % inhibition.

Surprisingly, none of the groups immunized one or three times with AAV-HL, AAV-mHL or AAV-mHL2 mounted antibody titers against the homologous or any other virus (Figure 22B). Also, contrasting the report by Hessel *et al.*, the combination of AAV-mHL1 + AAV-NP did only induce antibodies specific for NP but had otherwise no synergistic effect on the antibody response (Figure 22H). It appears that there might be a general barrier to an AAV-based immunization strategy employing headless HA. Thus, AAV-HL, AAV-mHL1, AAV-mHL2 and AAV-mHL1+NP were not included in the analysis described in the following sections.

As shown in Figure 22, D to G, AAV-HA, AAV-NP, AAV-cHA and WIV induced broadly reactive antibodies. AAV-HA induced antibodies reacted strongest with viruses from the H1N1 subtype, including the pandemic virus from 1918, and was otherwise restricted to group 1 influenza A virus subtypes, e.g. H5N1 (Figure 22D).

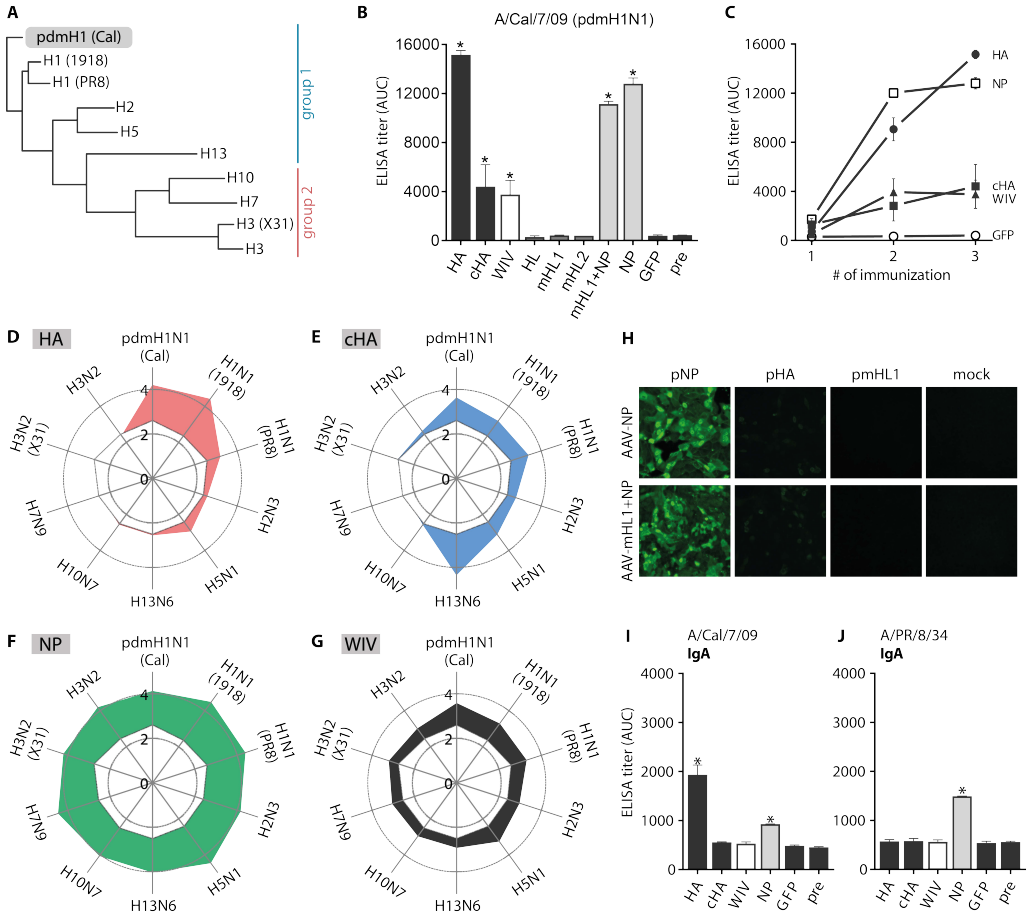

Figure 22: AAV-HA, AAV-cHA, AAV-NP and WIV induced broadly reactive antibodies

(**A**) Phylogenetic tree of influenza viruses used for serological analysis. (**B**) Cal/7/9-specific total antibody ELISA titers in pooled pre-challenge sera (mean ± SD of tech. replicate). (**C**) Cal/7/9-specific total antibody ELISA titers in pooled serum over time (mean ± SD of tech. replicate). (**D** to **G**) Total antibody ELISA titers in pooled pre-challenge sera against the influenza viruses indicated at the end of each axis of the web-diagram (colored area: specific reactivity of the immune serum indicated above each web-diagram; white area in center: background sero-reactivity of AAV-GFP group). (**H**) Immunofluorescence staining of MDCKII cells 48 h after transfection with the plasmids expressing the antigen indicated above each panel. Cells were fixed, permeabilized and incubated with pooled pre-challenge serum of AAV-NP or AAV-mHL+NP immunized animals and suited secondary antibody (green) (n=2) (**I** and **J**) Cal/7/9- (I) or PR8-specific IgA antibody ELISA titers in pooled pre-challenge sera (mean ± SD of tech. replicate). *p<0.05 (in comparison to AAV-GFP)

The AAV-cHA induced antibodies, though binding less strongly to viruses from the H1N1 subtype compared to AAV-HA, showed overall a stronger binding intensity to all other group 1 viruses (Figure 22E). However, both AAV-cHA and AAV-HA induced antibodies did not react with group 2 viruses. Interestingly, AAV-NP and WIV induced antibodies reacted with all tested influenza viruses including H3N2 and H7N9 viruses (Figure 22, F and G). However, binding intensity was weaker for the WIV compared to the AAV-NP immunized group.

IgA antibodies were shown to confer potent protection against respiratory pathogens due to their transudation into the respiratory mucosa (*125*). Here, serum IgA levels were analyzed, which can serve as a crude estimator for mucosal IgA levels, which might in fact be even higher. Interestingly, Cal/7/9-specific serum IgA were only found in animals immunized with AAV-HA or AAV-NP, whereas broadly reactive IgA against PR8 were only detected in AAV-NP immunized animals (Figure 22, I and J).

In summary, these results indicate that i.n. immunization with AAV-vectors efficiently induced influenza-specific immune responses even in the presence of high titers of AAV9-neutralizing serum antibodies. Intriguingly, binding breadth of the antibodies varied depending on the antigen used for immunization.

4.5. BROADLY REACTIVE ANTIBODIES ARE NON-NEUTRALIZING IN VITRO

To analyze the functionality of the antibody response, several serological analyses were performed, which are described in the following sections.

First, hemagglutination inhibition (HAI) and neutralizing antibody titers in the sera were determined. HAI^{pos} antibodies, which block the RBS and interfere with attachment, currently represent the gold standard for evaluation of influenza vaccine immunogenicity. Neutralizing antibodies, however, do not necessarily bind to the RBS, but might inhibit later steps of the viral replication cycle as well (*208*). To measure effects on the late replication cycle, a modified version of a classical microneutralization (MN) assay was performed (*375*).

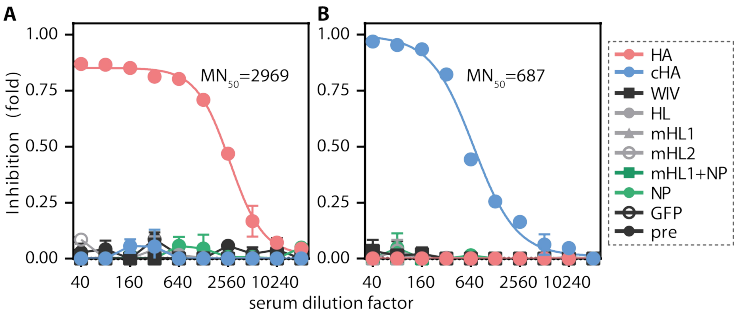

C

		HA	cHA	WIV	NP	GFP	pre
pdmH1N1	HAI	640	<40	<40	<40	<40	<40
(A/Cal/7/09)	MNT_{50}	2794	<40	<40	<40	<40	<40
H1N1	HAI	<40	<40	<40	<40	<40	<40
(A/PR/8/34)	MNT_{50}	<40	<40	<40	<40	<40	<40
H3N2	HAI	<40	<40	<40	<40	<40	<40
(A/X31)	MNT_{50}	<40	<40	<40	<40	<40	<40
H13N6	HAI	<40	160	<40	<40	<40	<40
	MNT_{50}	<40	1047	<40	<40	<40	<40

Figure 23: MN-positive and HAI-positive antibodies act virus strain specific
(**A** and **B**) 2-fold serial dilutions of pooled pre-challenge sera were incubated with Cal/7/9 (A) or H13N6 (B) virus for 1 h and added to MDCKII cells for 1 h, before cells were washed and fresh serum dilutions were added. After 24 h, Influenza virus antigen was detected by immuno-peroxidase staining. Inhibition was calculated and the MN_{50} value is indicated (mean ± SD of tech. replicate; curve: non-linear regression curve). (**C**) Mean HAI and MN_{50} titers (n=2-3 in tech. duplicates) in pooled pre-challenge sera against the indicated viruses.

Here, serum antibodies are not only present during attachment, but constantly throughout the viral replicative cycle. HAI^{pos} and MN^{pos} antibodies against Cal/7/9 could only be detected in sera of mice immunized with AAV-HA (Figure 23, A and C). However, these antibodies were strain specific and no other tested viruses from the H1N1 (PR8), H3N2 (X31) or H13N6 subtype could be inhibited or neutralized (Figure 23C). Sera from AAV-cHA immunized mice were HAI^{pos} and MN^{pos} against H13N6, but negative towards all other tested viruses (Figure 23, B and C). Notably, as the H13 HA-head domain is included in cHA3, the AAV-cHA immunized group encounters the H13 HA-head domain during their prime immunization (Figure 20A). Unexpectedly, WIV did not induce any HAI^{pos} or MN^{pos} antibodies. AAV-NP and AAV-GFP were negative in these assays (Figure 23C). Thus, HAI^{pos} and MN^{pos} antibodies seem to be specific for the HA-head domain of the virus which is encountered during the first immunization, resembling data obtained in the first immunogenicity study (Figure 18, Figure 23).

4.6. AAV-HA AND AAV-CHA INDUCE ANTIBODIES AGAINST THE HA-HEAD AND HA-STALK DOMAIN

Induction of antibodies against the HA-head and HA-stalk domain.

The absence of broadly reactive HAI^{pos} and MN^{pos} serum antibodies suggested the presence of other antibody specificities against regions apart from the RBS or classical antigenic sites within the HA-head region (see 1.2.4). Therefore, the binding specificities of the AAV-vector vaccine induced HA-specific serum antibodies were determined in more detail.

First, differences in binding of the serum antibodies to the HA1 and HA2 subunit of four different viruses from the H1N1 subtype spanning more than 90 years of influenza virus evolution were analyzed via immunoblots (Figure 24A). HA1 contains the HA-head domain, whereas most of the stalk is contained within HA2. Beforehand, the input virus amount loaded on the SDS-PAGE was adjusted to yield equal intensities of HA2 after detection with a commercially available HA2-specific antibody (Figure 24B; anti-HA2 (ctrl.)). Notably, all sera were tested in the same dilution (1:500) allowing comparison of the relative abundance of the respective antibodies recognizing HA1 and HA2 between the vaccine groups. AAV-HA induced sera detected the HA1 subunit of Cal/7/9 (pdm2009) and of A/Brevig Mission/1/1918 (pdm1918), but not of PR8 (1934) and another seasonal H1N1 virus, A/Brisbane/59/2007 (2007) (Figure 24B). This differential binding pattern to HA1 reflects the closer phylogenetic relationship between the amino acid sequences of both the complete HA proteins and the HA1 subunit of the pandemic viruses from 2009 and 1918 compared to the viruses from 1934 and 2007 (Figure 24, A and C). In contrast to that, the highly conserved HA2 domain of all four H1N1 viruses could be detected by antibodies in the AAV-HA induced sera (Figure 24, B and C).

The presence of antibodies against HA1 and HA2 in the AAV-HA sera could also be verified in an epitope screen with overlapping 15-mer peptides of the Cal/7/9 HA (Figure 24, E to G). Five surface exposed peptides were identified which reacted significantly stronger with AAV-HA serum compared to AAV-GFP serum (Figure 24G).

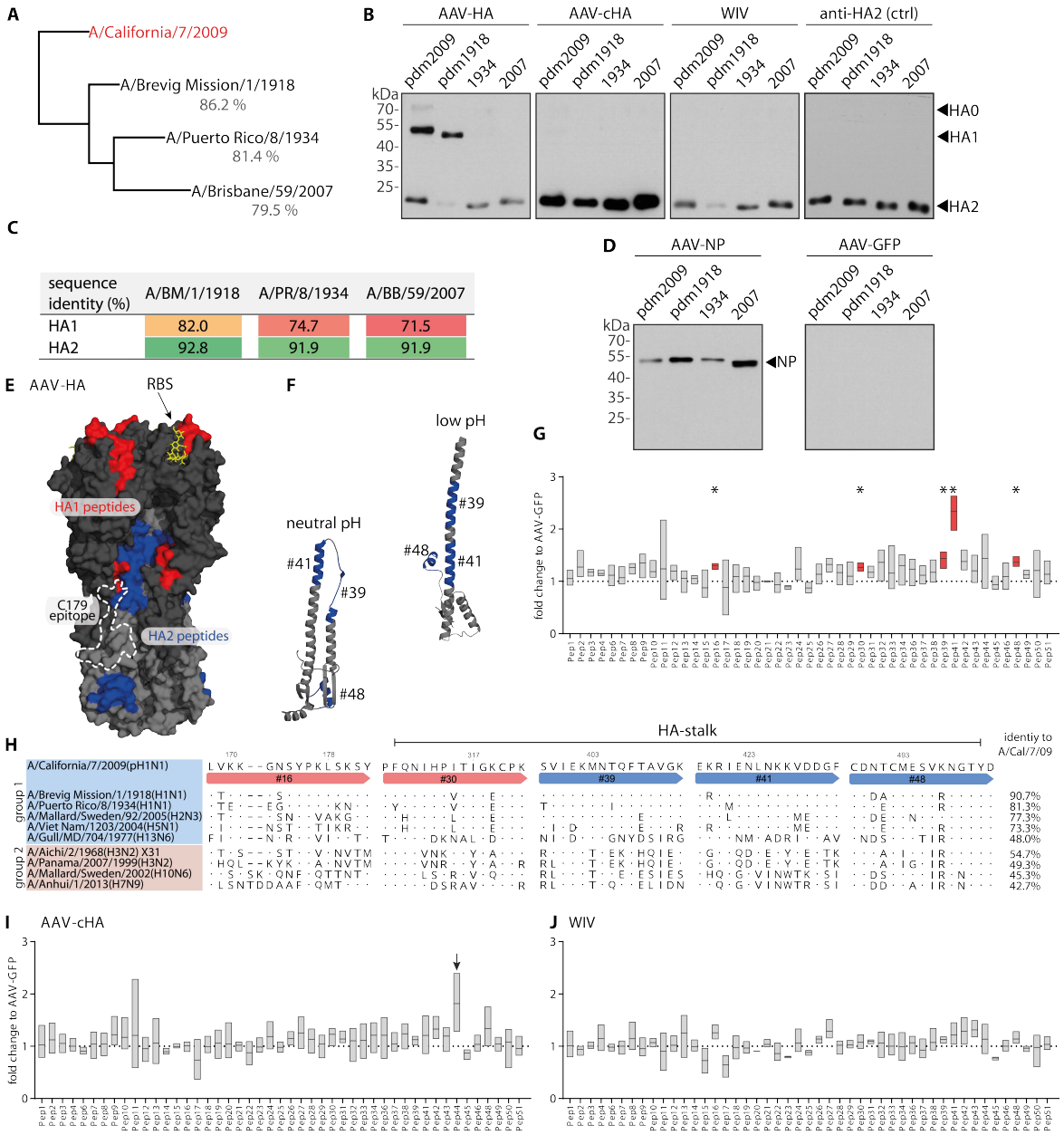

Figure 24: Induction of distinct antibody binding specificities

(**A**) Phylogenetic tree with sequence identities of the complete HA sequences of the H1N1 viruses used for immunoblot analysis. (**B**) Immunoblot analysis of purified H1N1 viruses separated under denaturing conditions. Uncleaved HA0 and the cleavage products HA1 and HA2 were detected with 1:500 diltuion of pooled pre-challenge serum indicated above each panel. Beforhand, loading was normalized to yield comparable signals with an commercial anti-HA2 antibody (n=3). (**C**) Sequence identity of HA1 and HA2 of the indicated viruses compared to Cal/7/9. (**D**) Immunoblot analysis as shown in (B). NP was detected with AAV-NP pooled pre-challenge serum. AAV-GFP pooled pre-challenge serum served as negative control (n=3). (**E**) Significant peptides identified with the epitope screen with AAV-HA pooled pre-challenge sera were mapped onto HA1 (red) and HA2 (blue) of the trimeric HA (PDB: 3UBE). The position of the RBS (yellow) and the C179 epitope (dashed line) is indicated. (**F**) Epitopes #39, #41 which were identified in the epitope screen with AAV-HA are located at the upper end of the alpha-helices, while epitope #48 is located at the membrane proximal end (blue). Upon conformational changes of HA2, the alpha-helical structure of peptide #41 and #48 seems to be maintained. (**G**) Results of the 15-mer Cal/7/9 peptide screen with AAV-HA pooled pre-challenge serum. Data is shown as fold change over AAV-GFP signal (n=3 in tech. duplicates). *p<0.05. Floating bars represent mean and range. (**H**) Amino acids at the positions identified in the peptide screen with AAV-HA serum in the HA sequence of the influenza viruses used for serological assays. The amino acid identity to the Cal/7/9 sequence of the peptides in the HA-stalk compared to Cal/7/9 sequence is indicated. (**I** and **J**) Results of the 15-mer Cal/7/9 peptide screen with AAV-cHA or WIV pooled pre-challenge serum. Arrow points at the stronger but non-significant binding peptide #44 (I).

Mapping of those peptides onto the three dimensional structure of H1N1 HA revealed that the identified epitopes include the RBS (HA1; peptide #16; amino acid positions 168-182), an epitope at the lateral site of the head locate in a cleft between two HA monomers (HA1 + HA2; peptides #30 and #39/#41; amino acid positions 308-322, 398-412, and 418-432), and one epitope at the membrane proximal end of the HA-stalk domain (HA2; peptide #48, amino acid positions 488-502) (Figure 24E). Apparently, upon structural changes of HA2 as consequence of a pH change, only the conformation of peptide #39 seems to change, while peptides #41 and #48 remain in their alpha helical structure (Figure 24E) (see below). Furthermore, the amino acid positions in the HA-stalk identified in the epitope screen appeared to be more conserved among group 1 influenza A viruses with which AAV-HA induced serum reacted in the aforementioned ELISA analyses compared to group 2 viruses (Figure 24H, Figure 22). This might explain the limitation of reactivity towards group 1 influenza A viruses seen with the AAV-HA induced sera (Figure 22).

As expected, AAV-cHA induced very strong HA2-specific antibodies that reacted with all four viruses in the immunoblot analysis (Figure 24B). Interestingly, also WIV induced an HA2-specific antibody response which, however, was weaker compared to AAV-cHA. No significantly binding peptides could be identified in the epitope screen with these sera, which might reflect lower overall antibody titers in the AAV-cHA and WIV sera (Figure 24, I and J). However, with AAV-cHA sera one non-surface exposed peptide (#44) appeared to show a trend towards increased binding compared to AAV-GFP control group (1.8-fold increase, p-value: 0.128, Figure 24I).

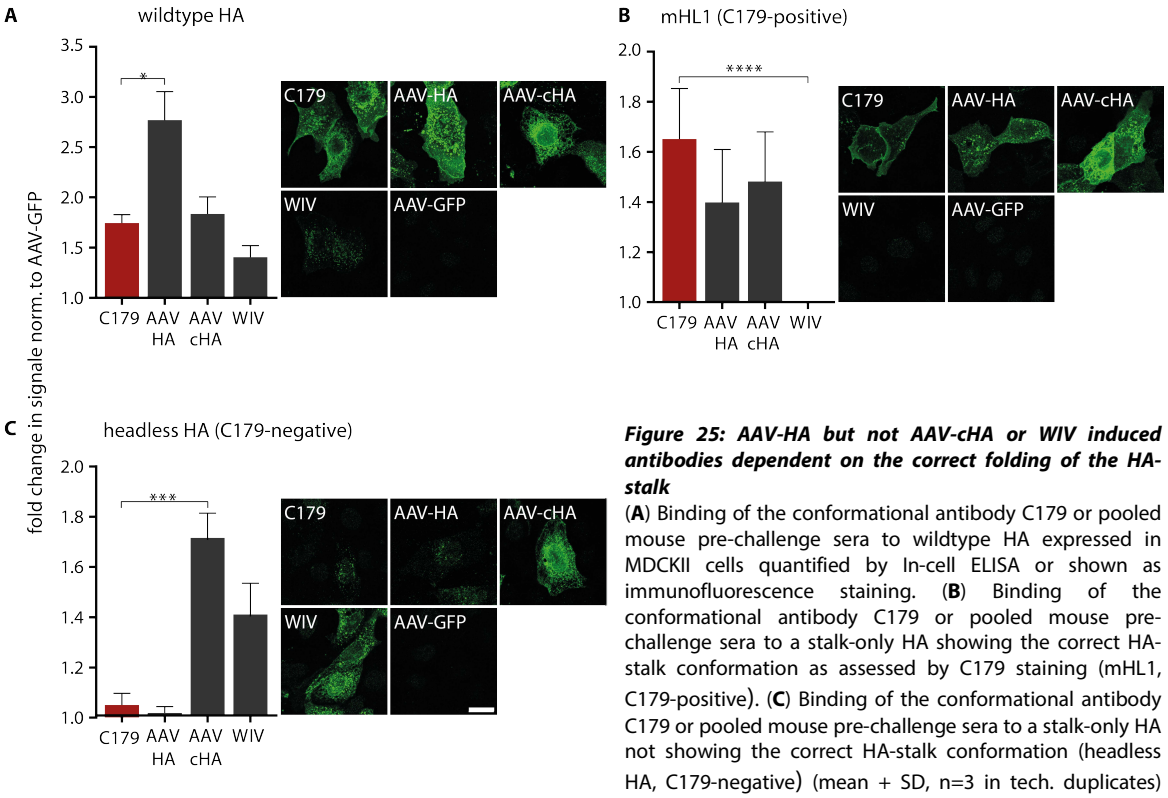

Figure 25: AAV-HA but not AAV-cHA or WIV induced antibodies dependent on the correct folding of the HA-stalk

(**A**) Binding of the conformational antibody C179 or pooled mouse pre-challenge sera to wildtype HA expressed in MDCKII cells quantified by In-cell ELISA or shown as immunofluorescence staining. (**B**) Binding of the conformational antibody C179 or pooled mouse pre-challenge sera to a stalk-only HA showing the correct HA-stalk conformation as assessed by C179 staining (mHL1, C179-positive). (**C**) Binding of the conformational antibody C179 or pooled mouse pre-challenge sera to a stalk-only HA not showing the correct HA-stalk conformation (headless HA, C179-negative) (mean + SD, n=3 in tech. duplicates) (scale bar: 20 µm). *p<0.05; ***p<0.01, ****p<0.001

Dependence on conformation of the HA-stalk domain on antibody binding

Several HA-stalk reactive antibodies, such as the prototypic C179, recognize conformational epitopes (*193*). To assess the influence of conformation of the HA-stalk on serum antibody reactivity binding was assessed by immunofluorescence and quantified via in-cell ELISA to different HA-antigens either showing the correct HA-stalk conformation (wildtype HA and mHL1) or not (headless HA) as indicated by C179-binding (Figure 15, Figure 25, A to C). Interestingly, AAV-HA sera resembled the binding profile of C179, as binding was only apparent to the correctly folded stalk (Figure 25). However, results from the immunoblot analyses shown in Figure 24B, which was done under denaturing conditions indicate that in polyclonal context of the serum also non-conformational antibodies must be present. In addition to the results shown in Figure 24 binding to mHL1 lacking the H1 head region further validates that AAV-HA immunization in fact induced HA-stalk reactive antibodies (Figure 25, B and C).

AAV-cHA induced sera reacted with all tested antigens irrespective of the conformation of the HA-stalk (Figure 25). WIV induced sera behaved comparable to AAV-cHA induced sera, with the only difference that no binding to the truncated mHL1 was detectable, indicating that mHL1 might lack the major epitope recognized by antibodies in WIV induced sera (Figure 25, A to C).

Influence of pH-dependent conformational changes on antibody binding

Upon acidification of the endosome HA needs to undergo a major conformational change which eventually results in fusion of the viral and endosomal membrane and release of the viral genome into the cytoplasm (Figure 5).

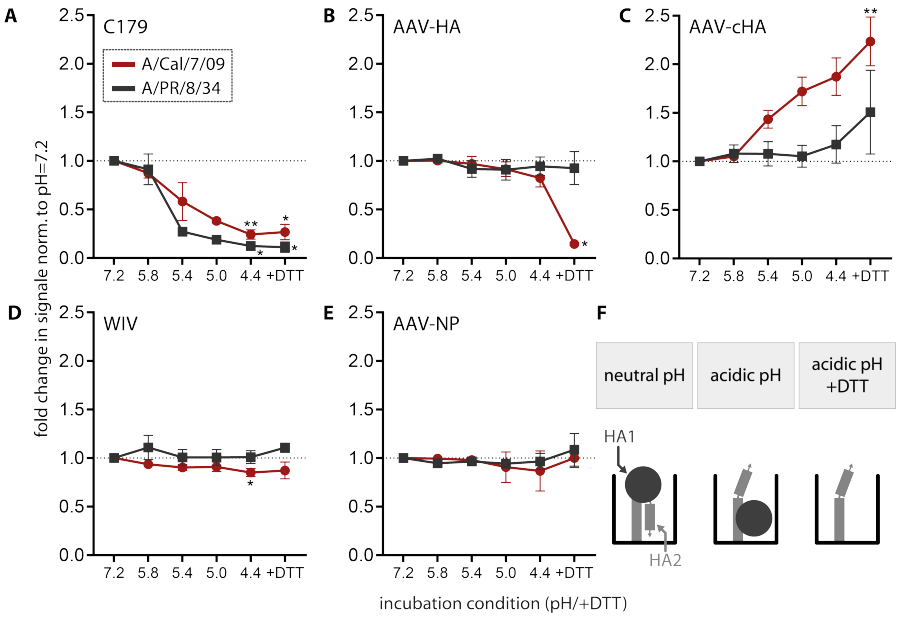

Figure 26: AAV-HA and AAV-cHA induced sera bind differentially to the pre- and post-fusion HA-stalk
(**A** to **E**) Binding of C179 (A) or AAV-HA (B), AAV-cHA (C), WIV (D) or AAV-NP (E) pooled pre-challenge sera to Cal/7/9 or PR8 virus particles which were pre-incubated at pH=7.2, 5.8, 5.4, 5.0, 4.4 or 4.4 + DTT, to induced pH-dependent conformational changes in HA or to remove the HA1 subunit (+DTT) (mean + SD, n=3 in tech. duplicates). (**F**) Schematic principle of the experiment. Upon acidification conformational changes are induced in HA2 which lead to the exposition of the fusion peptide. By the addition of the reducing agent DTT disulfide bonds between HA1 and HA2 are solved and HA1 can be removed from the system by washing. Conformational antibodies such as C179 do not recognize the low pH form of HA (A). *p<0.05, **p<0.01 (in comparison to pH=7.2)

As mechanism to inhibit viral replication, some HA-stalk specific antibodies were shown to interfere with theses conformational changes (see 1.3.3) (*200*). To execute this effect, HA-stalk reactive antibodies require to recognize the HA pre-fusion conformation are required. Thus, binding of mouse sera to HA at a pH-range from neutral (7.2) to acidic (4.4) was analyzed to determine the presence of antibodies binding to the pre- and/or post-fusion HA-stalk region. Additionally, the reducing agent DTT was added at acidic pH to remove the HA1 subunit from the HA protein (Figure 26F).

As expected, already at a slightly acidic pH=5.4 binding of C179 to HA of Cal/7/9 or PR8 virus particles was reduced and the removal of HA1 (+DTT) had no further effect (Figure 26A). Sera induced by AAV-HA bound to Cal/7/9 HA unless HA1 subdomain was removed, indicating that binding to the homologous HA is mediated mainly by antibodies directed against the HA-head domain (Figure 26B). Removal of HA1 had, however, no effect on AAV-HA induced serum binding to PR8 (Figure 26B). This further supported the findings from the immunoblot analysis, which already indicated that binding to PR8 by AAV-HA induced sera is mainly mediated by antibodies against HA2 (Figure 24). Interestingly, AAV-HA induced stalk antibodies did, unlike C179, bind also to the low pH conformation of HA (Figure 25, A and B). This corroborates the aforementioned findings from the immunoblot analysis that AAV-HA induced sera contain non-conformational antibodies which apparently recognize epitopes that appear not to be largely restructured upon acid induced conformational changes of HA (Figure 24F).

Intriguingly, AAV-cHA induced sera reacted even stronger with the low pH conformation of HA, indicating that some otherwise buried epitopes might become more accessible upon conformational change (Figure 26C). In fact, peptide #44, which showed increase reactivity in the epitope screen with AAV-cHA induced serum, is not exposed on the surface of HA, but located at the interior of the trimeric HA-stalk (data not shown). Hence, it might become more accessible during conformational change of the HA resulting in increased reactivity (Figure 26C). WIV induced antibody binding did not vary with pH or after the addition of DTT which was also the case for AAV-NP sera (Figure 26, D and E).

These results showed that AAV-HA was the only vaccine to induce antibodies against the HA-head and –stalk of H1N1 viruses including those used for the challenge infections, while AAV-cHA and unexpectedly WIV did induce stalk antibodies.

4.7. Non-neutralizing antibodies activate Fc-gamma receptors

As shown in section 4.5, MN^{pos} and HAI^{pos} antibodies could be detected in AAV-HA and AAV-cHA immunized mice. These antibodies, however, reacted virus strain-specific (Figure 23). Broadly binding to non-homologous virus strains thus seems to be mediated by HAI^{neg} and MN^{neg} antibodies. These antibodies might execute their protective effect via different mechanisms such as FcR-mediated effector functions, including ADCC or ADP (*95, 96, 223*). Therefore, it was analyzed whether the influenza-specific serum antibodies could activate FcγR employing a recently developed reporter assay which allows for separate measurement of the activation of the four murine FcγRI, IIB, III and IV (*225*) (Figure 27A, see 3.8.7). As shown in Figure 27B, all vaccines induced Cal/7/9-specific antibodies that could activate all four murine FcγR.

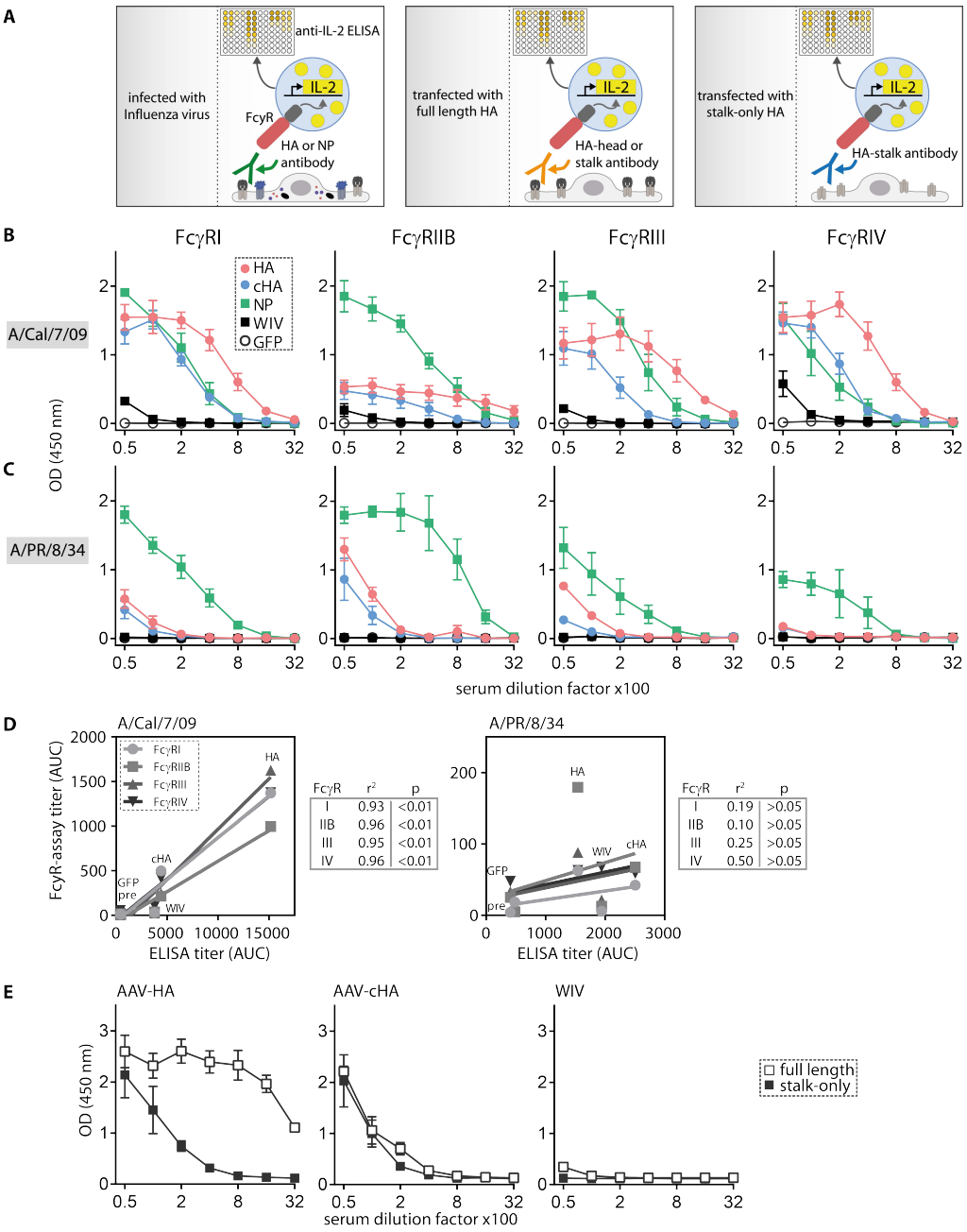

Figure 27: AAV-vectored but not inactivated vaccines broadly activate FcγR
(**A**) Schematic drawing of the principle of the different settings of the FcγR-assay. MDCKII cells were either infected with influenza viruses (left), which allows measurement of FcγR-activating antibodies against any viral protein, or transfected with full length HA (middle), which allows measurement of HA-specific antibodies against the head and the stalk, or transfected with a stalk-only HA (right), which allows measurement of HA-specific antibodies against the stalk. FcγR-cells and read-out of the assay (IL-2 ELISA) is the same with each setup. (**B**) Cal/7/9 virus-specific activation of murine FcγRI, FcγRIIB, FcγRIII or FcγRIV by antibodies in pooled pre-challenge sera. (**C**) PR8 virus-specific activation of murine FcγRI, FcγRIIB, FcγRIII or FcγRIV by antibodies in pooled pre-challenge sera. (mean ± SEM, n=3 in tech. duplicates) (**D**) Linear regression between serum ELISA titer and FcγR assay titer against the influenza virus indicated above each panel. (**E**) Activation of FcγR-IV by antibodies against the full-length HA or a stalk-only HA in the pooled pre-challenge sera indicated above each panel. (mean ± SEM, n=2 in tech. duplicates)

However, AAV-HA, AAV-NP and AAV-cHA led to an overall stronger activation compared to WIV. On the contrary, only the AAV-vectored vaccines but not WIV did induce PR8-specific FcγR-activating antibodies (Figure 27C). Notably, PR8 FcγR-activating antibody and total antibody titers did not correlate (Figure 27D). Thus, AAV-HA and AAV-cHA vaccination

induced higher amounts of broadly-reactive FcγR-activating antibodies in proportion to total antibodies than WIV vaccination (Figure 27D). Interestingly, AAV-NP vaccination induced antibodies showed unexpectedly potent FcγR-activation against Cal/7/9 and PR8 and also appeared to activate the inhibitory FcγRIIB more potently compared to the HA-antibodies induced by AAV-HA and AAV-cHA (Figure 27, B and C).

Initially it was proposed in the literature that only HA-stalk antibodies rely on activation of FcγR to execute their protective effect. However, this view has recently been changed and now acknowledges that apparently all broadly reactive antibodies require activation of FcγR to mediate protection (*223*). To dissect HA-head and -stalk specific FcγR-activating antibody activities, the experimental setup of the FcγR-assay was modified. In contrast to the setup described above, in which MDCK cells where infected with influenza viruses and, thus, express all influenza proteins, uninfected MCDK cells were transfected either with full length HA (pAAV-HA) or a stalk-only construct lacking the HA-head (pAAV-mHL1+TM) (Figure 27A). Since the HA-stalk domain is present in both setups serum-specific differences in the activation of the FcγR-assay are likely due to the presence of additional non-stalk-binding FcγR-activating antibodies. In fact, in the sera of AAV-HA immunized mice a signal increase was apparent when the FcγR assay was performed with full length HA compared to the stalk-only construct, indicating that antibodies against sites that are only present in the context of the full length HA, e.g. the HA-head, can activate FcγR, too (Figure 27E). In contrast to that, AAV-cHA sera, which contain only HA-stalk antibodies, yielded comparable signals under both experimental conditions. WIV induced signals were barely above background level.

These results indicate that vaccination with AAV-HA, AAV-cHA and AAV-NP leads to a more potent induction of broadly reactive FcγR-activating antibodies compared to WIV. Furthermore, AAV-HA, unlike AAV-cHA, induced FcγR-activating antibodies against the HA-head and -stalk domain of H1N1 viruses.

4.8. AAV-HA, AAV-cHA AND AAV-NP BUT NOT WIV INDUCE BROADLY PROTECTIVE IMMUNITY

To evaluate the extent and breadth of protection of the AAV-vectored vaccines, immunized mice were infected with lethal doses of homologous Cal/7/9, heterologous PR8 or heterosubtypic X-31 (H3N2) viruses. Survival and weight loss was monitored during a 14 days period. Mice reaching 20 % weight loss were euthanized and lungs were collected to determine the virus load by plaque assay. Eventually, surviving mice were euthanized at 14 days post infection and lungs were harvested, too.

After challenge with Cal/7/9, 100 % of AAV-HA, AAV-NP and AAV-mHL1+NP immunized mice were protected, while all mice of the negative control (AAV-GFP) succumbed to the infection by day eight (Figure 28A). AAV-cHA and WIV immunized animals were partially protected (80 %; 4/5). Interestingly, whereas animals of all other groups showed a mean maximum weight loss of up to 10 %, AAV-HA immunized animals did not lose weight (Figure 28, B and C). This is most likely due to the presence of neutralizing antibodies conferring sterile immunity only in these animals (Figure 23C). However, as expected, all animals surviving the challenge period were able to eventually clear the virus from their lungs (Figure 28D).

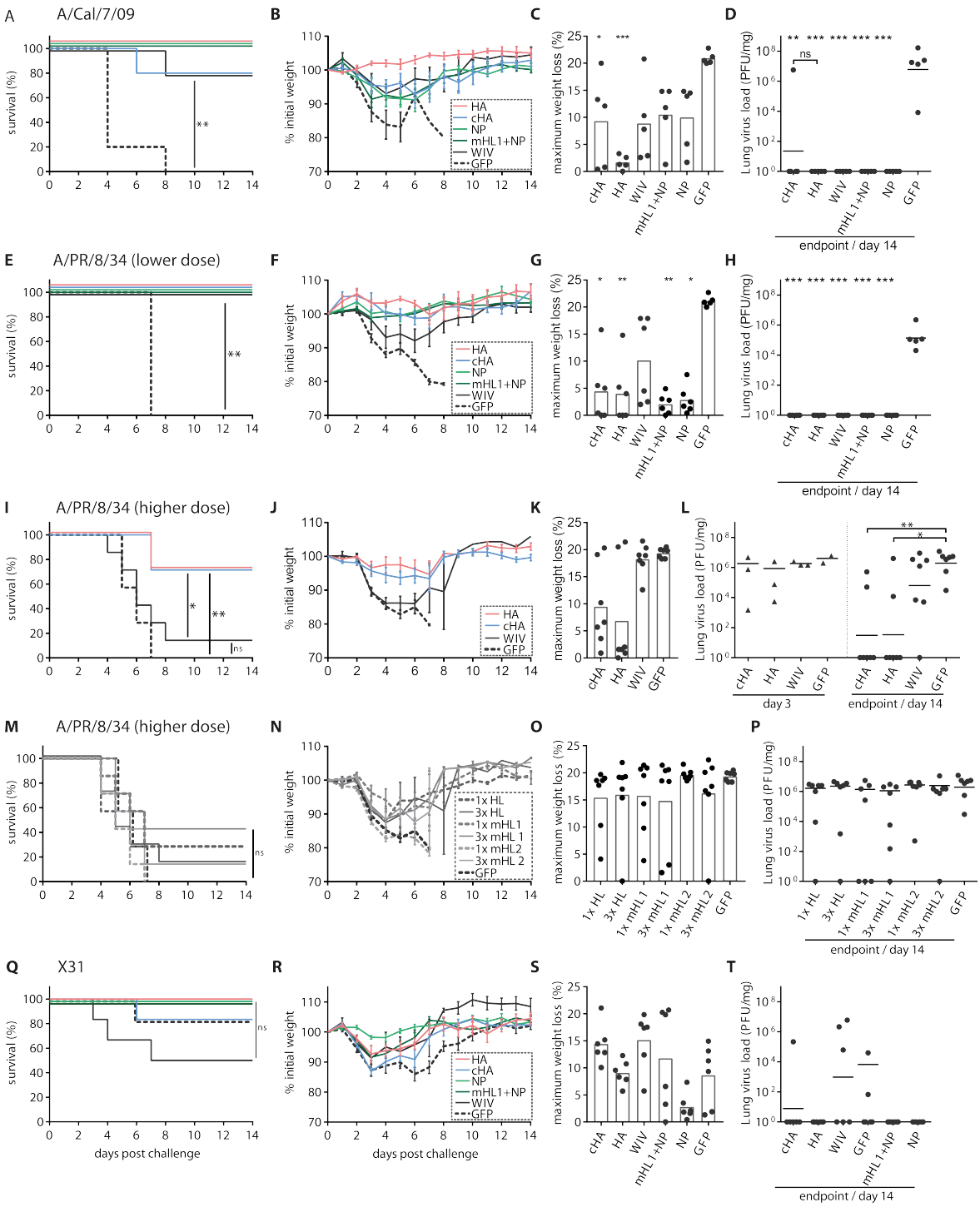

Figure 28: AAV-HA, AAV-cHA and AAV-NP protect against homologous and heterologous challenge

(**A** to **D**) Kaplan-Meier plots (A), relative weight loss (B), maximum weight loss (C) and lung virus titers at the individual endpoint or at 14 days post infection (D) of mice infected with Cal/7/9. (**E** to **H**) Kaplan-Meier plots (E), relative weight loss (F), maximum weight loss (G) and lung virus titers at the individual endpoint or at 14 days post infection (H) of mice infected with the lower dose of PR8. (**I** to **L**) Kaplan-Meier plots (I), relative weight loss (J), maximum weight loss (K) and lung virus titers at day 3 post infection, the individual endpoint or at 14 days post infection (L) of AAV-HA, AAV-cHA, WIV or AAV-GFP immunized mice infected with the higher dose of PR8. (**M** to **P**) Kaplan-Meier plots (M), relative weight loss (N), maximum weight loss (O) and lung virus titers at the individual endpoint or at 14 days post infection (P) of AAV-HL, AAV-mHL1, AAV-mHL2 or AAV-GFP immunized mice infected with the higher dose of PR8. (**Q** to **T**) Kaplan-Meier plots (Q), relative weight loss (R), maximum weight loss (S) and lung virus titers at the individual endpoint or at 14 days post infection (T) of mice infected with X31. (weight curves: mean ± SEM, max. weight loss bars: mean, lung virus titers lines: geometric mean). $^{ns}p \geq 0.05$, *$p < 0.05$, **$p < 0.01$, ***$p < 0.001$ (in comparison to AAV-GFP, or as indicated)

Next, heterologous protection against another H1N1 strain, PR8, was evaluated. Although being 100 % lethal for AAV-GFP immunized mice, this first challenge with a lower dose of PR8 did not reveal any differences regarding survival of the vaccinated groups (Figure 28E). However, WIV vaccinated animals did show an increased mean maximum weight loss of up to 10 %, while all AAV-vector immunized animals did show an only moderate mean maximum weight loss of about 3 - 4.5 %, which was significantly less compared to the AAV-GFP group (21 %) (Figure 28, F and G). As seen for the Cal/7/9 challenge, all surviving animals were eventually able to clear the virus also in the absence of neutralizing antibodies against PR8 (Figure 28H, Figure 23C).

To evaluate the influence of HA-specific non-neutralizing antibodies on survival, the heterologous PR8 challenge was repeated with a higher virus dose. Here, the majority (71 %; 5/7) of the AAV-HA and AAV-cHA immunized animals were protected from the infection (Figure 28I). This was also reflected by less mean maximum weight loss of only up to 10 % seen in surviving animals from these groups (Figure 28, J and K). In contrast, all AAV-GFP immunized animals had to be euthanized and only one WIV immunized animal survived the challenge with the higher PR8 dose, with both groups showing increased mean maximum weight loss of about 18-19 % (Figure 28, I to K). Notably, a single AAV-GFP immunized animal survived the PR8 challenge without weight loss and any sign of disease, and furthermore remained PR8 seronegative (data not shown), suggesting a failure during inoculation of the challenge virus. This one animal was therefore excluded from the analyses. During the second PR8 challenge a subset of animals was sacrificed on day three post infection to analyze the course of viral replication during the challenge period. Interestingly, all animals showed comparable virus titers in their lungs at this early time point, indicating that due to the lack of PR8-specific neutralizing antibodies no sterile immunity was achieved (Figure 28L). However, at the end of the challenge period, only AAV-HA and AAV-cHA immunization led to significantly reduced virus titers in the lungs of the mice compared to AAV-GFP (Figure 28L). AAV-HL, AAV-mHL1 and AAV-mHL2 immunized groups were challenged with the higher dose of PR8, too. As expected, due to the complete lack of a vaccine induced influenza-specific immune response, none of the animals was protected, which was associated with severe weight loss and uncontrolled virus replication in the lungs (Figure 28, M to P).

Finally, a heterosubtypic challenge infection with X31 was performed. Unfortunately, the used challenge dose was set too low and induced only 17 % lethality in the negative control group (AAV-GFP, 1/6) (Figure 28Q). In fact, lethality was more pronounced in the WIV immunized animals (50 %, 3/6). 100 % of the AAV-HA, AAV-NP and AAV-mHL1+NP immunized mice were protected while AAV-cHA immunization protected 83 % (5/6). Interestingly, AAV-NP immunized animals did show very little mean maximum weight loss compared to the other groups, indicating a protective effect which is however concealed by the too low challenge dose (Figure 28, R and S). Correspondingly, virus replication was not detectable in animals surviving the challenge (Figure 28T).

In summary, these results show that AAV-HA, AAV-cHA and AAV-NP immunization reduced symptom severity and showed superior protective effect against homologous and heterologous challenge compared to vaccination with the inactivated virus vaccine.

4.9. AAV-VECTOR IMMUNIZATION HAS A PROTECTIVE EFFECT IN FERRETS

Ferrets have become the gold standard animal model for research on influenza, as they are naturally susceptible to the virus, and the clinical course of infection resembles aspects of the human disease including fever, lethargy, as well as signs of upper and lower respiratory tract infection (*385*). This is in part due to the comparable distribution of the influenza virus receptors in the respiratory tract of ferrets and humans.

Consequently, the ferret model has not only been used to assess virulence of emerging pandemic strains, which is of high public health relevance, but also to evaluate a series of avant-garde vaccines including approaches using different kinds of broadly reactive antigens and/or virus vectors (*276, 278, 281, 297, 366*) (see 1.3.7). However, so far an active vaccination strategy employing AAV-vectors in ferrets has not been described in the literature.

Thus, to evaluate whether AAV-vectored vaccines expressing HA are immunogenic and protective in ferrets, groups of four ferrets were immunized intranasally three times in four week intervals with $1.875x10^{12}$ vg of AAV-HA, AAV-cHA or AAV-GFP (Figure 29A). As a control, one group received twice an intramuscular application of the human seasonal quadrivalent inactivated vaccine (QIV) of season 2017/2018 (*Influsplit Tetra*). Notably, the H1N1 component of the seasonal vaccine has been changed from Cal/7/9 to A/Michigan/45/2015 (H1N1)pdm. However, ferret convalescent sera raised against Cal/7/9 reacted undistinguishably also with Michigan/45/2015 (*386*). Before each and after the last immunization, serum samples were obtained from the animals. Animals were challenged with a non-lethal dose of the early (H1N1)pdm isolate A/Mexico/InDRE4487/2009 which has been shown to be highly virulent in ferrets (*387*). During the following three days, ferrets were monitored daily for clinical signs of influenza including changes in activity and respiratory signs. Also, temperature and body weight were measured daily and nasal wash samples were obtained in which virus titers were determined. At day three post infection animals were sacrificed and nasal turbinates, trachea and lungs were collected and either processed for titration of virus or histological examination (Figure 29A).

Interestingly, not only the QIV immunized but also some of the animals which were immunized with AAV-HA or AAV-cHA remained AAV9 seronegative throughout the vaccination period (Figure 29B). Nevertheless, all ferrets of the aforementioned groups mounted robust total antibody titers against Cal/7/9, which constantly and significantly increased over time only in AAV-HA immunized animals (Figure 29C). Resembling data obtained in mice only AAV-HA vaccination induced HAI^{pos} and MN^{pos} antibodies against Cal/7/9, which could also cross-neutralize A/Michigan/45/2015 (Figure 29D).

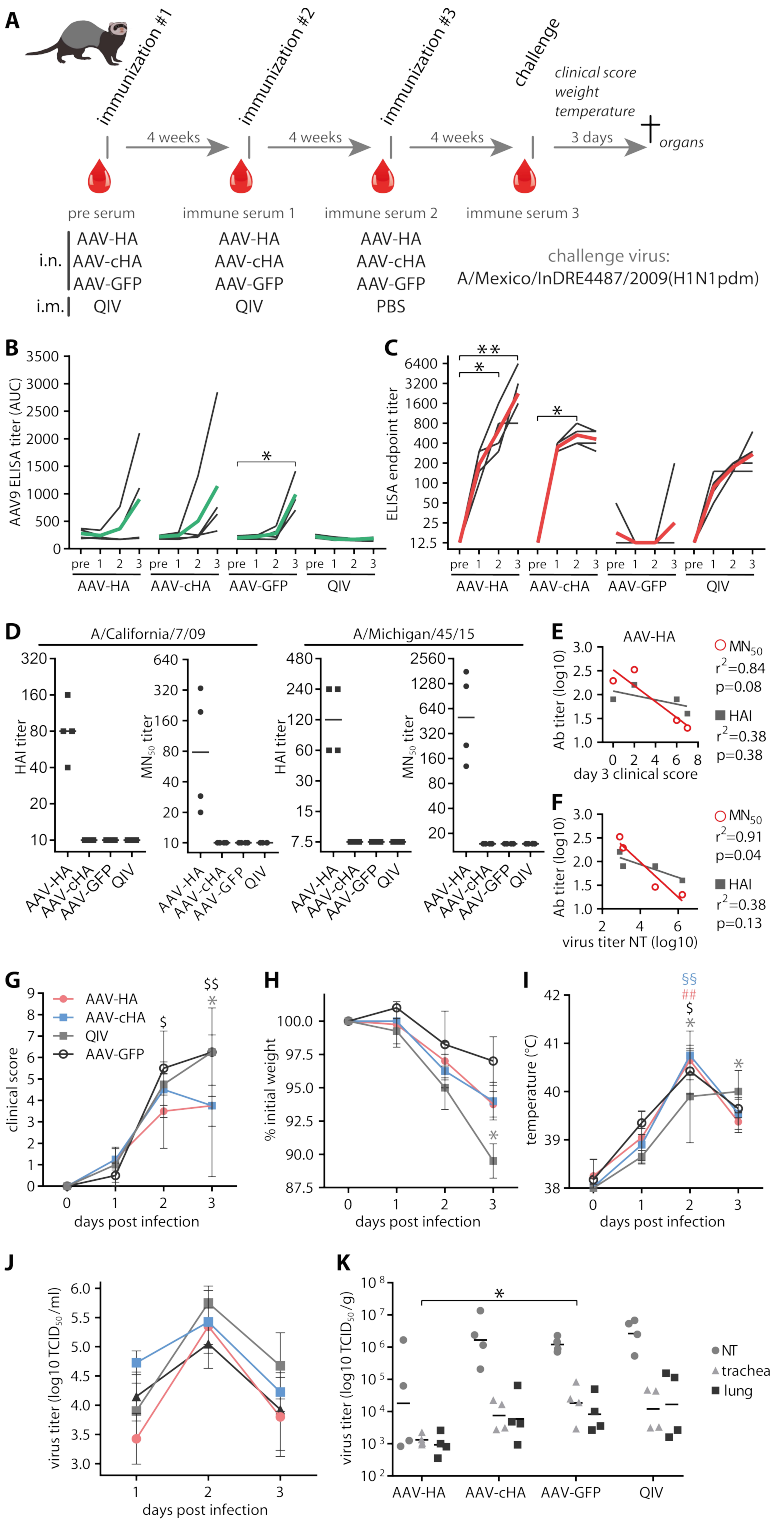

Figure 29: AAV-HA and AAV-cHA show symptomatic protection in ferrets

(**A**) Four ferrets per group were intranasally immunized three times in four week intervals with AAV-HA, AAV-cHA or AAV-GFP. A control group was intramuscularly immunized two times with the inactivated influenza vaccine of season 2017/18 (*Influsplit tetra*) (QIV). Before each and after the last immunization, serum was obtained from the animals in which serological parameters were analyzed. All ferrets were challenged with 10^5 $TCID_{50}$ an (H1N1)pdm virus. During the three days challenge period clinical signs, body temperature and weight was measured. Nasal washes were performed daily. At day three post infection all animals were sacrificed and nasal turbinates, trachea and lung was harvested. (**B**) AAV9-specific antibody response in individual ferret sera over time (black lines: individual animals, green lines: mean). (**C**) Cal/7/9-specific antibody response in individual ferret sera over time (black lines: individual animals, red: mean). (**D**) HAI and MN_{50} titers of individual ferrets against the virus indicated above the panels (line: geometric mean). (**E**) Correlation of HAI or MN_{50} titer with day 3 clinical score of AAV-HA immunized animals. The coefficient of correlation (r^2) and p-value is indicated to the right. (**F**) Correlation of HAI or MN_{50} titer with virus titers in nasal turbinates (NT) of AAV-HA immunized animals. (**G**) Mean clinical signs as expressed by a clinical score over time (mean ± SD). AAV-GFP: $^{\$}p<0.05$, $^{\$\$}p<0.01$; QIV: *p<0.01 (compared to day 0). (**H**) Mean body temperature over time (mean ± SD). AAV-HA: $^{\#\#}p<0.01$; AAV-cHA: $^{\S\S}p<0.01$; AAV-GFP: $^{\$}p<0.05$; QIV: *p<0.05 (compared to day 0). (**I**) Mean relative weight loss over time (mean ± SD). QIV: *p<0.05 (compared to day 0). (**J**) Virus titers in nasal washes over time (mean ± SD). (**K**) Virus titers at day three post infection in homogenates of nasal turbinates (NT), trachea and lung as determined by $TCID_{50}$ assay (line: geometric mean). *p<0.05, **p>0.01

Upon challenge with influenza virus, all animals rapidly developed signs of influenza, including serous nasal exudation, congestion, frequent sneezing and wheezing and depression (Figure 29G). However, only AAV-GFP (2 and 3 dpi) and QIV (3 dpi) immunized animals showed a significant increase of clinical score over time (Figure 29G). From day two on, AAV-HA and AAV-cHA immunized animals started to recover as evidenced by a regain of normal activity

and improvement of respiratory signs (Figure 29G). With AAV-HA immunized animals, higher MN^{pos} or HAI^{pos} serum antibody titers were associated with lower clinical scores (Figure 29E).

Upon infection, all animals lost weight irrespective of the immunization (Figure 29H). However, only QIV immunized animals showed a significant weight loss over time (about 10 % at 3 dpi) (Figure 29H). Weight loss in AAV-HA and AAV-cHA immunized was more moderate (about 6 %), and unexpectedly AAV-GFP immunized animals lost least weight (3 %) (Figure 29H). Fever peaked in all animals at day two post infection (Figure 29I). While the body temperature was no longer increased statistically significant at 3 dpi compared to the initial value in AAV-HA, AAV-cHA and AAV-GFP immunized animals, QIV immunized animals still had significantly higher temperature at this time point (Figure 29I). Prominent virus replication in the respiratory tract was apparent in all animals, corresponding to the fact that clinical signs of influenza were seen in all animals, too. Nasal wash titers peaked on 2 dpi in all groups but otherwise revealed no marked differences between the groups (Figure 29J). Nevertheless, AAV-HA immunized ferrets showed reduced virus titers in tissue homogenates of the nasal turbinates, trachea and lung, while all other groups showed comparable and high virus titers (Figure 29K). In fact, reduced virus replication in the upper respiratory tract (i.e. nasal turbinates) was associated with higher MN^{pos} or HAI^{pos} serum antibody titers in AAV-HA immunized ferrets (Figure 29F).

Immuno-histochemical staining of influenza virus antigen revealed, too, that none of the animals was completely negative for virus replication (Figure 30, A to D). However, influenza virus antigen was detectable in lower amounts in the submucosal glands and the bronchi of AAV-HA immunized animals compared to all other groups (Figure 30, A, B, D). Interestingly, AAV-cHA immunized animals showed slightly increased antigen detection in these tissues compared to QIV and/or AAV-GFP (Figure 30, A, B, D). Lungs of AAV-HA immunized animals did show reduced virus antigen detection compared to animals from AAV-cHA or QIV groups. Unexpectedly, the lungs of AAV-GFP immunized animals seemed to be spared from influenza virus replication (Figure 30, C and D).

Also, histopathological changes were analyzed and scored. All ferrets developed typical signs of an influenza virus induced bronchio-interstitial pneumonia at varying degrees of severity. Damage of bronchi and bronchiols was most pronounced in AAV-GFP immunized animals, while lesions of lung interstitium as well as submucosal glands were more severe in AAV-cHA and QIV immunized animals (Figure 30E). Ferrets receiving AAV-HA appeared to show less severe lesions of the conducting airways and the lung compared to animals from the other groups. Furthermore, more prominent hyperplasia of type II pneumocytes was apparent in AAV-cHA and QIV vaccinated groups resulting in increased surfactant production and immigration of alveolar macrophages (Figure 30F). Interestingly, although the induction of bronchus-associated lymphoid tissue (BALT) could be observed in AAV-cHA and QIV immunized animals to a high extent, AAV-HA immunized animals only showed moderate BALT formation and it was completely absent in AAV-GFP immunized animals (Figure 30G).

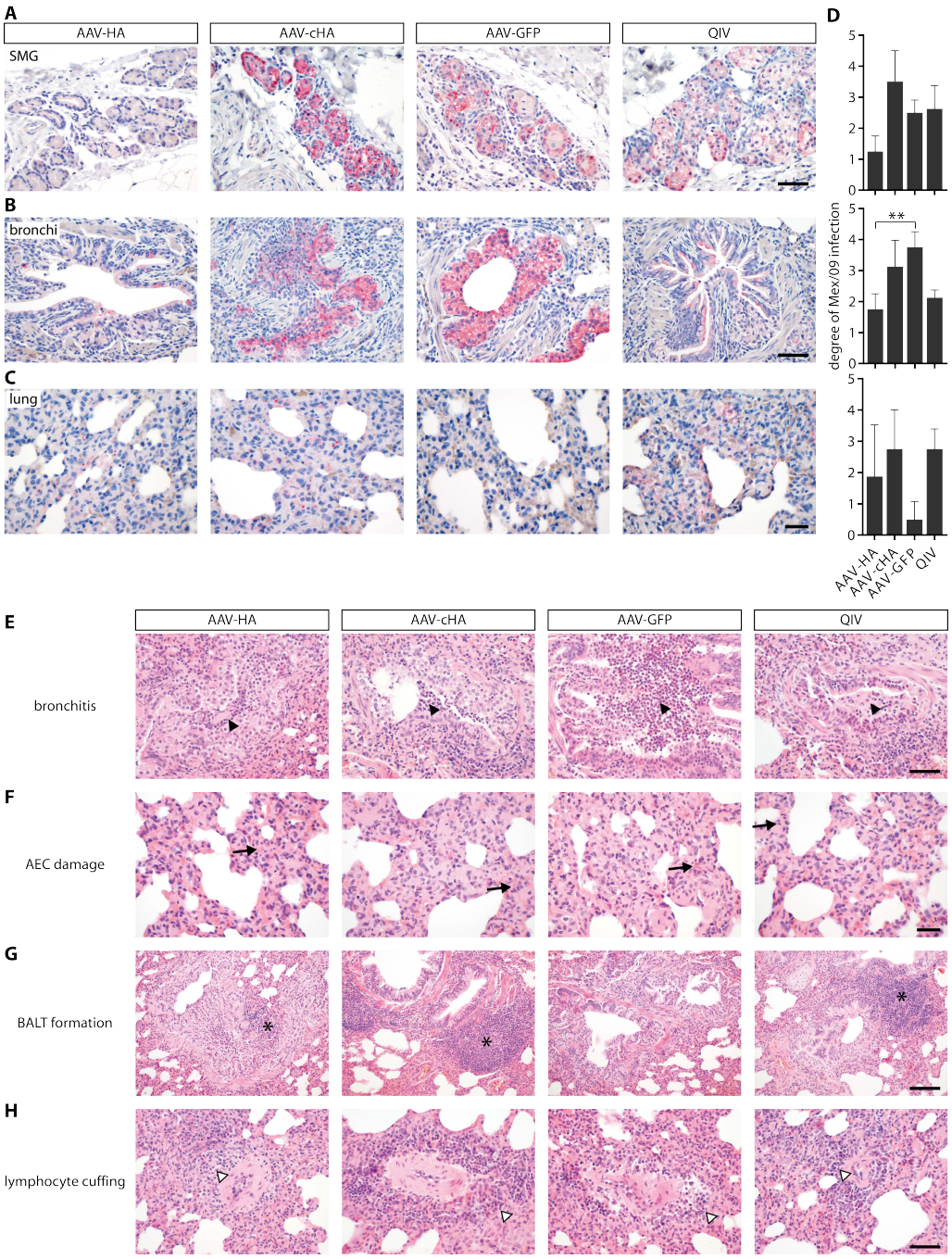

Figure 30: Immuno-histochemical and pathological examination of ferret respiratory tissue
(**A** to **C**) Immuno-histochemical staining of submucosal glands (SMG, bar 100 µm) (A), bronchi (bar 100 µm) (B) and lung parenchyme (bar 100 µm) (C) with anti-influenza antibody (red) and nuclei (blue). (**D**) Scoring of degree of infetion with influenza virus in the respective section of the respiratory tract (mean + SD). **p>0.01. (**E** to **H**) H&E staining showing inflammation in bronchial tissue (arrow heads, bar 100 µm) (E), damage of alveolar epethelial cells (AEC) (arrows, bar 50 µm) (F), BALT formation (asterisc, bar 200 µm) (G) and areas of lymphocyte cuffing (white arrow head, bar 100 µm) (H). Sample preparation and analysis (qualitative and quantitative) was done by K. Dietert and A. D. Gruber.

BALT formation can be induced upon immunologic stimulation, e.g. after infection or vaccination (*388*, *389*). This ectopic lymphoid tissue represents sites of local initiation and maintenance of a protective and regulatory adaptive immune response in the lung (*390*). In contrast to AAV-HA immunized ferrets, prominent perivascular lymphocyte cuffing was

observed in AAV-cHA, QIV and AAV-GFP immunized animals, indicating extensive recruitment of immune cells (Figure 30H). Taken together, these results indicated that AAV-HA and AAV-cHA have a protective effect in ferrets as both reduced severity of clinical signs. This, however, was associated with reduced virus replication in the respiratory tract and less pronounced pathology only in AAV-HA immunized ferrets.

5. DISCUSSION

Influenza remains to be a severe threat to public health. Currently, the only efficient prophylaxis is seasonal vaccination. The inactivated seasonal influenza vaccine induces antibodies mainly against highly variable regions in the head domain of the viral surface glycoprotein HA. Although these are neutralizing antibodies which can confer sterile immunity, their binding breath is very narrow and restricted to only a few strains of one influenza virus subtype. Since influenza viruses evolve quickly, the composition of the vaccine has to be adapted frequently to match circulating strains. This, however, can lead to vaccine mismatch when vaccine strains and circulating strains do not match. Under these circumstances, vaccine effectiveness can dramatically drop. Furthermore, even in years with good match with the circulating strains, vaccine effectiveness is only at about 60 % in healthy adults, while it is likely lower in groups being at high risk for influenza complications, such as the elderly (*183*). Also, the current seasonal vaccine does not provide protection against zoonotic or emerging pandemic strains. The urgent need for a broadly protective and long lasting vaccine has recently been acknowledged by public health authorities (*190, 191*). As a result, the National Institute of Allergy and Infectious Diseases (NIAID, USA) has released a 'strategic plan' for the development of a universal vaccine (*190*). According to this, improved understanding of influenza virus pathogenesis and of the immunity induced by the virus will help to define new correlates of protection (besides HAI titers) and aid rational vaccine design (*190*). Basic criteria of a universal vaccine were set up by the NIAID (Figure 31). Also, the WHO developed 'preferred product characteristics for next-generation influenza vaccines', which basically include the NIAID criteria, and also emphasize the need for new correlates of protection, including cell-mediated and FcγR-mediated immunity (*191*).

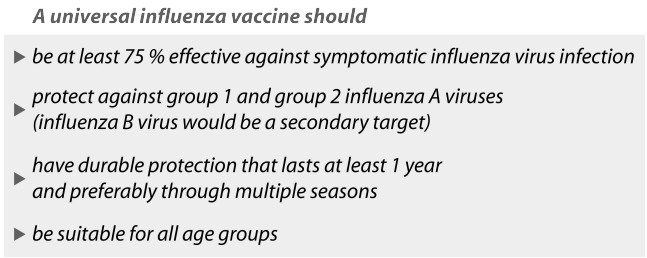

Figure 31: Criteria for a universal influenza vaccine
adapted from Erbelding *et al.*, J Infect Dis (2018)

Consequently, research has been (re)focusing on the topic intensively during the last decade with the goal of developing a vaccine which induces broadly reactive humoral and/or cellular immunity. With the discovery of broadly reactive antibodies against conserved regions in the HA protein, such as the HA-stalk domain, research on rationally designed antigens has been propelled. These antigens, including chimeric HA or headless HA, should allow circumvention of the immunodominance of the strain specific epitopes in the HA-head region. Also, other influenza virus proteins have gained interest as potential broadly reactive antigen candidates, such as NP, the extracellular domain of M2, and NA (*190*).

Although a growing body of work underlines the great potential of rationally designed broadly reactive antigen candidates, research on innovative vaccine delivery platforms such as viral vectors

and their influence on the immune response is considered important as well (*391*). With viral vector-based vaccination not only the transgene but also the vector itself shapes the immune response through its interaction with components of innate and adaptive immunity (*392*). Moreover, viral vectors enable targeting of the antigen to particular antigen processing pathways and/or compartments (e.g. mucosa) and thus activation of different arms of the immune system, which might not be activated by 'conventional' vaccines. Also, the stimulation of the immune system by components of the vector, and long persistence of vector and antigen can obviate the need for adjuvants (*392*). Most viral vectors can be produced in cell culture and do not rely on production in embryonated chicken eggs, a process which is not only costly and time consuming but also not ethically sound. However, viral vectors widely being used, such as Pox virus or Adenovirus vectors express viral gene products and induce strong inflammatory responses themselves, which might represent a safety risk. Moreover, they have to compete with high pre-existing immunity in the human population (*361*). In contrast to that, AAV-vector are 'gutless', meaning they only express the transgene product (*361*). AAV-vectors appear to induce less strong inflammatory responses upon administration which might be linked to their apparent inability to efficiently infect APC (*393*). This amounts to weaker activation of CTL and neutralizing antibody responses against the vector capsid, enabling stable and durable expression of the transgene (*394*). Hence, induction of strong immune responses against antigens from several pathogens has been reported using AAV-vectors (*361*). Although pre-existing immunity is an issue with some AAV serotypes, others, including AAV9, show low sero prevalence of neutralizing factors in the human population (*319*). Furthermore, AAV-vectors are environmentally stable and can be freeze dried (*371*). This, together with the opportunity for intranasal administration will likely ease the formulation and application of a vaccine based on AAV-vectors. Importantly, AAV-vectors are the first viral vectors to be licensed in Europe and the USA for use as gene therapy vectors (*395*). Thus, they represent a highly promising candidate for clinical evaluation as a virus vector-based vaccine carrier against influenza.

AAV-vectors have demonstrated in several *in vivo* studies their suitability as expression vectors for broadly reactive antibodies (*365-367*). However, these studies focused on the expression of monoclonal antibodies, whereas the polyclonality of a humoral immune response was shown to enhance the potency of HA-stalk antibodies (*264*). Development of active immunization strategies, which can induce polyclonal responses, is thus of high relevance. However, so far only very few studies focused on AAV-vectors as carriers for an active influenza vaccine, none of which had the goal of a broadly reactive vaccine (*362-364*). Therefore, in this study the potential of AAV-vectors as carriers for a broadly reactive influenza vaccine was evaluated in mice, and for the first time in ferrets.

Antigens and vectors

All antigens used in this study are based on Cal/7/9 virus, a prototype of (H1N1)pdm viruses, which caused the most recent pandemic in 2009 and which have been circulating since 2010 in humans. Only recently the Cal/7/9 component of the seasonal vaccine was replaced by the closely

related (H1N1)pdm-like virus A/Michigan/45/2015. The Cal/7/9 HA itself seems to show some peculiarities compared to other contemporary H1 HA, as it appears to be less stable and less glycosylated, thus resembling rather the HA of viruses which circulated before 1947, including the HA of the 1918 pandemic H1N1 virus (*396-398*). This might influence immunogenicity, given that heavy glycosylation can shield epitopes within HA from recognition by the immune system (*397*).

Initially, it appeared that the induction of antibodies against conserved epitopes in HA, i.e. the stalk, requires antigens such as cHA or headless HA. These antigens have been shown in several studies to be immunogenic when applied as protein antigen (*273-275, 277, 280, 288, 289, 297, 298*), as inactivated or life attenuated influenza virus vaccine (*281*), or viral (*276, 278, 279*) and DNA vector (*274, 275, 277, 280*). Thus, besides wildtype antigens (HA, NP) also three different cHA and three different headless HA were evaluated in this thesis, which all contained the HA-stalk of Cal/7/9.

Several HA-stalk reactive antibodies have been described to bind conformational epitopes, including the prototypic C179 (*194*). The chimeric HA constructs cHA1 (H2 head – H1 stalk) and cHA2 (H10 head – H1 stalk) have in contrast to cHA3 (H13 head – H1 stalk) not been described before (*271*). While it could be shown here that cHA3 contains the intact C179 epitope, it was partially misfolded in cHA1 and cHA2. Notably, although giving a first impression of the conformation of distinct epitopes, binding of a single antibody might not allow inference of the conformation of the complete HA-stalk, as for example the cHA3-like construct described in the aforementioned publication was not bound by another conformational antibody, 6F12 (*271*).

Furthermore, different previously published headless HA design concepts were adapted in this thesis to the Cal/7/9 HA sequence. Interestingly, although key residues used for the design of the different headless HA antigens were conserved between the influenza strains used in the original publications and Cal/7/9, some differences were observed between the Cal/7/9-based constructs generated in this thesis and the headless HA antigens described in the original publications. The PR8-based headless HA, which was initially described by Steel *et al. (288)*, was shown to display a misfolded HA-stalk conformation, based on the finding that several conformational antibodies did not bind to the construct (*289*). This was also true for the Cal/7/9-based headless HA generated in this thesis, which displayed an incorrectly folded HA-stalk as indicated by the lack of C179 binding. In contrast to the construct described by Steel *et al.*, the three-dimensional structures of the modified headless HA construct #4900 (Impagliazzo *et al.*) and an intermediate design step of Gen6 (i.e. Gen3, Yassine *et al.*), each obtained after co-crystallization with a conformational antibody, align almost perfectly to each other, and the HA2 domain of Cal/7/9 HA, strongly indicating their overall correct conformation (Figure 32). Unfortunately, the three-dimensional structure of the Steel *et al.* headless HA has never been resolved. Of note, both modified headless HA construct described in the original publications lack the cognate HA TM region, as construct #4900 (mHL2) is a secreted protein, and Gen6 (mHL2) is fused to a carrier particle (*297, 298*). However, as the Steel *et al.*-like headless HA used herein does contain the TM region, also mHL1 and mHL2 versions were constructed and analyzed containing the Cal/7/9 TM

region. In contrast to results described for construct #4900, mHL2 and mHL2+TM did not seem to show a correctly folded stalk region, or at least not the correctly folded C179 epitope (*298*). mHL1, which is based on construct Gen6, could to some extent be detected with C179, whereas the addition of a TM region to this construct further appeared to stabilize the correct conformation of the HA-stalk. This effect has also been described by Yassine *et al.* after fusion of construct Gen6 to a carrier protein, thereby replacing the TM region (*297*). Notably, Impagliazzo *et al.* used two other conformational antibodies, CR6261 and CR9114, to assess and select for the correct conformation of construct #4900 during their design process (*298*). In contrast, as mentioned above, Yassine *et al.* co-crystalized construct Gen3 with C179 (Figure 32), and found the epitope of the antibody to be intact (*297*). Thus, inference of the correct conformation of the HA-stalk solely based on C179 binding might be biased in this case. Nevertheless, mHL1 and mHL2 appear to show greater differences regarding the conformation of the HA-stalk as would have been expected by the almost perfectly aligning structures of the parental constructs (Figure 32). Nevertheless, misfolded HA-stalk antigens were shown to induce antibodies against the native HA protein conformation (*289*).

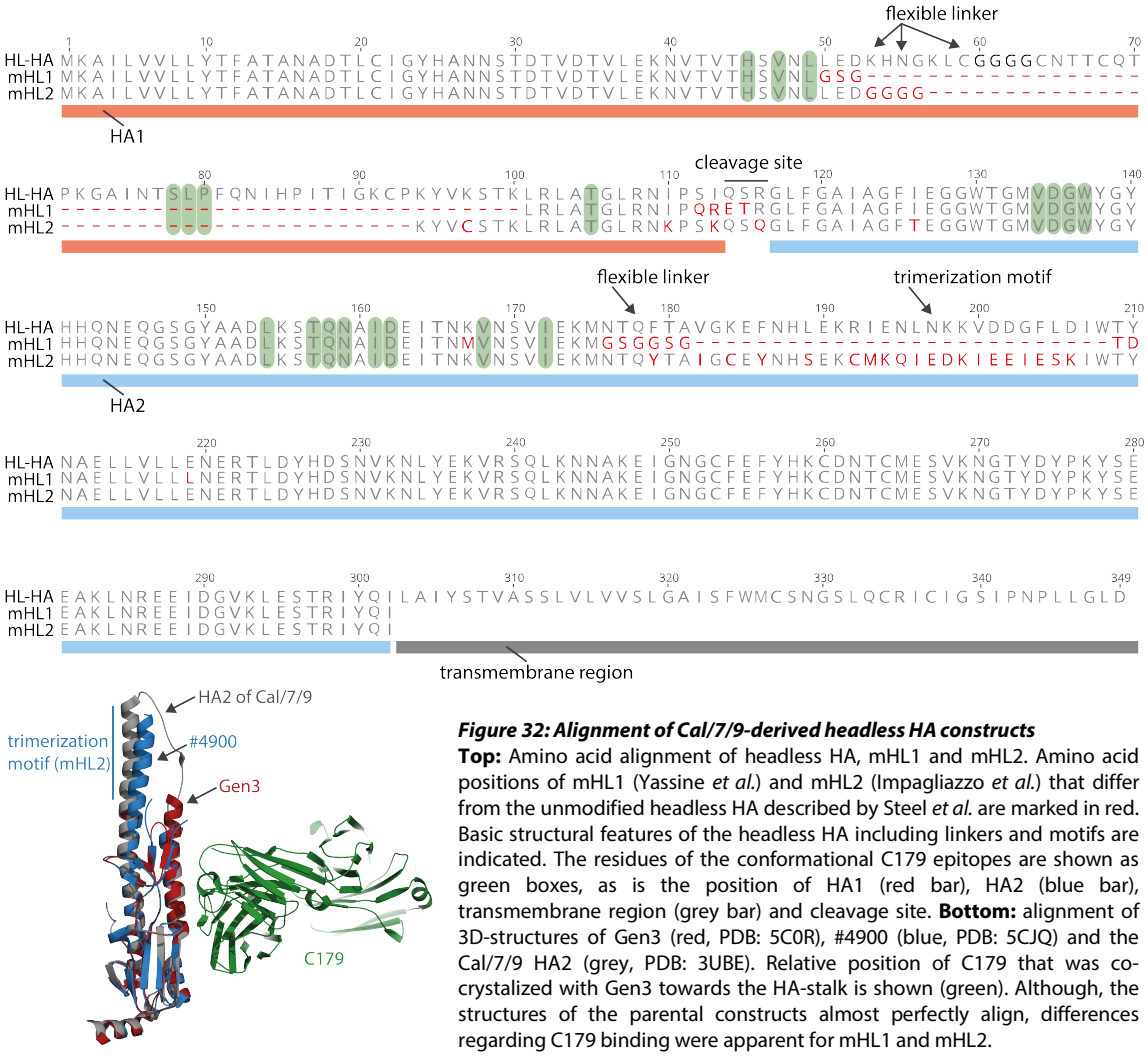

Figure 32: Alignment of Cal/7/9-derived headless HA constructs
Top: Amino acid alignment of headless HA, mHL1 and mHL2. Amino acid positions of mHL1 (Yassine *et al.*) and mHL2 (Impagliazzo *et al.*) that differ from the unmodified headless HA described by Steel *et al.* are marked in red. Basic structural features of the headless HA including linkers and motifs are indicated. The residues of the conformational C179 epitopes are shown as green boxes, as is the position of HA1 (red bar), HA2 (blue bar), transmembrane region (grey bar) and cleavage site. **Bottom:** alignment of 3D-structures of Gen3 (red, PDB: 5C0R), #4900 (blue, PDB: 5CJQ) and the Cal/7/9 HA2 (grey, PDB: 3UBE). Relative position of C179 that was co-crystalized with Gen3 towards the HA-stalk is shown (green). Although, the structures of the parental constructs almost perfectly align, differences regarding C179 binding were apparent for mHL1 and mHL2.

Hence, to which extent the conformation of the antigen will influence immunogenicity of HA-stalk epitopes remains elusive, especially in the context of AAV-vectored expression of the antigen from inside the cell, involving presentation of peptide and not protein antigen on MHC molecules. Thus, eventually this can only be assessed *in vivo*.

There were only minor differences regarding expression levels of the constructs. Whereas the cHA, headless HA, mHL1+TM and mHL2+TM showed a somewhat lower expression level, wildtype antigens (HA, NP) and mHL without TM (mHL1, mHL2) were expressed at higher levels. This might relate to the closer-to-optimum sequence of the latter constructs due to natural evolution (wildtype antigens) or design steps (mHL) enabling higher expression levels. Strong expression of the antigen from AAV-vectors in peripheral tissue was shown to be a prerequisite for efficient cross-presentation to the immune system and induction of a transgene-specific immune response (*399*). Moreover, shedding of antigen from AAV-vector transduced cells, as it occurred from *in vitro* cell cultures to high levels with the mHL proteins without TM (data not shown), was shown for other antigens to increase immunogenicity (*400*). Therefore, expression level and secretion was judged more important than correct conformation of the HA-stalk which is why mHL without TM region (i.e. mHL1 and mHL2) were used in the mouse study.

The purified AAV-vector stocks were highly infective and expression of all transgenes was confirmed *in vitro*. Furthermore, with the finally established purification protocol high quality AAV-vector preparations could be reproducibly produced. However, the aforementioned differences observed for each antigen on plasmid DNA-level were also apparent on the AAV-vector-level. This underlines the importance of a rigid assessment of quality of each vector to assure sufficient antigen production prior to experiments *in vivo* on both, plasmid DNA- and AAV-particle-level.

Intranasal application is advantageous over intramuscular immunization

In the first immunogenicity study in mice, different combinations of cHA and headless HA were applied intramuscularly (i.m.) to investigate, which vaccine regimen would induce the most potent HA-stalk-specific antibody response. I.m. immunization was used to allow better comparability and transferability of the results to preceding studies performed at the Robert Koch Institute (*362, 371*). Immunization with AAV-cHA induced broadly reactive antibodies against viruses from the H1N1 subtype, which were, however, non-neutralizing against Cal/7/9 virus, suggesting that these antibodies are directed towards non-classical antigenic sites, including the HA-stalk. These results are in line with other reports using cHA antigens (*274, 275, 278*). Interestingly, i.m. immunization with AAV-HA induced only Cal/7/9-specific antibodies during this initial immunogenicity study. This, however, was not corroborated by subsequent challenge studies, in which intranasal (i.n.) vaccination was used. Here, also AAV-HA immunization induced broadly reactive antibodies. This clearly underlines the impact of immunization route on the breadth and quality of the immune response, which needs to be distinguished more closely in follow up studies.

Notably, during the first immunogenicity study, only animals receiving three AAV-cHA immunizations mounted significant influenza virus-specific antibody titers. However, since immune responses were assessed three weeks after each immunization, animals receiving two immunizations were sacrificed at the time point when the other groups received their third immunization. Thus, it remains elusive, whether the third immunization was actually required to induce these antibody levels, or whether merely a longer time interval from the second immunization until sacrification of the animals would have sufficed. Furthermore, it became apparent that further refinements of the AAV-vector preparations and/or the administration process were required, as high variability was seen for antibody responses of individual animals and the antibody titers were overall relatively low.

Unexpectedly, in the first immunogenicity study, AAV-HL seemed to be completely non-immunogenic when given alone one to three times, or in combination with AAV-cHA. Also, priming with AAV-HL obviated the immunogenicity of subsequently applied AAV-cHA. This was most likely due to AAV9-specific serum neutralizing antibodies induced after prime immunization with AAV-HL, which might have prevented successful transduction with AAV-cHA. This is in stark contrast to other studies using headless HA (*288, 289*). In these studies, however, the headless HA was based on the more stable PR8 HA, or further stabilized by addition of a C-terminal trimerization domain. Moreover, the antigen was administered as combination of a DNA-vaccine (prime/boost) with a virus-like particle-vaccine (boost) (*288*), or as adjuvanted protein antigen (prime/boost) (*289*). Both studies report the induction of broadly reactive antibodies which, however, only provided partial homologous protection. This indicates that the headless HA itself is generally a suboptimal inducer of a *de novo* antibody response. Only after priming with a chimeric HA-DNA-vaccine (H9 head – H1 stalk), headless HA protein antigens induced complete homologous protection (*289*). However, this could not be recapitulated in the first immunogenicity study, in which no elevated antibody responses were triggered by AAV-cHA prime followed by AAV-HL immunization. Expression of foreign transgenes by AAV-vectors has been shown to occasionally induce immune tolerance towards the transgene (*400*). Apparently, this strongly depends on the administration route and the sub-cellular localization of the antigen (*400*). However, surface expressed wildtype HA has been shown in this thesis and by others to be immunogenic after transduction of muscle cells (*362, 393*). As the headless HA used herein is correctly targeted to the surface of the cell (data not shown), the lack of immunogenicity is more likely either associated with i) suboptimal amounts of *in vivo* produced transgene, which might lead to the induction of immune tolerance, or ii) the false conformation or lack of immunodominant epitopes in the headless HA protein, which furthermore might be outcompeted by the strongly immunogenic epitopes within the AAV-vector capsid (*401, 402*). To assess reasons for the failure of AAV-HL to induce influenza-specific antibodies, further experiments with modified headless HA were performed (see below).

The second mouse study was conducted to assess the protective efficacy of AAV-HA, AAV-cHA and AAV-HL against influenza virus challenge. Surprisingly, and in contrast to the aforementioned immunogenicity study, in this experiment mice remained influenza virus sero-

negative even after three immunizations with AAV-cHA. On the contrary, AAV-HA induced high Cal/7/9-specific neutralizing antibody titers comparable to those in the first study, which completely protected all animals against homologous challenge with Cal/7/9. It was hypothesized that the transgene expression in the murine muscle cells might have been too low as a consequence of low titers of infectious AAV-vector particles in the particular AAV-cHA preparations used for this study. Consequently, the production and purification methodology was further refined prior to the following studies to reproducibly yield high quality AAV-vector stocks. Another possibility is that AAV9-specific neutralizing serum antibodies interfered with transduction of the muscle cells. It has been shown before that AAV9-vectors can be re-administered into the respiratory tract even in the presence of AAV9-specific serum neutralizing antibodies (*369*). Thus, to circumvent AAV-vector neutralization by serum antibodies, mice received two additional i.n. immunizations. In fact, after these i.n. immunizations antibody titers could be induced in the AAV-cHA immunized group, which partially protected the animals from homologous challenge. At this stage of the project it was hypothesized that i.n. vaccination con not only circumvent neutralization of the vector by serum antibodies by might also lead to the induction of a stronger and/or broader immune response, because it resembles natural infection and activates canonical antigen processing pathways. This effect has also been shown for vaccination with LAIV in comparison to inactivated vaccine (*166*). Therefore, i.n. immunization was used for all subsequent studies in mice and ferrets.

Headless HA proteins appear to be generally non-immunogenic in the AAV-vector context

AAV-HL was completely non-immunogenic in the first two mouse studies, and also additional i.n. immunizations did not have the effect which was seen for the additional in AAV-cHA immunized mice, and thus mice were not protected against Cal/7/9 challenge during the challenge study. Nevertheless, the headless HA approach is appealing, because of its simplicity of just excluding all 'unwanted' epitopes from the antigen. Thus, the modified headless HA constructs were evaluated. Based on the results obtained with AAV-HL so far, reasons which could account for the lack of immunogenicity appeared to be either i) the amount of *in vivo* produced antigen, ii) its cellular localization and/or iii) the false conformation or lack of dominant epitopes in the HA-stalk. To assess these possible reasons, during the third study mice were i.n. immunized with AAV-HL, AAV-mHL1 or AAV-mHL2. As mentioned above, both mHL1 and mHL2 are strongly expressed *in vitro* and secreted from the cell. However, only AAV-mHL1 carries the at least partially correctly folded C179 epitope. Unexpectedly, not only all mice immunized with AAV-HL, but also all mice immunized with AAV-mHL1 and AAV-mHL2 remained sero-negative for influenza virus-specific antibodies after three immunizations. Thus, it seems unlikely that expression level, localization or conformation of the antigen account for the lack of immunogenicity of the AAV-vectored headless HA. Interestingly, the same phenomenon has been described before by Hessel *et al.*, using MVA-vectors expressing a headless HA based on A/Viet Nam/1203/2004 (H5N1) (MVA-hlHA) (*315*). MVA-hlHA would not induce protective immunity against homologous and heterologous challenge unless NP was co-expressed from the same vector

(MVA-hlHA-NP) (*315*). Herein, however, the combination of AAV-mHL1 + AAV-NP did not have this kind of effect. Comparable to immunization with AAV-NP alone, merely NP-specific immunity was induced by AAV-mHL1 + AAV-NP. Since headless HA and NP are co-expressed from the MVA-vector, each MVA-vector transduced cell will likely express both proteins at a time (*315*). In this case, NP-specific B-cells, which are likely not as rare as HA-stalk-specific B-cells, might pick up headless HA protein as well during antigen uptake from dying cells resulting in the presentation of headless HA-derived peptides on MHCII molecules. This could lead to the more efficient activation of headless HA-specific T-cells and, thus, could accelerate antibody responses towards headless HA, which might not be efficiently activated by solitary expressed headless HA. In fact, Hessel *et al.* described absence of influenza-specific $CD4^+$ T-cells when mice were vaccinated with MVA-hlHA alone, supporting such a scenario (*315*). Unfortunately, they did not differentiate between HA- and NP-specific cellular and humoral responses in their study (*315*). Here, due to the constrained coding capacity of the AAV-vector genome (ca. 4.7 kb max. vector size, (*403*)), mHL1 and NP had to be expressed separately from two AAV-vectors. This might have resulted in a too low number of cells expressing both antigens for this intermolecular help to happen. This hypothesis comes with the caveat that HA (and thus most likely also mHL1) and NP do not interact with each other, which should decrease the likelihood for concomitant uptake by a B-cell, especially when one of the proteins is secreted from the transduced cell as it is the case with mHL1 (*404*). The success of other headless HA-based vaccines might therefore also be connected to their ability to activate B-cells in a T-cell-independent manner through cross-linking of the B-cell receptors, as antigens are for example displayed in high density on carrier particles (*288, 297*). However, headless HA which completely lack dominant HA epitopes appear to be poor inducers of immune responses, especially in the presence of other immunodominant epitopes for instance from the AAV-vector capsid. Thus, a virus vectored approach solely based on headless HA does currently not seem to be feasible.

AAV-vectored antigen expression mitigates antibody immunodominance

In the third study in mice, AAV-HA, AAV-cHA and AAV-NP induced high homologous antibody titers after i.n. immunization. Also, variability among animals from each immunization group could be minimized (data not shown), which was either related to the higher quality of the AAV-vector preparations used for this study, or was a consequence of the i.n. immunization itself, which enabled a more controlled administration and uptake of the vaccine. During the third study, AAV-vectored vaccines were also for the first time compared to i.n. immunization with WIV.

Although high titers of AAV9-specific neutralizing serum antibodies were induced, a strong increase of homologous Cal/7/9-specific antibody titers over the complete immunization period was seen, especially with AAV-HA vaccination. Notably, AAV-HA immunization rather led to a constant Cal/7/9-specific antibody titer increase over the immunization period, whereas no clear boosting effect of immunizations #2 and #3 was seen. Thus, it remains elusive whether the second and third immunization were required, or whether a single immunization would have sufficed to

induce protective influenza-specific antibody titers with AAV-HA. As vaccination with the cHA is commonly done with a sequential regimen comprising three immunizations (*274, 275, 278*), AAV-HA was applied three times to allow for direct comparison with the AAV-cHA vaccine. Therefore, the option of a 'one-shot' vaccine has not been evaluated yet, and requires further investigation. As mentioned above, studies regarding the minimum required number of AAV-vectored cHA to induce broadly reactive HA-stalk antibodies would also be informative. Due to the long-lasting AAV-vector-mediated transgene expression, a vaccine requiring only one immunization seems feasible and would be most convenient regarding implementation in humans as well (*332*).

Interestingly, in the third study in mice, i.n. immunization with AAV-HA induced broadly reactive antibodies against several group 1 influenza A viruses, including the 1918 pandemic H1N1 and H5N1. As mentioned above, this was not the case after i.m. vaccination in the first immunogenicity study. Compared to the i.m. or parenteral administration route, mucosal immunization has been shown before to induce more broadly reactive antibodies also after immunization with inactivated or live attenuated vaccines (*166, 405*).

As expected, AAV-HA induced MN^{pos} and HAI^{pos} antibodies, which were, however, Cal/7/9-specific and did not bind to the PR8 HA. The amino acid sequence of the PR8 and Cal/7/9 HA1 subunits are only distantly related and diverge from each other by about 25 %. Also, IgA antibodies triggered by AAV-HA immunization were Cal/7/9-specific. IgA antibodies were shown to play an important role during protection from influenza virus infection due to their high local abundance within the respiratory tract (*125*). Notably, serum IgA was measured, which can however serve as surrogate for mucosal IgA, the concentration of which might even be higher in the lung compared to the serum (*125*). However, antibody responses against PR8 lacked detectable amounts of IgA, indicating that broadly reactive antibodies against this and likely other viruses rather belong to other Ig isotypes, such as IgG.

HA conformational change ELISA indicated that binding of AAV-HA induced sera to the homologous Cal/7/9 virus was largely mediated by HA-head antibodies, as removal of the Cal/7/9 HA1 subunit by DTT treatment led to an almost complete loss of reactivity. However, AAV-HA induced sera also appeared to contain a large proportion of broadly reactive antibodies towards the HA-stalk, as removal of the PR8 HA1 subunit would not lead to a loss of reactivity. This finding was somewhat surprising, since the induction of antibodies against the HA-stalk domain was only expected for immunization with cHA. In fact, immunization with AAV-cHA triggered

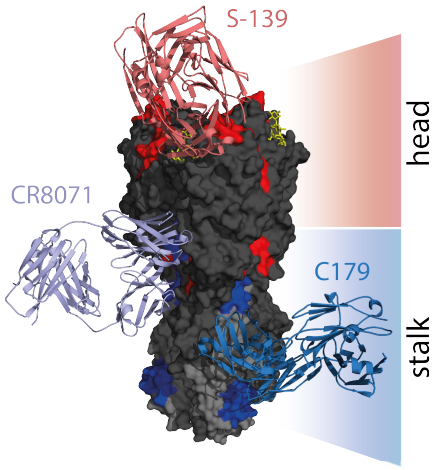

Figure 33: Footprints of well characterized broadly reactive antibodies overlap with epitopes recognized by AAV-HA induced antibodies
Peptides identified in the peptide screen with AAV-HA induced serum were mapped on the 3D-structure of HA as in Figure 24E. Additionally, structures of broadly reactive antibodies S-139 (PDB: 4GMS), CR8071 (PDB: 4FQJ) and C179 (PDB: 4HLZ) were aligned to the HA structure.

high levels of HA-stalk antibodies, which recapitulated findings from other studies using cHA protein antigens (*274, 275*).

Unlike C179, AAV-HA induced antibodies also strongly bound to PR8 HA at post fusion pH. Judged by the three-dimensional structures of the pre- and post-fusion HA, the conformation of some of the epitopes identified in the peptide screen (peptide #39, #41, #48) with AAV-HA induced sera seems to be largely maintained upon conformational changes of the HA-stalk. Though located in close proximity, the C179 epitope, i.e. the N-terminal part of a short-alpha helix in the HA-stalk extending to the fusion peptide, is completely restructured upon conformational change, which might explain the difference seen for C179 and the AAV-HA induced antibodies (*194*). The presence of both strain-specific antibodies against the HA-head and broadly reactive HA-stalk antibodies could also be confirmed with the immunoblot analysis. Here, AAV-HA induced sera could detect HA1 and HA2 subunit of two closely related H1N1 viruses, whereas binding to the more distantly related H1N1 viruses, such as PR8, was mediated by HA2 antibodies. Furthermore, the peptide screen revealed that AAV-HA induced antibodies not only bind to residues in HA1, e.g. the RBS (positions 168-182), but also to the lateral part of the HA-head domain (positions 308-322), and the membrane proximal part of the stalk domain (positions 389-412 and 418-432), thus including amino acid residues in HA1 and HA2. Moreover, the identified sites were in close proximity or overlapped with the footprints of well described broadly reactive HA-specific antibodies against the head and the stalk, such as S-139 (RBS) (*204*), CR8071 (lateral head) (*202*), or C179 (membrane proximal stalk) (*194*) (Figure 33).

Interestingly, the above mentioned results indicated that AAV-HA induced sera contain non-conformational stalk antibodies, which were able to bind to denatured antigen in conformational change ELISA and immunoblot analysis or to peptides. Results from in-cell ELISA, however, indicated that AAV-HA induced sera also contain a substantial proportion of conformational HA-stalk antibodies. Here, AAV-HA induced antibodies behaved comparable to the prototypic conformational HA-stalk antibody C179, and bound HA-stalk constructs only when they displayed the correctly folded C179 epitope. Interestingly, the difference in reactivity between AAV-HA and AAV-cHA induced sera towards the natively folded antigen as measured by in-cell ELISA was not as pronounced as against the denatured antigen in the immunoblot analysis, which further supports the idea that AAV-HA sera contain a considerable proportion of conformational HA-stalk antibodies, whereas AAV-cHA induced antibodies seemed to be largely non-conformational (see below). Further experiments assessing the prevalence of different antibody specificities after AAV-HA immunization in more detail (e.g. on a monoclonal antibody or B-cell level) would be highly informative.

The HA-stalk antibodies induced by AAV-cHA and AAV-HA showed quite different binding characteristics. Unlike AAV-HA, AAV-cHA induced antibodies bound the HA-stalk irrespective of the presence or absence of the correctly folded C179-epitope in the in-cell ELISA. Also, AAV-cHA induced antibodies showed stronger binding to denatured antigen in the immunoblot analysis compared to AAV-HA. Possibly, the at least partially misfolded conformation of the HA-stalk of cHA1 and cHA2, which were used for immunization #2 and #3, influenced the antibody

response and led to these findings. Intriguingly, these antibodies bound even stronger to the post fusion HA conformation at low pH in the conformational change ELISA. Cryo-electron microscopy structures of a representative chimeric HA (H5 head – H1 stalk) revealed that it adopts a more open HA-head and a tilted stalk domain configuration (*406*). The authors argued that the functionality of the cHA is unaltered by this non-naturally occurring conformation (*406*). However, this might as well change immunogenicity of the antigen, since otherwise buried epitopes within the HA-stalk could become more recognizable by the immune system. In fact, antibodies could be detected in AAV-cHA induced sera, which showed a trend towards increased binding to a peptide (#44) which is located at the inside of the trimeric HA-stalk. Thus, also the cHA used in this thesis might exhibit a more open conformation influencing the immune response. Although the AAV-cHA induced antibodies bind the post fusion conformation of HA the extent of their contribution to protection is questionable, since the post-fusion conformation of HA is present only during late attachment steps in the acidified endosome. Unfortunately, the epitope screen did not reveal further significantly binding peptides with AAV-cHA and WIV induced sera. In contrast to AAV-HA, AAV-cHA and WIV immunization induced lower antibody titers against Cal/7/9. These might have been too low to detect significant binders with the screening protocol used here.

AAV-cHA induced MN^{pos} and HAI^{pos} antibodies, which were specific for the head of the H13 HA which was included in cHA3 and thus used for prime immunization of these animals. The lack of MN^{pos} and HAI^{pos} antibodies against other influenza viruses, including the parental viruses of the cHA which were used for immunization #2 and #3, recapitulates findings from other studies (*278*) and is in accordance with the hypothesized mode of action of the cHA: Upon sequential immunization with different cHA, re-focusing of the immune-response from dominant neutralizing epitopes in the HA-head to non-neutralizing epitopes in the stalk occurs (*278*). Although in the challenge studies described in this thesis the neutralizing antibodies against the 'irrelevant' exotic H13 HA-head did likely not provide protection against the infection with H1N1 viruses, they might become advantageous in a real-world setting when the head region of the cHA happens to match the HA of a newly emerging virus. The cHA-head used for vaccination would then have to be chosen appropriately to match for instance strains with high zoonotic potential, e.g. H5N1.

In conclusion, AAV-vectored immunization seemed to mitigate the immunodominance of variable epitopes in the HA-head, allowing induction of antibodies against subdominant epitopes as well. Hence, not only AAV-vectored vaccination with a sequence of cHA could induce HA-stalk antibodies, but also immunization with wildtype HA. Important factors leading to this effect were most likely continuous generation of antigen by respiratory cells after mucosal immunization, and the lung-specific environment, which influences processing and presentation of antigen to cells of the adaptive immune system. This possibly resulted in more effective priming of rare B-cells recognizing conserved epitopes in the HA-stalk. Further experiments for example comparing different administration routes (i.n. versus i.m.) and antigen forms (AAV-vectored

versus protein antigen) will be required to evaluate the exact reason for the mitigation of the immunodominance.

Both AAV-HA and AAV-cHA induced antibody responses were restricted in their reactivity to group 1 influenza A viruses. This restriction seems to represent a major hurdle for the development of a universal influenza vaccine and has thus been reported in several studies before (*268, 274*). Eventually, further studies need to be conducted to expand protection to both antigenic groups, for example by the inclusion of another vaccine component from antigenic group 2, such as H3, or use of an inter-group-stalk consensus construct.

Unexpectedly, also WIV vaccination induced HA-stalk antibodies, which showed exceptionally broad reactivity against all tested influenza A viruses. WIV-induced sera, however, appeared completely negative in the MN and HAI assays. Product batch-specific difference in the HA1 and HA2 content of the inactivated virus preparation could account for the peculiar breadth and specificity of the immune response (*192*), though the batch's HA content, i.e. HA1 and HA2, was analyzed and confirmed by the supplier, i.e. the NIBSC. Thus, this seems rather unlikely. However, it was shown that the i.n. route in contrast to parenteral vaccination is able to induce a broadened immunity, which might also have been the case here (*405*). Interestingly, the binding of WIV induced antibodies was independent of the conformation of the HA-stalk in the immunoblot analysis and independent of the pH-induced conformational changes in ELISA. However, in the in-cell ELISA binding to the extensively truncated mHL1 was completely absent. This indicates that the dominant epitope recognized by WIV induced antibodies is likely located in the upper part of the HA (-stalk).

Finally, AAV-NP induced a remarkably potent broadly reactive antibody response covering all tested virus from both antigenic groups of influenza A viruses. This reactivity breadth is most likely associated with the high conservation of the NP proteins of the tested viruses. In contrast to AAV-HA and AAV-cHA, this response included broadly reactive IgA. However, rather than being specifically induced to higher relative amounts by AAV-NP immunization, the higher levels of PR8-specific IgA most likely resulted from higher absolute overall serum antibody levels against PR8 in these animals. There is increasing evidence that NP-specific antibodies play an important role during protection from unmatched influenza viruses (*143, 233*). Since NP is the major stimulus for the induction of protective CTL responses, NP-specific T-cells likely play a major role during protection as well (*362, 371*). These were not analyzed in this project since the main focus was on HA-mediated immunity, which is mainly mediated by humoral immune responses. Notably, a similar project performed at the Robert Koch Institute focused on AAV-NP-induced cellular immunity (*371*). In the respective study, however, though strong NP-specific CTL responses could be measured in AAV-NP immunized mice, cell mediated immunity was not able to protect against heterologous challenge with a PR8 virus. In fact, the CTL were unable to efficiently execute cytotoxic effector functions *in vivo* (*371*). This might have resulted from a ca. 10-fold lower dose of AAV-vector or the i.m. route which was used for immunization (*371*), which was in this thesis shown to result in weaker immune responses compared to i.n. immunization. Further studies including measurement of AAV-NP induced cell mediated

immunity in the context of broad protection will be required to analyze the impact of antibody mediated versus cell mediated immunity against the internal viral NP.

AAV-HA, AAV-cHA and AAV-NP mediated protection is associated with increased capacity to induce FcγR-activating antibodies

Several studies described that non-neutralizing antibodies confer protection via interference with later steps of the viral life cycle. These include inhibition of the conformational changes of HA, which are required for fusion of the viral and cellular membrane, or prevention of release of progeny virus from infected cells (*208, 223, 224, 229*). The MN-assay which was performed herein not only allowed for measurement of inhibitory effects on attachment and/or fusion, but also on release and maturation of the virions, since serum was constantly present throughout multicycle replication of the virus (*375*). However, no influence on infectivity of the viruses or interference with their release into the supernatant (data not shown) by cross-reactive antibodies could be found in AAV-vector immunized animals. Though the polyclonality of the mouse sera might conceal effects of some minor antibody specificities, it appears that inhibition of steps in the viral replicative cycle thus seems not to account for broad protection seen with the AAV-vectored vaccines.

Activation of FcγR by broadly reactive antibodies was shown to play an important role for protection in the mouse model (*201, 222*). The presence of FcγR- or ADCC-activating antibodies has also been shown in humans (*213, 407*). Furthermore, these human antibodies conferred protection after passive serum transfer into mice (*408*). Although there is growing evidence that high ADCC-activating antibody titers are associated with low viral replication and less severe disease, pre-existing immunity in humans hampers research, which could ultimately prove functionality and relevance of FcγR-activating antibody-mediated protection (*218, 232, 409*). ADCC-activating antibodies are induced early in life, and their titers increase over a lifetime (*213, 410, 411*). In fact, repetitive natural infection and vaccination with inactivated vaccine was shown to boost ADCC-activating antibodies in children and adults (*218-221, 411-414*). However, an inactivated vaccine failed to induce ADCC-activating antibodies in influenza-naïve macaques (*216*). Only infection with influenza virus mounted ADCC-activating antibodies in these animals (*216*). Also, H7N9 LAIV vaccination of H7N9-HAI^{neg} human subjects did not mount detectable ADCC-activating antibodies levels until subjects received a booster vaccination with inactivated vaccine (*221*), while children receiving booster vaccination with LAIV after LAIV priming did not mount ADCC-activating antibodies (*218*). The authors argue that the latter finding might be due to suboptimal antigen production by LAIV in the respective study (*218*). This indicates that broadly reactive FcγR-activating antibodies are not readily induced in humans by currently licensed vaccines, but seem to require innovative vaccine approaches including adjuvants, heterologous prime-boost regimens, or viral vector-vaccines (*415*).

Here, a recently developed reporter assay was used which allows for the measurement of influenza virus-specific activation of each of the four murine type I FcγR (I to IV) by serum from AAV-vector or WIV vaccinated mice (*225*). Interestingly, AAV-HA, AAV-cHA and AAV-NP

vaccination induced high Cal/7/9-specific FcγR-activating antibody titers, while WIV vaccination only induced marginal reactivity. Even more striking, PR8-specific FcγR-activation was not detected in WIV-induced sera. In contrast, AAV-HA, AAV-cHA and AAV-NP vaccination induced broadly reactive FcγR-activating antibodies against PR8. Notably, this was not due to the lack of binding antibodies in the WIV immunization group, as all vaccines induced high titers of Cal/7/9- and PR8-specific antibodies. Potent activation of FcγR and requirement on the FcγR-activated effector mechanisms to mediate protection was in particular shown for broadly reactive antibodies against the HA-stalk (*222*). Interestingly, in contrast to the HA-stalk antibodies induced by AAV-HA and AAV-cHA immunization, stalk antibodies induced by WIV could not potently activate FcγR. As mentioned above, the failure of inactivated vaccine to induce ADCC-activating antibodies has been shown before in macaques while only influenza virus infection could induce/boost a functional antibody response in this study (*216*). Thus, the AAV-vectored vaccines seem to be able to activated cognate antigen processing pathways, which would also become active during natural infection and, thus, induce and boost superior functional FcγR-activating antibody response compared to WIV.

Activating and inhibitory type I FcγR are (co-)expressed on most immune cell types (*120*). Thus, the response of a particular cell is modulated depending on the relative abundance of each receptor (*416*). Also, relative abundance of antibodies activating one particular FcγR influences regulation of the immune response (*120*). With AAV-HA and AAV-cHA induced sera, however, only modest differences were apparent with respect to the activation of the individual four murine FcγR: FcγRIIB seemed to be less strongly activated by Cal/7/9-specific antibodies in the sera of AAV-HA and AAV-cHA immunized mice, and FcγRIV less strongly by PR8-specific antibodies compared to the respective other receptors. The induction of such a potent homologous and heterologous FcγR-activating antibody response by AAV-NP was unexpected. In fact, AAV-NP was the only vaccine which also showed a protective effect towards the heterosubtypic X31, which might also be conferred by FcγR-activating antibodies. Notably, the internal viral protein NP seems to be expressed also on the surface of cells (*114, 234*). Furthermore, an AAV-NP transduced 293T cell culture released NP into the cell culture supernatant (data not shown), increasing the likelihood for interaction of the antibody molecule with the otherwise internal viral protein. In humans, broadly reactive NP-specific antibodies were shown to mediate protection via ADCC (*233, 417*). Aside from activation of ADCC, NP-specific FcγR-activating antibodies might also be involved in regulation of the immune response, as the inhibitory FcγRIIB seems to be more potently activated by AAV-NP induced sera compared to other vaccines (against Cal/7/9) or FcγR (against PR8). Activation of FcγRIIB can for example regulate the B-cell repertoire and lead to survival of higher affinity B-cells (*135*). However, as mentioned above, the true impact of FcγR-mediated protection and the underlying effector mechanisms, as well as the influence of T-cell-mediated immunity on protection needs to be defined in more detail in additional studies in immunocompromised FcγR-KO (e.g. Fcer1g KO mouse) or CTL-deficient (e.g. CD8 KO mouse) mice. In addition, further experiments in FcγR-class-specific KO mice (e.g. FcgγRIIb^{-} mouse)

could reveal the influence of the slightly differential activation of the individual FcγR by AAV-HA, AAV-cHA and AAV-NP vaccines on regulation of the immune response.

AAV-cHA seemed to induce lower FcγR-activating titers compared to AAV-HA. In AAV-HA immunized mice, the higher amount of total antibodies against Cal/7/9 might as well include a higher absolute amount of FcγR-activating antibodies against this virus. In fact, Cal/7/9-specific total and FcγR-activating antibody titers in the vaccine groups were proportional to each other. Against PR8, however, AAV-HA immunization also induced slightly higher titers of FcγR-activating antibodies, though less total antibody titers were induced compared to AAV-cHA. Thus, AAV-HA immunization seems to induce a greater fraction of FcγR-activating antibodies. Amount of antigen, as well as conformation of the HA-stalk was shown to influence the induction of broadly reactive antibodies (*297, 298*). Since AAV-HA is expressed to high amounts and displays the native HA conformation, this might positively influence the functional antibody response. Besides FcγR-activating antibodies against the HA-stalk, also broadly reactive non-RBS binding antibodies against the head were shown to activate FcγR (*223*). These might complement the potency of FcγR-activation of the HA-stalk antibodies, resulting in increased overall FcγR-activation. In fact, by measuring the induction of FcγR by antibodies which bind either to the complete HA or a truncated stalk-only construct, it could be shown that AAV-HA but not AAV-cHA induced FcγR-activating antibodies against epitopes present only in the context of the full length HA, such as the HA-head. Data obtained with the peptide screen suggested that these antibodies bind to the epitope at the lateral side of HA-head, which includes amino acid in HA1 (positions 308-322), and HA2 (positions 389-412 and 418-432). As the cHA contain exotic HA-head domains, the immune responses evoked by AAV-cHA immunization will likely lack antibodies against these epitopes in the H1 HA-head domain. Thus, with respect to the potent induction of FcγR-activating antibodies against H1N1 viruses, AAV-HA seems to be advantageous over AAV-cHA.

During homologous challenge infection with Cal/7/9, sterile immunity was achieved in AAV-HA immunized mice, which was most likely mediated by neutralizing antibodies against this virus. The absence of neutralizing antibodies in AAV-cHA and WIV immunized mice suggests that FcγR-activating antibodies accounted for the observed partial homologous protection, given that the relatively low titers of FcγR-activating antibodies in WIV immunized mice were high enough to mediate protection. In fact, already low concentrations of FcγR-activating antibodies can confer protection (*222*). AAV-NP immunized mice, which also lacked neutralizing antibodies, might as well be protected through FcγR-mediated effector mechanisms. However, T-cell mediated effector mechanisms likely also play a role during homologues protection (*362, 371*). Further experiments in immuno-compromised mice (B-cell (e.g. muMt$^-$ mouse) or CTL-deficient (e.g. CD8 KO mouse)) could, therefore, help to unravel the involved arms of the immune response and mediators of protection.

During heterologous challenge infection with PR8, high FcγR-activating antibody titers in AAV-HA, AAV-cHA and AAV-NP immunized mice were associated with increased survival and/or less severe weight loss. As mentioned above, in another study T-cells induced by AAV-NP

immunization were shown to be non-functional *in vivo* against PR8 infection, suggesting that FcγR-mediated effector mechanisms could account for the AAV-NP-mediated heterologous protection seen in this thesis (*371*). Notably, in the respective study different immunization conditions were used, which might limit comparability to the results described in this thesis. WIV immunized animals lacking broadly reactive FcγR-activating antibodies were not protected against heterologous challenge. Protection of the AAV-vector immunized groups was associated with clearance of virus in the lung at the end of the challenge period (day 14). Although initial infection of the respiratory tissue could not be prevented due to the absence of pre-existing neutralizing antibodies, FcγR-mediated effector mechanism seem to become active later on, which eventually mediate clearance of the virus infection.

Induction of antibody-dependent enhancement of disease (ADE) during infection with several viruses including influenza virus has been shown (*238, 239*). Hereby, concomitant binding of a non-neutralizing antibody to the virus and the FcγR may result in enhanced uptake of viruses into the FcγR bearing cells and thus increased replication (*238, 239*). However, no signs for ADE were apparent in any of the AAV-vector immunized mice.

Jegaskanda *et al.* illustrated the putative role of neutralizing and non-neutralizing but FcγR-activating antibodies as shown in Figure 34 (*418*). According to this, in case of infection with a matched influenza virus, neutralizing antibodies can confer sterile immunity and prevent infection completely.

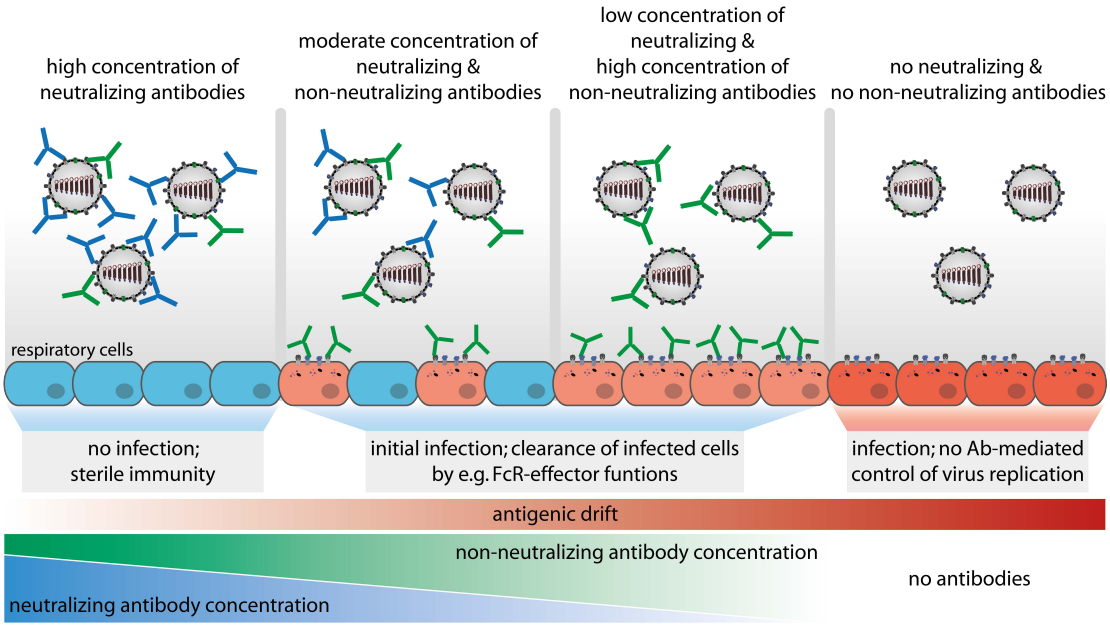

Figure 34: Protection against homologous and drifted influenza virus strains is conferred by neutralizing and non-neutralizing antibodies
In case of an infection with homologous influenza virus, matched neutralizing and HAI^{pos} antibodies (blue) confer sterile immunity and prevent infection (blue cells). Non-neutralizing antibodies (green) presumably play a minor role during infection with homologous viruses. Strain-specific, neutralizing antibodies are limited with respect to their binding breadth, and might not completely prevent infection with a drifted virus variant. However, broadly reactive, non-neutralizing antibodies help to rapidly limit and clear infection through activation of FcγR-mediated mechanisms, such as ADCC, thereby reducing disease severity (light red cells). Without any antibody, no control and clearance of virus infection can of course be mediated (dark red cells). (adapted from Jegaskanda *et al.*, Hum Vacc Immunother (2017))

However, with increased antigenic distance to the homologous strain, protection is mediated by broadly-reactive, non-neutralizing antibodies which are able to activate FcγR (*418*). In conclusion, the aforementioned findings indicate that AAV-HA is able to induce both neutralizing antibodies that confer sterile immunity against a homologous strain, and broadly protective antibodies against heterologous viruses, which confer protection via FcγR-mediated effector functions.

In conclusion, AAV-vectored vaccines, particularly AAV-HA and AAV-NP, induced and boosted superior FcγR-activating antibody responses compared to WIV, which were associated with homologous and heterologous protection. Thus, AAV-vectors could potentially be used in humans as stand-alone vaccine to induce, boost, and maintain robust broadly protective functional antibody responses. In this respect, and as criteria set by health authorities require the protection of a universal vaccine to last for a minimum of one year (Figure 31), longevity of AAV-vector vaccine induced immunity is of high importance and should be assessed in follow-up studies. Furthermore, AAV-vector vaccines could also act as primer-vaccine to induce broad basal immunity, which could be expanded in case of an unforeseen pandemic by, for example, immunization with a non-perfectly matching inactivated vaccine. This would help to bridge time until better matched vaccines are available. However, the interplay of AAV-vector and inactivated vaccine has not yet been analyzed, and further experiments are required to gain understanding of the requirements for optimal induction of a broadly protective immune response.

AAV-HA and AAV-cHA show a protective effect in ferrets

Since the first isolation of influenza A virus, ferrets have represented the gold-standard animal model for influenza in humans (*152*). The main reasons for this are their natural susceptibility to most human influenza viruses and the close resemblance of human influenza in ferrets (*385*). Hence, while focusing on HA-mediated immunity, the protective efficacy of i.n. immunization with AAV-HA and AAV-cHA was evaluated in ferrets, and compared to i.m. immunization with human QIV of the season 2017/18. The latter represents the vaccination recommendation for influenza virus naïve individuals by the STIKO (*160*).

Interestingly, during the complete immunization period, some of the ferrets receiving AAV-HA and AAV-cHA remained AAV9 sero-negative, although all of these animals developed Cal/7/9-specific total antibody titers. Several factors might influence the extent of immunity against the AAV-vector capsid including route of administration, vector purity, vector dose, and AAV serotype, as well as peculiarities of the transgene. Unfortunately, data from another ferret study using AAV9 did not include information about capsid-specific antibodies (*366*). It is, however, unlikely that AAV9-specific antibody titers were below the detection limit of the ELISA (i.e. a serum dilution of 1:100), since administration of AAV-vectors usually readily induces relatively high titers of AAV-specific antibodies in mice and larger animals including humans (*359*). Thus, reason and relevance of this finding remain elusive.

Most likely due to the strong and long-lasting transgene expression, immunization with AAV-HA led to a stronger induction of antibody titers against Cal/7/9 compared to immunization with

QIV. As for results obtained in the mouse studies, it would be highly interesting to investigate in ferrets whether even a single immunization with AAV-HA would have sufficed to induce protective antibody titers. In congruence with results obtained in mice, only AAV-HA but not AAV-cHA induced MN^{pos} and HAI^{pos} antibodies against Cal/7/9. Unexpectedly, QIV induced total antibodies but no neutralizing antibodies. However, this has also been observed in other ferret studies, indicating that the human vaccine has a rather low immunogenicity in these animals (*281*).

AAV-HA immunized ferrets were partially protected against signs of disease and showed less virus replication in the respiratory tract compared to the other groups. Moreover, MN^{pos} antibody titers correlated inversely with virus titers in nasal turbinates, suggesting that robust local protective immunity was induced at the side of administration of the AAV-HA vector. In fact, the highest expression of transgene was shown directly at the site of administration of AAV-vectors expressing reporter genes in the nostrils of ferrets (*366*). Since the nasal mucosa is the first site in contact with intruding respiratory pathogens, the establishment of local immunity by direct targeting of the antigen to the mucosa could enhance the protective efficacy of a vaccine (*419*). Notably, viral titers in trachea and lung of AAV-HA immunized animals were also reduced compared to the other groups, but did not differ enough from each other within the AAV-HA group to reveal any correlation with MN^{pos} antibody titers.

The induction of bronchus-associated lymphoid tissue (BALT) has been implicated in the initiation and maintenance of an adaptive mucosal immune response (*390, 420*). Viral infection-induced BALT was also shown in ferrets challenged with A/Mexico/InDRE4487/2009 (H1N1)pdm at seven days post infection, and even earlier post infection in mice (three days) (*421, 422*). However, the lack of BALT in AAV-GFP immunized ferrets indicates that its formation in the other vaccine groups is rather associated with the immunization and not a consequence of the challenge infection itself. The induction of BALT was shown after intranasal and intravenous immunization with inactivated vaccine (*389, 423*). In the ferret study described in this thesis, it appears that also i.m. immunization with QIV could induce BALT. Interestingly, less distinct formation of BALT was seen in AAV-HA compared to AAV-cHA and QIV immunized ferrets. Influenza virus infection was shown to result in enlargement of pre-existing BALT structures (*424*). The lower virus load, which was associated with the presence of neutralizing antibodies in AAV-HA immunized ferrets, might have led to a less pronounced stimulation of immune cells migrating into BALT and, thus, less enlarged BALT structures. This might, however, be an advantage, since less marked influx of immune cells might also diminish the risk for tissue damage in AAV-HA immunized animals (*425*). Further analyses of the immunological mechanisms involved in establishment of AAV-vector induced influenza immunity in ferrets will be required.

AAV-cHA immunized ferrets were partially protected against signs of disease but did not show reduced viral replication in the respiratory tract. Most likely other protective mechanisms apart from neutralization, such as FcγR-mediated effector mechanisms, account for the observed symptomatic protection. Unfortunately, measurement of FcγR-activating antibodies in ferret sera was not possible with the murine FcγR-receptor reporter assay (data not shown). However, it was

shown that a human-specific FcγRIV assay shows some cross-reactivity with ferret sera, which would allow at least an approximation of the amount of FcγR-activating antibodies (*278*). The impact of FcγR-receptor mediated immunity for protection in the ferret model needs to be addressed in further studies.

Unexpectedly, QIV immunized animals were not protected against disease and developed symptoms comparable to the AAV-GFP immunized negative control group. As the time interval between vaccination and challenge could influence the protective efficacy of a vaccine, it might be argued that vaccination with QIV closer to the time point of challenge infection would have induced a more effective protection. However, also vaccination with TIV four weeks (and not eight weeks as in the study presented in this thesis) in advance to challenge infection did not provide protection in another study, in which inactivated vaccine also showed low efficacy (*281*). Therefore, timing might not be as relevant, but a low immunogenicity of the inactivated vaccine in ferrets seems to account for the low efficacy.

A more widespread infection also to the lower respiratory tract was shown for (H1N1)pdm virus compared to seasonal strains, which are normally restricted to infection of the upper respiratory tract and the trachea (*387, 426*). Unexpectedly, AAV-GFP immunized animals seemed to be free from influenza replication in the lung as indicated by immunohistochemistry (IHC). Notably, this not necessarily contradicts findings from the virus titration of lung homogenates, in which AAV-GFP immunized ferrets shows comparably high virus titers as AAV-cHA and QIV immunized animals. As homogenates contain lung lobes as well as bronchi, this might conceal a more distinct spatial distribution of virus replication within the respective tissue compartments, which can only be resolved with IHC. In fact, the overall IHC-score of the lungs reflected data of the homogenate virus titration quite well (not shown). Infection of the lower respiratory tract was shown to result in more severe disease (*426*). The presence of neutralizing antibodies against (H1N1)pdm in AAV-HA immunized animals likely led to the reduction of virus replication in the complete respiratory tract, which ameliorated inflammation and severity of disease in these animals. In AAV-GFP immunized animals, however, virus apparently did just not reach the alveoli and, therefore, did not cause as severe alveolar damage as in the AAV-cHA and QIV immunized groups. This might also explain why AAV-GFP immunized animals lost least weight. Correspondingly, also no hyperplasia of type II pneumocytes was seen in AAV-GFP immunized mice. Nevertheless, AAV-GFP immunized animals showed a more severe infection and inflammation of the upper respiratory tract compared to the other vaccine groups, and these animals were not symptomatically protected. It can only be speculated on the reason for this phenomenon, but it was shown that immune pressure, imposed for instance by the presence of antibodies in the upper respiratory tract, can force a change of tropism of the virus, which might have occurred here (*427*). However, variability introduced by the low animal number, experimental variance and the outbred genetic background of the ferrets might also account for some differences. Thus, further experiments will be required to define the exact mechanism behind and the relevance of this phenomenon.

Interestingly, AAV-cHA immunized ferrets seemed to show slightly increased tissue inflammation. Non-neutralizing antibodies have been shown to occasionally enhance virus uptake and disease (*235, 238, 239*). This effect could have also played a role in the study described here. However, due to the low number of animals and the high variability associated with the outbreeding of the ferrets, it might be premature to speak of antibody-dependent enhancement of disease. As mentioned above, such an effect has not been observed with AAV-cHA in mice. This has, however, to be considered cautiously and requires further attention.

Nevertheless, a protective effect of AAV-HA and AAV-cHA was demonstrated for the first time in a sub-lethal ferret infection model. However, only AAV-HA immunized ferrets showed reduced virus replication and tissue damage. Symptomatic protection would already have a huge impact on public health, since most influenza infections progress without need for medical attendance or even hospitalization, which is, however, causing high costs for health systems, too (*190*). Further experiments in ferrets are warranted to explore the protective efficacy of AAV-vectored vaccines against heterologous virus infections.

Perspective

AAV-vectors expressing influenza virus antigens were shown in this thesis to induce superior broadly protective immunity in mice compared to an inactivated vaccine. The protective mechanism likely includes the activation of FcγR-mediated cytotoxic or regulatory effector functions. Interestingly, vaccination with AAV-vectors appears to mitigate the immunodominance of virus-specific epitopes in the HA-head, focusing the immune response to epitopes within the conserved HA-stalk. Furthermore, for the first time an active AAV-vectored vaccine was shown to be protective in ferrets against homologous challenge in direct comparison to the gold-standard human inactivated vaccine, which had little to no effect.

As discussed above, further studies will be required to further develop the AAV-vectors as carriers for broadly reactive influence vaccines according to the criteria set up by health authorities (Figure 31). The 75 % efficacy criterion against symptomatic influenza could already be met. Further studies should include on the one hand the assessment of the exact mechanisms by which AAV-vectored vaccines mediate protection, which likely includes FcγR-activated mechanisms. On the other hand further immunization regimens should be assessed to extent the protective breadth to both antigenic groups of influenza a viruses. This could be achieved by combination of different AAV-vectored HA components (e.g. H1 and H3), or by combination of these with AAV-NP. Furthermore, also evaluation of AAV-vectored expression of other promising broadly reactive antigen candidates such as the viral neuraminidase would be highly interesting.

Due to the aforementioned advantageous of AAV-vectors, including their excellent safety profile, their licensure for use in humans and clinical grade manufacturability, AAV-vectors belong to the best suited candidates among viral vectors for clinical evaluation as influenza vaccine carriers. Taken together, findings from both animal models justify progression to clinical evaluation of the AAV-vectored vaccine, in particular of the most promising candidates AAV-HA and AAV-NP. Thus, AAV-vectors might eventually be useable in a naïve human population to efficiently prime a broadly reactive immunity, or to boost and maintain such a response in influenza experienced individuals. Influenza remains to be a disease with extreme impact on public health, not least due to the low efficacy of current vaccines. In this thesis, the beneficial influence of AAV-vectors on the immunogenicity of influenza virus antigens could be demonstrated, which might help to develop a more effective and broadly reactive influenza vaccine.

BIBLIOGRAPHY

1. J. W. McCauley *et al.*, 'ICTV 9th Report (2011) - Orthomyxoviridae', (https://talk.ictvonline.org/ictv-reports/ictv_9th_report/negative-sense-rna-viruses-2011/w/negrna_viruses/209/orthomyxoviridae), 2011.
2. B. M. Hause *et al.*, 'Characterization of a novel influenza virus in cattle and Swine: proposal for a new genus in the Orthomyxoviridae family'. *mBio* **5**, e00031-00014 (2014)
3. R. G. Webster *et al.*, 'Evolution and ecology of influenza A viruses'. *Microbiological reviews* **56**, 152-179 (1992)
4. A. D. M. E. Osterhaus *et al.*, 'Influenza B Virus in Seals'. *Science (New York, N.Y.)* **288**, 1051 (2000)
5. S. Tong *et al.*, 'A distinct lineage of influenza A virus from bats'. *Proceedings of the National Academy of Sciences* **109**, 4269-4274 (2012)
6. S. Tong *et al.*, 'New World Bats Harbor Diverse Influenza A Viruses'. *PLoS pathogens* **9**, e1003657 (2013)
7. C. Rohm *et al.*, 'Characterization of a novel influenza hemagglutinin, H15: criteria for determination of influenza A subtypes'. *Virology* **217**, 508-516 (1996)
8. WHO, 'Fact Sheet on avian Influenza ', (http://www.who.int/mediacentre/factsheets/avian_influenza/en/), 2014.
9. WHO, 'Influenza (Seasonal) Fact Sheet on Influenza No. 211', (http://www.who.int/mediacentre/factsheets/fs211/en/), 2018.
10. Y. Matsuzaki *et al.*, 'Clinical Features of Influenza C Virus Infection in Children'. *The Journal of infectious diseases* **193**, 1229-1235 (2006)
11. L. G. Baum *et al.*, 'Sialyloligosaccharides of the respiratory epithelium in the selection of human influenza virus receptor specificity'. *Acta histochemica. Supplementband* **40**, 35-38 (1990)
12. V. K. Weinheimer *et al.*, 'Influenza A viruses target type II pneumocytes in the human lung'. *The Journal of infectious diseases* **206**, 1685-1694 (2012)
13. CDC, 'Flu Symptoms & Complications', (https://www.cdc.gov/flu/consumer/symptoms.htm), 2017.
14. N. A. Molinari *et al.*, 'The annual impact of seasonal influenza in the US: measuring disease burden and costs'. *Vaccine* **25**, 5086-5096 (2007)
15. P. Palese, 'Influenza: old and new threats'. *Nat Med* **10**, S82-87 (2004)
16. CDC, 'Influenza - Past Pandemics', (https://www.cdc.gov/flu/pandemic-resources/basics/past-pandemics.html), 2017.
17. N. P. Johnson *et al.*, 'Updating the accounts: global mortality of the 1918-1920 "Spanish" influenza pandemic'. *Bulletin of the history of medicine* **76**, 105-115 (2002)
18. WHO, 'Cumulative number of confirmed human cases for avian influenza A(H5N1) reported to WHO, 2003-2018', (http://www.who.int/influenza/human_animal_interface/2016_06_13_tableH5N1.pdf?ua=1), 2018.
19. M. Imai *et al.*, 'A Highly Pathogenic Avian H7N9 Influenza Virus Isolated from A Human Is Lethal in Some Ferrets Infected via Respiratory Droplets'. *Cell Host & Microbe* (2017)
20. M. Linster *et al.*, 'Identification, characterization, and natural selection of mutations driving airborne transmission of A/H5N1 virus'. *Cell* **157**, 329-339 (2014)
21. S. Herfst *et al.*, 'Airborne transmission of influenza A/H5N1 virus between ferrets'. *Science* **336**, 1534-1541 (2012)
22. M. Kates *et al.*, 'Origin of lipids in influenza virus'. *Cold Spring Harbor symposia on quantitative biology* **27**, 293-301 (1962)
23. S. L. Zebedee *et al.*, 'Influenza A virus M2 protein: monoclonal antibody restriction of virus growth and detection of M2 in virions'. *J Virol* **62**, 2762-2772 (1988)
24. T. Noda *et al.*, 'Architecture of ribonucleoprotein complexes in influenza A virus particles'. *Nature* **439**, 490-492 (2006)
25. K. G. Murti *et al.*, 'Localization of RNA polymerases on influenza viral ribonucleoproteins by immunogold labeling'. *Virology* **164**, 562-566 (1988)
26. E. C. Hutchinson *et al.*, 'Conserved and host-specific features of influenza virion architecture'. *Nature communications* **5**, 4816 (2014)
27. R. W. Compans *et al.*, 'Structure of the Ribonucleoprotein of Influenza Virus'. *Journal of Virology* **10**, 795-800 (1972)
28. U. Desselberger *et al.*, 'The 3' and 5'-terminal sequences of influenza A, B and C virus RNA segments are highly conserved and show partial inverted complementarity'. *Gene* **8**, 315-328 (1980)
29. R. Flick *et al.*, 'Promoter elements in the influenza vRNA terminal structure'. *RNA (New York, N.Y.)* **2**, 1046-1057 (1996)
30. M. T. Hsu *et al.*, 'Genomic RNAs of influenza viruses are held in a circular conformation in virions and in infected cells by a terminal panhandle'. *Proc Natl Acad Sci U S A* **84**, 8140-8144 (1987)
31. E. Fodor *et al.*, 'The influenza virus panhandle is involved in the initiation of transcription'. *J Virol* **68**, 4092-4096 (1994)
32. H. M. Wise *et al.*, 'A complicated message: Identification of a novel PB1-related protein translated from influenza A virus segment 2 mRNA'. *J Virol* **83**, 8021-8031 (2009)
33. W. Chen *et al.*, 'A novel influenza A virus mitochondrial protein that induces cell death'. *Nat Med* **7**, 1306-1312 (2001)
34. B. W. Jagger *et al.*, 'An overlapping protein-coding region in influenza A virus segment 3 modulates the host response'. *Science (New York, N.Y.)* **337**, 199-204 (2012)
35. A. V. Vasin *et al.*, 'Molecular mechanisms enhancing the proteome of influenza A viruses: an overview of recently discovered proteins'. *Virus research* **185**, 53-63 (2014)
36. S. Yamayoshi *et al.*, 'Identification of a Novel Viral Protein Expressed from the PB2 Segment of Influenza A Virus'. *J Virol* **90**, 444-456 (2015)
37. Y. Muramoto *et al.*, 'Identification of novel influenza A virus proteins translated from PA mRNA'. *J Virol* **87**, 2455-2462 (2013)
38. S. J. Watowich *et al.*, 'Crystal structures of influenza virus hemagglutinin in complex with high-affinity receptor analogs'. *Structure (London, England : 1993)* **2**, 719-731 (1994)
39. W. Weis *et al.*, 'Structure of the influenza virus haemagglutinin complexed with its receptor, sialic acid'. *Nature* **333**, 426-431 (1988)
40. I. A. Wilson *et al.*, 'Structure of the haemagglutinin membrane glycoprotein of influenza virus at 3 A resolution'. *Nature* **289**, 366-373 (1981)
41. E. Nobusawa *et al.*, 'Comparison of complete amino acid sequences and receptor-binding properties among 13 serotypes of hemagglutinins of influenza A viruses'. *Virology* **182**, 475-485 (1991)
42. G. N. Rogers *et al.*, 'Receptor determinants of human and animal influenza virus isolates: differences in receptor specificity of the H3 hemagglutinin based on species of origin'. *Virology* **127**, 361-373 (1983)

43. G. N. Rogers *et al.*, 'Receptor binding properties of human and animal H1 influenza virus isolates'. *Virology* **173**, 317-322 (1989)
44. R. J. Connor *et al.*, 'Receptor specificity in human, avian, and equine H2 and H3 influenza virus isolates'. *Virology* **205**, 17-23 (1994)
45. J. N. Couceiro *et al.*, 'Influenza virus strains selectively recognize sialyloligosaccharides on human respiratory epithelium; the role of the host cell in selection of hemagglutinin receptor specificity'. *Virus research* **29**, 155-165 (1993)
46. A. S. Gambaryan *et al.*, 'Specification of receptor-binding phenotypes of influenza virus isolates from different hosts using synthetic sialylglycopolymers: non-egg-adapted human H1 and H3 influenza A and influenza B viruses share a common high binding affinity for 6'-sialyl(N-acetyllactosamine)'. *Virology* **232**, 345-350 (1997)
47. C. W. Naeve *et al.*, 'Mutations in the hemagglutinin receptor-binding site can change the biological properties of an influenza virus'. *J Virol* **51**, 567-569 (1984)
48. G. N. Rogers *et al.*, 'Single amino acid substitutions in influenza haemagglutinin change receptor binding specificity'. *Nature* **304**, 76-78 (1983)
49. M. N. Matrosovich *et al.*, 'Avian influenza A viruses differ from human viruses by recognition of sialyloligosaccharides and gangliosides and by a higher conservation of the HA receptor-binding site'. *Virology* **233**, 224-234 (1997)
50. C. T. Hardy *et al.*, 'Egg fluids and cells of the chorioallantoic membrane of embryonated chicken eggs can select different variants of influenza A (H3N2) viruses'. *Virology* **211**, 302-306 (1995)
51. K. Shinya *et al.*, 'Avian flu: influenza virus receptors in the human airway'. *Nature* **440**, 435-436 (2006)
52. M. Matrosovich *et al.*, 'Early alterations of the receptor-binding properties of H1, H2, and H3 avian influenza virus hemagglutinins after their introduction into mammals'. *J Virol* **74**, 8502-8512 (2000)
53. A. Vines *et al.*, 'The role of influenza A virus hemagglutinin residues 226 and 228 in receptor specificity and host range restriction'. *J Virol* **72**, 7626-7631 (1998)
54. K. S. Matlin *et al.*, 'Infectious entry pathway of influenza virus in a canine kidney cell line'. *J Cell Biol* **91**, 601-613 (1981)
55. J. Chen *et al.*, 'Structure of the hemagglutinin precursor cleavage site, a determinant of influenza pathogenicity and the origin of the labile conformation'. *Cell* **95**, 409-417 (1998)
56. S. A. Wharton *et al.*, 'Studies of influenza haemagglutinin-mediated membrane fusion'. *Virology* **149**, 27-35 (1986)
57. W. Weissenhorn *et al.*, 'Atomic structure of the ectodomain from HIV-1 gp41'. *Nature* **387**, 426-430 (1997)
58. C. M. Carr *et al.*, 'A spring-loaded mechanism for the conformational change of influenza hemagglutinin'. *Cell* **73**, 823-832 (1993)
59. P. Chambers *et al.*, 'Heptad repeat sequences are located adjacent to hydrophobic regions in several types of virus fusion glycoproteins'. *The Journal of general virology* **71 (Pt 12)**, 3075-3080 (1990)
60. C. W. Ward *et al.*, 'Influenza virus haemagglutinin. Structural predictions suggest that the fibrillar appearance is due to the presence of a coiled-coil'. *Australian journal of biological sciences* **33**, 441-447 (1980)
61. A. Helenius, 'Unpacking the incoming influenza virus'. *Cell* **69**, 577-578 (1992)
62. L. H. Pinto *et al.*, 'Influenza virus M2 protein has ion channel activity'. *Cell* **69**, 517-528 (1992)
63. J. F. Cros *et al.*, 'An unconventional NLS is critical for the nuclear import of the influenza A virus nucleoprotein and ribonucleoprotein'. *Traffic (Copenhagen, Denmark)* **6**, 205-213 (2005)
64. I. Ulmanen *et al.*, 'Role of two of the influenza virus core P proteins in recognizing cap 1 structures (m7GpppNm) on RNAs and in initiating viral RNA transcription'. *Proc Natl Acad Sci U S A* **78**, 7355-7359 (1981)
65. S. J. Plotch *et al.*, 'A unique cap(m7GpppXm)-dependent influenza virion endonuclease cleaves capped RNAs to generate the primers that initiate viral RNA transcription'. *Cell* **23**, 847-858 (1981)
66. G. X. Luo *et al.*, 'The polyadenylation signal of influenza virus RNA involves a stretch of uridines followed by the RNA duplex of the panhandle structure'. *J Virol* **65**, 2861-2867 (1991)
67. L. L. Poon *et al.*, 'Direct evidence that the poly(A) tail of influenza A virus mRNA is synthesized by reiterative copying of a U track in the virion RNA template'. *J Virol* **73**, 3473-3476 (1999)
68. G. L. Smith *et al.*, 'Synthesis and cellular location of the ten influenza polypeptides individually expressed by recombinant vaccinia viruses'. *Virology* **160**, 336-345 (1987)
69. W. W. Wu *et al.*, 'The directionality of the nuclear transport of the influenza A genome is driven by selective exposure of nuclear localization sequences on nucleoprotein'. *Virol J* **6**, 68 (2009)
70. G. P. Leser *et al.*, 'Influenza virus assembly and budding in raft-derived microdomains: a quantitative analysis of the surface distribution of HA, NA and M2 proteins'. *Virology* **342**, 215-227 (2005)
71. J. G. Magadan *et al.*, 'Influenza A virus hemagglutinin trimerization completes monomer folding and antigenicity'. *J Virol* **87**, 9742-9753 (2013)
72. D. N. Hebert *et al.*, 'Glucose trimming and reglucosylation determine glycoprotein association with calnexin in the endoplasmic reticulum'. *Cell* **81**, 425-433 (1995)
73. C. S. Copeland *et al.*, 'Assembly of influenza hemagglutinin trimers and its role in intracellular transport'. *J Cell Biol* **103**, 1179-1191 (1986)
74. M. Veit *et al.*, 'Palmitoylation of influenza virus proteins'. *Biochemical Society transactions* **41**, 50-55 (2013)
75. J. T. Perez *et al.*, 'Influenza A virus-generated small RNAs regulate the switch from transcription to replication'. *Proc Natl Acad Sci U S A* **107**, 11525-11530 (2010)
76. N. C. Robb *et al.*, 'NS2/NEP protein regulates transcription and replication of the influenza virus RNA genome'. *The Journal of general virology* **90**, 1398-1407 (2009)
77. F. T. Vreede *et al.*, 'Model suggesting that replication of influenza virus is regulated by stabilization of replicative intermediates'. *J Virol* **78**, 9568-9572 (2004)
78. G. Neumann *et al.*, 'Influenza A virus NS2 protein mediates vRNP nuclear export through NES-independent interaction with hCRM1'. *The EMBO journal* **19**, 6751-6758 (2000)
79. L. Brunotte *et al.*, 'The nuclear export protein of H5N1 influenza A viruses recruits Matrix 1 (M1) protein to the viral ribonucleoprotein to mediate nuclear export'. *The Journal of biological chemistry* **289**, 20067-20077 (2014)
80. J. S. Rossman *et al.*, 'Influenza virus assembly and budding'. *Virology* **411**, 229-236 (2011)
81. M. Gerber *et al.*, 'Selective packaging of the influenza A genome and consequences for genetic reassortment'. *Trends Microbiol* **22**, 446-455 (2014)
82. P. M. Colman *et al.*, 'Structure of the catalytic and antigenic sites in influenza virus neuraminidase'. *Nature* **303**, 41-44 (1983)
83. P. Palese *et al.*, 'Inhibition of influenza virus replication in tissue culture by 2-deoxy-2,3-dehydro-N-trifluoroacetylneuraminic acid (FANA): mechanism of action'. *The Journal of general virology* **33**, 159-163 (1976)
84. P. Palese *et al.*, 'Characterization of temperature sensitive influenza virus mutants defective in neuraminidase'. *Virology* **61**, 397-410 (1974)

85. S. Bertram *et al.*, 'Influenza and SARS-coronavirus activating proteases TMPRSS2 and HAT are expressed at multiple sites in human respiratory and gastrointestinal tracts'. *PloS one* **7**, e35876 (2012)
86. E. Bottcher-Friebertshauser *et al.*, 'Cleavage of influenza virus hemagglutinin by airway proteases TMPRSS2 and HAT differs in subcellular localization and susceptibility to protease inhibitors'. *J Virol* **84**, 5605-5614 (2010)
87. H. Kido *et al.*, 'Cellular proteinases trigger the infectivity of the influenza A and Sendai viruses'. *Molecules and cells* **9**, 235-244 (1999)
88. M. L. Perdue *et al.*, 'Virulence-associated sequence duplication at the hemagglutinin cleavage site of avian influenza viruses'. *Virus research* **49**, 173-186 (1997)
89. A. Stieneke-Grober *et al.*, 'Influenza virus hemagglutinin with multibasic cleavage site is activated by furin, a subtilisin-like endoprotease'. *The EMBO journal* **11**, 2407-2414 (1992)
90. D. A. Steinhauer, 'Role of hemagglutinin cleavage for the pathogenicity of influenza virus'. *Virology* **258**, 1-20 (1999)
91. S. Tripathi *et al.*, 'The amazing innate immune response to influenza A virus infection'. *Innate immunity* **21**, 73-98 (2015)
92. A. Iwasaki *et al.*, 'Innate immunity to influenza virus infection'. *Nature reviews. Immunology* **14**, 315-328 (2014)
93. N. Said-Sadier *et al.*, 'Alarmins, inflammasomes and immunity'. *Biomedical journal* **35**, 437-449 (2012)
94. M. Terajima *et al.*, 'Complement-dependent lysis of influenza a virus-infected cells by broadly cross-reactive human monoclonal antibodies'. *J Virol* **85**, 13463-13467 (2011)
95. W. He *et al.*, 'Alveolar macrophages are critical for broadly-reactive antibody-mediated protection against influenza A virus in mice'. *Nature communications* **8**, 846 (2017)
96. C. E. Mullarkey *et al.*, 'Broadly Neutralizing Hemagglutinin Stalk-Specific Antibodies Induce Potent Phagocytosis of Immune Complexes by Neutrophils in an Fc-Dependent Manner'. *mBio* **7**, (2016)
97. R. Cioncada *et al.*, 'Vaccine adjuvant MF59 promotes the intranodal differentiation of antigen-loaded and activated monocyte-derived dendritic cells'. *PloS one* **12**, e0185843 (2017)
98. J. McGill *et al.*, 'Innate immune control and regulation of influenza virus infections'. *Journal of leukocyte biology* **86**, 803-812 (2009)
99. K. M. Kenneth *et al.*, *Janeway Immunology*. (Springer Spektrum, ed. 7, 2009), vol. 7, pp. 1093.
100. M. A. Miller *et al.*, 'Endogenous antigen processing drives the primary CD4+ T cell response to influenza'. *Nat Med* **21**, 1216-1222 (2015)
101. A. DiPiazza *et al.*, 'Pandemic 2009 H1N1 Influenza Venus reporter virus reveals broad diversity of MHC class II-positive antigen-bearing cells following infection in vivo'. *Scientific reports* **7**, 10857 (2017)
102. M. M. Hufford *et al.*, 'The effector T cell response to influenza infection'. *Curr Top Microbiol Immunol* **386**, 423-455 (2015)
103. G. L. Chen *et al.*, 'Comparison of a live attenuated 2009 H1N1 vaccine with seasonal influenza vaccines against 2009 pandemic H1N1 virus infection in mice and ferrets'. *The Journal of infectious diseases* **203**, 930-936 (2011)
104. H. Hamada *et al.*, 'Multiple redundant effector mechanisms of CD8+ T cells protect against influenza infection'. *Journal of immunology (Baltimore, Md. : 1950)* **190**, 296-306 (2013)
105. J. Sun *et al.*, 'Effector T cells control lung inflammation during acute influenza virus infection by producing IL-10'. *Nat Med* **15**, 277-284 (2009)
106. E. Grant *et al.*, 'Nucleoprotein of influenza A virus is a major target of immunodominant CD8+ T-cell responses'. *Immunology and cell biology* **91**, 184-194 (2013)
107. F. Gotch *et al.*, 'Cytotoxic T lymphocytes recognize a fragment of influenza virus matrix protein in association with HLA-A2'. *Nature* **326**, 881-882 (1987)
108. G. T. Belz *et al.*, 'Compromised influenza virus-specific CD8(+)-T-cell memory in CD4(+)-T-cell-deficient mice'. *J Virol* **76**, 12388-12393 (2002)
109. S. M. Haeryfar *et al.*, 'Regulatory T cells suppress CD8+ T cell responses induced by direct priming and cross-priming and moderate immunodominance disparities'. *Journal of immunology (Baltimore, Md. : 1950)* **174**, 3344-3351 (2005)
110. W. Gerhard, 'The role of the antibody response in influenza virus infection'. *Curr Top Microbiol Immunol* **260**, 171-190 (2001)
111. K. K. McKinstry *et al.*, 'Memory CD4+ T cells protect against influenza through multiple synergizing mechanisms'. *The Journal of clinical investigation* **122**, 2847-2856 (2012)
112. K. D. Zens *et al.*, 'Memory CD4 T cells in influenza'. *Curr Top Microbiol Immunol* **386**, 399-421 (2015)
113. T. Wu *et al.*, 'Lung-resident memory CD8 T cells (TRM) are indispensable for optimal cross-protection against pulmonary virus infection'. *Journal of leukocyte biology* **95**, 215-224 (2014)
114. R. Bodewes *et al.*, 'In vitro assessment of the immunological significance of a human monoclonal antibody directed to the influenza a virus nucleoprotein'. *Clin Vaccine Immunol* **20**, 1333-1337 (2013)
115. J. T. Voeten *et al.*, 'Use of recombinant nucleoproteins in enzyme-linked immunosorbent assays for detection of virus-specific immunoglobulin A (IgA) and IgG antibodies in influenza virus A- or B-infected patients'. *Journal of clinical microbiology* **36**, 3527-3531 (1998)
116. C. Chiu *et al.*, 'Antiviral B cell and T cell immunity in the lungs'. *Nat Immunol* **16**, 18-26 (2015)
117. B. O. Lee *et al.*, 'CD4 T cell-independent antibody response promotes resolution of primary influenza infection and helps to prevent reinfection'. *Journal of immunology (Baltimore, Md. : 1950)* **175**, 5827-5838 (2005)
118. R.-P. Sekaly, 'The failed HIV Merck vaccine study: a step back or a launching point for future vaccine development?'. *The Journal of experimental medicine* **205**, 7-12 (2008)
119. S. P. Buchbinder *et al.*, 'Efficacy assessment of a cell-mediated immunity HIV-1 vaccine (the Step Study): a double-blind, randomised, placebo-controlled, test-of-concept trial'. *Lancet (London, England)* **372**, 1881-1893 (2008)
120. F. Nimmerjahn *et al.*, 'Fcgamma receptors as regulators of immune responses'. *Nature reviews. Immunology* **8**, 34-47 (2008)
121. B. Cortina-Ceballos *et al.*, 'Longitudinal analysis of the peripheral B cell repertoire reveals unique effects of immunization with a new influenza virus strain'. *Genome medicine* **7**, 124 (2015)
122. Y. Fu *et al.*, 'A broadly neutralizing anti-influenza antibody reveals ongoing capacity of haemagglutinin-specific memory B cells to evolve'. *Nature communications* **7**, 12780 (2016)
123. G. A. Kirchenbaum *et al.*, 'Infection of Ferrets with Influenza Virus Elicits a Light Chain-Biased Antibody Response against Hemagglutinin'. *Journal of immunology (Baltimore, Md. : 1950)* (2017)
124. Y. Avnir *et al.*, 'Molecular signatures of hemagglutinin stem-directed heterosubtypic human neutralizing antibodies against influenza A viruses'. *PLoS pathogens* **10**, e1004103 (2014)
125. Y. Asahi *et al.*, 'Protection against influenza virus infection in polymeric Ig receptor knockout mice immunized intranasally with adjuvant-combined vaccines'. *Journal of immunology (Baltimore, Md. : 1950)* **168**, 2930-2938 (2002)

126. P. Bruhns, 'Properties of mouse and human IgG receptors and their contribution to disease models'. *Blood* **119**, 5640-5649 (2012)
127. A. Pincetic *et al.*, 'Type I and type II Fc receptors regulate innate and adaptive immunity'. *Nat Immunol* **15**, 707-716 (2014)
128. F. Nimmerjahn *et al.*, 'FcgammaRIV: a novel FcR with distinct IgG subclass specificity'. *Immunity* **23**, 41-51 (2005)
129. T. T. Wang *et al.*, 'Anti-HA Glycoforms Drive B Cell Affinity Selection and Determine Influenza Vaccine Efficacy'. *Cell* **162**, 160-169 (2015)
130. P. Sondermann *et al.*, 'The 3.2-A crystal structure of the human IgG1 Fc fragment-Fc gammaRIII complex'. *Nature* **406**, 267-273 (2000)
131. K. Kato *et al.*, 'A conformational change in the Fc precludes the binding of two Fcgamma receptor molecules to one IgG'. *Immunology today* **21**, 310-312 (2000)
132. A. M. Duchemin *et al.*, 'Clustering of the high affinity Fc receptor for immunoglobulin G (Fc gamma RI) results in phosphorylation of its associated gamma-chain'. *The Journal of biological chemistry* **269**, 12111-12117 (1994)
133. P. Sondermann *et al.*, 'General mechanism for modulating immunoglobulin effector function'. *Proceedings of the National Academy of Sciences* **110**, 9868-9872 (2013)
134. R. Jefferis *et al.*, 'IgG-Fc-mediated effector functions: molecular definition of interaction sites for effector ligands and the role of glycosylation'. *Immunological reviews* **163**, 59-76 (1998)
135. S. Bournazos *et al.*, 'Fcgamma Receptor Function and the Design of Vaccination Strategies'. *Immunity* **47**, 224-233 (2017)
136. S. Jegaskanda *et al.*, 'Fc or not Fc; that is the question: Antibody Fc-receptor interactions are key to universal influenza vaccine design'. *Hum Vaccin Immunother* 0 (2017)
137. M. J. Smyth *et al.*, 'Activation of NK cell cytotoxicity'. *Molecular immunology* **42**, 501-510 (2005)
138. S. S. Metkar *et al.*, 'Human neutrophils lack granzyme A, granzyme B, and perforin'. *Blood* **104**, 905-906; author reply 907-908 (2004)
139. A. Manda *et al.*, 'Neutrophil extracellular traps in physiology and pathology'. *Central-European Journal of Immunology* **39**, 116-121 (2014)
140. T. Frensing *et al.*, 'Influenza virus intracellular replication dynamics, release kinetics, and particle morphology during propagation in MDCK cells'. *Applied microbiology and biotechnology* **100**, 7181-7192 (2016)
141. J. Fan *et al.*, 'Preclinical study of influenza virus A M2 peptide conjugate vaccines in mice, ferrets, and rhesus monkeys'. *Vaccine* **22**, 2993-3003 (2004)
142. M. R. Sandbulte *et al.*, 'Cross-reactive neuraminidase antibodies afford partial protection against H5N1 in mice and are present in unexposed humans'. *PLoS medicine* **4**, e59 (2007)
143. D. M. Carragher *et al.*, 'A novel role for non-neutralizing antibodies against nucleoprotein in facilitating resistance to influenza virus'. *Journal of immunology (Baltimore, Md. : 1950)* **181**, 4168-4176 (2008)
144. Aaron G. Schmidt *et al.*, 'Viral Receptor-Binding Site Antibodies with Diverse Germline Origins'. *Cell* **161**, 1026-1034 (2015)
145. X. Yu *et al.*, 'Neutralizing antibodies derived from the B cells of 1918 influenza pandemic survivors'. *Nature* **455**, 532-536 (2008)
146. A. J. Caton *et al.*, 'The antigenic structure of the influenza virus A/PR/8/34 hemagglutinin (H1 subtype)'. *Cell* **31**, 417-427 (1982)
147. W. Gerhard *et al.*, 'Antigenic structure of influenza virus haemagglutinin defined by hybridoma antibodies'. *Nature* **290**, 713-717 (1981)
148. D. L. Hovanec *et al.*, 'Antigenic structure of the hemagglutinin of influenza virus B/Hong Kong/8/73 as determined from gene sequence analysis of variants selected with monoclonal antibodies'. *Virology* **139**, 384-392 (1984)
149. D. C. Wiley *et al.*, 'Structural identification of the antibody-binding sites of Hong Kong influenza haemagglutinin and their involvement in antigenic variation'. *Nature* **289**, 373-378 (1981)
150. N. C. Wu *et al.*, 'A Perspective on the Structural and Functional Constraints for Immune Evasion: Insights from Influenza Virus'. *Journal of molecular biology* **429**, 2694-2709 (2017)
151. G. Pappas *et al.*, 'Insights into infectious disease in the era of Hippocrates'. *International journal of infectious diseases : IJID : official publication of the International Society for Infectious Diseases* **12**, 347-350 (2008)
152. W. Smith *et al.*, 'A VIRUS OBTAINED FROM INFLUENZA PATIENTS'. *The Lancet* **222**, 66-68 (1933)
153. C. Hannoun, 'The evolving history of influenza viruses and influenza vaccines'. *Expert review of vaccines* **12**, 1085-1094 (2013)
154. I. Barberis *et al.*, 'History and evolution of influenza control through vaccination: from the first monovalent vaccine to universal vaccines'. *Journal of Preventive Medicine and Hygiene* **57**, E115-E120 (2016)
155. C. ACIP, 'Antiviral Agents for the Treatment and Chemoprophylaxis of Influenza'. *MMWR* **60**, (2011)
156. WHO, 'WHO Model List of Essential Medicines'. (2017)
157. Aerzteblatt, 'Tamiflu: ECDC-Gutachten bewertet Neuraminidase-Hemmer weiter positiv'. *Aerzteblatt* (2017)
158. F. G. Hayden *et al.*, 'Baloxavir Marboxil for Uncomplicated Influenza in Adults and Adolescents'. *The New England journal of medicine* **379**, 913-923 (2018)
159. RKI, 'Empfehlungen der Ständigen Impfkommission (STIKO) am Robert Koch-Institut – 2017/2018'. *Epidemiologisches Bulletin* **34**, (2017)
160. R. K. Institut, 'Epidemiologisches Bulletin - Empfehlungen der STIKO beim RKI 2018/2019'. **34**, (2018)
161. A. al-Mazrou *et al.*, 'Comparison of adverse reactions to whole-virion and split-virion influenza vaccines in hospital personnel'. *CMAJ : Canadian Medical Association journal = journal de l'Association medicale canadienne* **145**, 213-218 (1991)
162. L. M. Dunkle *et al.*, 'Randomized Comparison of Immunogenicity and Safety of Quadrivalent Recombinant Versus Inactivated Influenza Vaccine in Healthy Adults 18-49 Years of Age'. *The Journal of infectious diseases* **216**, 1219-1226 (2017)
163. C. Herzog *et al.*, 'Eleven years of Inflexal V-a virosomal adjuvanted influenza vaccine'. *Vaccine* **27**, 4381-4387 (2009)
164. C. A. Robertson *et al.*, 'Fluzone(R) Intradermal Quadrivalent Influenza Vaccine'. *Expert review of vaccines* **15**, 1245-1253 (2016)
165. ECDC, 'Types of seasonal influenza vaccines', (https://ecdc.europa.eu/en/seasonal-influenza/prevention-and-control/vaccines/types-of-seasonal-influenza-vaccine), 2017.
166. R. B. Belshe *et al.*, 'Live attenuated versus inactivated influenza vaccine in infants and young children'. *The New England journal of medicine* **356**, 685-696 (2007)
167. P. K. Tosh *et al.*, 'Flu myths: dispelling the myths associated with live attenuated influenza vaccine'. *Mayo Clinic proceedings* **83**, 77-84 (2008)
168. S. E. Ohmit *et al.*, 'Prevention of antigenically drifted influenza by inactivated and live attenuated vaccines'. *The New England journal of medicine* **355**, 2513-2522 (2006)
169. PEI, 'Liste Pandemischer Impfstoffe',

(https://www.pei.de/DE/arzneimittel/impfstoff-impfstoffe-fuer-den-menschen/influenza-grippe/pandemische-influenzaimpfstoffe/pandemische-influenzaimpfstoffe-node.html), 2018.
170. P. C. Soema *et al.*, 'Current and next generation influenza vaccines: Formulation and production strategies'. *Eur J Pharm Biopharm* **94**, 251-263 (2015)
171. WHO. (2018).
172. C. Gerdil, 'The annual production cycle for influenza vaccine'. *Vaccine* **21**, 1776-1779 (2003)
173. D. D. Raymond *et al.*, 'Influenza immunization elicits antibodies specific for an egg-adapted vaccine strain'. *Nat Med* (2016)
174. J. A. Tree *et al.*, 'Comparison of large-scale mammalian cell culture systems with egg culture for the production of influenza virus A vaccine strains'. *Vaccine* **19**, 3444-3450 (2001)
175. C. Y. Chan *et al.*, 'Preflucel(R): a Vero-cell culture-derived trivalent influenza vaccine'. *Expert review of vaccines* **11**, 759-773 (2012)
176. A. Doroshenko *et al.*, 'Trivalent MDCK cell culture-derived influenza vaccine Optaflu (Novartis Vaccines)'. *Expert review of vaccines* **8**, 679-688 (2009)
177. M. S. Lee *et al.*, 'A cell-based backup to speed up pandemic influenza vaccine production'. *Trends Microbiol* **20**, 103-105 (2012)
178. I. W. Li *et al.*, 'Differential susceptibility of different cell lines to swine-origin influenza A H1N1, seasonal human influenza A H1N1, and avian influenza A H5N1 viruses'. *Journal of clinical virology : the official publication of the Pan American Society for Clinical Virology* **46**, 325-330 (2009)
179. K. Haq *et al.*, 'Immunosenescence: influenza vaccination and the elderly'. *Current opinion in immunology* **29**, 38-42 (2014)
180. PEI, 'Liste zugelassende Grippeimfpstoffe', (https://www.pei.de/DE/arzneimittel/impfstoff-impfstoffe-fuer-den-menschen/influenza-grippe/influenza-grippe-node.html), 2018.
181. A. Vrdoljak *et al.*, 'Induction of broad immunity by thermostabilised vaccines incorporated in dissolvable microneedles using novel fabrication methods'. *Journal of controlled release : official journal of the Controlled Release Society* **225**, 192-204 (2016)
182. D. Christensen *et al.*, 'Seasonal Influenza Split Vaccines Confer Partial Cross-Protection against Heterologous Influenza Virus in Ferrets When Combined with the CAF01 Adjuvant'. *Frontiers in immunology* **8**, 1928 (2017)
183. M. Rondy *et al.*, 'Effectiveness of influenza vaccines in preventing severe influenza illness among adults: A systematic review and meta-analysis of test-negative design case-control studies'. *J Infect* **75**, 381-394 (2017)
184. H. Xie *et al.*, 'H3N2 Mismatch of 2014–15 Northern Hemisphere Influenza Vaccines and Head-to-head Comparison between Human and Ferret Antisera derived Antigenic Maps'. *Scientific reports* **5**, 15279 (2015)
185. E. A. Belongia *et al.*, 'Variable influenza vaccine effectiveness by subtype: a systematic review and meta-analysis of test-negative design studies'. *The Lancet Infectious Diseases* **16**, 942-951 (2016)
186. E. Dube *et al.*, 'Vaccine hesitancy: an overview'. *Human vaccines & immunotherapeutics* **9**, 1763-1773 (2013)
187. ECDC, 'Seasonal Influenza Vaccination in Europe'. *Technical Report* (2017)
188. Nature, 'Science must get ready for the next global flu crisis: A universal flu vaccine is the only serious defence against a future flu pandemic. '. *Nature* **553**, 1 (2018)
189. A. Nicoll *et al.*, 'Low effectiveness undermines promotion of seasonal influenza vaccine'. *The Lancet. Infectious diseases* **13**, 7-9 (2013)
190. E. J. Erbelding *et al.*, 'A Universal Influenza Vaccine: The Strategic Plan for the National Institute of Allergy and Infectious Diseases'. *The Journal of infectious diseases* **218**, 347-354 (2018)
191. J. R. Ortiz *et al.*, 'Report on eighth WHO meeting on development of influenza vaccines that induce broadly protective and long-lasting immune responses: Chicago, USA, 23–24 August 2016'. *Vaccine* **36**, 932-938 (2018)
192. P. N. Graves *et al.*, 'Preparation of influenza virus subviral particles lacking the HA1 subunit of hemagglutinin: unmasking of cross-reactive HA2 determinants'. *Virology* **126**, 106-116 (1983)
193. Y. Okuno *et al.*, 'A common neutralizing epitope conserved between the hemagglutinins of influenza A virus H1 and H2 strains'. *J Virol* **67**, 2552-2558 (1993)
194. C. Dreyfus *et al.*, 'Structure of a classical broadly neutralizing stem antibody in complex with a pandemic H2 influenza virus hemagglutinin'. *J Virol* **87**, 7149-7154 (2013)
195. H. Hoag, 'A universal problem'. *Nat Med* **19**, 12-14 (2013)
196. P. S. Lee *et al.*, 'Structural characterization of viral epitopes recognized by broadly cross-reactive antibodies'. *Curr Top Microbiol Immunol* **386**, 323-341 (2015)
197. A. M. Hashem, 'Prospects of HA-based universal influenza vaccine'. *BioMed research international* **2015**, 414637 (2015)
198. D. C. Ekiert *et al.*, 'Antibody recognition of a highly conserved influenza virus epitope'. *Science (New York, N.Y.)* **324**, 246-251 (2009)
199. M. Throsby *et al.*, 'Heterosubtypic neutralizing monoclonal antibodies cross-protective against H5N1 and H1N1 recovered from human IgM+ memory B cells'. *PloS one* **3**, e3942 (2008)
200. D. C. Ekiert *et al.*, 'A Highly Conserved Neutralizing Epitope on Group 2 Influenza A Viruses'. *Science (New York, N.Y.)* **333**, 843-850 (2011)
201. D. Corti *et al.*, 'A neutralizing antibody selected from plasma cells that binds to group 1 and group 2 influenza A hemagglutinins'. *Science (New York, N.Y.)* **333**, 850-856 (2011)
202. C. Dreyfus *et al.*, 'Highly conserved protective epitopes on influenza B viruses'. *Science (New York, N.Y.)* **337**, 1343-1348 (2012)
203. R. H. Friesen *et al.*, 'A common solution to group 2 influenza virus neutralization'. *Proc Natl Acad Sci U S A* **111**, 445-450 (2014)
204. P. S. Lee *et al.*, 'Heterosubtypic antibody recognition of the influenza virus hemagglutinin receptor binding site enhanced by avidity'. *Proc Natl Acad Sci U S A* **109**, 17040-17045 (2012)
205. R. Yoshida *et al.*, 'Cross-protective potential of a novel monoclonal antibody directed against antigenic site B of the hemagglutinin of influenza A viruses'. *PLoS pathogens* **5**, e1000350 (2009)
206. X. Zhu *et al.*, 'A unique and conserved neutralization epitope in H5N1 influenza viruses identified by an antibody against the A/Goose/Guangdong/1/96 hemagglutinin'. *J Virol* **87**, 12619-12635 (2013)
207. K. E. Neu *et al.*, 'Heads, stalks and everything else: how can antibodies eradicate influenza as a human disease?'. *Current opinion in immunology* **42**, 48-55 (2016)
208. B. Brandenburg *et al.*, 'Mechanisms of Hemagglutinin Targeted Influenza Virus Neutralization'. *PloS one* **8**, e80034 (2013)
209. G. S. Tan *et al.*, 'Characterization of a Broadly Neutralizing Monoclonal Antibody That Targets the Fusion Domain of Group 2 Influenza A Virus Hemagglutinin'. *Journal of Virology* **88**, 13580-13592 (2014)
210. S. Yamayoshi *et al.*, 'A Broadly Reactive Human Anti-hemagglutinin Stem Monoclonal Antibody That Inhibits Influenza A Virus Particle Release'. *EBioMedicine* (2017)

211. T. J. Wohlbold *et al.*, 'Hemagglutinin Stalk- and Neuraminidase-Specific Monoclonal Antibodies Protect against Lethal H10N8 Influenza Virus Infection in Mice'. *J Virol* **90**, 851-861 (2016)
212. K. B. O'Brien *et al.*, 'A protective role for complement C3 protein during pandemic 2009 H1N1 and H5N1 influenza A virus infection'. *PloS one* **6**, e17377 (2011)
213. M. Terajima *et al.*, 'High Antibody-Dependent Cellular Cytotoxicity Antibody Titers to H5N1 and H7N9 Avian Influenza A Viruses in Healthy US Adults and Older Children'. *The Journal of infectious diseases* **212**, 1052-1060 (2015)
214. A. W. Mesman *et al.*, 'Influenza virus A(H1N1)2009 antibody-dependent cellular cytotoxicity in young children prior to the H1N1 pandemic'. *J Gen Virol* **97**, 2157-2165 (2016)
215. S. Jegaskanda *et al.*, 'Age-associated cross-reactive antibody-dependent cellular cytotoxicity toward 2009 pandemic influenza A virus subtype H1N1'. *The Journal of infectious diseases* **208**, 1051-1061 (2013)
216. S. Jegaskanda *et al.*, 'Standard trivalent influenza virus protein vaccination does not prime antibody-dependent cellular cytotoxicity in macaques'. *J Virol* **87**, 13706-13718 (2013)
217. R. D. de Vries *et al.*, 'Influenza virus-specific antibody dependent cellular cytoxicity induced by vaccination or natural infection'. *Vaccine* **35**, 238-247 (2017)
218. S. Jegaskanda *et al.*, 'Generation and Protective Ability of Influenza Virus-Specific Antibody-Dependent Cellular Cytotoxicity in Humans Elicited by Vaccination, Natural Infection, and Experimental Challenge'. *Journal of Infectious Diseases* **214**, 945-952 (2016)
219. W. Zhong *et al.*, 'Antibody-Dependent Cell-Mediated Cytotoxicity to Hemagglutinin of Influenza A Viruses After Influenza Vaccination in Humans'. *Open forum infectious diseases* **3**, ofw102 (2016)
220. W. Zhong *et al.*, 'Vaccination with 2014-15 Seasonal Inactivated Influenza Vaccine Elicits Cross-Reactive Anti-HA Antibodies with Strong ADCC Against Antigenically Drifted Circulating H3N2 Virus in Humans'. *Viral immunology* **29**, 259-262 (2016)
221. M. Sobhanie *et al.*, 'Evaluation of the Safety and Immunogenicity of a Candidate Pandemic Live Attenuated Influenza Vaccine (pLAIV) Against Influenza A(H7N9)'. *The Journal of infectious diseases* **213**, 922-929 (2016)
222. D. J. DiLillo *et al.*, 'Broadly neutralizing hemagglutinin stalk-specific antibodies require FcgammaR interactions for protection against influenza virus in vivo'. *Nat Med* **20**, 143-151 (2014)
223. D. J. DiLillo *et al.*, 'Broadly neutralizing anti-influenza antibodies require Fc receptor engagement for in vivo protection'. *The Journal of clinical investigation* **126**, 605-610 (2016)
224. G. S. Tan *et al.*, 'Broadly-Reactive Neutralizing and Non-neutralizing Antibodies Directed against the H7 Influenza Virus Hemagglutinin Reveal Divergent Mechanisms of Protection'. *PLoS pathogens* **12**, e1005578 (2016)
225. S. Van den Hoecke *et al.*, 'Hierarchical and redundant roles of activating FcgammaRs in protection against influenza disease by M2e-specific IgG1 and IgG2a antibodies'. *J Virol* (2017)
226. W. He *et al.*, 'Epitope specificity plays a critical role in regulating antibody-dependent cell-mediated cytotoxicity against influenza A virus'. *Proc Natl Acad Sci U S A* (2016)
227. F. Cox *et al.*, 'HA Antibody-Mediated FcgammaRIIIa Activity Is Both Dependent on FcR Engagement and Interactions between HA and Sialic Acids'. *Frontiers in immunology* **7**, 399 (2016)
228. P. E. Leon *et al.*, 'Optimal activation of Fc-mediated effector functions by influenza virus hemagglutinin antibodies requires two points of contact'. *Proceedings of the National Academy of Sciences of the United States of America* **113**, E5944-E5951 (2016)
229. C. J. Henry Dunand *et al.*, 'Both Neutralizing and Non-Neutralizing Human H7N9 Influenza Vaccine-Induced Monoclonal Antibodies Confer Protection'. *Cell host & microbe* **19**, 800-813 (2016)
230. P. Palese, 'Influenza: A broadly protective antibody'. *Nature* **551**, 310-311 (2017)
231. C. Shen *et al.*, 'A multimechanistic antibody targeting the receptor binding site potently cross-protects against influenza B viruses'. *Sci Transl Med* **9**, (2017)
232. H. A. Vanderven *et al.*, 'Fc functional antibodies in humans with severe H7N9 and seasonal influenza'. *JCI insight* **2**, (2017)
233. S. Jegaskanda *et al.*, 'Human seasonal influenza A viruses induce H7N9-cross-reactive antibody-dependent cellular cytotoxicity (ADCC) antibodies that are directed towards the nucleoprotein'. *The Journal of infectious diseases* (2016)
234. J. W. Yewdell *et al.*, 'Expression of influenza A virus internal antigens on the surface of infected P815 cells'. *Journal of immunology (Baltimore, Md. : 1950)* **126**, 1814-1819 (1981)
235. S. Khurana *et al.*, 'Vaccine-induced anti-HA2 antibodies promote virus fusion and enhance influenza virus respiratory disease'. *Sci Transl Med* **5**, 200ra114 (2013)
236. S. A. Valkenburg *et al.*, 'Stalking influenza by vaccination with pre-fusion headless HA mini-stem'. *Scientific reports* **6**, 22666 (2016)
237. C. Bernelin-Cottet *et al.*, 'A Universal Influenza Vaccine Can Lead to Disease Exacerbation or Viral Control Depending on Delivery Strategies'. *Frontiers in immunology* **7**, 641 (2016)
238. H. Ochiai *et al.*, 'Infection enhancement of influenza A NWS virus in primary murine macrophages by anti-hemagglutinin monoclonal antibody'. *Journal of medical virology* **36**, 217-221 (1992)
239. M. Tamura *et al.*, 'Antibodies to Ha and Na Augment Uptake of Influenza-a Viruses into Cells Via Fc Receptor Entry'. *Virology* **182**, 211-219 (1991)
240. N. Chai *et al.*, 'Two Escape Mechanisms of Influenza A Virus to a Broadly Neutralizing Stalk-Binding Antibody'. *PLoS pathogens* **12**, e1005702 (2016)
241. K. Tharakaraman *et al.*, 'Broadly neutralizing influenza hemagglutinin stem-specific antibody CR8020 targets residues that are prone to escape due to host selection pressure'. *Cell host & microbe* **15**, 644-651 (2014)
242. J. Sui *et al.*, 'Structural and functional bases for broad-spectrum neutralization of avian and human influenza A viruses'. *Nat Struct Mol Biol* **16**, 265-273 (2009)
243. C. A. Thomson *et al.*, 'Pandemic H1N1 Influenza Infection and Vaccination in Humans Induces Cross-Protective Antibodies that Target the Hemagglutinin Stem'. *Frontiers in immunology* **3**, 87 (2012)
244. A. K. Wheatley *et al.*, 'H5N1 Vaccine-Elicited Memory B Cells Are Genetically Constrained by the IGHV Locus in the Recognition of a Neutralizing Epitope in the Hemagglutinin Stem'. *Journal of immunology (Baltimore, Md. : 1950)* **195**, 602-610 (2015)
245. D. De Marco *et al.*, 'A Non-VH1-69 Heterosubtypic Neutralizing Human Monoclonal Antibody Protects Mice against H1N1 and H5N1 Viruses'. *PloS one* **7**, e34415 (2012)
246. L. Pappas *et al.*, 'Rapid development of broadly influenza neutralizing antibodies through redundant mutations'. *Nature* **516**, 418-422 (2014)
247. Y. Avnir *et al.*, 'IGHV1-69 polymorphism modulates anti-influenza antibody repertoires, correlates with IGHV utilization shifts and varies by ethnicity'. *Scientific reports* **6**, 20842 (2016)

248. J. Wrammert *et al.*, 'Rapid cloning of high-affinity human monoclonal antibodies against influenza virus'. *Nature* **453**, 667-671 (2008)
249. D. Angeletti *et al.*, 'Understanding and Manipulating Viral Immunity: Antibody Immunodominance Enters Center Stage'. *Trends Immunol* **39**, 549-561 (2018)
250. A. H. Ellebedy *et al.*, 'Induction of broadly cross-reactive antibody responses to the influenza HA stem region following H5N1 vaccination in humans'. *Proc Natl Acad Sci U S A* **111**, 13133-13138 (2014)
251. V. I. Zarnitsyna *et al.*, 'Multi-epitope Models Explain How Pre-existing Antibodies Affect the Generation of Broadly Protective Responses to Influenza'. *PLoS pathogens* **12**, e1005692 (2016)
252. S. F. Andrews *et al.*, 'Immune history profoundly affects broadly protective B cell responses to influenza'. *Sci Transl Med* **7**, 316ra192 (2015)
253. D. Angeletti *et al.*, 'Defining B cell immunodominance to viruses'. *Nat Immunol* **18**, 456-463 (2017)
254. J. Wrammert *et al.*, 'Broadly cross-reactive antibodies dominate the human B cell response against 2009 pandemic H1N1 influenza virus infection'. *The Journal of experimental medicine* **208**, 181-193 (2011)
255. N. Pica *et al.*, 'Hemagglutinin stalk antibodies elicited by the 2009 pandemic influenza virus as a mechanism for the extinction of seasonal H1N1 viruses'. *Proc Natl Acad Sci U S A* **109**, 2573-2578 (2012)
256. F. Krammer *et al.*, 'Hemagglutinin Stalk-Reactive Antibodies Are Boosted following Sequential Infection with Seasonal and Pandemic H1N1 Influenza Virus in Mice'. *J Virol* **86**, 10302-10307 (2012)
257. G. M. Li *et al.*, 'Pandemic H1N1 influenza vaccine induces a recall response in humans that favors broadly cross-reactive memory B cells'. *Proc Natl Acad Sci U S A* **109**, 9047-9052 (2012)
258. P. Palese *et al.*, 'Why do influenza virus subtypes die out? A hypothesis'. *mBio* **2**, (2011)
259. F. Krammer, 'Strategies to induce broadly protective antibody responses to viral glycoproteins'. *Expert review of vaccines* **16**, 503-513 (2017)
260. M. S. Miller *et al.*, 'Neutralizing antibodies against previously encountered influenza virus strains increase over time: a longitudinal analysis'. *Sci Transl Med* **5**, 198ra107 (2013)
261. R. Nachbagauer *et al.*, 'Age Dependence and Isotype Specificity of Influenza Virus Hemagglutinin Stalk-Reactive Antibodies in Humans'. *mBio* **7**, (2016)
262. R. Nachbagauer *et al.*, 'Defining the antibody cross-reactome directed against the influenza virus surface glycoproteins'. *Nat Immunol* (2017)
263. M. Mandelboim *et al.*, 'Significant cross reactive antibodies to influenza virus in adults and children during a period of marked antigenic drift'. *BMC Infect Dis* **14**, 346 (2014)
264. W. He *et al.*, 'Broadly neutralizing anti-influenza virus antibodies: enhancement of neutralizing potency in polyclonal mixtures and IgA backbones'. *J Virol* **89**, 3610-3618 (2015)
265. M. A. Moody *et al.*, 'H3N2 Influenza Infection Elicits More Cross-Reactive and Less Clonally Expanded Anti-Hemagglutinin Antibodies Than Influenza Vaccination'. *PloS one* **6**, e25797 (2011)
266. C. J. Henry Dunand *et al.*, 'Preexisting human antibodies neutralize recently emerged H7N9 influenza strains'. *The Journal of clinical investigation* **125**, 1255-1268 (2015)
267. D. Corti *et al.*, 'Heterosubtypic neutralizing antibodies are produced by individuals immunized with a seasonal influenza vaccine'. *The Journal of clinical investigation* **120**, 1663-1673 (2010)
268. I. Margine *et al.*, 'H3N2 influenza virus infection induces broadly reactive hemagglutinin stalk antibodies in humans and mice'. *J Virol* **87**, 4728-4737 (2013)
269. R. Nachbagauer *et al.*, 'Induction of broadly reactive anti-hemagglutinin stalk antibodies by an H5N1 vaccine in humans'. *J Virol* **88**, 13260-13268 (2014)
270. R. Hai *et al.*, 'Influenza viruses expressing chimeric hemagglutinins: globular head and stalk domains derived from different subtypes'. *J Virol* **86**, 5774-5781 (2012)
271. C. J. Chen *et al.*, 'Influenza A viruses expressing intra- or inter-group chimeric hemagglutinins'. *J Virol* (2016)
272. F. Krammer, 'Novel universal influenza virus vaccine approaches'. *Curr Opin Virol* **17**, 95-103 (2016)
273. P. H. Goff *et al.*, 'Adjuvants and immunization strategies to induce influenza virus hemagglutinin stalk antibodies'. *PloS one* **8**, e79194 (2013)
274. F. Krammer *et al.*, 'Chimeric hemagglutinin influenza virus vaccine constructs elicit broadly protective stalk-specific antibodies'. *J Virol* **87**, 6542-6550 (2013)
275. I. Margine *et al.*, 'Hemagglutinin stalk-based universal vaccine constructs protect against group 2 influenza A viruses'. *J Virol* **87**, 10435-10446 (2013)
276. F. Krammer *et al.*, 'Assessment of Influenza Virus Hemagglutinin Stalk-Based Immunity in Ferrets'. *Journal of Virology* **88**, 3432-3442 (2014)
277. F. Krammer *et al.*, 'H3 stalk-based chimeric hemagglutinin influenza virus constructs protect mice from H7N9 challenge'. *J Virol* **88**, 2340-2343 (2014)
278. R. Nachbagauer *et al.*, 'Hemagglutinin stalk immunity reduces influenza virus replication and transmission in ferrets'. *J Virol* (2015)
279. A. B. Ryder *et al.*, 'Vaccination with Vesicular Stomatitis Virus-Vectored Chimeric Hemagglutinins Protects Mice against Divergent Influenza Virus Challenge Strains'. *J Virol* **90**, 2544-2550 (2015)
280. M. E. Ermler *et al.*, 'Chimeric Hemagglutinin Constructs Induce Broad Protection against Influenza B Virus Challenge in the Mouse Model'. *J Virol* **91**, (2017)
281. R. Nachbagauer *et al.*, 'A universal influenza virus vaccine candidate confers protection against pandemic H1N1 infection in preclinical ferret studies'. *NPJ vaccines* **2**, 26 (2017)
282. E. C. T. Register, 'FLU D-SUIV-ADJ-001 (GSK Supraseasonal Universal Influenza Vaccine (Flu D-SUIV), chimeric strain cH8/1N1, AS03 adjuvanted trial)', (https://www.clinicaltrialsregister.eu/ctr-search/trial/2017-001584-20/BE), 2017.
283. T. T. Wang *et al.*, 'Vaccination with a synthetic peptide from the influenza virus hemagglutinin provides protection against distinct viral subtypes'. *Proc Natl Acad Sci U S A* **107**, 18979-18984 (2010)
284. M. Klausberger *et al.*, 'Globular Head-Displayed Conserved Influenza H1 Hemagglutinin Stalk Epitopes Confer Protection against Heterologous H1N1 Virus'. *PloS one* **11**, e0153579 (2016)
285. F. Krammer, 'The Quest for a Universal Flu Vaccine: Headless HA 2.0'. *Cell host & microbe* **18**, 395-397 (2015)
286. J. Chen *et al.*, 'A soluble domain of the membrane-anchoring chain of influenza virus hemagglutinin (HA2) folds in Escherichia coli into the low-pH-induced conformation'. *Proc Natl Acad Sci U S A* **92**, 12205-12209 (1995)
287. H. Sagawa *et al.*, 'The immunological activity of a deletion mutant of influenza virus haemagglutinin lacking the globular region'. *The Journal of general virology* **77 (Pt 7)**, 1483-1487 (1996)
288. J. Steel *et al.*, 'Influenza virus vaccine based on the conserved hemagglutinin stalk domain'. *mBio* **1**, (2010)
289. T. J. Wohlbold *et al.*, 'Vaccination with soluble headless hemagglutinin protects mice from challenge with divergent influenza viruses'. *Vaccine* **33**, 3314-3321 (2015)

290. G. Bommakanti *et al.*, 'Design of an HA2-based Escherichia coli expressed influenza immunogen that protects mice from pathogenic challenge'. *Proc Natl Acad Sci U S A* **107**, 13701-13706 (2010)
291. G. Bommakanti *et al.*, 'Design of Escherichia coli-expressed stalk domain immunogens of H1N1 hemagglutinin that protect mice from lethal challenge'. *J Virol* **86**, 13434-13444 (2012)
292. K. Uranowska *et al.*, 'Hemagglutinin stalk domain from H5N1 strain as a potentially universal antigen'. *Acta Biochim Pol* **61**, 541-550 (2014)
293. V. V. Mallajosyula *et al.*, 'Influenza hemagglutinin stem-fragment immunogen elicits broadly neutralizing antibodies and confers heterologous protection'. *Proc Natl Acad Sci U S A* **111**, E2514-2523 (2014)
294. V. V. Mallajosyula *et al.*, 'Hemagglutinin Sequence Conservation Guided Stem Immunogen Design from Influenza A H3 Subtype'. *Frontiers in immunology* **6**, 329 (2015)
295. Y. Lu *et al.*, 'Production and stabilization of the trimeric influenza hemagglutinin stem domain for potentially broadly protective influenza vaccines'. *Proc Natl Acad Sci U S A* **111**, 125-130 (2014)
296. F. Krammer *et al.*, 'A carboxy-terminal trimerization domain stabilizes conformational epitopes on the stalk domain of soluble recombinant hemagglutinin substrates'. *PloS one* **7**, e43603 (2012)
297. H. M. Yassine *et al.*, 'Hemagglutinin-stem nanoparticles generate heterosubtypic influenza protection'. *Nat Med* **21**, 1065-1070 (2015)
298. A. Impagliazzo *et al.*, 'A stable trimeric influenza hemagglutinin stem as a broadly protective immunogen'. *Science (New York, N.Y.)* **349**, 1301-1306 (2015)
299. B. M. Giles *et al.*, 'A computationally optimized broadly reactive antigen (COBRA) based H5N1 VLP vaccine elicits broadly reactive antibodies in mice and ferrets'. *Vaccine* **29**, 3043-3054 (2011)
300. D. J. Laddy *et al.*, 'Immunogenicity of novel consensus-based DNA vaccines against avian influenza'. *Vaccine* **25**, 2984-2989 (2007)
301. M. F. Ducatez *et al.*, 'Feasibility of reconstructed ancestral H5N1 influenza viruses for cross-clade protective vaccine development'. *Proc Natl Acad Sci U S A* **108**, 349-354 (2011)
302. A. Kamlangdee *et al.*, 'Mosaic H5 hemagglutinin provides broad humoral and cellular immune responses against influenza viruses'. *J Virol* (2016)
303. A. Kamlangdee *et al.*, 'Broad protection against avian influenza virus by using a modified vaccinia Ankara virus expressing a mosaic hemagglutinin gene'. *J Virol* **88**, 13300-13309 (2014)
304. R. A. Medina *et al.*, 'Glycosylations in the globular head of the hemagglutinin protein modulate the virulence and antigenic properties of the H1N1 influenza viruses'. *Sci Transl Med* **5**, 187ra170 (2013)
305. D. Eggink *et al.*, 'Guiding the immune response against influenza virus hemagglutinin toward the conserved stalk domain by hyperglycosylation of the globular head domain'. *J Virol* **88**, 699-704 (2014)
306. W. C. Liu *et al.*, 'Unmasking Stem-Specific Neutralizing Epitopes by Abolishing N-Linked Glycosylation Sites of Influenza Virus Hemagglutinin Proteins for Vaccine Design'. *J Virol* **90**, 8496-8508 (2016)
307. F. Berlanda Scorza *et al.*, 'Universal influenza vaccines: Shifting to better vaccines'. *Vaccine* (2016)
308. F. Krammer *et al.*, 'NAction! How Can Neuraminidase-Based Immunity Contribute to Better Influenza Virus Vaccines?'. *mBio* **9**, (2018)
309. S. Quinones-Parra *et al.*, 'Universal immunity to influenza must outwit immune evasion'. *Frontiers in microbiology* **5**, 285 (2014)
310. S. Chen *et al.*, 'Protection against multiple subtypes of influenza viruses by virus-like particle vaccines based on a hemagglutinin conserved epitope'. *BioMed research international* **2015**, 901817 (2015)
311. R. Li *et al.*, 'Mucosally administered Lactobacillus surface-displayed influenza antigens (sM2 and HA2) with cholera toxin subunit A1 (CTA1) Induce broadly protective immune responses against divergent influenza subtypes'. *Veterinary microbiology* **179**, 250-263 (2015)
312. A. Firsov *et al.*, 'Expression and Immunogenicity of M2e Peptide of Avian Influenza Virus H5N1 Fused to Ricin Toxin B Chain Produced in Duckweed Plants'. *Frontiers in chemistry* **6**, 22 (2018)
313. R. D. de Vries *et al.*, 'Viral vector-based influenza vaccines'. *Human vaccines & immunotherapeutics* **12**, 2881-2901 (2016)
314. H. C. Ertl, 'Viral vectors as vaccine carriers'. *Curr Opin Virol* **21**, 1-8 (2016)
315. A. Hessel *et al.*, 'MVA Vectors Expressing Conserved Influenza Proteins Protect Mice against Lethal Challenge with H5N1, H9N2 and H7N1 Viruses'. *PloS one* **9**, e88340 (2014)
316. N. B. T. Secrets), '$1-million price tag set for Glybera gene therapy'. *Nature biotechnology* (2015)
317. C. E. Thomas *et al.*, 'Progress and problems with the use of viral vectors for gene therapy'. *Nat Rev Genet* **4**, 346-358 (2003)
318. R. J. Chandler *et al.*, 'Genotoxicity in Mice Following AAV Gene Delivery: A Safety Concern for Human Gene Therapy?'. *Molecular therapy : the journal of the American Society of Gene Therapy* **24**, 198-201 (2016)
319. S. Boutin *et al.*, 'Prevalence of serum IgG and neutralizing factors against adeno-associated virus (AAV) types 1, 2, 5, 6, 8, and 9 in the healthy population: implications for gene therapy using AAV vectors'. *Human gene therapy* **21**, 704-712 (2010)
320. R. Calcedo *et al.*, 'Worldwide epidemiology of neutralizing antibodies to adeno-associated viruses'. *The Journal of infectious diseases* **199**, 381-390 (2009)
321. G. Gao *et al.*, 'Clades of Adeno-associated viruses are widely disseminated in human tissues'. *J Virol* **78**, 6381-6388 (2004)
322. R. W. Atchison *et al.*, 'ADENOVIRUS-ASSOCIATED DEFECTIVE VIRUS PARTICLES'. *Science (New York, N.Y.)* **149**, 754-756 (1965)
323. M. Mitchell *et al.*, 'Production, purification and preliminary X-ray crystallographic studies of adeno-associated virus serotype 9'. *Acta Crystallographica Section F: Structural Biology and Crystallization Communications* **65**, 715-718 (2009)
324. A. M. Mitchell *et al.*, 'AAV's anatomy: roadmap for optimizing vectors for translational success'. *Curr Gene Ther* **10**, 319-340 (2010)
325. K. I. Berns *et al.*, 'AAV: An Overview of Unanswered Questions'. *Human gene therapy* **28**, 308-313 (2017)
326. D. Grimm *et al.*, 'Small but increasingly mighty - Latest advances in AAV vector research, design and evolution'. *Human gene therapy* (2017)
327. Z. Wang *et al.*, 'Human Bocavirus 1 Is a Novel Helper for Adeno-Associated Virus Replication'. *J Virol* (2017)
328. M. Hosel *et al.*, 'Hepatitis B virus infection enhances susceptibility toward adeno-associated viral vector transduction in vitro and in vivo'. *Hepatology (Baltimore, Md.)* **59**, 2110-2120 (2014)
329. J. C. Grieger *et al.*, 'Production and characterization of adeno-associated viral vectors'. *Nature protocols* **1**, 1412-1428 (2006)

330. J. E. Rabinowitz *et al.*, 'Cross-packaging of a single adeno-associated virus (AAV) type 2 vector genome into multiple AAV serotypes enables transduction with broad specificity'. *J Virol* **76**, 791-801 (2002)
331. B. C. Schnepp *et al.*, 'Infectious Molecular Clones of Adeno-Associated Virus Isolated Directly from Human Tissues'. *Journal of Virology* **83**, 1456-1464 (2009)
332. P. D. Kessler *et al.*, 'Gene delivery to skeletal muscle results in sustained expression and systemic delivery of a therapeutic protein'. *Proceedings of the National Academy of Sciences of the United States of America* **93**, 14082-14087 (1996)
333. X. Xiao *et al.*, 'Efficient long-term gene transfer into muscle tissue of immunocompetent mice by adeno-associated virus vector'. *Journal of Virology* **70**, 8098-8108 (1996)
334. R. M. Kotin *et al.*, 'Characterization of a preferred site on human chromosome 19q for integration of adeno-associated virus DNA by non-homologous recombination'. *The EMBO journal* **11**, 5071-5078 (1992)
335. S. Daya *et al.*, 'Adeno-Associated Virus Site-Specific Integration Is Mediated by Proteins of the Nonhomologous End-Joining Pathway'. *Journal of Virology* **83**, 11655-11664 (2009)
336. J. C. Nault *et al.*, 'Recurrent AAV2-related insertional mutagenesis in human hepatocellular carcinomas'. *Nature genetics* **47**, 1187-1193 (2015)
337. H. Buning *et al.*, 'Adeno-associated Vector Toxicity-To Be or Not to Be?'. *Molecular therapy : the journal of the American Society of Gene Therapy* **23**, 1673-1675 (2015)
338. A. Srivastava *et al.*, 'AAV Infection: Protection from Cancer'. *Human gene therapy* **28**, 323-327 (2017)
339. J.-C. Nault *et al.*, 'Wild-type AAV Insertions in Hepatocellular Carcinoma Do Not Inform Debate Over Genotoxicity Risk of Vectorized AAV'. *Molecular Therapy* **24**, 660-661 (2016)
340. A. Ulusoy *et al.*, 'Dose Optimization for Long-term rAAV-mediated RNA Interference in the Nigrostriatal Projection Neurons'. *Molecular Therapy: the Journal of the American Society of Gene Therapy* **17**, 1574-1584 (2009)
341. N. Brown *et al.*, 'Adeno-Associated Virus Vectors and Stem Cells: Friends or Foes?'. *Human gene therapy* **28**, 450-463 (2017)
342. F. Salmon *et al.*, 'Safety profile of recombinant adeno-associated viral vectors: focus on alipogene tiparvovec (Glybera(R))'. *Expert review of clinical pharmacology* **7**, 53-65 (2014)
343. M. F. Dias *et al.*, 'Molecular genetics and emerging therapies for retinitis pigmentosa: Basic research and clinical perspectives'. *Progress in retinal and eye research* **63**, 107-131 (2018)
344. D. Huser *et al.*, 'High prevalence of infectious adeno-associated virus (AAV) in human peripheral blood mononuclear cells indicative of T lymphocytes as sites of AAV persistence'. *J Virol* (2016)
345. A. Srivastava, 'In vivo tissue-tropism of adeno-associated viral vectors'. *Curr Opin Virol* **21**, 75-80 (2016)
346. S. Pillay *et al.*, 'Host determinants of adeno-associated viral vector entry'. *Curr Opin Virol* **24**, 124-131 (2017)
347. A. M. Dudek *et al.*, 'An alternate route for adeno-associated virus entry independent of AAVR'. *J Virol* (2018)
348. S. Pillay *et al.*, 'An essential receptor for adeno-associated virus infection'. *Nature* **530**, 108-112 (2016)
349. S. Pillay *et al.*, 'AAV serotypes have distinctive interactions with domains of the cellular receptor AAVR'. *J Virol* (2017)
350. M. Nonnenmacher *et al.*, 'Adeno-associated virus 2 infection requires endocytosis through the CLIC/GEEC pathway'. *Cell host & microbe* **10**, 563-576 (2011)
351. S. Uhrig *et al.*, 'Successful target cell transduction of capsid-engineered rAAV vectors requires clathrin-dependent endocytosis'. *Gene therapy* **19**, 210-218 (2012)
352. M. E. Nonnenmacher *et al.*, 'Syntaxin 5-dependent retrograde transport to the trans-Golgi network is required for adeno-associated virus transduction'. *J Virol* **89**, 1673-1687 (2015)
353. A. Girod *et al.*, 'The VP1 capsid protein of adeno-associated virus type 2 is carrying a phospholipase A2 domain required for virus infectivity'. *The Journal of general virology* **83**, 973-978 (2002)
354. P. J. Xiao *et al.*, 'Cytoplasmic trafficking, endosomal escape, and perinuclear accumulation of adeno-associated virus type 2 particles are facilitated by microtubule network'. *J Virol* **86**, 10462-10473 (2012)
355. S. C. Nicolson *et al.*, 'Recombinant adeno-associated virus utilizes host cell nuclear import machinery to enter the nucleus'. *J Virol* **88**, 4132-4144 (2014)
356. R. A. Schwartz *et al.*, 'Adeno-associated virus replication induces a DNA damage response coordinated by DNA-dependent protein kinase'. *J Virol* **83**, 6269-6278 (2009)
357. M. D. Weitzman *et al.*, 'Recruitment of wild-type and recombinant adeno-associated virus into adenovirus replication centers'. *J Virol* **70**, 1845-1854 (1996)
358. A. Wistuba *et al.*, 'Subcellular compartmentalization of adeno-associated virus type 2 assembly'. *J Virol* **71**, 1341-1352 (1997)
359. C. Vandamme *et al.*, 'Unraveling the complex story of immune responses to AAV vectors trial after trial'. *Human gene therapy* (2017)
360. D. M. McCarty, 'Self-complementary AAV vectors; advances and applications'. *Molecular therapy : the journal of the American Society of Gene Therapy* **16**, 1648-1656 (2008)
361. K. Nieto *et al.*, 'AAV Vectors Vaccines Against Infectious Diseases'. *Frontiers in immunology* **5**, 5 (2014)
362. I. Sipo *et al.*, 'Vaccine protection against lethal homologous and heterologous challenge using recombinant AAV vectors expressing codon-optimized genes from pandemic swine origin influenza virus (SOIV)'. *Vaccine* **29**, 1690-1699 (2011)
363. J. Lin *et al.*, 'A new genetic vaccine platform based on an adeno-associated virus isolated from a rhesus macaque'. *J Virol* **83**, 12738-12750 (2009)
364. K. Q. Xin *et al.*, 'A novel recombinant adeno-associated virus vaccine induces a long-term humoral immune response to human immunodeficiency virus'. *Human gene therapy* **12**, 1047-1061 (2001)
365. A. B. Balazs *et al.*, 'Broad protection against influenza infection by vectored immunoprophylaxis in mice'. *Nature biotechnology* **31**, 647-652 (2013)
366. M. P. Limberis *et al.*, 'Intranasal antibody gene transfer in mice and ferrets elicits broad protection against pandemic influenza'. *Sci Transl Med* **5**, 187ra172 (2013)
367. V. S. Adam *et al.*, 'Adeno-associated virus 9-mediated airway expression of antibody protects old and immunodeficient mice against influenza virus'. *Clin Vaccine Immunol* **21**, 1528-1533 (2014)
368. M. P. Limberis *et al.*, 'Vectored expression of the broadly neutralizing antibody FI6 in mouse airway provides partial protection against a new avian influenza A virus, H7N9'. *Clin Vaccine Immunol* **20**, 1836-1837 (2013)
369. M. P. Limberis *et al.*, 'Adeno-associated virus serotype 9 vectors transduce murine alveolar and nasal epithelia and can be readministered'. *Proc Natl Acad Sci U S A* **103**, 12993-12998 (2006)
370. C. L. Bell *et al.*, 'The AAV9 receptor and its modification to improve in vivo lung gene transfer in mice'. *The Journal of clinical investigation* **121**, 2427-2435 (2011)
371. K. Fiddeke, 'Evaluierung von Nukleoprotein-kodierenden AAV-Vektoren als breitenwirksame Influenza-Impfstoffe', *Dissertation*, Freie Universität Berlin, (2016).

372. S. E. Reed *et al.*, 'Transfection of mammalian cells using linear polyethylenimine is a simple and effective means of producing recombinant adeno-associated virus vectors'. *Journal of virological methods* **138**, 85-98 (2006)
373. B. Strobel *et al.*, 'Comparative Analysis of Cesium Chloride- and Iodixanol-Based Purification of Recombinant Adeno-Associated Viral Vectors for Preclinical Applications'. *Human gene therapy methods* **26**, 147-157 (2015)
374. F. Sonntag *et al.*, 'The assembly-activating protein promotes capsid assembly of different adeno-associated virus serotypes'. *J Virol* **85**, 12686-12697 (2011)
375. W. He *et al.*, 'Measuring the neutralization potency of influenza A virus hemagglutinin stalk/stem-binding antibodies in polyclonal preparations by microneutralization assay'. *Methods* **90**, 95-100 (2015)
376. WHO, 'Manual on Animal Influenza Diagnosis and Surveillance', 2002.
377. A. Meliani *et al.*, 'Determination of anti-adeno-associated virus vector neutralizing antibody titer with an in vitro reporter system'. *Human gene therapy methods* **26**, 45-53 (2015)
378. E. Corrales-Aguilar *et al.*, 'A novel assay for detecting virus-specific antibodies triggering activation of Fcgamma receptors'. *J Immunol Methods* **387**, 21-35 (2013)
379. E. Corrales-Aguilar *et al.*, 'Human Cytomegalovirus Fcγ Binding Proteins gp34 and gp68 Antagonize Fcγ Receptors I, II and III'. *PLoS pathogens* **10**, e1004131 (2014)
380. D. Kugel *et al.*, 'Intranasal administration of alpha interferon reduces seasonal influenza A virus morbidity in ferrets'. *J Virol* **83**, 3843-3851 (2009)
381. L. Walz *et al.*, 'Sialidase-Inhibiting Antibody Titers Correlate with Protection from Heterologous Influenza Virus Strains of the Same Neuraminidase Subtype'. *J Virol* (2018)
382. K. Dietert *et al.*, 'Spectrum of pathogen- and model-specific histopathologies in mouse models of acute pneumonia'. *PloS one* **12**, e0188251 (2017)
383. WHO, 'WHO recommendations on the composition of influenza virus vaccines', (http://www.who.int/influenza/vaccines/virus/recommendations/en/), 2018.
384. N. M. Bouvier *et al.*, 'Animal Models for Influenza Virus Pathogenesis and Transmission'. *Viruses* **2**, 1530-1563 (2010)
385. T. Enkirch *et al.*, 'Ferret models of viral pathogenesis'. *Virology* **479-480**, 259-270 (2015)
386. WHO, 'Recommended composition of influenza virus vaccines for use in the 2017/2018 northern hemisphere influenza season', (http://www.who.int/influenza/vaccines/virus/recommendations/201703_recommendation.pdf?ua=1), 2017.
387. I. Meunier *et al.*, 'Virulence differences of closely related pandemic 2009 H1N1 isolates correlate with increased inflammatory responses in ferrets'. *Virology* **422**, 125-131 (2012)
388. T. Tschernig *et al.*, 'Bronchus-Associated Lymphoid Tissue (BALT) Is Not Present in the Normal Adult Lung but in Different Diseases'. *Pathobiology* **68**, 1-8 (2000)
389. S. Halle *et al.*, 'Induced bronchus-associated lymphoid tissue serves as a general priming site for T cells and is maintained by dendritic cells'. *The Journal of experimental medicine* **206**, 2593 (2009)
390. J. E. Moyron-Quiroz *et al.*, 'Role of inducible bronchus associated lymphoid tissue (iBALT) in respiratory immunity'. *Nat Med* **10**, 927-934 (2004)
391. A. Kumar *et al.*, 'Novel Platforms for the Development of a Universal Influenza Vaccine'. *Frontiers in immunology* **9**, 600 (2018)
392. M. A. Liu, 'Immunologic basis of vaccine vectors'. *Immunity* **33**, 504-515 (2010)
393. A. Sarukhan *et al.*, 'Successful interference with cellular immune responses to immunogenic proteins encoded by recombinant viral vectors'. *J Virol* **75**, 269-277 (2001)
394. K. Jooss *et al.*, 'Immunity to adenovirus and adeno-associated viral vectors: implications for gene therapy'. *Gene therapy* **10**, 955-963 (2003)
395. FDA, 'Aproved Products - LUXTURNA', (https://www.fda.gov/biologicsbloodvaccines/cellulargenetherapyproducts/approvedproducts/ucm589507.htm), 2018.
396. E. Y. Klein *et al.*, 'Stability of the Influenza Virus Hemagglutinin Protein Correlates with Evolutionary Dynamics'. *mSphere* **3**, e00554-00517 (2018)
397. M. D. Tate *et al.*, 'Playing hide and seek: how glycosylation of the influenza virus hemagglutinin can modulate the immune response to infection'. *Viruses* **6**, 1294-1316 (2014)
398. C. D. O'Donnell *et al.*, 'Effect of Priming with H1N1 Influenza Viruses of Variable Antigenic Distances on Challenge with 2009 Pandemic H1N1 Virus'. *Journal of Virology* **86**, 8625-8633 (2012)
399. C. Kurts *et al.*, 'Major histocompatibility complex class I-restricted cross-presentation is biased towards high dose antigens and those released during cellular destruction'. *The Journal of experimental medicine* **188**, 409-414 (1998)
400. A. Sarukhan *et al.*, 'Factors influencing cross-presentation of non-self antigens expressed from recombinant adeno-associated virus vectors'. *The journal of gene medicine* **3**, 260-270 (2001)
401. R. Schirmbeck *et al.*, 'The immunogenicity of adenovirus vectors limits the multispecificity of CD8 T-cell responses to vector-encoded transgenic antigens'. *Molecular therapy : the journal of the American Society of Gene Therapy* **16**, 1609-1616 (2008)
402. A. Kim *et al.*, 'Distorted Immunodominance by Linker Sequences or other Epitopes from a Second Protein Antigen During Antigen-Processing'. *Scientific reports* **7**, 46418 (2017)
403. J. Y. Dong *et al.*, 'Quantitative analysis of the packaging capacity of recombinant adeno-associated virus'. *Human gene therapy* **7**, 2101-2112 (1996)
404. S. Alam *et al.*, 'CD4 T Cell Help Is Limiting and Selective during the Primary B Cell Response to Influenza Virus Infection'. *Journal of Virology* **88**, 314-324 (2014)
405. T. M. Tumpey *et al.*, 'Mucosal delivery of inactivated influenza vaccine induces B-cell-dependent heterosubtypic cross-protection against lethal influenza A H5N1 virus infection'. *J Virol* **75**, 5141-5150 (2001)
406. E. E. Tran *et al.*, 'Cryo-electron Microscopy Structures of Chimeric Hemagglutinin Displayed on a Universal Influenza Vaccine Candidate'. *mBio* **7**, (2016)
407. A. W. Mesman *et al.*, 'Influenzavirus A(H1N1)2009 antibody-dependent cellular cytotoxicity in young children prior to the H1N1 pandemic'. *The Journal of general virology* (2016)
408. H. Jacobsen *et al.*, 'Influenza Virus Hemagglutinin Stalk-Specific Antibodies in Human Serum are a Surrogate Marker for In Vivo Protection in a Serum Transfer Mouse Challenge Model'. *mBio* **8**, (2017)
409. J. K. Park *et al.*, 'Evaluation of Preexisting Anti-Hemagglutinin Stalk Antibody as a Correlate of Protection in a Healthy Volunteer Challenge with Influenza A/H1N1pdm Virus'. *mBio* **9**, (2018)
410. G. Hashimoto *et al.*, 'Ability of human cord blood lymphocytes to mediate antibody-dependent cellular cytotoxicity against influenza virus-infected cells'. *Infection and immunity* **42**, 214-218 (1983)
411. H. A. Vanderven *et al.*, 'Antibody-Dependent Cellular Cytotoxicity Responses to Seasonal Influenza Vaccination in Older Adults'. *The Journal of infectious diseases* **217**, 12-23 (2017)

412. S. Jegaskanda *et al.*, 'Cross-Reactive Influenza-Specific Antibody-Dependent Cellular Cytotoxicity Antibodies in the Absence of Neutralizing Antibodies'. *The Journal of Immunology* **190**, 1837-1848 (2013)
413. R. D. de Vries *et al.*, 'Influenza virus-specific antibody dependent cellular cytoxicity induced by vaccination or natural infection'. *Vaccine* (2016)
414. R. D. de Vries *et al.*, 'Primary Human Influenza B Virus Infection Induces Cross-Lineage Hemagglutinin Stalk-Specific Antibodies Mediating Antibody-Dependent Cellular Cytoxicity'. *The Journal of infectious diseases* **217**, 3-11 (2017)
415. C. J. Wei *et al.*, 'Elicitation of Broadly Neutralizing Influenza Antibodies in Animals with Previous Influenza Exposure'. *Sci Transl Med* **4**, 147ra114 (2012)
416. C. Rosales *et al.*, 'Fc receptors: Cell activators of antibody functions'. *Advances in Bioscience and Biotechnology* **04**, 21-33 (2013)
417. H. A. Vanderven *et al.*, 'What Lies Beneath: Antibody Dependent Natural Killer Cell Activation by Antibodies to Internal Influenza Virus Proteins'. *EBioMedicine* **8**, 277-290 (2016)
418. S. Jegaskanda *et al.*, 'Fc or not Fc; that is the question: Antibody Fc-receptor interactions are key to universal influenza vaccine design'. *Human vaccines & immunotherapeutics* **13**, 1-9 (2017)
419. H. Yusuf *et al.*, 'Current prospects and future challenges for nasal vaccine delivery'. *Human vaccines & immunotherapeutics* 1-12 (2016)
420. J. E. Moyron-Quiroz *et al.*, 'Persistence and responsiveness of immunologic memory in the absence of secondary lymphoid organs'. *Immunity* **25**, 643-654 (2006)
421. S. S. Huang *et al.*, 'Differential pathological and immune responses in newly weaned ferrets are associated with a mild clinical outcome of pandemic 2009 H1N1 infection'. *J Virol* **86**, 13187-13201 (2012)
422. S. Sun *et al.*, 'Age-related sensitivity and pathological differences in infections by 2009 pandemic influenza A (H1N1) virus'. *Virol J* **8**, 52 (2011)
423. B. A. Askonas *et al.*, 'Formation of specific antibodies and γ-globulin in vitro. A study of the synthetic ability of various tissues from rabbits immunized by different methods'. *Biochemical Journal* **68**, 252-261 (1958)
424. J. Rangel-Moreno *et al.*, 'The development of inducible bronchus-associated lymphoid tissue depends on IL-17'. *Nat Immunol* **12**, 639-646 (2011)
425. D. Damjanovic *et al.*, 'Immunopathology in influenza virus infection: Uncoupling the friend from foe'. *Clinical Immunology* **144**, 57-69 (2012)
426. Y. Itoh *et al.*, 'In vitro and in vivo characterization of new swine-origin H1N1 influenza viruses'. *Nature* **460**, 1021-1025 (2009)
427. L. A. Reperant *et al.*, 'Linking influenza virus tissue tropism to population-level reproductive fitness'. *PloS one* **7**, e43115 (2012)

LIST OF FIGURES

LIST OF TABLES

ABBREVIATIONS

AAV ..... Adeno-associated virus
AAVR ..... Adeno-associated virus receptor
ADCC ..... antibody-dependent cellular cytotoxicity
ADE ..... antibody-dependent enhancement of disease
ADP ..... antibody-dependent phagocytosis
AdV ..... Adenovirus
APC ..... antigen presenting cell
BALT ..... bronchus-associated lymphoid tissue
BCR ..... B-cell receptor
$CD103^{+*}$ DC, $CD11b^{+}$ DC, pDC ..... dendritic cell subsets with specialized functions
CDR ..... complementary determining region
C_H ..... antibody heavy chain constant region
cHA ..... chimeric HA
C_L ..... antibody light chain constant region
CMV ..... Cytomegalovirus
cRNA ..... complementary RNA
CTL ..... cytotoxic T lymphocyte
DC ..... dendritic cell
dpi ..... days post infection
DTT ..... Dithiothreitol
ELISA ..... enzyme-linked immunosorbent assay
EM ..... electron microscopy
FcγR ..... Fcγ-receptor
FcγR-KO mouse ..... FcγR knock out mouse
GFP ..... green fluorescent protein
GMP ..... good manufacturing practice
GPI ..... glycosylphosphatidylinositol
HA or H ..... hemagglutinin
HA0 ..... precursor protein of the HA monomer
HA1 and HA2 ..... subunits of the HA monomer
HAI ..... hemagglutination inhibition
headless HA ..... headless HA
i.m. ..... intramuscular
i.n. ..... intranasal
IFN ..... interferon
Ig (IgM, IgD, IgG, IgE, IgA) ..... immunoglobulin (immunoglobulin isotypes)
IHC ..... immunohistochemistry

IL-2 ..... interleukin 2
ITAM motif ..... immune receptor tyrosine-based activation motif
ITIM motif ..... immune receptor tyrosine-based inhibitory motif
ITR ..... inverted terminal repeat
kDA ..... Kilo Dalton
LAIV ..... life attenuated Influenza vaccine
M1, M2 ..... matrix protein 1or 2
MAP-kinase ..... mitogen-activated protein kinase
MHCI ..... major histocompatibility complex class I molecule
MHCII ..... major histocompatibility complex class II molecule
mHL1 or mHL2 ..... modified headless HA 1 or 2
mHL1+TM or mHL2+TM ..... modified headless HA 1 or 2 with transmembrane domain
MN assay ..... microneutralization assay
MVA virus ..... Modified vaccine virus Ankara virus
NA or N ..... neuraminidase
NAI ..... neuraminidase activity inhibition
NEP ..... nuclear export protein
NK cell ..... natural killer cell
NP ..... nucleoprotein
NS1 and NS2 ..... nonstructural proteins 1 and 2
PA, PB1 and PB2 ..... polymerase subunits (acid, basic 1 and basic 2)
PBMC ..... peripheral blood mononuclear cell
PFU ..... plaque forming unit
RBS ..... receptor binding site
RdRp ..... RNA-dependent-RNA-Polymerase
RNP ..... ribonucleoprotein
$TCID_{50}$ ..... 50 % tissue culture infectious dose
T_{CM}, T_{EM} or T_{RM} ..... memory T-cell subsets
T_{FH}, T_H17 or T_{Reg} ..... regulatory $CD4^+$ T-cell subsets
TIV or QIV ..... trivalent or quadrivalent inactivated Influenza vaccine
TM ..... transmembrane region
TNFα ..... tumor necrosis factor α
V(D)J segments ..... gene segments that are recombined to build up an antibody's chains
vg ..... viral genomes
V_H ..... antibody heavy chain variable region
V_L ..... antibody light chain variable region
VLP ..... virus-like particle
VP1, VP2, VP3 ..... AAV capsid proteins
vRNA ..... viral RNA
VSV ..... Vesicular stomatitis virus
WIV ..... whole inactivated virus